UNIVERSITY OF GENOA

POLYTECHNIC SCHOOL

DIME

Dipartimento di Ingegneria Meccanica, Energetica, Gestionale e dei Trasporti

PhD Thesis

XXXIII Cycle

MICROTURBINE BASED ENERGY HUB DESIGN AND MANAGEMENT IN A DISTRIBUTED GENERATION APPROACH

Supervisor:

Chiar.ma Prof. Ing. Loredana Magistri

Co-Supervisor:

Dott. Ing. Massimo Rivarolo

Candidate:

Ing. Diego Rattazzi

Year: 2021

UNIVERSITÀ DEGLI STUDI DI GENOVA

SCUOLA POLITECNICA

DIME

Dipartimento di Ingegneria Meccanica, Energetica,

Gestionale e dei Trasporti

Tesi di Dottorato

DOTTORATO DI RICERCA IN INGEGNERIA DELLE MACCHINE E DEI SISTEMI PER L'ENERGIA, L'AMBIENTE E I TRASPORTI

CICLO XXXIII

PROGETTAZIONE E GESTIONE DI HUB ENERGETICI BASATI SU MICROTURBINE IN UN APPROCCIO DI GENERAZIONE DISTRIBUITA

Relatore:

Chiar.ma Prof. Ing. Loredana Magistri

Co-relatore:

Dott. Ing. Massimo Rivarolo

Candidato:

Ing. Diego Rattazzi

Anno: 2021

Table of Contents

List of Figures ... 1
List of Tables ... 6
Nomenclature ... 8
Symbols ... 10
Abstract ... 12
1 Distributed Generation: an introduction ... 15
1.1 Italian energy policies ... 19
1.1.1 Incentives and policies direction ... 19
1.1.2 Grid connection limits and regulations ... 25
1.2 Distributed Generation Technologies ... 29
1.2.1 Traditional generators ... 33
1.2.2 Non - Traditional generators ... 35
2 A residential case study: ENVISION ... 45
2.1 Southern Demo Description ... 46
2.1.1 System layout and technologies implemented ... 51
2.2 System modelling ... 66
2.2.1 Solar façade panels model ... 66
2.2.2 Heat Pump model ... 70
2.3 System configuration optimization ... 84
2.3.1 Panel configuration ... 84
2.3.2 System sizing ... 86
2.4 Control strategy development ... 95
2.4.1 W-ECoMP Description ... 100
2.4.2 District cases management ... 101
2.4.3 Single system analysis ... 115
2.4.4 Control algorithm for the Savona Demosite ... 124
2.5 Preliminary test campaign ... 135
3 A maritime application of Distributed Generation ... 145
3.1 GEI Project ... 149
3.1.1 Micro Gas Turbine with LNG ... 151
3.1.2 PEM Fuel Cells with Hydrogen ... 156

3.1.3 Systems comparison at steady-state level ... 162
3.1.4 Time-variant analysis ... 170
3.2 HELM Tool ... 210
3.2.1 HELM Applications and studies ... 215
3.2.2 HELM in a maritime Distributed Generation application ... 221
4 Conclusions ... 232
5 References ... 235

List of Figures

Figure 1 Share of renewables in power generation in the Sustainable Development Scenario [1] 15
Figure 2 Renewable power generation by technology in the Sustainable Development Scenario [2] 16
Figure 3 "Trickling down" paradigm 17
Figure 4 PV electricity production in Italy [5] 18
Figure 5 Energy Flows in 2017 [6] 18
Figure 6 Energy system transition scheme [5] 19
Figure 7 Different grid Inertia for a system with or without inverter [18] 29
Figure 8 DG installed power and number of plants per primary source, Italy [26] 32
Figure 9 DG production overall trend, Italy [26] 32
Figure 10 Distributed Generation Technologies Classifications [27] 33
Figure 11 Microturbine scheme [31] 35
Figure 12 Electricity cost by source [32] 37
Figure 13 Evolution of fuel cell installed power in terms of applications (left) and type (right) [34] 38
Figure 14 Different Fuel Cell types, operational scheme [35] 38
Figure 15 Energy storages categories [37] 40
Figure 16 Electric Vehicles selling projection [39] 41
Figure 17 Generation units efficiency, comparison between DG technologies and centralized ones [35] 42
Figure 18 Energy consumption by sector in EU-28 [40] 43
Figure 19 ENVISION logo 45
Figure 20 ENVISION Consortium [43] 46
Figure 21 Savona Smart-Polygeneration micro-Grid [44] 47
Figure 22 Savona Campus DHN 48
Figure 23 Savona Campus map 49
Figure 24 ENVISION Area initial status A 50
Figure 25 ENVISION Area initial status B 50
Figure 26 ENVISION Area initial status C 50
Figure 27 ENVISION Area initial status D 50
Figure 28 Before 50
Figure 29 After 50
Figure 30 ENVISION system layout 51
Figure 31: 1960s residential building 52
Figure 32: Renovated 1960s residential building 52
Figure 33: 3D model of demo façade 52
Figure 34: Intersection of the demo façade 52
Figure 35: Fluid distribution pipes model 53
Figure 36: Fluid distribution pipes SolarBEAT 53
Figure 37: Section view of pipe on panel 53
Figure 38: Mounting system model 54
Figure 39: Mounting system SolarBEAT 54
Figure 40 ENVISION Area buildings dimensions, SE view 54

Figure 41 ENVISION Area buildings dimensions, NW view 54
Figure 42 Heat Pump operational scheme and PH Diagram [45] 55
Figure 43 ENVISION Heat pump Scheme 56
Figure 44 ENEREN Heat Pump Dimensions 57
Figure 45 mGT installation building 60
Figure 46 mGT draw 60
Figure 47 Operational scheme of considered mGT 61
Figure 48 ENVISION mGT drawing 61
Figure 49 500 litres Thermal Energy Storage in Savona Campus 64
Figure 50 Inertial storage tank draw 64
Figure 51 Inertial storage tank dimensions 64
Figure 52 Savona Campus Laboratories thermal dissipators 65
Figure 53 ENVISION Southern Demosite rendering 66
Figure 54 Façade panel performances curve 67
Figure 55 Incidence of solar radiation 67
Figure 56 $\eta 0$ dependence on incidence angle 68
Figure 57 Solar Panel Control Volume 69
Figure 58 Black Uncovered Panel parity plot 70
Figure 59 Red Uncovered Panel parity plot 70
Figure 60 White Uncovered Panel parity plot 70
Figure 61 HP cycle on R1233zd(E) T-s diagram 71
Figure 62 HP scheme 72
Figure 63 Evaporator Simulink Model 73
Figure 64 Compressor map 74
Figure 65 Compressor delays 75
Figure 66 Compressor Simulink Model 75
Figure 67 Condenser Simulink model 76
Figure 68 Expansion valve delays 77
Figure 69 Expansion valve Simulink Model 77
Figure 70 Control system Simulink model 78
Figure 71 HP simplified Simulink model 78
Figure 72 Moving boundary approach for HP Condenser 79
Figure 73 Calculation scheme for Heat Exchanger in a moving boundary approach 80
Figure 74 Error of main model parameters compared to the experimental data provided by Mayekawa 82
Figure 75 Ub coefficient comparison with a literature study 83
Figure 76 Series or parallel Panels interconnection 84
Figure 77 COP for different configurations in hot season 85
Figure 78 COP for different configurations in cold season 85
Figure 79 Inlet and Outlet temperature for the panels in different configurations 86
Figure 80 DHN Inlet temperature 86
Figure 81 Simulated Layout 87
Figure 82 Matlab Simulink Model Layout 88
Figure 83 Thermal demand for 20 apartments of 52 m^2 89
Figure 84 Temperature deviation of water inlet of HP's evaporator (Winter) 89
Figure 85 Heat Pump COP variation with temperatures [56] 90

Figure 86 Temperature deviation of water inlet of HP's evaporator (Summer)...................... 92
Figure 87 Split daily costs of ENVISION solution on a yearly base... 94
Figure 88 Overview of district heating temperature range due to heat generation technologies and sources [64].. 96
Figure 89 Technical triangle for HP integration into DHN [64].. 97
Figure 90 Technical triangle in four different scenarios [64]... 98
Figure 91 Traditional Heat coverage (on the Left) considering building refurbishment and Innovative management (on the right) considering the use of only innovative energy sources [64]... 99
Figure 92 Schemes for: (A) traditional fossil fuel-based DH and (B) heat pump placement options in advanced DH [64]... 99
Figure 93 W-ECoMP description 100
Figure 94 Example of off-design curves in W-ECoMP... 101
Figure 95 Smart-grid configuration on W-ECoMP... 102
Figure 96 Smart Grid Electric management in a winter scenario... 105
Figure 97 Smart Grid Thermal management in a winter scenario 105
Figure 98 mGTs partial load in a winter scenario 106
Figure 99 COP of Heat Pumps in a winter scenario 107
Figure 100 Smart Grid Electric management in a summer scenario..................................... 107
Figure 101 Smart Grid thermal management in a summer scenario..................................... 108
Figure 102 mGT partial load in a summer scenario.. 109
Figure 103 COP of Heat Pumps in a summer scenario 109
Figure 104 DHN configuration on W-ECoMP 110
Figure 105 DHN management in a winter scenario.. 111
Figure 106 COP on a daily basis in a winter scenario 112
Figure 107 Heat Pumps partial load on a daily basis in a winter scenario............................ 112
Figure 108 DHN management in a summer scenario... 113
Figure 109 COP on a daily basis in summer scenario 114
Figure 110 Heat Pumps partial load on a daily basis in summer scenario 114
Figure 111 W-ECoMP simulation layout.. 116
Figure 112 Electric management in a characteristic winter day 117
Figure 113 Thermal management in a characteristic winter day.. 117
Figure 114 Storage daily usage on the winter scenario.. 118
Figure 115 Electric management in a characteristic summer day 119
Figure 116 Thermal management in a characteristic summer day.. 119
Figure 117 Storage daily usage on the summer scenario.. 120
Figure 118 Electrical (left) and thermal (right) management in a winter scenario 120
Figure 119 Electrical (left) and thermal (right) management in a summer scenario 121
Figure 120 Yearly operational costs detail.. 122
Figure 121 Voice of cost for LCOE and LCOH calculations 123
Figure 122 LCOH and LCOE for the scenario with higher electric demand........................ 123
Figure 123 Levelized cost of energy for ENVISION system compared to alternative and conventional energy systems [69]... 124
Figure 124 MPC Controller Scheme 125
Figure 125 MPC Concept description... 126
Figure 126 Optimization problem solution... 128

Figure 127 HP state-space model for MPC ... 129
Figure 128 mGT state-space model ... 130
Figure 129 Case study MPC structure ... 131
Figure 130 Electric (top) and thermal (bottom) system management ... 132
Figure 131 MPC controlled variables ... 132
Figure 132 HP and mGT actual thermal production ... 133
Figure 133 Advanced MPC description for ENVISION system ... 134
Figure 134 ENVISION advanced MPC layout in Matlab Simulink ... 134
Figure 135 Preliminary Demo at Savona ... 136
Figure 136 PreDemo layout ... 136
Figure 137 Temperature sensors detail ... 137
Figure 138 Ambient conditions for morning August day by SOLCAST ... 138
Figure 139 Temperature trends for the panels during August morning ... 138
Figure 140 Heat produced by ENVISION panels, August morning ... 139
Figure 141 Ambient conditions for afternoon August day by SOLCAST ... 139
Figure 142 Temperature trends for the panels during August afternoon ... 140
Figure 143 Heat produced by ENVISION panels, August afternoon ... 140
Figure 144 Daily Ambient conditions for September, SOLCAST data (left), Savona Campus data (right) ... 141
Figure 145 Temperature trends for the panels September day ... 141
Figure 146 Daily monitoring of panels heat production in September ... 142
Figure 147 Transport sectors comparison [75] ... 145
Figure 148 IMO Logo ... 146
Figure 149 ECAs and potential ECAs [76] ... 146
Figure 150 SOx limitations [73] ... 147
Figure 151 NOx limitations [73] ... 147
Figure 152 CO_2 emissions limitation trend by IMO regulations [74] ... 148
Figure 153 Royal Princess cruise ship ... 149
Figure 154 Electrical scheme for DG on board ... 151
Figure 155 Membrane LNG tank ... 154
Figure 156 Membrane LNG tank description ... 154
Figure 157 Type C LNG tank layout ... 155
Figure 158 Bi-lobed LNG Tank Type C ... 156
Figure 159 PEMFC schematic of the operation ... 157
Figure 160 Structure of a PEMFC Stack ... 158
Figure 161 PEMFC fuelled by H_2 layout ... 159
Figure 162 PEM Hydrogenics HD 30 characteristic curve [86] ... 160
Figure 163 Linde cryogenic Hydrogen tank ... 161
Figure 164 Economic analysis of the two main solutions in comparison with SoA (MFO with ICE) ... 169
Figure 165 Energy system layout in W-ECoMP ... 175
Figure 166 ZG1 electrical management ... 176
Figure 167 ZG1 Thermal management ... 177
Figure 168 ZG2 Electrical management ... 177
Figure 169 ZG2 Thermal management ... 177
Figure 170 ZG3 Electrical management ... 178

Figure 171 ZG3 Thermal management 178
Figure 172 ZG 1 electrical management warm ambient 182
Figure 173 ZG 1 Thermal management warm ambient 182
Figure 174 ZG 2 Electrical management warm ambient 183
Figure 175 ZG 2 Thermal management warm ambient 183
Figure 176 ZG 3 Electrical management warm ambient 183
Figure 177 ZG 3 Thermal management warm ambient 184
Figure 178 ZG 1 Electric management cold ambient 191
Figure 179 ZG 1 Thermal management cold ambient 191
Figure 180 ZG 2 Electric management cold ambient 191
Figure 181 ZG 2 Thermal management cold ambient 192
Figure 182 ZG 3 Electric management cold ambient 192
Figure 183 Thermal management cold ambient 192
Figure 184 ZG 1 Electric management warm ambient 196
Figure 185 ZG 1 Thermal management warm ambient 196
Figure 186 ZG 2 Electric management warm ambient 197
Figure 187 ZG 2 Thermal management warm ambient 197
Figure 188 ZG 3 Electric management warm ambient 197
Figure 189 ZG 3 Thermal management warm ambient 198
Figure 190 Hybrid solution layout 204
Figure 191 ZG 3 Electric management for hybrid solution in cold ambient 205
Figure 192 ZG 3 Thermal management for hybrid solution in cold ambient 205
Figure 193 mGT LCOE comparison 209
Figure 194 PEMFC LCOE comparison 209
Figure 195 HELM Logo 210
Figure 196 Fuel Oil Tank Map 211
Figure 197 HELM Tool logical scheme 212
Figure 198 X_i Values for the weight performance parameter 213
Figure 199 HELM User interface 214
Figure 200 Impact of Emissions relevance parameter on the overall score for the main technologies 217
Figure 201 HELM resulting scores 220
Figure 202 Costa Diadema main characteristics 221
Figure 203 Hotel electrical load 222
Figure 204 HELM screenshot with the implemented technologies 224
Figure 205 HELM Score results for Case 1 225
Figure 206 Score detail for PEM+LH2 and ICE+LNG solutions 225
Figure 207 Detailed data for mGT and SOFC solutions 226
Figure 208 HELM score results for Case 2 227
Figure 209 Case 2 Score detail for PEM+LH_2, ICE+MeOH, ICE+FO, ICE+NH_3 227
Figure 210 Details on the values provided by HELM for mGT+LNG, ICE+LNG, ICE+FO 228

List of Tables

Table 1 Main Fuel Cells characteristic [33] 40
Table 2 Total Available surface for ENVISION panels installation 55
Table 3 ENVISION HP Dimensioning 56
Table 4 HP Performances, Scenario A 57
Table 5 HP Performances, Scenario B 58
Table 6 HP Performances, Scenario C 58
Table 7 ENVISION HP main characteristics 58
Table 8 Air intake characteristics 61
Table 9 Heat recovery unit characteristics 62
Table 10 Gas specifications 62
Table 11 mGT Electrical characteristics 62
Table 12 Wind Thermal Losses coefficient [s/m] 68
Table 13 Panel Thermal Capacity [kJ/K] 69
Table 14 Evaporator Characteristics [49] 73
Table 15 Condenser Characteristics [49] 76
Table 16 PI control coefficients 77
Table 17 First guess set of equations 81
Table 18 Equations system for condenser solution 81
Table 19 Simulated scenarios 88
Table 20 Economic and environmental assessment (Winter) 91
Table 21 Economic and environmental assessment (Summer) 92
Table 22 Yearly Economic and environmental assessment 93
Table 23 Thermo economic results for boiler 94
Table 24 Heat Pumps properties 102
Table 25 CHP unit properties 103
Table 26 Trendlines for electric loads used on summer (top) and winter (bottom) [66] 104
Table 27 Percentage of time spent by each mGT in a certain working condition, winter scenario 106
Table 28 Percentage of time spent by each mGT in a certain working condition, summer scenario 108
Table 29 Heat Pump properties 111
Table 30 Preliminary MPC parameters 131
Table 31 Panels efficiency 143
Table 32 Royal Princess main characteristics 149
Table 33 Engines on board 150
Table 34 Units distribution on board 151
Table 35 mGT Capstone 800s technical specifications 152
Table 36 LNG tanks dimensioning 153
Table 37 800 kWe PEMFC specifications 159
Table 38 Volumes and weights comparison 164
Table 39 Efficiency comparison 166
Table 40 Economic comparison 168
Table 41 LCOE evaluation for the studied technologies 170

Table 42 Thermal and Electrical load profile for warm and cold external ambient, overall cruise ship 171
Table 43 Thermal and Electrical load profile for warm and cold external ambient, ZG 1 .. 172
Table 44 Thermal and Electrical load profile for warm and cold external ambient, ZG 2 .. 173
Table 45 Thermal and Electrical load profile for warm and cold external ambient, ZG 3 .. 174
Table 46 W-ECoMP input data for mGT simulations 175
Table 47 Electrical and thermal management of mGTs in the three different ZGs 176
Table 48 mGT ON/OFFs on a monthly basis 179
Table 49 Partial Loads and efficiency of mGTs for each ZG in a cold ambient (in descending order) 179
Table 50 Electrical and thermal management of mGTs in the three different ZGs in warm ambient 182
Table 51 mGT ON/OFFs on a monthly basis, warm ambient 184
Table 52 Partial Loads and efficiency of mGTs for each ZG in a warm ambient (in descending order) 185
Table 53 Economic data 187
Table 54 Cold ambient weekly costs per ZGs 187
Table 55 Warm ambient weekly costs per ZGs 188
Table 56 Costs and fuel consumptions on a yearly basis for the whole cruise ship 189
Table 57 W-ECoMP input data for mGT simulations 190
Table 58 Electrical and thermal management of PEMFCs in the three different ZGs in cold ambient 191
Table 59 PEMFCs ON/OFFs on a monthly basis, cold ambient 193
Table 60 Partial Loads and efficiency of PEMFCs for each ZG in a cold ambient (in descending order) 193
Table 61 Electrical and thermal management of PEMFCs in the three different ZGs in warm ambient 196
Table 62 PEMFCs ON/OFFs on a monthly basis, warm ambient 198
Table 63 Partial Loads and efficiency of PEMFCs for each ZG in a warm ambient (in descending order) 199
Table 64 Economic hypothesis 201
Table 65 Cold ambient weekly costs per ZGs 201
Table 66 Warm ambient weekly costs per ZGs 202
Table 67 Costs and fuel consumptions on a yearly basis for the whole cruise ship 203
Table 68 Boiler consumption, costs and emissions with PEMFC application 204
Table 69 Electrical and thermal management of Hybrid solution in ZG 4 in cold ambient . 205
Table 70 Partial Loads and efficiency for PEMFCs and mGTs in ZG 3, cold ambient 206
Table 71 Costs and fuel consumptions on a yearly basis for the whole cruise ship, Hybrid solution 207
Table 72 Boiler consumption, costs and emissions with Hybrid application 207
Table 73 Different technologies comparison (in brackets the data including the use of the boiler) 207
Table 74 LCOE of the considered technologies 208
Table 75 Containers for storage system 218
Table 76 Costa Diadema Technical Data 222
Table 77 HELM Database validation on GEI Data 229

Nomenclature

ATO	Antimony Tin Oxide
BoP	Balance of Plant
CCGT	Combined-Cycle Gas Turbine
CH_2	Compressed Hydrogen
CHP	Combined Heat and Power
COP	Coefficient Of Performance
CSP	Concentrated Solar Power
DER	Distributed Energy Resources
DG	Distributed Generation
DHN	District Heating Network
DHW	Domestic Hot Water
EB	Energy Balance
ECA	Emission Control Area
EES	Energy Storage System
EV	Electric Vehicles
FC	Fuel Cell
FO	Fuel Oil
GHG	Green House Gases
HEX	Heat Exchanger
HFO	Heavy Fuel Oil
HP	Heat Pump
HT	High Temperature
HV	High Voltage
ICE	Internal Combustion Engine
IMO	International Maritime Organization
LCOE	Levelized Cost of Electricity
LCOH	Levelized Cost of Heat
LH_2	Liquid Hydrogen
LHV	Lower Heating Value
LNG	Liquid Natural Gas
LT	Low Temperature
LV	Low Voltage
MCFC	Molten Carbonate Fuel Cell
MEA	Membrane Electrode Assembly
mGT	micro Gas Turbine
MIMO	Multi Input Multi Output
MDO	Marine Diesel Oil
MFO	Marine Fuel Oil
MGO	Marine Gas Oil
MPC	Model Predictive Control
MSD	Market for Dispatching Service

MV	Medium Voltage
MVZ	Main Vertical Zone
NECA	NOx Emission Control Area
NG	Natural Gas
NIR	Near InfraRed
PAFC	Phosphoric Acid Fuel Cell
PEMFC	Polymer Electrolyte Membrane Fuel Cell
PI	Proportional-Integrative
PID	Proportional Integrative Derivative
PV	PhotoVoltaic
RES	Renewable Energy Sources
SECA	Sulphur Emission Control Area
SG	Smart Grid
SISO	Single Input and a Single Output
SoA	State of the Art
SOFC	Solid Oxide Fuel Cell
SPM	Smart Polygernetation Microgrid
TES	Thermal Energy Storage
TRL	Technology Readiness Level
ZG	Zonal Group

Symbols

A_{panel}	[m^2]	Panel Surface
β	-	Pressure Ratio
C	[kJ/K]	Thermal Capacity
$c_{p_{H2O}}$	[kJ/kgK]	Water Specific Heat
$c_{p_{sink}}$	[kJ/kgK]	DHN circuit Fluid Specific Heat
$c_{p_{source}}$	[kJ/kgK]	ENVISION Panels circuit Fluid Specific Heat
Dhi	[W/ m^2]	Direct Solar Radiation horizontal surface
$Delta_{TML,Eva}$	-	Temperature Logarithmic Difference in Heat Pump Evaporator
$Delta_{TML,Cond}$	-	Temperature Logarithmic Difference in Heat Pump Condenser
λ	[m]	Heat-Exchanger two-phases region length
$\dot{m}_{H2O}$	[kg/s]	Water Mass flow rate
$\dot{m}_{sink}$	[kg/s]	Connection to DHN Water Mass flow rate
$\dot{m}_{source}$	[kg/s]	ENVISION Panels circuit Mass flow rate
$\dot{m}_{workingFluid}$	[kg/s]	Heat Pump working fluid Mass flow rate
η_{comp}	-	Heat Pump compressor efficiency
G	[kW/ m^2]	Solar Radiation
Ghi	[W/ m^2]	Global Solar Radiation horizontal surface
h	[kJ/kg]	Enthalpy
P_{el}	[kW]	Heat Pump electric consumption
p_{cond}	[bar]	Heat Pump condenser pressure
p_{eva}	[bar]	Heat Pump evaporator pressure
Q_{cond}	[kW]	Heat produced by HP (in the condenser)
Q_{eva}	[kW]	Heat absorbed by HP (in the evaporator)
$Q_{lossesWind}$	[kW]	Thermal losses due to wind presence
Q_{panel}	[kW]	Heat produced by ENVISION Panel
$T_{ambient}$	[K]	Ambient Temperature
$T_{avg_{panel}}$	[K]	Average Panel temperature
ΔT_{cond}	[K]	Outlet-Inlet water temperature in condenser
T_{cond}	[K]	Heat pump Condenser temperature
T_{eva}	[K]	Heat pump Evaporator temperature
$T_{sink,in}$	[K]	Return temperature from the DHN
$T_{sink,out}$	[K]	Outlet temperature to the DHN
$T_{source,in}$	[K]	Temperature from the panels
$T_{source,out}$	[K]	Return temperature to the panels
$u_{WindVelocity}$	[m/s]	Wind Velocity
U	kW/(m^{2}K)	Global Heat Exchange Coefficient
U_b	kW/(m^{2}K)	Global Heat Exchange Coefficient, two phases region
U_s	kW/(m^{2}K)	Global Heat Exchange Coefficient, single phase region

Abstract

This thesis is focused on the analysis of distributed generation potential and drawbacks in different scenarios. The analysis is divided into three main chapters with the aim of describing the technical and normative framework that regulates the distributed generation application, before moving in the detail of two different applications: a residential and a maritime one. The use of micro Gas Turbines is one of the most promising solutions towards the large diffusion of distributed generation of both thermal and electric energy, anyway, it is worth to mention also other technologies such as Renewables, Fuel Cells and Internal Combustion Engines.

The residential application is developed within the H2020 Envision project that aims to foster the transition to positive energy buildings increasing the active surfaces for energy production for solar radiation. In this context, the University of Genoa is responsible for one of the two main demosites, where Envision technologies are tested in interaction with a Smart Polygeneration Microgrid. To do that, a detailed study of the thermo-economic performances of the involved technologies has been developed in order to proper dimension and design the demosite components. In particular, it has been necessary to model and analyse the performance of thermal solar façade panels connected to a Heat Pump, with the aim of evaluating the best configuration of the system and its proper management in interconnection with a District Heating Network. Furthermore, the presence of a micro Gas Turbine, to provide also electric energy, requires more detailed management of the system obtained through a thermo-economic analysis that gives the basis for the tuning of a Model Predictive Control through the experimental campaign. Furthermore, the results obtained from a preliminary test campaign for analysing the impact of insulation on the back of a panel are reported in the conclusion of this section. The overall activities represent a strong and solid basis on which rely during the experimental campaign, in terms of configuration, installation and control of the system.

The second application of distributed generation presented in this work refers to a maritime scenario. In this context, a detailed study has been developed in order to understand if the use of micro Gas Turbines and/or PEM Fuel Cells is suitable for Distributed Generation on board of cruise ship. In particular, taking into account the application, the choice of the best solution has to consider not only energetic performances but also aspects related to volumes and weights that could affect the available payload of the vessel. To do that, a steady-state analysis has been developed, in detail, with the scope of analysing and comparing the different solutions in terms of economy, energy and dimensions. After that, a deeper study has been performed in a time-variant scenario, where it has been considered the proper management of the system. This analysis highlights the promising performances of PEM Fuel Cells at partial load, while on the other hand, the mGTs show better behaviour in a CHP application. All those aspects have been considered, evaluating also the performances in terms of emissions for the considered technologies when compared to Internal combustion engines fuelled by LNG. This activity has been the first step towards the development of a

comparison tool, HELM, that is able to compare different energy generation solutions for maritime application depending on the considered scenario, suggesting which can be the most suitable solution taking into account the relevance of the main evaluation categories: volumes, weights, costs and emissions.

1 Distributed Generation: an introduction

Decarbonisation and technological development are increasing reliance on renewable technologies, primarily variable weather-dependent resources such as wind and solar. Looking at Figure 1, reporting the share of renewables in power generation considering the European Sustainable Development Scenario, we can state that a huge increase of this share is expected in the upcoming 10 years, moving from a value of 28% to almost 50%. Among Renewable Energy Sources (RES), the largest increase is linked to solar energy. Figure 2 underlines this aspect, showing the evolution of the energy share, in terms of the total amount of energy per year, supplied by RES considering the contribution of different typologies. The Hydropower source (violet one) is the already most exploited among RES, while wind and solar energy (orange and yellow ones) still have a huge potential to be used.

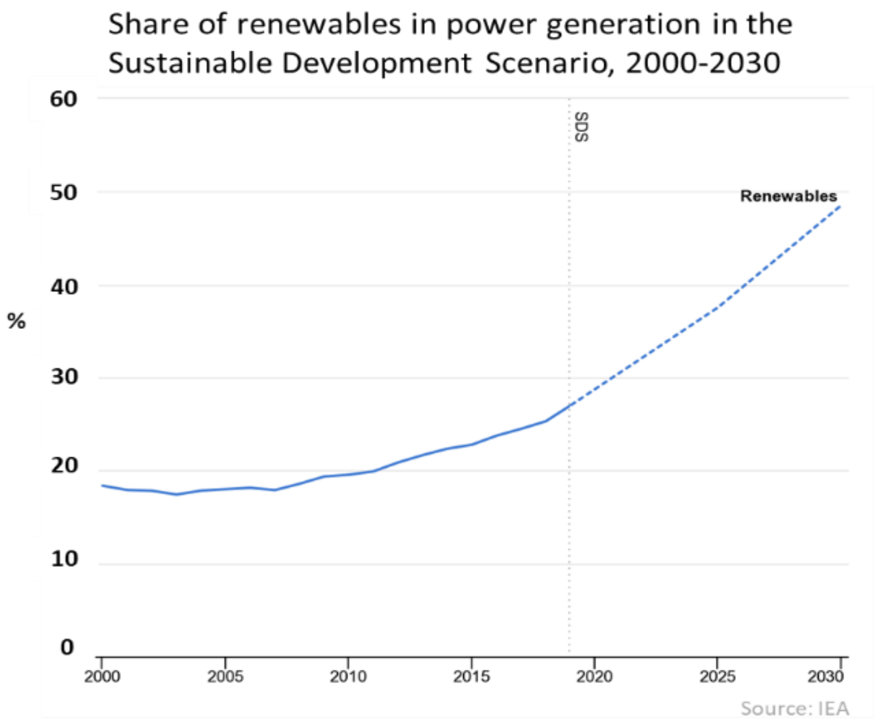

Figure 1 Share of renewables in power generation in the Sustainable Development Scenario [1]

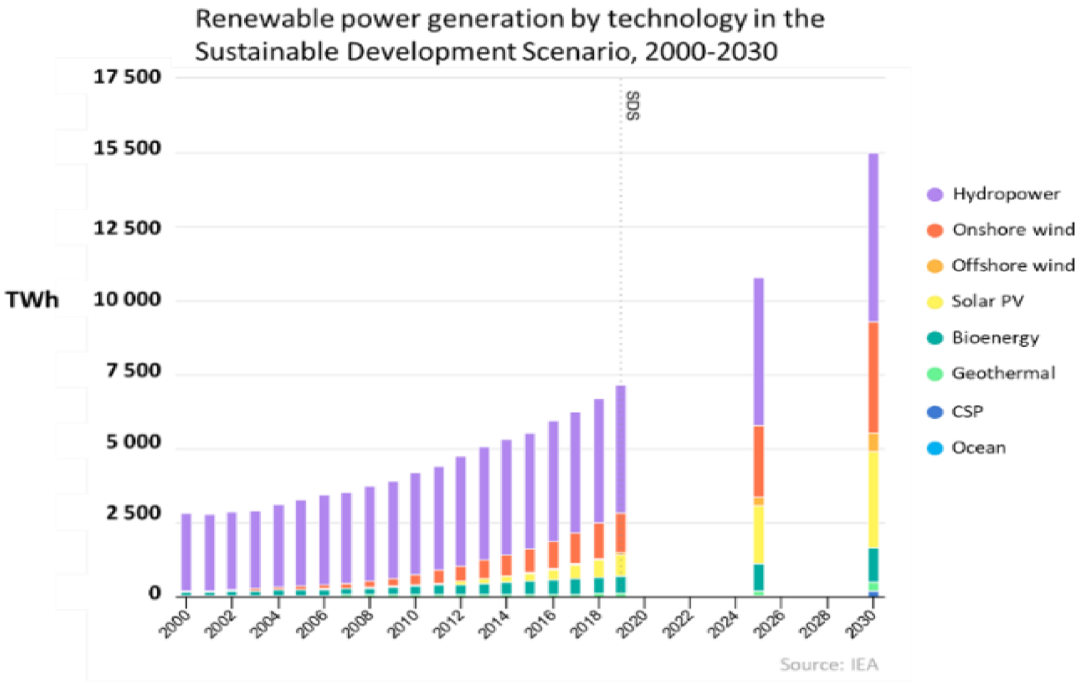

Figure 2 Renewable power generation by technology in the Sustainable Development Scenario [2]

Power systems are indeed facing relevant changes due to the increasing shares of variable RES; this leads to a larger request for flexibility. On the other hand, the consequent decrease of traditional sources supply deprives the power system from their programmable and flexible contribution.

From this scenario irrupt Distributed Energy Resources (DERs), a diverse array of technologies including gas-fired distributed generation, solar photovoltaics (PVs), small- and medium-sized wind farms, electric vehicles, energy storage, and demand-side management. These DERs, unlike traditional centralized units, are characterized by their small capacities (from 5 kW up to 300 MW), their diverse nature (generation, storage, responsive demand, or any combination thereof), and their connection to electricity distribution grids (centralized power unit are usually connected to transmission network). DERs, if properly integrated, may have the potential to deliver not only the valuable electricity services that are traditionally provided by centralized generating units, but also new services enabled by their distributed nature [3].

Therefore, the community has to face the end of the so-called “Trickling down” paradigm [3]. This name refers to the scenario where we have been living under for more than a century: large power plants inject power into the transmission network via step-up transformers (400 kV and/or 275 kV); that power, covering long distances in transmission lines, is brought by step-down transformers in substations to lower voltages into the meshed high-voltage distribution network (130 kV). Then, other transformers in smaller substations bring the power to lower voltages in the medium-voltage distribution grid (33 kV and/or 11 kV). Finally, the so-called distribution transformers, located in special-purpose poles in the streets or hidden in large buildings or underground, bring power to the consumers located nearby (380V or 240V). Figure 3 shows schematically this traditional power system paradigm.

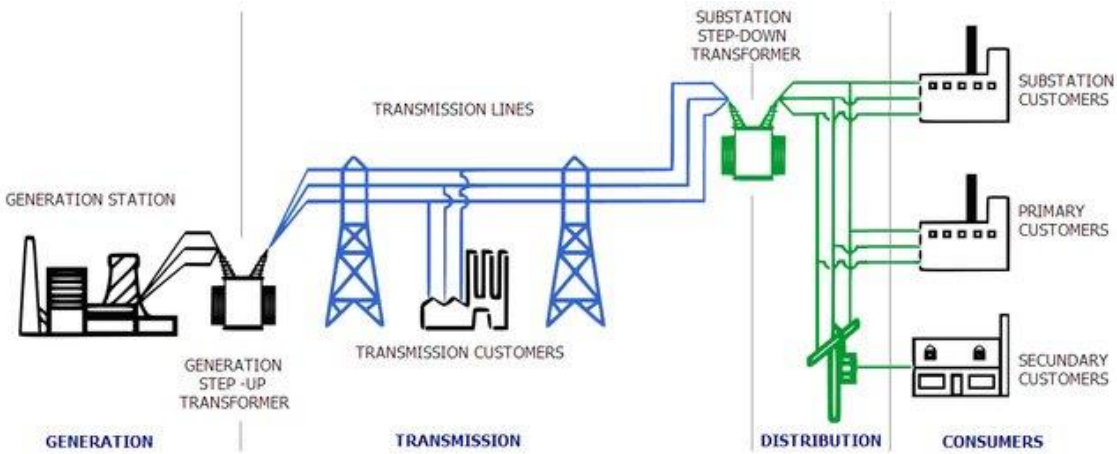

Figure 3 "Trickling down" paradigm

Electrical distribution grids were traditionally designed as 'passive' networks, containing mainly loads. In such power systems, power flows uni-directionally, from the high voltage transmission grid to the loads in the lower voltage levels of the system. The cited penetration levels of DER transform distribution grids to 'active' systems which, together with loads, contain high shares of generators and energy storage devices. This new system structure implies bi-directional power flows between distribution and transmission systems; indeed, distribution grids will be responsible for the power export in periods when local generation exceeds consumption. This evolution brings higher complexity in the management of distribution systems, but also open to new possibilities in the optimisation of the overall system by allowing distribution systems to participate actively in the system operation and by allowing DER to participate actively in the distribution system management [4]. In many countries, renewables generation units could be located in a particular exploitable area (such as Solar Energy in the South of Italy, Figure 4). It is then possible to have the majority of the electricity generation located at the lower voltage levels of the distribution network in a specific part of the country, while the power demand is more uniformly located in the territory (as reported for the Italian case in Figure 5). This scenario leads to substantial power flows with large potential impacts at all voltage levels. Indeed, these flows could impact a country's transmission system and interconnections with neighbouring systems.

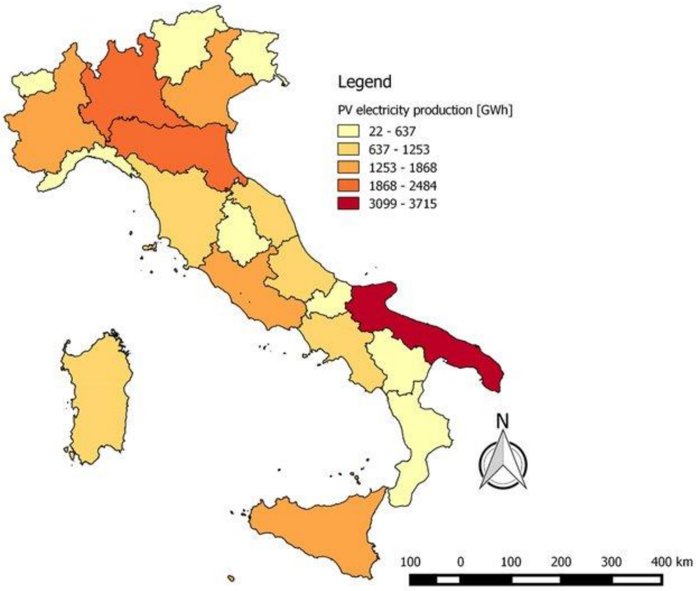

Figure 4 PV electricity production in Italy [5]

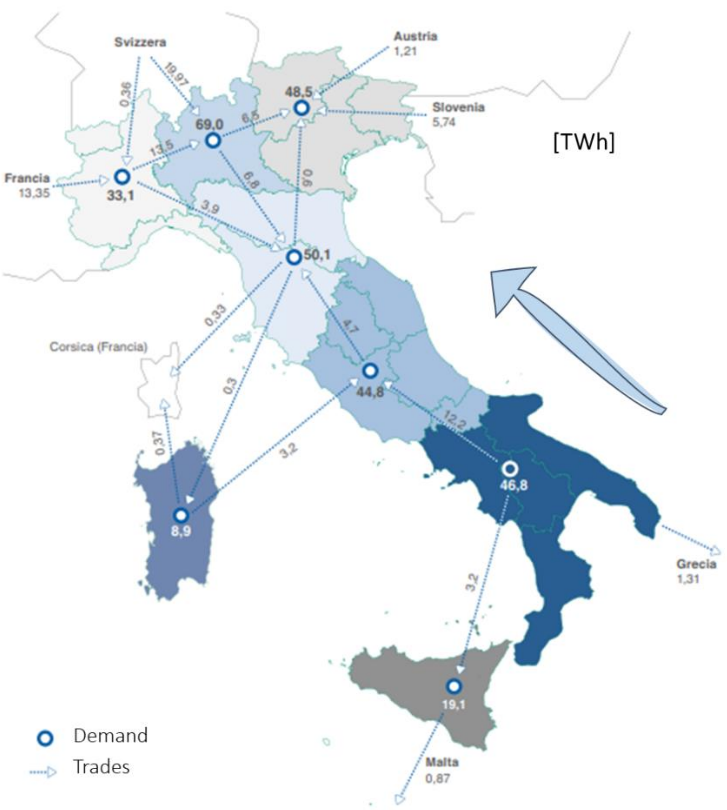

Figure 5 Energy Flows in 2017 [6]

Generally speaking, the architecture of the energy system is to be approached in a new way of thinking, where the old strict boundaries among users and producers, transmission and distribution become more blurry. A big effort is therefore needed in terms of policies and regulations in this future grid concept. European Countries are working in order to adapt and upgrade the regulatory framework with the vision of a future where RES and Distributed Generation will have a major role.

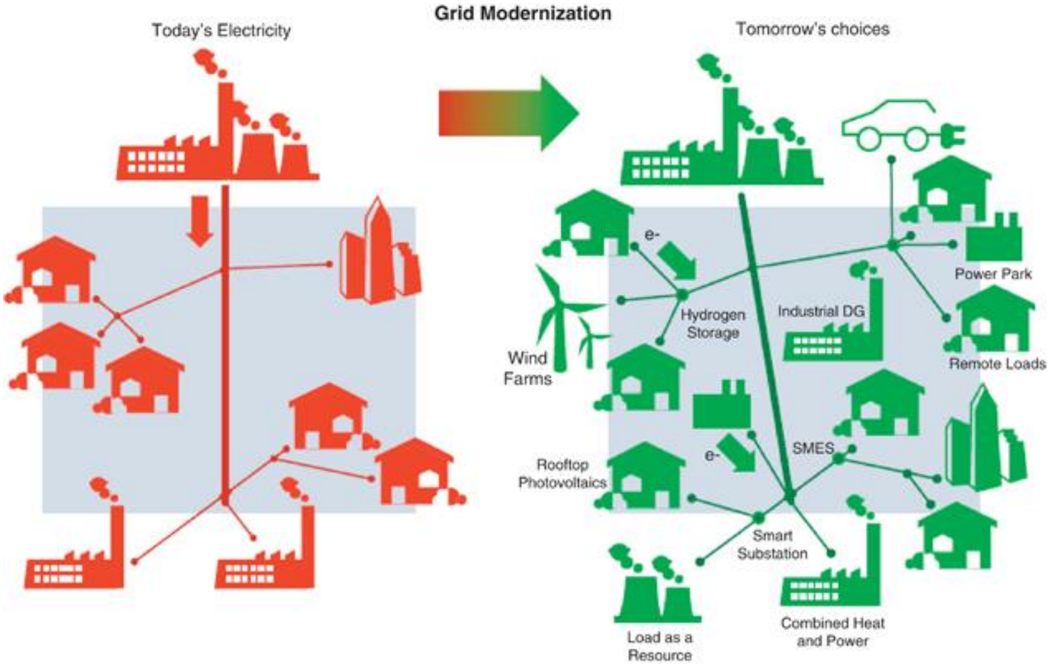

Figure 6 Energy system transition scheme [5]

1.1 Italian energy policies

Energy policies are established interacting between several, possibly conflicting, targets. The security of demand-supply will always be the first key target in any energy policy, although the emphasis on supply security can differ over time and geographies depending on different factors. In the last decades, energy policies have focused also on the limitation of the negative environmental impact related to energy production and transmissions. The type of environmental problems addressed has shifted over time, moving from local pollution to a more global perspective emphasized by the climate change problem. The third target relates to cost minimization, aiming to supply energy in a cost-efficient way. Talking about this economic aspect, the regulation authorities sometimes focus a bit narrower, with a strong emphasis on e.g. low prices and industrial competitiveness, which is not necessarily the same thing as an economic efficient supply [4].

A particular focus on the Italian context is developed in this section, detailing the regulatory framework on what the Italian legislator is working to face the cited changes and to track the environmental sustainability objectives. It is worth underlining that most of the directives implemented at National level are developed in compliance with European Union guidelines.

1.1.1 Incentives and policies direction

The Italian electricity sector is evolving rapidly owing to the effects of the profound energy transition, focused on achieving sustainability goals and improving system security. The most significant elements of the new model are the integration and management of renewable energy, energy efficiency, grid digitalisation and storage systems. A brief description of the evolution of Italian policies in towards the target of pollutant reduction is here presented.

To promote and increase the use of renewable energy sources in **electricity production** and to create demand for electricity from renewable energy sources, the Italian government introduced in 1999 an annual obligation for electricity producers and importers to input a minimum quota of energy produced using renewable energy sources into the national electricity system. This quota was equal to 2% of the electrical energy produced or imported from non-renewable sources in the previous year, in excess of 100 GWh/year. An energy operator could discharge its obligation by either producing the entire minimum quantity of energy from renewable sources by itself or by purchasing the whole or part of an equivalent amount, or the related rights (green certificates), from other producers. Green Certificates evidence the renewable attributes of the electricity generated. From 1 January 2016, Green Certificates were replaced by a feed-in premium mechanism known as GRIN. The new mechanism guarantees the payment of a tariff by the GSE (Gestore Servizi Energetici) on the net production of energy.

In 2005, an incentive system specifically dedicated to solar photovoltaic plants, known as Conto Energia, was introduced. Conto Energia consisted of the payment of fixed incentive tariffs for 20 years starting from the date of entry into operation of the relevant photovoltaic plant (depending upon the capacity of the plant and the level of integration of the plant). Conto Energia is no longer in place for new photovoltaic plants because the budget was reached in July 2013. Projects aimed at increasing energy efficiency may be eligible to obtain White Certificates (also known as energy efficiency certificates). White Certificates are tradable instruments that give proof-of-end-use energy savings. The scheme aims at supporting the production of thermal energy from renewables and high-performance cogeneration units as well as small-scale interventions of energy efficiency for private persons and the public administration.

A simplified sale and purchase arrangement are other tools offered by the GSE under which producers are paid a minimum guaranteed price for every kWh. Producers with small-sized plants and a nominal electrical capacity up to 1 MW may benefit from this scheme for the first 2 million kWh per year fed into the grid, with the possibility of receiving more if the hourly zonal prices prove to be more advantageous.

Through the net metering service, producers or users may feed into the grid the electricity that they generate on-site, but do not consume immediately, and take from the grid part or all of the electricity that they need at a different time. This system applies to renewable energy plants having a capacity up to 200kW commissioned after 31 December 2007 and to high efficiency combined heat and power plants with a capacity up to 200 kW. Under this service, the producer receives a yearly net metering contribution from GSE. This contribution refunds the producer or user for part of the costs incurred for importing electricity from the grid. The energy produced by renewable energy plants has interconnection and dispatch priority. Moreover, the national Transmission System Operator (Terna) and the operators of the local distribution grids, have the obligation to connect every plant that makes a connection request to the grids that they operate. A request to be connected to the power grid can be filled before the construction of the plant is completed, or even started, because no time limit is set as to how long before the start of operations the request can be filed. The request to be connected to the power grid must be filed with either the operator of the local distribution grid if the capacity requested is below 10 GW, or Terna, if the capacity requested is equal to or more than 10 GW.

In 2017, the Italian government approved the National Energy Strategy setting out future policy goals for the electricity sector. The objective is to make the national energy system more competitive, sustainable and secure. Italy has already achieved its 2020 renewable energy targets, with energy from renewable energy sources accounting for 17.5 % of total energy consumption in 2015, in comparison with the 17 % target to be reached by 2020. The main new priority goals, included in PNIEC 2018, are set as follows [7]:

- to achieve the target of a 30% share of renewable energy sources on total energy consumption by 2030;
- to foster low energy-consumption initiatives having the best cost/benefit ratio, to achieve 32.5% of energy savings by 2030 and give impetus to the Italian energy efficiency industry (e.g., construction of energy-efficient buildings and installation of energy-efficient facilities);
- to speed up the decarbonisation of the energy system, starting from the use of coal in power generation, and to introduce progressive measures spanning the entire energy process, thereby achieving significant environmental and health benefits, and contributing to the attainment of European targets;
- to launch the capacity market to guarantee system adequacy, maintaining the necessary gas-fired capacity (with priority to flexible capacity) and integrating new resources into the market (e.g., cross-border renewable-energy power-generating units, storage systems, active demand-side management), further strengthening interconnections with neighbouring countries, increasing the capacity of storage systems, implementing grid projects to integrate renewables, and increase the resilience of the system;
- to decrease primary consumption of oil products by 13.5 Mtoe by 2030 when compared with 2015 levels;
- to double investments in clean-energy research and development, from €222 million in 2013 to €44 million in 2021.

The objectives of the Italian energy policy up to 2030, set precisely by the SEN (Strategia Energetica Nazionale; National Energy Strategy) 2017 [8], provide for significant development of Renewable Energy Sources (RES) and Distributed Generation with an expected integration of about 35-40 GW of new photovoltaic plants, mainly attested at the level of distribution networks. This to reach, in 2030, 70 TWh of electricity from photovoltaic plants (+180% compared to 2017), or 39% of the entire gross production of electricity from renewable sources (equal to 184 TWh). It is clear that, for the reasons set out above, the adjustment of the distribution networks becomes crucial to accommodate the significant increase in estimated Distributed Generation (about additional 3GWh/year by photovoltaics alone). With the Legislative Decree no. 28 of 3 March 2011, the authority highlighted the vision to incentivize distributed generation towards digitalization, providing that [9]:

- "Electricity distributors that carry out modernization works according to smart grid concepts are entitled to a higher return on invested capital for the distribution service, limited to the above-mentioned modernization works " (article 18, paragraph 1)
- Smart grid interventions "consist primarily of systems for the control, regulation and management of loads and production units, including electric car charging systems".

Decree-Law no. 34 of 30 April 2019 (Growth Decree-Law) [10] established a contribution in favour of municipalities, up to a maximum of € 500 million for the year 2019 from the Development and Cohesion Fund (FSC) for interventions related to investments in the field of energy efficiency and sustainable territorial development. The contributions referred are intended for public works in the field of:

- energy efficiency, including public lighting, energy saving in public buildings and public housing, and the installation of installations for the production of energy from renewable sources;
- sustainable territorial development, including work on sustainable mobility, adaptation and safety of schools, public buildings and municipal heritage and the removal of architectural barriers.

Starting from the year 2020, for the above-mentioned projects, the Growth Decree-Law has authorized the implementation of a multi-year funding program, whose actual resources are distributed among municipalities with a population of fewer than 1,000 inhabitants, assigning to each municipality a contribution of an equal amount.

The effort of Italian regulations focuses also on **buildings**, in order to promote and enhance the presence of Renewable Energy System and also reducing the energy consumptions. With the Annex 3 of Legislative Decree 28/2011 [9] are identified obligations for the integration of renewable sources in new buildings or buildings undergoing a major renovation, in force since 31 May 2012. These obligations are currently established in terms of percentage shares (increasing over the years) of the supply with renewable sources of the energy needs of the building for the provision of heating, cooling and hot water services. In particular, it is foreseen that in the case of new buildings or buildings undergoing major renovations, the thermal energy production systems must be designed and built in such a way as to ensure simultaneous compliance with the supply, through the use of energy produced by systems powered by renewable sources, of 50% of the expected consumption of domestic hot water and the following percentages of the sum of the expected consumption of domestic hot water, heating and cooling:

- 20% when the application for the relevant building title is submitted from 31 May 2012 to 31 December 2013;
- 35% when the application for the relevant building permit is submitted from 1 January 2014 to 31 December 2016;
- 50% when the application for the relevant building permit is issued from 1 January 2017 (then extended to 2018).

Regarding situations where it is technically impossible to comply with the obligations to reach the energy requirements of buildings subject to first level renovation, the possibility of a procedure for the installation of the mandatory quota by the owner on another building, even if not owned by the owner, or transfer to the local authority that can accumulate them in order to reach quotas suitable for interventions on public buildings is assessed.

Considering the ambitious goals set by the National Energy Strategy in 2017 [8], incentives on **electric vehicles** (EV) result fundamental to encourage their development. Indeed, the state of the art of electric vehicle charging station in Italy is [11]:

- 420 EV public charging stations installed in 60 provinces (out of these 300 are installed by ENEL); Quick/Slow charging (3 KW and 22 KW) and fast charging (43 KW) have been developed
- Fast charging stations (AC 43 KW and DC 50 KW) under test (to be initially used in gasoline filling station);
- 2500 EVs introduced in 2012 (mostly light-duty quadricycles);
- Agreements with regions and municipalities to foster electric mobility (infrastructure);
- Focus on interoperability between energy operators.

The Law 190/2014 (art.1 comma 232) [12] sets a gradual ban on the circulation of category M2 and M3 motor vehicles fuelled with petrol and diesel (Euro 0) from 1 January 2019 and provision for a ban on the circulation of category M2 and M3 motor vehicles fuelled with petrol and diesel (Euro 0 and Euro 1) in-service contracts from 1 January 2018. In the 2017 Stability Law, the Government launched a substantial financing plan for the renewal of the road rolling stock used for Local Public Transport for the period 2019-2033. These include electric and natural gas buses for the integration and replacement of the existing bus fleet. During discussions with Regions and local authorities, it was also decided to proceed with the establishment of an interinstitutional political table for discussion and consultation on transport, composed of the Ministries of Infrastructure, Economic Development and Environment, as well as Regions and local authorities. It is proposed to accelerate the provisions of paragraph 10 of Article 18 of the Legislative Decree 257/2016 [13] providing that public administrations, bodies and institutions dependent or controlled by them, Regions, local authorities and utilities for activities carried out in provinces with high PM10 particulate matter pollution, at the time of replacement of their car fleet, buses and public utility vehicles, including those for municipal waste collection, are required to purchase at least 30% by 2022, 50% by 2025 and 85% by 2030 of electric and hybrid vehicles with external charging, methane and hydrogen, and electric or methane in the case of buses. The first measures in this sense have already been introduced, with effect from March 2019 to December 2021, and consist in granting a contribution to those who purchase a vehicle with CO2 emissions of less than 70 g/km and an official price of less than €50,000. The contribution is differentiated by emission classes (0-20 g/km and 21-70 g/km) and depending on whether or not a vehicle approved in classes from Euro 1 to Euro 4 is scrapped, and ranges from €1,500 to €6,000. The same law provides for the experimentation of innovative means of transport for personal mobility with mainly electric propulsion, such as segways, hoverboards and scooters. On the other hand, the law provides, for the same period, the payment of a tax for the purchase of M1 category vehicles, if the CO2 emissions are higher than 160 g/km. The tax varies from €1,100 to €2,500 depending on emissions. In addition, the Decree-Law n.34 of April 2019 (Growth Decree-Law)[10] established that those who, in 2019, purchase, also under the financial lease, and register in Italy a brand new electric or hybrid vehicle of categories L1e, L2e, L3e, L4e, L5e, L6e and L7e and who deliver a vehicle for scrapping are entitled to a contribution equal to 30% of the purchase price, up to a maximum of 3,000 € if the vehicle delivered for scrapping is in the Euro 0, 1, 2 or 3 category.

In the last decades, the regulator approach for the introduction of innovative solutions in the system is to precede a stage experimental to the regulation phase at full throttle. A key element of the "pilot projects" is to carry out tests on real and limited cases. A list of experiences of regulation through "pilot project" is here reported [14]:

- smart grid (Deliberation ARG/ elt 39 10)
- electric mobility (Deliberation ARG/ elt 242 10)
- storage systems (Deliberation ARG/ elt 199 11)
- participation of distributed generation in the MSD, Market for Dispatching Service (Deliberation 300/2017/ eel)

The approach chosen by the Italian legislator to test the experiences of regulation in a really limited environment (pilot projects) before issuing general measures, has certainly made it possible to effectively frame intervention actions to implement a gradual demarcation of electricity networks. Nevertheless, the process of "smartization", involving multiple subjects with different interests, makes difficult the identification of a single business model for all the actors involved. This process still presents many critical points that require the intervention of the regulator both in technical and social acceptability [15]. Concerning the technical criticalities, the studies carried out have shown that, although the technological solutions (e.g. communication devices, sensors, etc.) are generally available and mature in their sector of reference (e.g. ICT), they are not always effectively interoperable and therefore cannot be easily integrated into Smart Grids due to lack of homogeneity or languages and mechanisms of communication and cooperation [15]. Of a different nature from the previous point, but equally relevant to concretely promote the "smartization" of current electricity networks, is the criticality related to social acceptability. The implementation of smart networks requires the active involvement of end consumers who must accept a new way of energy management based on sharing their data and consumption habits. Only after a detailed consumption profiling, for example, will the distribution companies, or third-party companies involved in the management of the SG, be able to implement management logics optimised and propose customer-specific participation mechanisms or charging systems. On the other hand, it is easy to see that consumer willingness to participate will be highly dependent on an effective understanding of both the economic and environmental benefits of active participation. Therefore, regulatory interventions aimed at defining possible incentive mechanisms for participation and national communication campaigns will certainly be fundamental tools for the success of Smart Grids (SG) projects. In this scenario, the promotion of social acceptability passes through:

1. regulatory interventions aimed at defining possible mechanisms to encourage participation;
2. communication campaigns aimed at illustrating the usefulness of active participation in SG projects;
3. search for technological solutions that enable a user-friendly way of participation (e.g. through apps or Web-oriented tools now widely used in other sectors).

1.1.2 Grid connection limits and regulations

As described in the previous sections, the deeper presence of Distributed Generation systems requires more flexibility in the grid system, to do that smart management of the network is required. Currently, in Italy, 100% of HV/MV substations (>2000) and only 25% of MV/LV Secondary Substations (>100.000 MV/LV SubStations) are remotely controlled [11]. Several thousand pole-top MV switches are remotely controlled and few installations of remote control of LV breakers are present.
Other important technical aspects are related to grid connection. The presence of distributed generation mostly connected to the distribution grid could change the connection methods; therefore, a clear vision on the Italian grid connection standards is presented. The current Italian regulations on grid connection standards, for all voltage levels, are subject to the approval of the Regulatory Authority for Energy, Networks and Environment (ARERA). The connection of users to the Transmission Networks, in particular, is subject to the requirements of the so-called “Grid Code”, which is issued by the Italian Transmission System Operator (TERNA), with the approval of ARERA. The connection of users to the Medium Voltage and Low Voltage Distribution Networks is instead subject to the prescriptions of the CEI regulations. In particular:

- Technical standard CEI 0-16 is the reference for the connection of active and passive users to the HV and MV networks of electricity distribution companies;
- Technical standard CEI 0-21 establishes the modalities for the connection of active and passive users to the LV networks of electricity distribution undertakings.

Considering grid connection, it is relevant to understand also the role of **storage systems** in order to clarify in which regulation context have to refer. A storage system is considered to be a production plant (or generation group of a plant) powered by non-renewable sources

[16]. As a transitional measure, the procedural and economic conditions for high-efficiency cogeneration plants shall apply. From the point of view of the connection to the grid with the Deliberation 642/2014/R/eel [17], it has been established that the technical requirements of V1 to the 3rd edition of CEI 0-16 and V1 to the 2nd edition of CEI 0-21 must be obligatorily met by all storage systems. A storage system is defined as a set of devices, equipment and management and control logic, functional to absorb and release electricity, designed to operate continuously in parallel with the grid with the obligation to connect third parties or capable of causing an alteration of the exchange profiles with the electricity grid (input and/or withdrawal). The storage system may or may not be integrated with a production plant (if any). This does not include systems used in emergency conditions which, therefore, only come into operation when the power supply from the electricity grid is interrupted for reasons beyond the control of the person who has the availability.

Within grid connection regulations, there are also relevant aspects related to **grid services** that the different producers connected to the grid could or must provide. These services have always been peculiar of programmable energy producers; but considering the increasing share of non-programmable energy producers, the need for a reassessment of the regulatory aspects related to grid services becomes evident. In particular including also non-programmable producers in the group of suppliers for these fundamental services. At the beginning of 2010, only for high power wind plants (connected to TSO) and for the new construction ones, became mandatory the provision of some automatic grid services, including the reduction of power in case of need (service previously provided only by the larger programmable plants) [18]. The observability of production has also been extended, every 4 seconds by Terna, as already foreseen for larger programmable plants. This contributes to reducing the reserve margins that must be supplied for the safety of the electrical system [18].

Then, from 2012 to 2015, also for distributed generation units has been planned the obligatory provision of some grid services. Among these, the mandatory installation, on systems that have been in operation since 1 April 2013 and on existing installations with an installed power higher than 6 kW, of devices (inverters, where provided, and interface protection devices) with the aim of preventing the disconnection of plants as long as the grid frequency remains in the range of 47.5-51.5 Hz (as the largest plants), rather than the previous range of 49.7-50.3 Hz, avoiding the safety problems caused by the sudden shutdowns of the small generation systems, currently no longer negligible [18]. This aspect, therefore, increases the responsibility of distributed generation units in the grid frequency maintaining. Furthermore, for all wind and photovoltaic systems (including existing ones) connected to medium voltage networks and having a power equal to or greater than 100 kW, has been set mandatory the installation of disconnection systems to be used to guarantee the safety and grid stability (generally the production from RES is privileged but there are cases where disconnections are needed, e.g. very significant low demands).

In parallel, in order to reduce the gap between RES and programmable sources, it has been tried to promote better forecasts of the electric energy introduced in the grid. Then it is possible to extend the discipline of the grid imbalances also to the not programmable RES. This contributes to reducing the reservoir margins that must be supplied for the safety of the electric system, avoiding that the costs due to the lack of predictability affect only the general consumers.

Recently, the opening of MSD (Market for Dispatching Service) to demand, non-programmable renewable sources and distributed generation (including storages) by increasing the availability of resources for ancillary services (also called flexibility resources), was initiated through pilot projects in 2017, with deliberation 300/2017/eel [19]. This innovation is particularly relevant in the current context where the system is experiencing a reduction in the number of programmable plants (especially thermoelectric) that have historically provided ancillary services [20].

The ancillary services, related to the Italian regulation are [20]:

- **Frequency control**: it refers to the need to guarantee that the grid frequency is within a specific range of the nominal frequency (50 Hz). A mismatch between electricity generation and demand causes variations in frequency, so control services are required to bring the frequency back to its nominal value and ensure it does not vary out of range. Three different levels of control are present:
    - *Primary operating reserve*: it consists in making available bandwidth of capacity to an automatic regulation device able to modulate the power, both increasing and decreasing, in response to a frequency variation (in Italy, within 15 s for the half band and 30 s for the whole band). Through this resource, it is possible to automatically correct in real-time, for a few seconds, the instantaneous imbalances between total production and requirements total of the entire interconnected European electricity system. The primary reserve must be continuously available and must be distributed within the system electric uniformly (1.5% of the maximum power of the power plant). It represents a fast and short-term action. This level in Italy is a duty for the high programmable power plants (> 10 MW) and therefore, there is no remuneration.
    - *Secondary operating reserve*: it consists in making available bandwidth of capacity to an automatic regulation device able to modulate the power, both increasing and decreasing, on the basis of the level signal received (in Italy within 200 s). The secondary reserve, if necessary, is automatically activated on all previously selected units and has a duration a few minutes. This level of reserve in Italy is provided within the MSD.
    - *Tertiary operating reserve*: it consists in making reserves available with respect to a maximum or minimum power in the scheduling of the enabled units or in the willingness to accept modifications to the enabled unit scheduling for the purpose of constituting tertiary

operating reserve. The tertiary frequency control falls within a number of categories that differ according to the time within which it is supplied and the duration of the supply (in Italy, the tertiary reserve is identified as "ready" when delivered within 15 minutes with a gradient of 50 MW/min for at least 120 minutes, the "rotating reserve" is delivered within 15 minutes for at least 120 minutes and the "replacement reserve" delivered within 120 minutes with a gradient of 0.67 MW/min and without duration limits). This level is provided within MSD.

- *Balancing:* it consists in the activation, in real-time and in order to guarantee the equilibrium between demand and supply, of the supplied tertiary operating reserve. This level is provided within MSD.

- **Voltage control**: consumer loads expect voltage within a certain range, and the regulators require it be within a certain per cent of the nominal voltage. In Italy, this control is a duty for the programmable power plants (> 10 MW). Two levels of voltage control can be considered:
    - *Primary voltage control*: it consists in subordinating the reactive power production of a generation group (or groups belonging to a plant) to an automatic regulation device able to modulate the reactive power supplied by the generation group (or groups) on the basis of the deviation of the voltage at the terminals of the same generation group (or on the HV busbars of the production plant) compared to a reference value.
    - *Secondary voltage control*: it consists in subordinating the reactive power production of the generation groups, belonging to the same plant, to an automatic centralized regulation device able to modulate the reactive power supplied by each of these groups on the basis of the deviation of the voltage on some nodes predefined by the System Operator (pilot nodes).
- **Power grid congestion management:** it belongs to the ex-ante phase, with the aim to provide changes in the scheduled services in order to make them physically feasible. This service is provided within MSD.
- **Load interruptibility:** it consists of the availability by end customers enabled to interrupt the load (for example, in Italy, within 200 ms in case of instant interruptibility). This service is more related to large plants able to supply their loads with their own back-up systems. The remuneration for this service is provided via bi-lateral contracts, with pre-selected users via auctions.
- **Load rejection:** it consists of the service provided by energy production systems able to remain in steady operating conditions when the generation group itself is disconnected from the grid, powering its auxiliary services. Therefore, these systems are able to provide a fast reconnection to the grid, once that the grid problems are

solved. This service is mainly provided as a duty by large power plants appropriately selected in relation to their size and geographic location.

- **Black start**: it consists of the availability of a power generation group to participate in the implementation of the restart plan of the electric system defined and coordinated by the System Operator. This service in Italy is mainly provided as a duty by Hydroelectric system and gas plant.

Another important aspect concerning the grid connection and ancillary services is the so-called "grid Inertia". Indeed, the power plants supplied by RES and equipped with inverter are characterized by low inertia; therefore, in case of a particular issue in the grid, the frequency decreases rapidly. On the other hand, with thermoelectric plants, the presence of rotating masses guarantees intrinsically higher inertia: in this case, the frequency decreases slower than the previous case. This aspect is described in Figure 7.

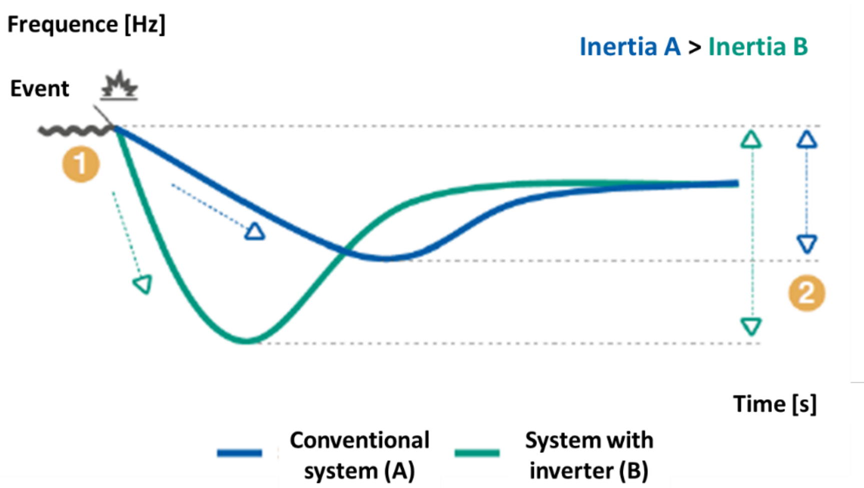

Figure 7 Different grid Inertia for a system with or without inverter [18]

This paragraph was necessary in order to frame the aspects of distributed and innovative generation within a regulatory framework. In the next sections, the focus will be more on the technical and technological aspects of Distributed Generation.

1.2 Distributed Generation Technologies

Distributed Generation is an approach that uses small-scale technologies and renewable energy sources to produce energy where it is most useful: close to the end-user. This guarantees a reduction of costs, boosting reliability with lower environmental impact than traditional methods of power generation. We have grown in a world where giant coal, gas, or hydroelectric power stations generated electricity that was then distributed by a centralised grid. While that worked well enough when demand was limited and predictable, reliability of supply has now emerged as an issue even in many major developed economies because of the demands that an ever-more electrified world places on the grid [21]. Energy security is linked sometimes basically to the diversification of primary energy supplies, while other interpretations connect energy security to the reliability of the electricity system.

Under the first interpretation, the diversification of primary energy supplies (both renewables and not) proper of distributed generation could certainly represent a benefit. Considering the second interpretation, the reflections related to DG possible benefits become more complex. As summarized in [22] IEA (in 2002) stated that distributed generation can contribute to reducing the risks and costs of blackouts. Therefore, in this view, distributed generation is seen as an instrument that leads to the reduction of private costs and risks for electricity customers in case of system failures. On the other hand, CIRED (in 1999) claims that distributed generation does not contribute to system security, but it would have a negative effect. This negative impact on system security occurs when the share of non-dispatchable generation capacity increases. Examples of such units are wind turbines, photovoltaic systems and cogeneration units closely dependent to heat demand. These units cannot be centrally controlled due to the natural variability of their power supply. As a result, there is an increased need to regulate the (back-up) power. This aspect has been treated in detail in the previous section, showing that issues related to the increasing share of non-programmable units in the grid have been and are continuously faced by the Regulatory Authority.

Many different definitions of Distributed Generation can be found, some referring to the size, others refer to the primary energy source or to the close position to an end-users. A clear and concise definition of DG is provided by the European Union in the Deliberation 2009/72/CE [23]: "*Distributed Generation systems are electricity generating plants that are connected to a distribution network rather than the transmission network*". Previously, the Italian Authority had defined and analyzed distributed generation as the set of generation plants with a nominal capacity of less than 10 MVA, taking its bearings from certain regulatory references such as Law no. 239/04 and considering that, historically, plants with a capacity of less than 10 MVA have always been treated as "irrelevant" plants for the purposes of managing the overall electricity system. Anyway, from 2012, also the Italian Authority agreed to the DG definition provided by 2009/72/CE.

Distributed generation refers to a variety of technologies that generate electricity in connection to the distribution grid, such as solar panels and combined heat and power. Distributed generation may serve a single structure, such as a home or business, or it may be part of a microgrid (a smaller grid that is also tied into the larger electricity delivery system), such as at a major industrial facility, a military base, or a large college campus. Therefore, DG can help support the delivery of clean, reliable power to additional customers and reduce electricity losses along transmission and distribution lines [24].

Distributed Generation can have a positive impact on the environment when its use reduces the amount of electricity that must be generated at centralized power plants, in turn, can also reduce the environmental impacts of centralized generation. In detail [24]:

- Existing cost-effective distributed generation technologies can be used to generate electricity at homes and businesses using renewable energy resources such as solar and wind.

- Distributed generation can harness the energy that might otherwise be wasted—for example, through a combined heat and power system.
- By using local energy sources, distributed generation reduces or eliminates the “line loss” (wasted energy) that happens during transmission and distribution in the electricity delivery system.

On the other hand, distributed generation can also lead to possible negative environmental impacts [24]:

- Distributed generation systems require a “footprint” (they take up space), and because they are located closer to the end-user, some distributed generation systems might be unpleasant to the eye or cause land-use concerns.
- Some distributed generation technologies, such as waste incineration, biomass combustion, and combined heat and power, may require water for steam generation or cooling.
- Distributed energy technologies may cause some negative environmental issues at the end of their useful life when they are replaced or removed.
- Distributed generation systems that use combustion may be less efficient than centralized power plants due to efficiencies of scale.
- Distributed generation technologies that involve combustion—particularly burning fossil fuels—can produce many of the same types of impacts as larger fossil-fuel-fired power plants, such as air pollution. These impacts may be smaller in scale than the impacts from a large power plant but may also be closer to populated areas.

It is worth noting that the aspects related to pollutant emissions can be mitigated, considering the possible interconnection to a smart grid (moving from standard distribution grid to smart ones). In this case, proper management of the different technologies interconnected to the distribution grid could lead to higher overall efficiencies and, therefore, lower overall emissions.

Other benefits related to the exploitation of Distributed Generation are presented in [25] :

- Reduction of dependence on major power plants. This results in eliminating the need to erect new big power generation and deferral of new capacity.
- Dependence on long-distance national transmission grid reduction (releasing transmission lines capacities). This leads to a limitation of costs related to the installation of new transmission lines and guarantees a reduction of congestion in the existing transmission lines.
- Reduction of price volatility in energy markets.
- The presence of DG units enhances or preserves the system reliability by having a back-up generation; at the same time the flexibility for system operators increases.
- Acceleration towards the innovative system, pushing on the retirement of old (and pollutant) units.

- Increases energy security by diversifying energy sources and reducing dependence on complex large systems.
- Increases personal, business and regional self-sufficiency.
- Lower environmental impact and greenhouse gas emissions; due to the fact that a large section of DG units is based on renewables or low emission generators

The last point gives us the cue to focus more in detail on the technologies that are employed in DG, in order to understand which are the primary sources involved in this process and the peculiarities related to the different technologies.

Focusing on the Italian scenario, Figure 8 highlights that, talking about Distributed Generation penetration, it is important to distinguish if we consider the installed power or the number of installed plants. The solar fields are characterized by their small size, mainly local at building scale; while wind farms and hydro system are characterized by larger size in terms of power installed, same consideration can be done for Distributed thermal plant, mostly used as Combined Heat and Power (CHP) units. Therefore, considering the power installed, thermal plants represent a significative portion of the distributed generation share. Although, Figure 9 illustrates the trend of DG in the last years, where the share connected to conventional thermal sources is decreasing with a consequent increase in the solar PV presence.

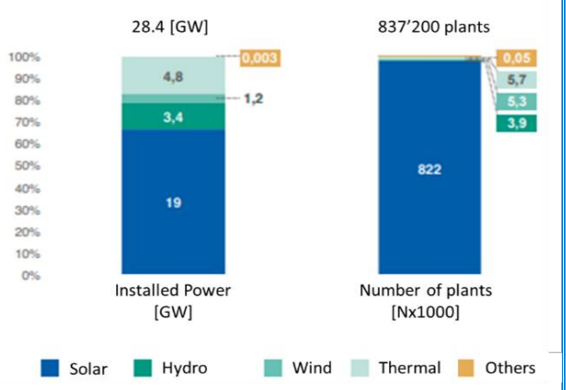

Figure 8 DG installed power and number of plants per primary source, Italy [26]

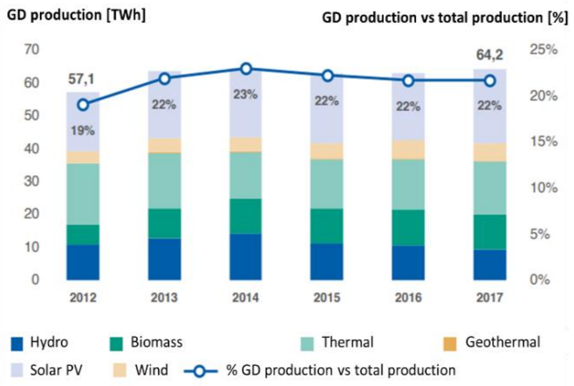

Figure 9 DG production overall trend, Italy [26]

As seen in Figure 8 and Figure 9, Terna categorizes the DG technologies depending on the primary energy source used. Following this scheme, we purpose a brief description of the technologies involved in DG as reported in Figure 10. The traditional generators are the common thermal power plant, fuelled by Natural Gas or Diesel; while among the non-traditional generators are included renewable devices, batteries and Fuel Cells.

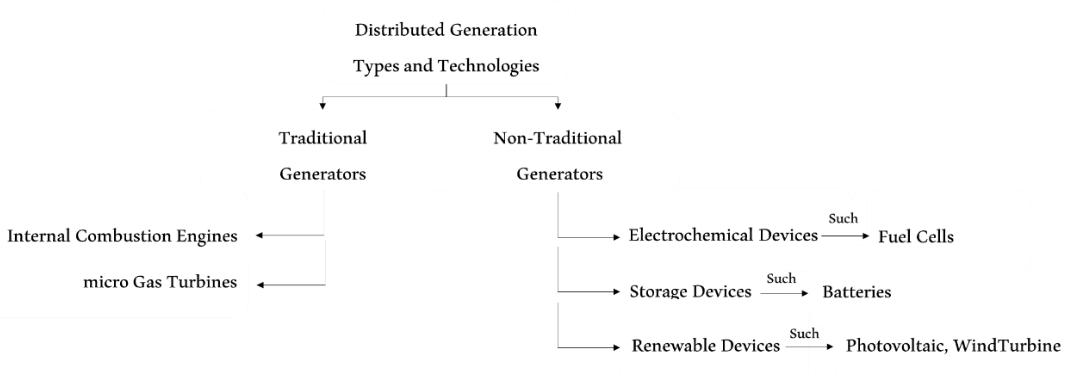

Figure 10 Distributed Generation Technologies Classifications [27]

1.2.1 Traditional generators

Traditional generators are energy systems that convert primary energy into profitable electric and/or thermal energy via combustion. The large majority of this kind of plant is not feasible for the small sizes related to DG, therefore steam power plants, combined cycles and large gas turbine power systems will not be treated in this part. While the most interesting applications for DG, considering their power size and dimensions, are Internal Combustion Engines (ICEs) and micro Gas Turbines (mGTs). The interest in this generators consists mainly on their application as Combined Heat Power (CHP) units; producing simultaneously thermal and electrical power the overall efficiency of the unit increase dramatically, making interesting the application of these traditional generators also in a small scale, especially for residential purpose.

1.2.1.1 Internal Combustion Engines

Internal Combustion Engines are the most technically mature technology among the DG units [28]. ICEs are commonly known for applications in the transport sector (automotive and maritime), but stationary engine/generator applications for power production is getting an increase in interest. Internal combustion engines and heat recovery methods are the cornerstones of Combined Heat and Power systems at all scales [29]. For universities, hospitals, data centres, and municipal utilities, ICE technology is the most common way to provide standby power in case of electric utility fail [29]. Different sizes are available (from 5kWe for small residential application up to several MW) and different fuels can be coupled with this technology. An internal combustion engine converts fuel energy into mechanical power. This mechanical power is used to turn a shaft in the engine, then a generator is present to convert the rotational motion into power. Two different ignition methods are possible:

- *Spark ignition*: a spark is introduced into the cylinder (from a spark plug) at the end of the compression stroke and.
- *Compression ignition*: where the fuel-air mixture spontaneously ignites when the compression raises it to a high enough temperature.

Fast-burning fuels, like gasoline and natural gas, are commonly used in spark-ignition engines, while compression ignition performs better with slow-burning fuels, like diesel. An internal combustion engine can operate in two main cycles: the four strokes cycle and the two strokes cycle. Two strokes engines are lighter, simpler and less expensive to manufacture. They have a greater power to weight ratio, but they have lower efficiency and they require lubrication oil to be fed with fuel. Considering the reduction of emissions, different innovative fuels (such as Methanol and Ammonia) are currently investigated in order to mitigate pollutants especially for what concerns the maritime sector. This aspect will be investigated in detail in the maritime section of this work.

1.2.1.2 Micro Gas Turbines

Microturbines are energy generators with a power size from 15 to 300 kW. The most effective fuel to minimize emissions is clearly Natural Gas. Natural gas is also the fuel choice for small businesses from where derives the commonly used name micro Gas Turbine (mGT). Usually, the natural gas requires compression to the ambient pressure at the compressor inlet of the microturbine. The compressor outlet pressure is nominally three to four atmospheres mainly working with natural gas. The basic principle is based on open cycle gas turbines, but they present several typical features, such as: variable speed, high-speed operation, compact size, simple operability, easy installation, low maintenance, air bearings, low NOx emissions and usually a recuperator that increase overall system performances [30]. First applications of microturbines are related to the automotive sector between 1950 and 1970, but the use of this equipment in the energy market increased between 1980 and 1990 when the demand for DG started to increase [30].
The main characteristics related to mGTs are:

- Variable rotation: the turbine rotates with a speed that varies between 30’000 and 120’000 rpm depending on the manufacturer;
- High-frequency electric alternator: the generator operates with a converter for AC/DC. In addition, the alternator itself is the engine starter;
- Reliability: some microturbines have already reached 30’000 hours of operation including shutdown and maintenance. Although, the expected lifetime for an mGT is around 10 years;
- Simplicity: the generator is placed in the same turbine shaft being relatively easy to be manufactured and maintained. Moreover, it presents great potential for inexpensive and large-scale manufacturing;
- Compact: easy installation and maintenance;
- High noise levels: to reduce noise levels during operation, microturbines require a specific acoustic system. This problem is specifically relevant in case of residential applications;
- Air-cooled bearings: the use of air bearings avoid lubricants contamination by combustion products, prolongs the equipment useful life and reduces maintenance costs;
- Efficiency: microturbine manufacturers generally use heat recovery of exhaust gas to heat the air intake of the combustion chamber, thus achieving a thermal efficiency of 30%.

Some microturbines can operate with different fuels, other the cited Natural Gas. Thanks to the digital control software, implemented inside these machines, it is possible to work with different fuels without significant changes to the hardware. mGTs, like any other power generation units, produce large amounts of heat in the process of converting fuel into electricity. In average, more than two-thirds of the energy content of the input fuel is converted into heat. Conventional power plants discard this waste heat, however, distributed generation technologies, due to their load-appropriate size and sitting, enable this heat to be recovered [30]. CHP plants produce heat and electricity at or near the load side with an overall efficiency up to 85% and operating costs lower than other applications. The hot exhaust gas from mGTs is produced at a reliable temperature for cogeneration applications. The recovered heat is generally used for hot water heating (mainly residential) or low-pressure steam applications. Figure 11 shows the scheme of a microturbine system: the recuperator acts as a pre-heater in order to minimize the fuel combustion, increasing the overall system efficiency. A water-gas heat exchanger is installed in CHP configuration, in order to absorb heat from the exhaust gases.

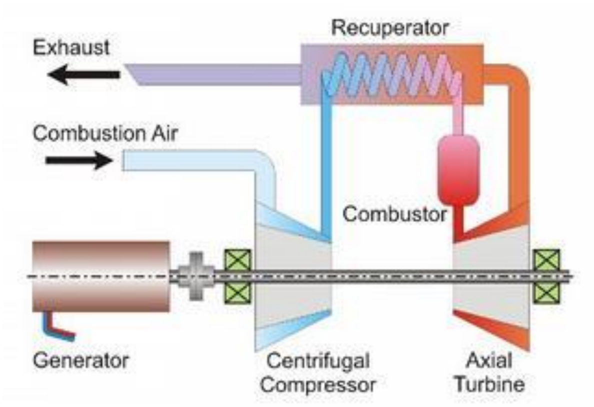

Figure 11 Microturbine scheme [31]

1.2.2 Non - Traditional generators

Innovative generation units are getting more and more relevance due to their potential in the increasing of energy savings and pollutant emissions. These technologies are generally characterized by their high efficiency and very low pollutant emissions. The size of non-traditional generators is commonly quite small, therefore they fit perfectly with DG applications. Innovative generation units can be classified depending on the primary energy source; renewables are certainly the large majority of these technologies, but a relevant role is represented also by Fuel Cells and Batteries.

1.2.2.1 Renewables

Among renewables, the main technologies employed in DG are bases on solar and wind. Especially solar power fits perfectly with the small scale required for DG; while wind power generation is basically at large scale and therefore connected to the transmission lines, but several applications of small wind generators are already installed.

- **Wind turbine technology:** Wind energy, in the past, has been commonly used for practical purposes in the agricultural field (windmill). Nowadays, large and modern wind turbines operate together in wind farms to produce electricity. Small turbines are used at the residential level to help meet localized energy needs. Currently, the largest market share is represented by horizontal-axis, medium to large size grid-connected wind turbines (capacity greater than 100kWe) and it is expected, also, that this technology will dominate the development in the near future [28]. The design of the aerodynamic rotor diameters strictly depends on the installation environment, with the aim of maximizing the yearly energy harvest. On high-wind speed sites, usually smaller rotor diameters are used with an aerodynamic profile that will reach the maximum efficiency between 14–16 m/s. For low-wind sites, larger rotors will be used but with an aerodynamic profile that will reach the maximum efficiency already between 12–14 m/s. Capital and maintenance costs represent a non-negligible aspect for wind applications Currently, three-bladed wind turbines dominate the market for grid-connected, horizontal-axis wind turbines [28]. The benefits of three-bladed wind turbines are the easy handle of rotor inertia and the ‘‘better’’ visual aesthetics, with a lower noise level than two-bladed wind turbines. Both aspects are important considerations for wind turbine utilization in highly populated areas. Furthermore, three-bladed wind turbines are suitable for a wider range of wind velocity and lead to higher efficiency and balance. Two-bladed wind turbines, on the other hand, have the advantage that the tower top weight is lighter and, therefore, the whole supporting structure can be built lighter, with lower costs. Currently, most wind turbine manufacturers, are working on larger wind turbines, in the multi-megawatt range [28].
- **Solar technologies:** this kind of technologies can be used for both thermal (Solar thermal panels) and electricity production (Photovoltaic panels). Therefore, their use can be considered for DG of electricity and also local thermal production (with the chance of a connection to District Heating Networks). In this introduction, we will focus more on PV, while the thermal distributed production will be analysed more in detail in a dedicated section. The solar electric production by photovoltaic cells represents one of the most promising options for a sustainability energy provision compliant with the world’s future energy requirements [28]. In the past, PV panels have been based on the silicon wafers also used in microelectronics, currently, the transition towards the second generation of thin-film technology is leading to lower costs. At the same time, the residential rooftop application of photovoltaics had a continuous increase, providing the market growth needed for price reduction [28]. These cost reduction, thanks to the both cited aspects, led to a strong decrease of PV panels prices towards a competitive price level for electricity production also on a large scale, as reported in Figure 12.

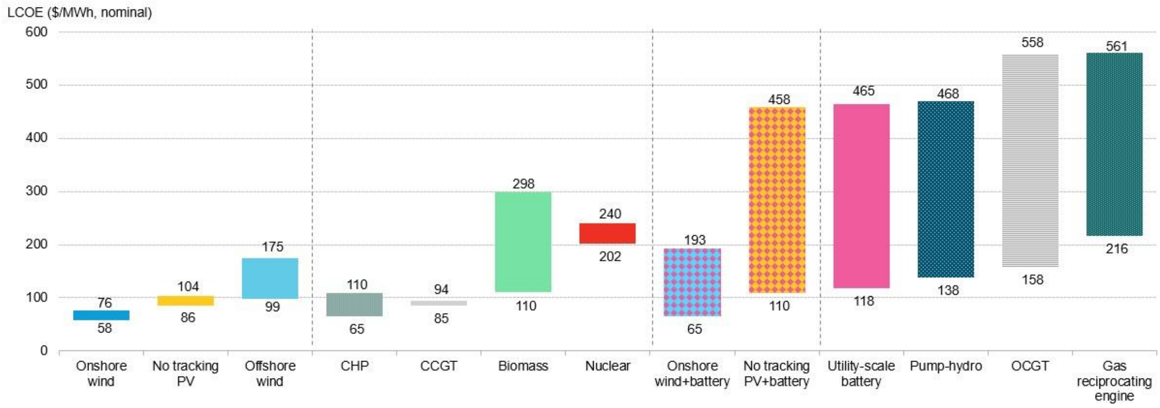

Figure 12 Electricity cost by source [32]

1.2.2.2 Fuel Cells

A Fuel Cell (FC) is an energy conversion device that produces electricity and heat via electrochemical process combining a gaseous fuel (hydrogen-based) and an oxidant gas (oxygen from the air) through electrodes and across an ion-conducting electrolyte, water is the only exhaust. The principal characteristic of a fuel cell is its ability to convert chemical energy directly to electrical energy, without any combustion. Therefore, the overall conversion efficiency is significantly higher (close to 50%) than any conventional thermomechanical system. One of the main benefits of FC is their almost zero-noise behaviour since there are no moving parts. Auxiliary components are required to generate electrical power with a fuel cell stack. These components are usually referred to as the balance of plant (BoP). One class of BoP components is used to supply fuel and oxidant to the stack (e.g. pumps, blowers and compressors). High-temperature fuel cells are often equipped with burners to heat the system up during start-up. Although high-temperature fuel cells are usually cooled with cathode air, the temperature gradients in low-temperature fuel cells are too small to achieve sufficient cooling in this way. Therefore, for these units, a separate cooling system is needed [33]. Since fuel cells generate DC power with variable voltage and current, power conditioning equipment, such as DC/AC inverters, is used to generate electricity at grid voltage and frequency. The cited BoP components are the only responsible for the noise related to fuel cells applications. Fuel cells offer several technical advantages, such as modularity, good partial load characteristics and dynamic response. On the other hand, it is worth notice that one of the main reasons that are slowing down FC applications is their high costs. The other main limiting aspect is linked to Hydrogen use that is costly (H_2 production and delivery costs) and requires delicate management (high-pressure tanks or cryogenic storages). The US Department of Energy (DOE) has published a market report in 2016, whose results are shown in Figure 13.

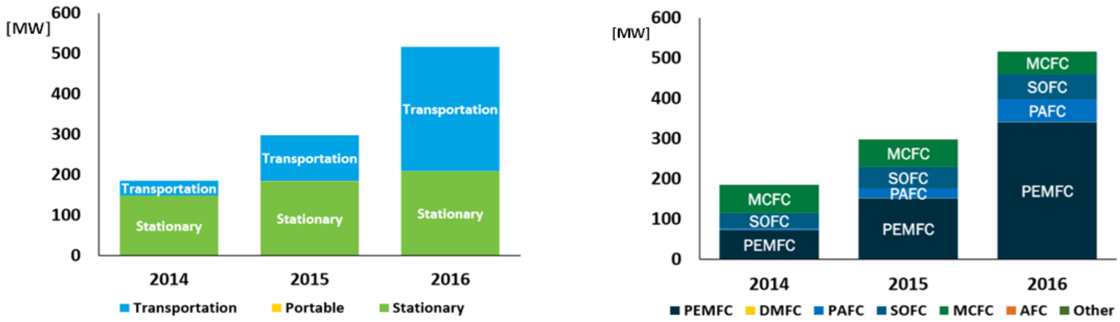

Figure 13 Evolution of fuel cell installed power in terms of applications (left) and type (right) [34]

A significant increase in installed power by fuel cells is occurring in these years, mainly in the transportation sector. This increase is mainly related to the great exploitation of PEMFCs in the transport sector. Although, a variety of fuel cell types with distinct characteristics is currently present in the market. The most relevant are the Low and High-Temperature Polymer Electrolyte Membrane Fuel Cell (LT/HT-PEMFC), Phosphoric Acid Fuel Cell (PAFC), Molten Carbonate Fuel Cell (MCFC) and Solid Oxide Fuel Cell (SOFC).

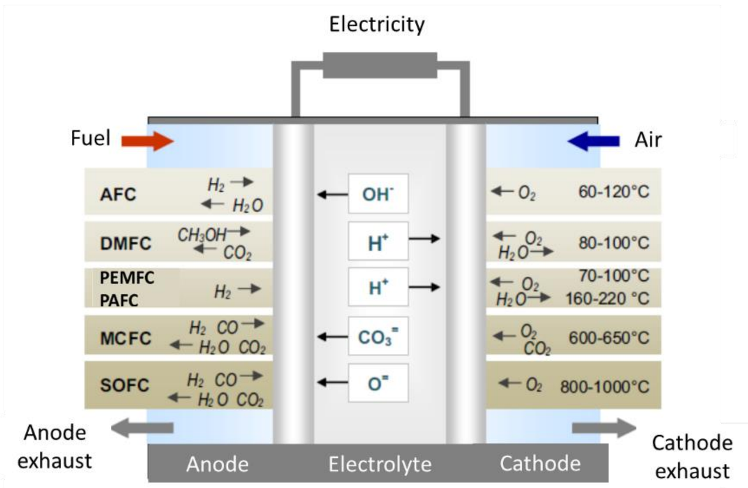

Figure 14 Different Fuel Cell types, operational scheme [35]

- **PEMFC:** this fuel cell uses as electrolyte a polymeric membrane with high proton conductivity and operates in a temperature range between 70 and 100 °C; they are mainly developed for traction and small generation/cogeneration (1-250 kW) [35] They can be divided in Low-Temperature PEMFC (LT-PEMFC) and High-Temperature PEMFC (HT-PEMFC). The *LT-PEMFC* has known rapid development in the last decades and achieved high power densities and good transient performance. Its membrane consists of a proton-conducting wetted polymer (commonly Nafion). The need for a wet membrane, while the gas-diffusion pores have to remain dry, dictates an operational temperature of 65 and 85 °C, in order to do not vaporize the water. Considering the relatively low-temperature range, the use of platinum is required to catalyse the electrochemical reaction [33]. Another important disadvantage of the low operating temperature is the limited tolerance to fuel impurities. In particular, carbon monoxide (CO) deactivates the catalyst, because of its strong surface adsorption at low temperatures. A membrane that combines a polymer electrolyte with a phosphoric acid has been developed in order to operate in a higher temperature region (over 100 °C). These PEMFC are known as High-Temperature PEMFC (*HT-PEMFC*). In this configuration, platinum can be replaced with cheaper catalysts, such as nickel, in the high-temperature fuel cell classes. Furthermore, the sensitivity to fuel impurities has strongly decreased. Another advantage is the opportunity to use high-temperature waste heat and steam, for example in a bottoming cycle or for fuel processing. On the other hand, the main drawback of this solution is related to their slow dynamics and low durability [36], not really performant in case of transport applications.

- **PAFC:** the membrane of Phosphoric Acid Fuel Cell consists of a silicon carbide matrix saturated with liquid phosphoric acid; working in a temperature range between 140 to 200 °C, the required platinum loading decreases, while the CO tolerance increases. The low power density and durability issues have so far limited the commercial success of the PAFC [33].
- **MCFC:** Molten Carbonate Fuel Cell uses as electrolyte a solution of alkaline carbonates melted at the operating temperature of the cell (650-700°C) and contained in a porous ceramic matrix; they are mainly suitable for the generation of electricity and cogeneration from few hundred kW to several MW. This technology represents a relatively mature solution among high-temperature fuel cell. Indeed, MCFCs are commercially available but still struggle with high cost, limited lifetime and low power density (particularly an issue for transport applications) [33].
- **SOFC:** Solid Oxide Fuel Cells operate at very high temperature (about 900-1000 °C) to guarantee a sufficient conductivity to the electrolyte, made of ceramic material (zirconium oxide doped with yttrium oxide). These cells are particularly promising for electricity generation and cogeneration from a few kW to several MW. The lower temperature classes are mainly applied in stand-alone fuel cell products, with electrical efficiencies up to 60% [33], while the high-temperature SOFCs are designed for combined operation with gas turbines, where efficiencies over 70% are projected [33]. Their high operating temperature allows the internal reforming of fuels, eliminating the need for an external reforming unit and allowing the units to be used with a certain variety of fuels, mostly Natural Gas. They are also relatively resistant to small amounts of sulphur in the fuel, when compared to other types of fuel cells, and can therefore be used with hard coal gas. An additional advantage due to the high operating temperature is that the reaction kinetics is improved, eliminating the need for a catalyst. Although SOFC represents a promising solution, their current limited development state is mainly related to their mechanical vulnerability (ceramic material is particularly sensitive to vibrations) and high costs. Furthermore, there are some disadvantages related to their high temperatures: these cells require more time to be heated up to their operating temperature, it is also necessary to build this technology with robust and heat-

resistant materials and must be shielded to prevent heat loss (especially during start-up).

Table 1 summarizes the main peculiarities of the mentioned Fuel Cells technologies

Table 1 Main Fuel Cells characteristic [33]

Fuel Cell Type	Temperature range [°C]	Fuel	Poisonous substances	Internal reforming	Efficiency
LT-PEMFC	65-85	H_2	S, CO>10 ppm	No	40-60 % with H_2
HT-PEMFC, PAFC	140-200	H_2	S, CO>3%	No	40-60 % with H_2
MCFC	650-700	H_2, CO	S	Yes	40-55 % with NG
SOFC	500-1000	H_2, CO	S	Yes	45-60% with NG

1.2.2.3 Storages

Energy storage systems are considered enabling technologies for different DG functionalities such as active management of network assets, network flexibility, improve power quality, self-healing, and resiliency. In addition, energy storage systems are essential components for integrating the non-dispatchable renewable energy resources. Other applications for energy storage systems include micro-grids and electrification of remote areas, in which energy storage systems are used to minimize dependence on the main grid supply. Energy Storage Systems (ESS) can be classified depending on the energy form they are using in the storage process. There are five main categories, as reported in Figure 15.

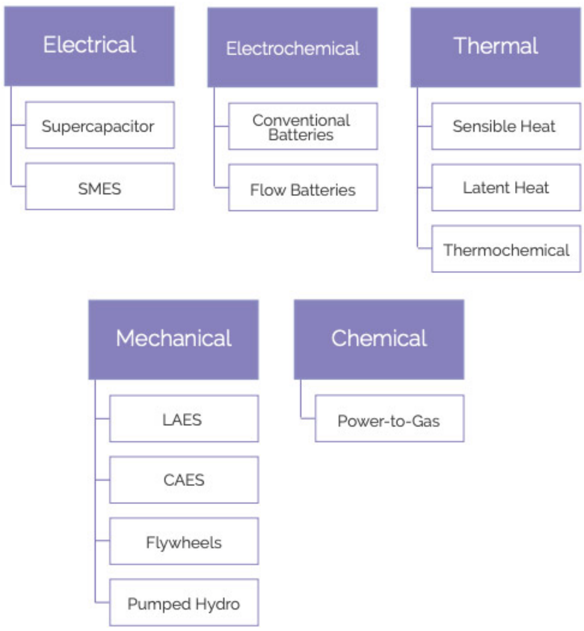

Figure 15 Energy storages categories [37]

The main used technologies in DG scenario are electrochemical storages and thermal storages. The presence of storages gives to the system manager one degree of freedom more to perform the optimized management of the generation units. In the case of CHP units, as an example, the presence of a storage guarantees to decouple electrical and thermal demands. Therefore, it is possible to manage the system tracking one demand or the other considering economic and/or environmental aspects. Usually, in this case, thermal storage (more economic) is preferable.

On the other hand, the use of electrochemical energy storages is getting more and more interesting considering the electric vehicle increasing share (Figure 16). The presence of these units in connection to the distribution grids is expected to have a huge impact on the grids and environment. Batteries contain a number of heavy metals and toxic chemicals. The disposing of them by the same process as regular household waste has raised concerns over soil contamination and water pollution. The Basel Convention on the Control of Trans-boundary Movements of Hazardous Wastes and their Disposal is the most comprehensive global environmental agreement on hazardous and other wastes. The Convention includes 172 Parties and aims to protect human health and the environment against the adverse effects resulting from the generation, management, transboundary movements and disposal of hazardous and other wastes, including batteries. Battery recycling aims to reduce the number of batteries being disposed of as municipal solid waste. Recycling plants in Europe have to comply with Directive 2006/66/EC, which requires a minimum recycling quota of 50%. From an economic point of view, the main drivers for recycling are cobalt (31,440 US$/t, 99.8%) and nickel (15,914 US$/t, 99.8%), followed by copper (6451 US$/t, grade A, LME) and lithium (6439 US$/t lithium carbonate, average prices June 2014–May 2015) [38].

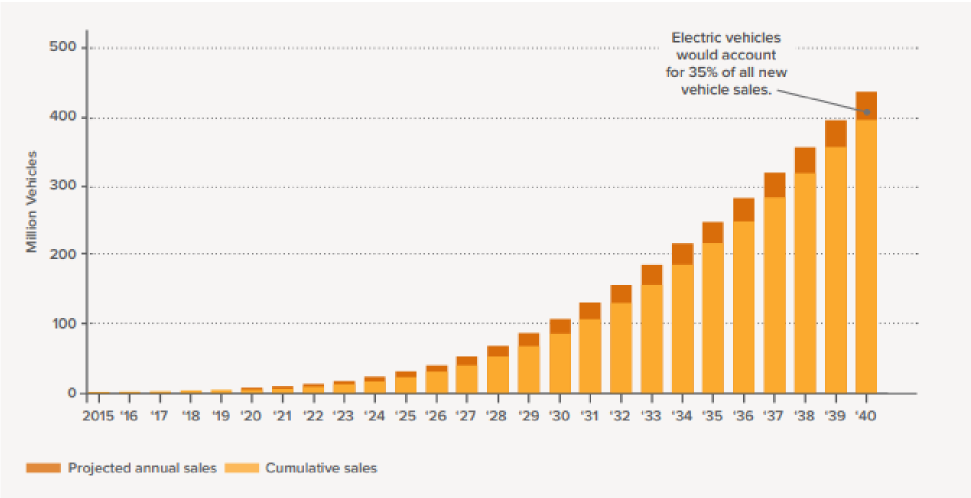

Figure 16 Electric Vehicles selling projection [39]

In this introduction, we have described the current and the foreseen energy scenario. In this context, where renewables will have an increasing role, the Distributed Generation approach looks like a necessity considering the currently available size for these systems. Furthermore, the trend towards wider use of DG shows an interesting potential with many benefits, such as size optimization and waste reduction. It is also worth notice that some critical aspects related to the management of the electrical grids have to be considered and properly managed in order to guarantee a reliable and safe massive introduction of these technologies in the energy market. Therefore, moving to the DG paradigm, the available fuelled technologies for Distributed Generation are reported in Figure 17 in comparison with standard centralized plants.

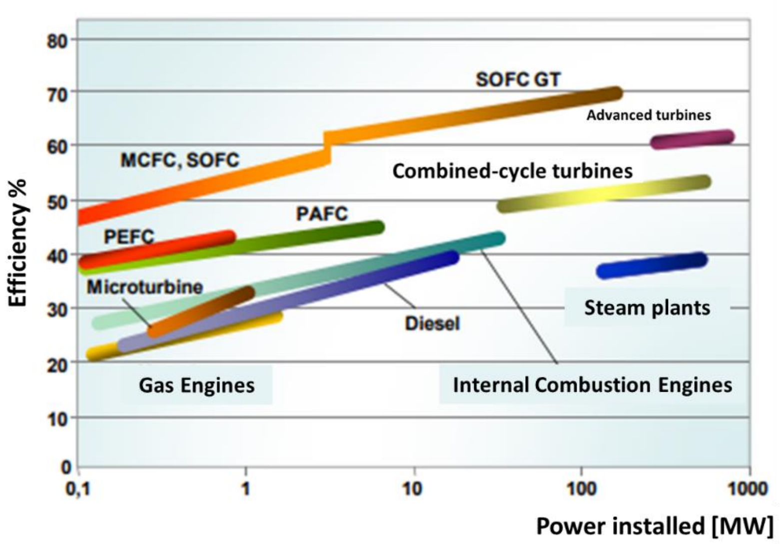

Figure 17 Generation units efficiency, comparison between DG technologies and centralized ones [35]

Among DG technologies, the most promising in terms of energy efficiency are the Fuel Cells that still present drawbacks in terms of costs and life cycle. Most mature technologies such as Internal Combustion Engines and micro Gas Turbine, represents a good compromise solution since that, accepting their lower efficiencies, are very competitive in terms of cost and system management.

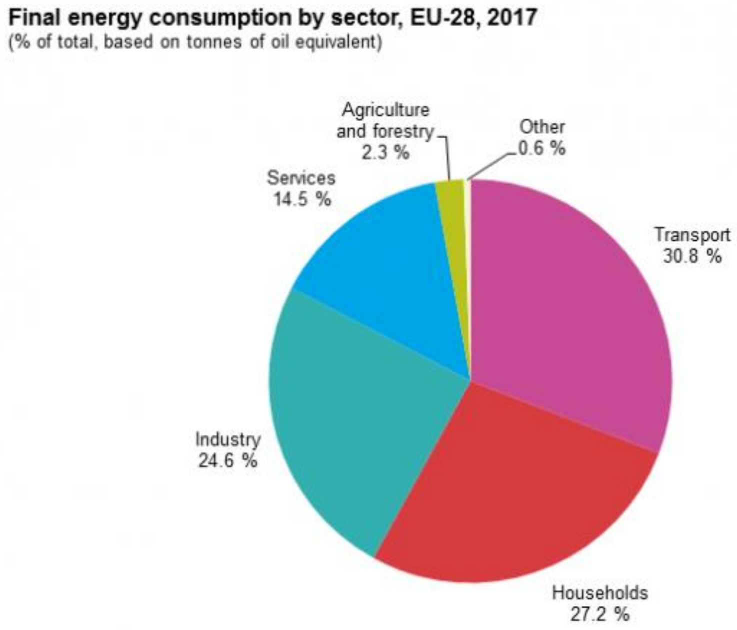

Figure 18 Energy consumption by sector in EU-28[40]

As reported in Figure 18, referring to Eurostat and IEA [41], the main energy consumptions in Europe are related to building and transport sectors. Therefore, the study presented in the next chapters of this thesis is focused on the development of the distributed generation approach in these two energy sectors. The use of micro Gas Turbines is studied in residential and transport sectors with the aim of evaluating their viability considering the different constrains set by the two sectors. In detail, the household application is related to the development of an energy hub in interaction with a poli-generation Smart Grid. In this case study the author has developed the design of the system (necessary for the proper selection of all the necessary components) and the management strategies with the aim of guaranteeing efficient and economic operations. For what concerns the transport application, the author has focused on the maritime sector, in particular the application of a DG approach onboard cruise ships. This has been possible via evaluating the most suitable technologies for this application considering the limitations in terms of weights and volumes when facing this kind of applications.

2 A residential case study: ENVISION

To mitigate the impact on climate change, related to residential energy consumptions, Europe sets the goal of an energy-neutral built environment in 2050 [42]. In order to meet this foreseen ambitious target, the building surfaces for solar energy harvesting should be maximized. Application of photovoltaic solar panels and/or collectors has increased considerably in recent years, but are mainly applied on roofs due to aesthetics, practical reasons and price. Efficient management of solar radiation on buildings could provide an enormous potential, considering that in EU28 a total of 60 billion m^2 of façade surfaces exists, and the current usage of solar radiation on opaque surfaces is still minimal. Including roof surfaces, the overall potential surfaces for solar energy harvesting could reach a total of 120 billion m^2 [43].

Figure 19 ENVISION logo

In this context ENVISION H2020 Project focuses on energy harvesting of the façade and works by absorbing an invisible part of the solar radiation (the near-infrared (NIR) part) allowing visible aspects to be retained. The harvesting of solar energy will be achieved via different "ENVISION technologies":

- Heat collecting non-transparent aesthetically pleasing façade elements by harvesting the NIR solar radiation;
- Heat harvesting ventilated glass by harvesting the NIR solar radiation,
- Electricity harvesting photovoltaic glazing solutions.

The interesting potential of these technologies is also linked to the foreseen need for a major renovation in the upcoming period, considering that approximately 85% of existing dwellings were built before 1990 with poor insulation ($R \leq 1.6$ m2K/W) [43]. To improve energy performance, a need exists for energy harvesting envelopes that separate the indoor from outdoor. ENVISION technologies increase the competitiveness and the needed renovation speed via simple and flexible solutions, thanks also to the different contribution of the partners involved in the consortium.

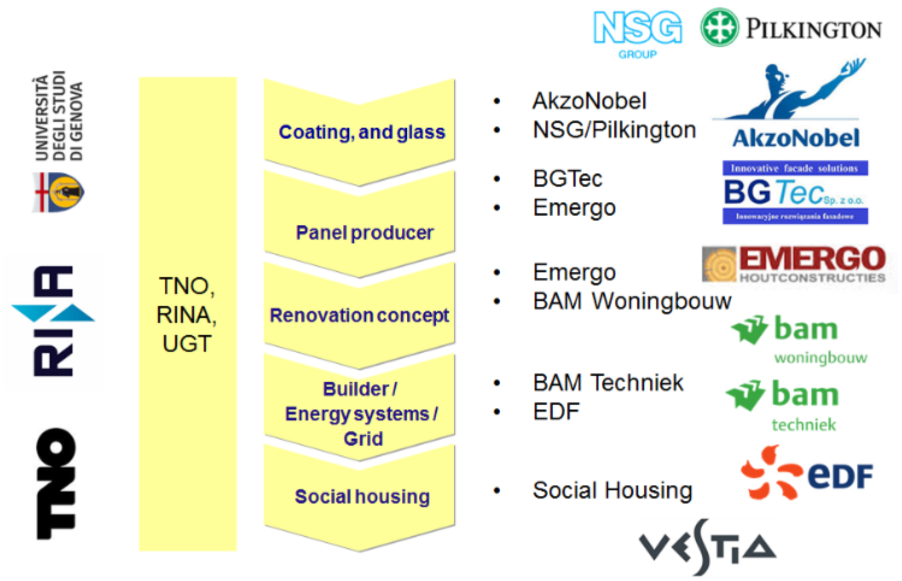

Figure 20 ENVISION Consortium [43]

The aim of ENVISION is to develop and test the cited technologies with the aim of reaching a Technology Readiness Level (TRL) of 7 or 8. To do that, different demosites ware developed to test different technologies in a different environment and at a different scale.

Northern Demosite: Vestia and BAM will apply the new technologies in the renovation of an apartment building. Apartment buildings or flats have large challenges as the amount of energy usage by the inhabitants is high, compared to the surfaces that can be used for energy harvesting. Achieving Near Zero Energy flats is a major challenge, especially considering the high number of flats that need renovation. To achieve a fast and simple implementation, the module can be replaced easily allowing upgrading by renewing the key elements, such as glass, collector, coating. Easy connection to the heating system should be taken care of.

Southern Demosite: The first one will be installed at the Savona Campus, one of the venues of the University of Genoa. In this demosite a single-detached house will be equipped with ENVISION technologies to investigate their coupling with the local smart electrical grid and a District Heating Network (DHN).

University of Genoa is responsible for the Southern Demo, therefore the focus of the presented work will be on this demosite, starting from the design, the control algorithm definition and the preliminary tests.

2.1 Southern Demo Description

As mentioned before, the ENVISION Southern Demo is responsible for testing some of the ENVISION technologies at District Level, evaluating their performances in interaction with a poly-generation smart grid. This is possible thanks to the installation of the system in the Savona Campus, where a Smart Polygeneration Micro (SPM) grid is present (Figure 21).

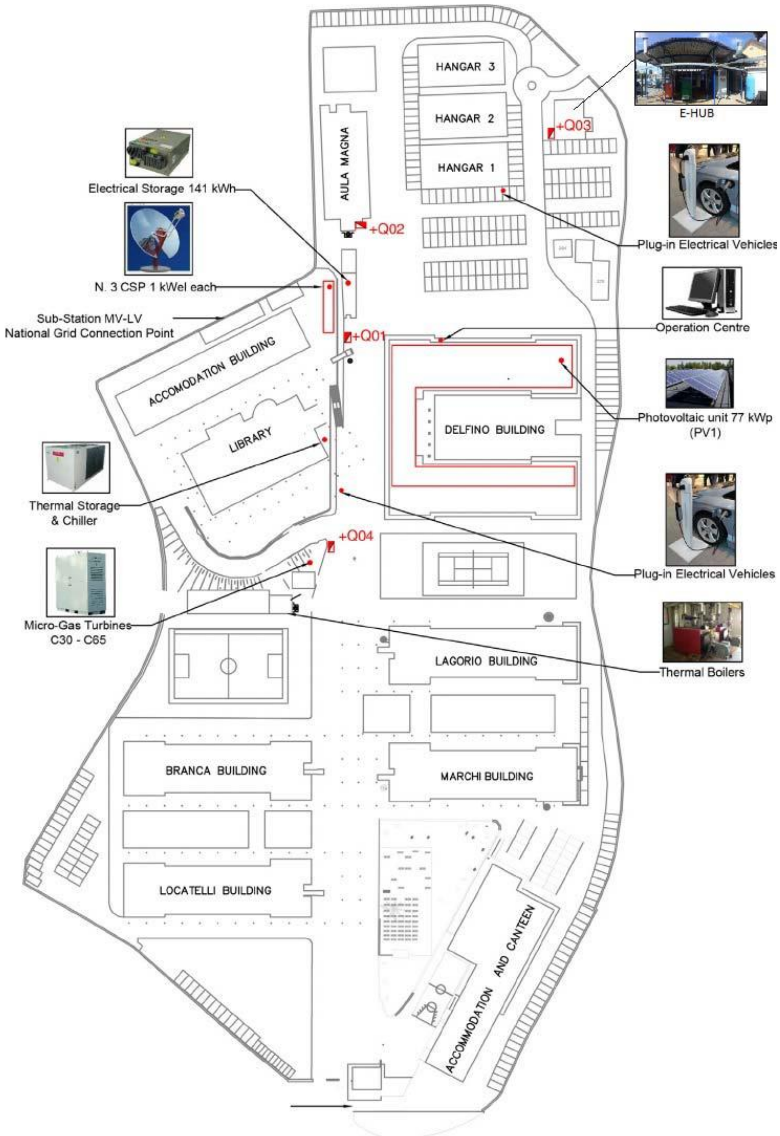

Figure 21 Savona Smart-Polygeneration micro-Grid [44]

The SPM installed in Savona includes several commercial CHP units, traditional prime movers and renewable generators, as it follows:

- 2x mGT Turbec T100 (100 kWe,165 kWth each);
- 1x mGT Capstone C30 (30 kWe, 49 kWth);
- 2x mGT Capstone C65 (65 kWe,112 kWth each);
- 1x ICE TANDEM T20 (20 kWe, 44 kWth);
- Photovoltaic roof, about 400m2 (peak power 77 kWe);
- 3x CSP dish Stirling units (1 kWe, 3 kWth each);
- 2x Natural gas boilers (500 kWth each);
- 4x Storage tanks for hot water (total volume: 12000 l).

The layout of the DHN, including the modification needed for ENVISION project, is presented in Figure 22.

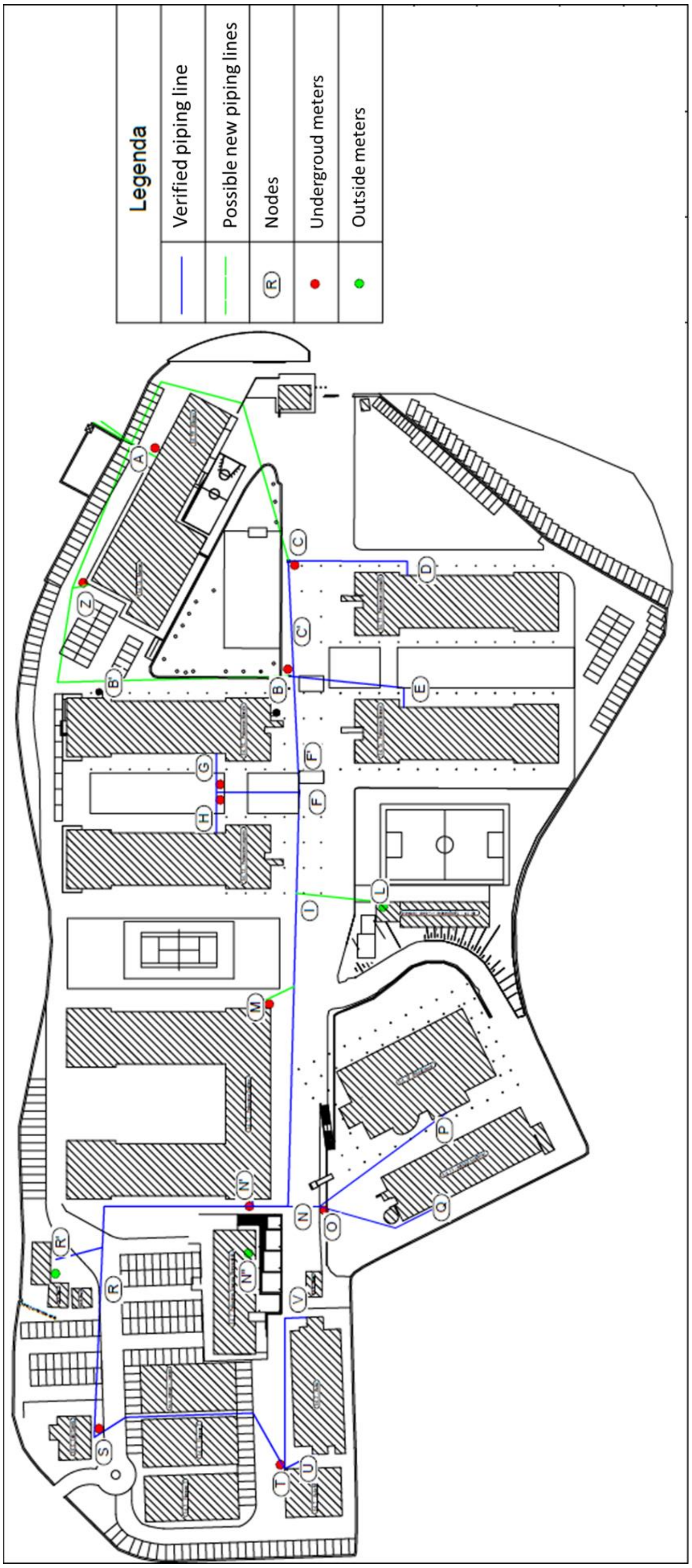

Figure 22 Savona Campus DHN

With ENVISION project new technologies will be added and connected to the SPM. The dedicated area for the installation of "ENVISION technologies" is the one highlighted in Figure 23 that has easy access to the DHN pipelines.

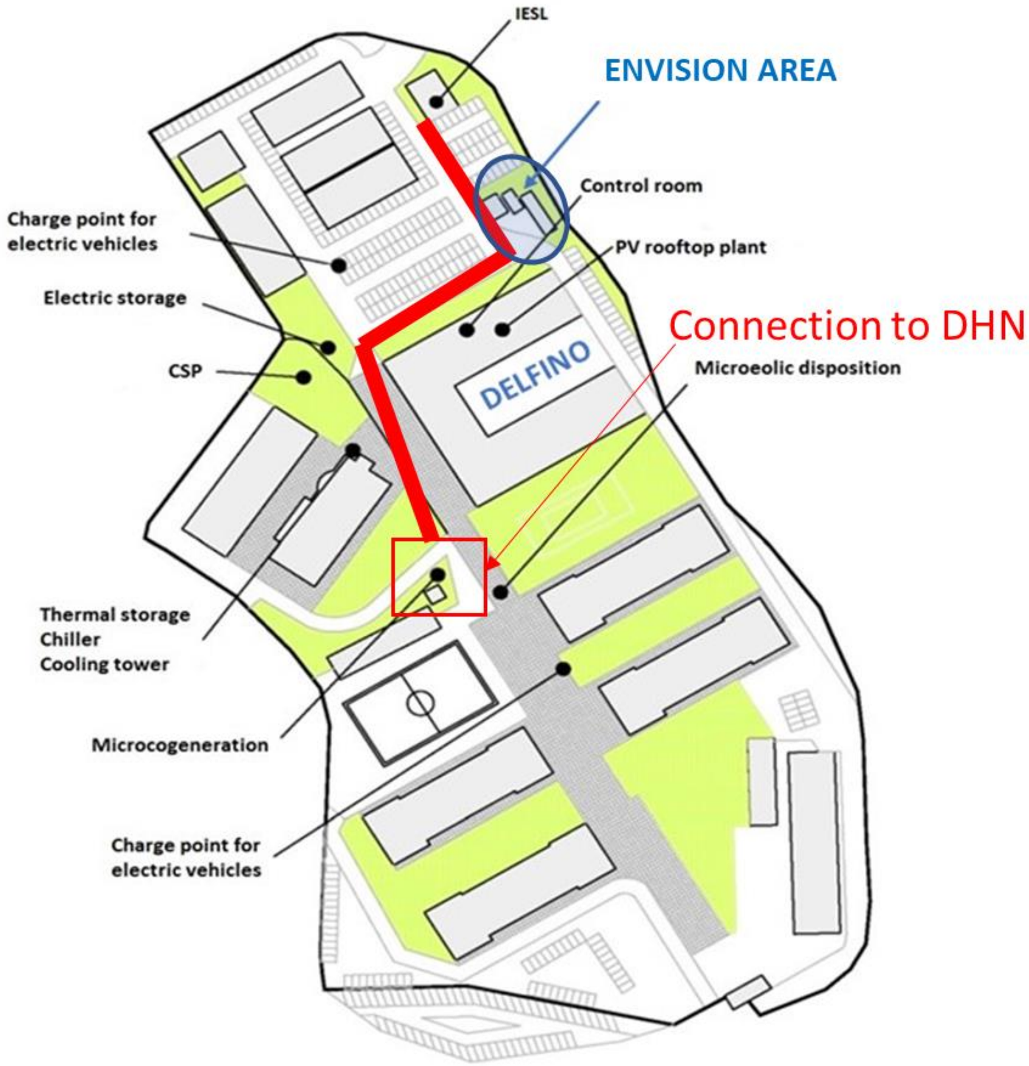

Figure 23 Savona Campus map

A detailed view of the ENVISION area is presented in Figure 24, Figure 25, Figure 26, and Figure 27 where it gets clear the need of renovation for the buildings in order to guarantee a safe and proper testing environment for the project.

Figure 24 ENVISION Area initial status A

Figure 25 ENVISION Area initial status B

Figure 26 ENVISION Area initial status C

Figure 27 ENVISION Area initial status D

The management of Savona Campus is responsible for the renovation of this area. A rendering representing the status of the ENVISION area after renovation is reported in Figure 28 and Figure 29.

Figure 28 Before

Figure 29 After

After this brief description of the environment where the ENVISION Southern Demo will take place, the next section will be focused on the technologies that are studied and implemented at Savona Campus.

2.1.1 System layout and technologies implemented

The aim of this demosite is to test technologies at district level thanks to the presence of SPM; therefore, a cogenerative system, producing both thermal and electrical energy is installed. The system layout is presented in Figure 30.

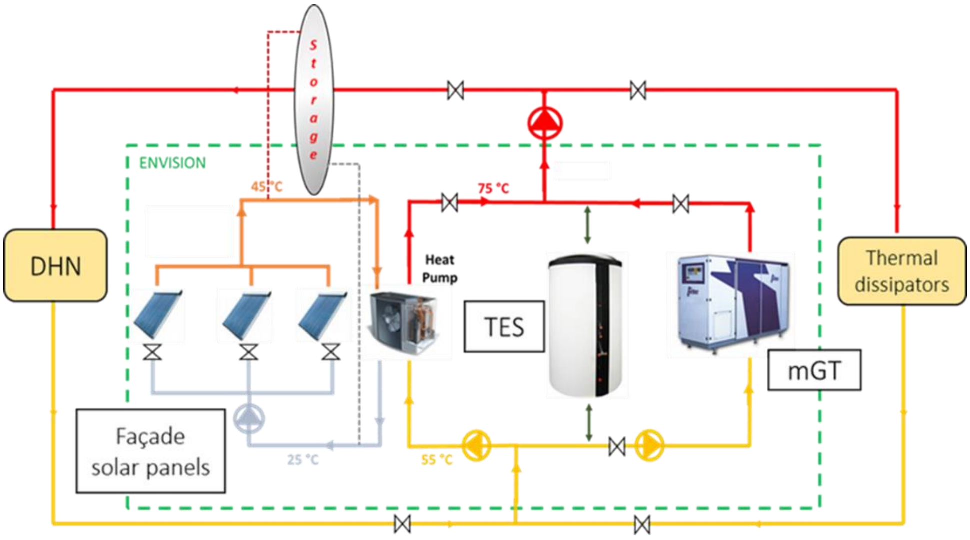

Figure 30 ENVISION system layout

The system consists of the use of several solar façade panels that are interconnected to a Heat Pump (HP). The presence of the HP is needed in order for coupling the temperatures provided by the panels (max 45°C), with the one required by the DHN (75-80 °C). Furthermore, to mitigate the fluctuations due to the variability of solar radiation, intermediate Inertial storage is installed. Considering the electric consumption related to the HP and the need to provide both thermal and electrical power to the SPM, a micro Gas Turbine in CHP configuration is installed with the aim to supply thermal power to the DHN and electrical power both to HP and the grid. As mentioned in the introduction, the presence of storage is fundamental in the management of CHP units, guaranteeing more independency between thermal and electrical demand tracking. This ENVISION-hub is then connected to the DHN of Savona Campus. Although, in order to be able to test different scenarios and environment, a connection to the thermal dissipators installed in Savona Campus is considered, giving flexibility to the experimental campaign.

In the following sections, a detailed description of the mentioned technology is provided.

2.1.1.1 Solar Façade Panels

The product developed in this project is a flexible solution for façade cladding with optional an integrated and invisible solar collector function. For the façade cladding, different colours can be chosen, giving to the designer or architect design freedom. The cladding can be used in combination with the different façade function such as door and window frames, parts of stone strip façade and other façade cladding materials. The collector function is integrated into the cladding and therefore “invisible”. It is then possible to select the parts surface area of the façade that is activated to harvest the solar energy with the collector function. The heat from the façade collector function can be used for domestic hot water preparation or as a source for a heat pump, as applied in Savona Campus. An example of thermal solar collectors mounted on the façades of buildings is demonstrated below. On the left, a standard 1960s residential building is shown, while on the right is reported the same building renovated with the thermal solar collectors on the façade.

Figure 31: 1960s residential building

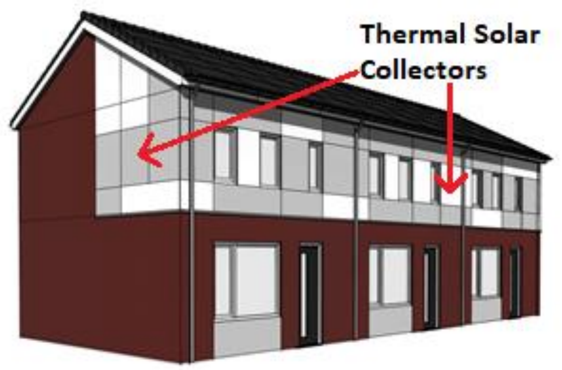

Figure 32: Renovated 1960s residential building

A more detailed 3D model of a prototype using the thermal solar collectors on a façade is presented in the next two pictures.

Figure 33: 3D model of demo façade

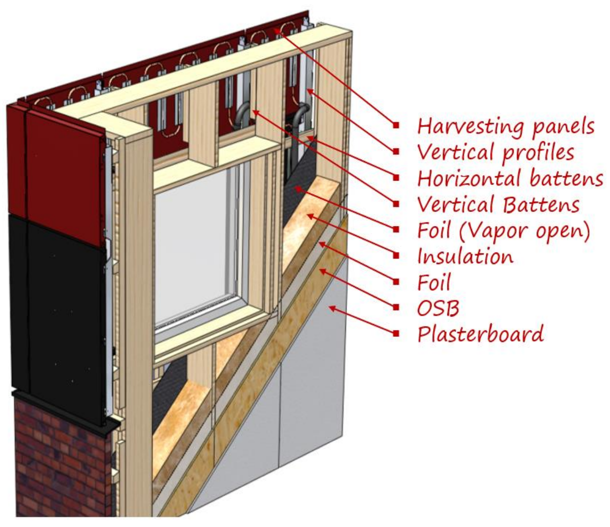

Figure 34: Intersection of the demo façade

To transport heat from the collector to the heat pump, buffer or the domestic hot water preparation, a fluid flows through pipes on the back of the panel. This fluid will absorb the heat. To connect the pipes on the collector plate, a heat-conducting metal is used, which is structurally bonded with a specially developed adhesive applied using high pressure. Thanks to this process, the pipes are completely enclosed (360°). This larger area of contact results in a significantly improved heat transfer and thus optimum efficiency. Simultaneously, the corrosion resistance is increased.

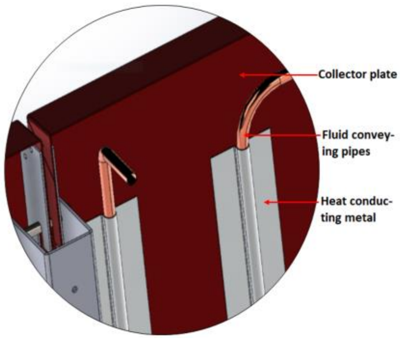

Figure 35: Fluid distribution pipes model

Figure 36: Fluid distribution pipes SolarBEAT

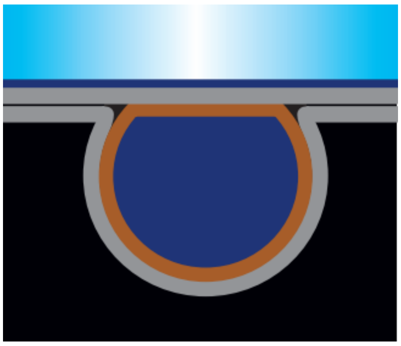

Figure 37: Section view of pipe on panel

Considering their installation on surfaces, like façades, that are mostly not perpendicular to solar radiation, the need to optimize the absorption on a larger wavelength (including NIR) gets fundamental. The basic principle to optimize heat absorbance in light coloured coatings, carried out in dedicated activities among the project, concluded that the NIR absorbance of especially light coatings can be increased using nanometer-sized antimony tin oxide (ATO) particles in conjunction with titanium dioxide (TiO2). However, the addition of ATO particles is not an ideal solution because it also leads to a decrease in the lightness of the coating. That is, ATO not only absorbs the invisible NIR waves, it also absorbs some of the visible light. For small quantities of added ATO, the drop in the lightness of the coating is small compared to the gain in (especially NIR) absorbance. But when larger amounts of ATO are added, the impact on the colour is becoming so big that pigments that are normally used in coatings (such as carbon black) can also be used to improve the NIR absorbance in a similar way. The different formulated colours, during the test performed by AzkoNobel, have shown to absorb more than 70% of the solar energy. The exceptions are (near) white colours, that are limited by a theoretical upper limit of 50% absorption.

The façade cladding has a mounting system that consists of an axis on the façade that falls in a slot in the collector panel. This way, the mounting of the panels will be easy and quick. When the panels are in place, they will be fixated using an L-profile with screws (Figure 38).

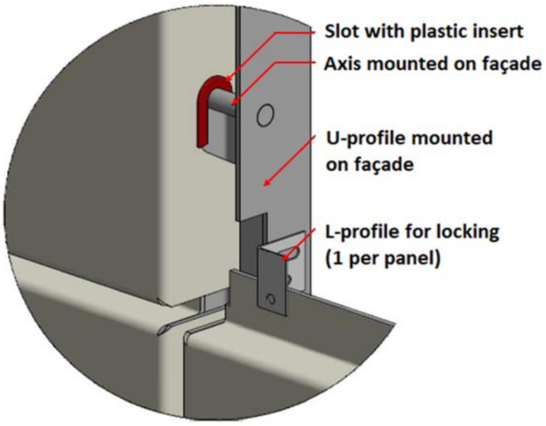

Figure 38: Mounting system model

Figure 39: Mounting system SolarBEAT

The panels will be installed in Savona Campus, with the aim of maximizing the available surface. At this scope, the different available buildings in the ENVISION Area have been analysed. Considering the dimensions of the three available buildings, as reported in Figure 40 and Figure 41.

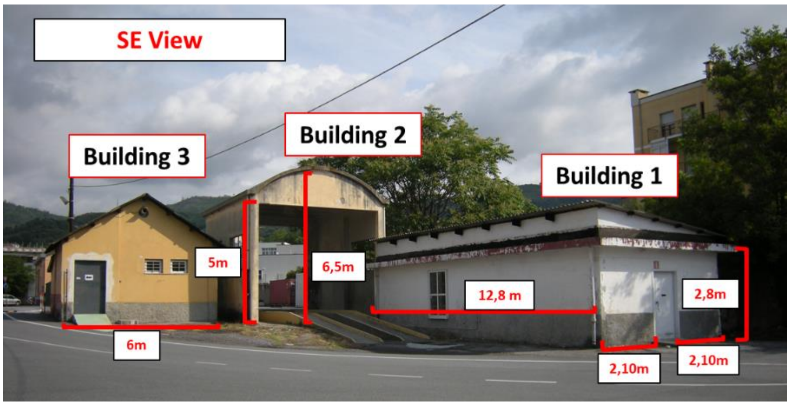

Figure 40 ENVISION Area buildings dimensions, SE view

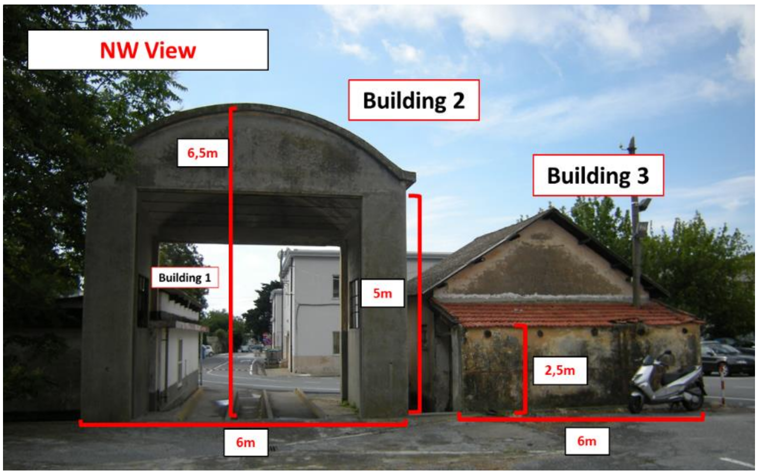

Figure 41 ENVISION Area buildings dimensions, NW view

The available surface calculated for the panels is presented in Table 2, where it is possible to conclude that the most promising building for panels installation is the Building 1, with a maximum available surface of **96 m²**. The choice of Building 1 has been performed considering that it is the most exposed building; furthermore Building 2 does not have the permit for being completely enclosed.

Table 2 Total Available surface for ENVISION panels installation

Total Available surface for façade panels installation					
Building 1		Building 2		Building 3	
Length SE [m]	4.2	Length [m]	5.9	Length NW [m]	6
Length NW [m]	5	Width [m]	6.6	Height NW[m]	1.5
Width [m]	12.8	Height [m]	5		
Height [m]	2.8				
Height NW [m]	2.5				
Tot Surface [m2]	95.94	Tot Surface [m2]	125	Tot Surface [m2]	9

Referring to the preliminary evaluation of the performances of the panels provided by the ENVISION consortium partners, it is estimated an overall maximum thermal power of **20-30 kWth** in relation to the available solar field.

2.1.1.2 Heat Pump

The heat pump will be applied in order to provide heat at the temperature required by the DHN (75°- 80°C). As a brief reminder, Figure 42 reports the working principle of a Heat Pump (HP). The low-temperature heat source, in the ENVISION case represented by the heat produced by the panels, is used to evaporate the working fluid. Then, with an external work input (mainly electric), the working fluid is compressed in order to reach higher temperatures. The user thermal load is supplied through a heat exchanger where the working fluid release heat to the sink. An expansion valve is used to close the cycle through an iso-enthalpic expansion.

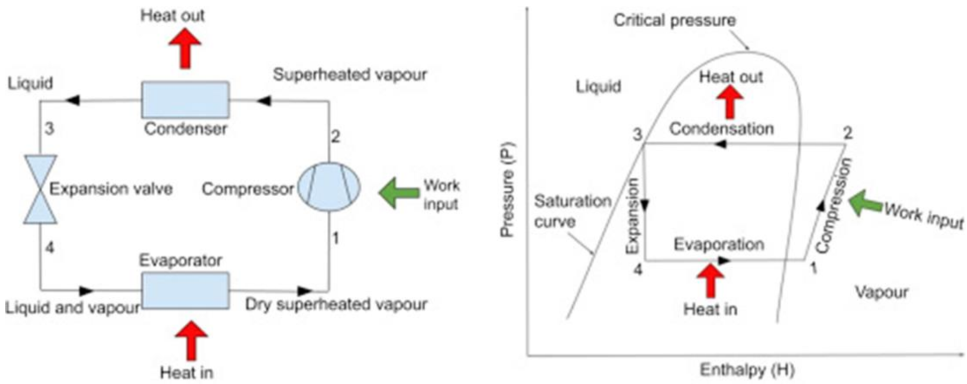

Figure 42 Heat Pump operational scheme and PH Diagram [45]

A preliminary dimensioning of the Heat Pump has been done in order to perform detailed and precise market research. The design has been developed by using an iterative process based on the following equations.

$$Q_{cond} = \dot{m}_{H2O} * c_{p_{H2O}} * \Delta T_{cond} \quad (1)$$

$$P_{el} = \frac{Q_{cond}}{COP} \quad (2)$$

$$Q_{eva} = Q_{cond} - P_{el} \quad (3)$$

The water mass flow rate is guessed in order to calculate the heat in output (Q_{cond}) that, once that is fixed the Coefficient Of Performance (COP), makes equal the heat absorbed by the HP evaporator (Q_{eva}) with the one produced by the thermal panels.

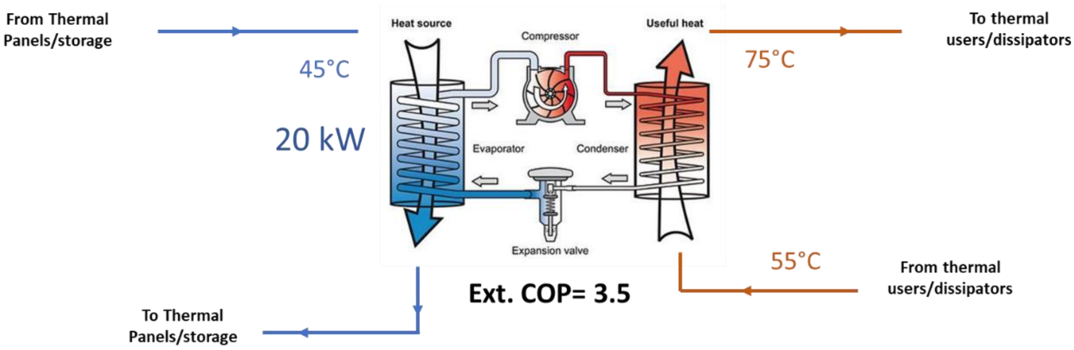

Figure 43 ENVISION Heat pump Scheme

Considering the hypothesis summarized in Figure 43, the resulting preliminary dimensioning for the Heat Pump is reported in Table 3.

Table 3 ENVISION HP Dimensioning

ENVISION HP	
H2O_Massflow_? [kg/s]	0.38
COP	3.5
Q_cond [kW]	31.51
P_el [kW]	9.00
Q_eva[kW]	22.51
error (Q_eva-Q_Panels)	0.0254%

Basing on these results, it has been performed market research investigating possible suppliers. Since the relatively small size of the required technology and the high-temperature gap between condenser-evaporator, it has not been possible to find standard products on the market. Therefore, a custom HP model has been needed and proposed by ENEREN (http://eneren.it/), *ENEREN EKW050K*.

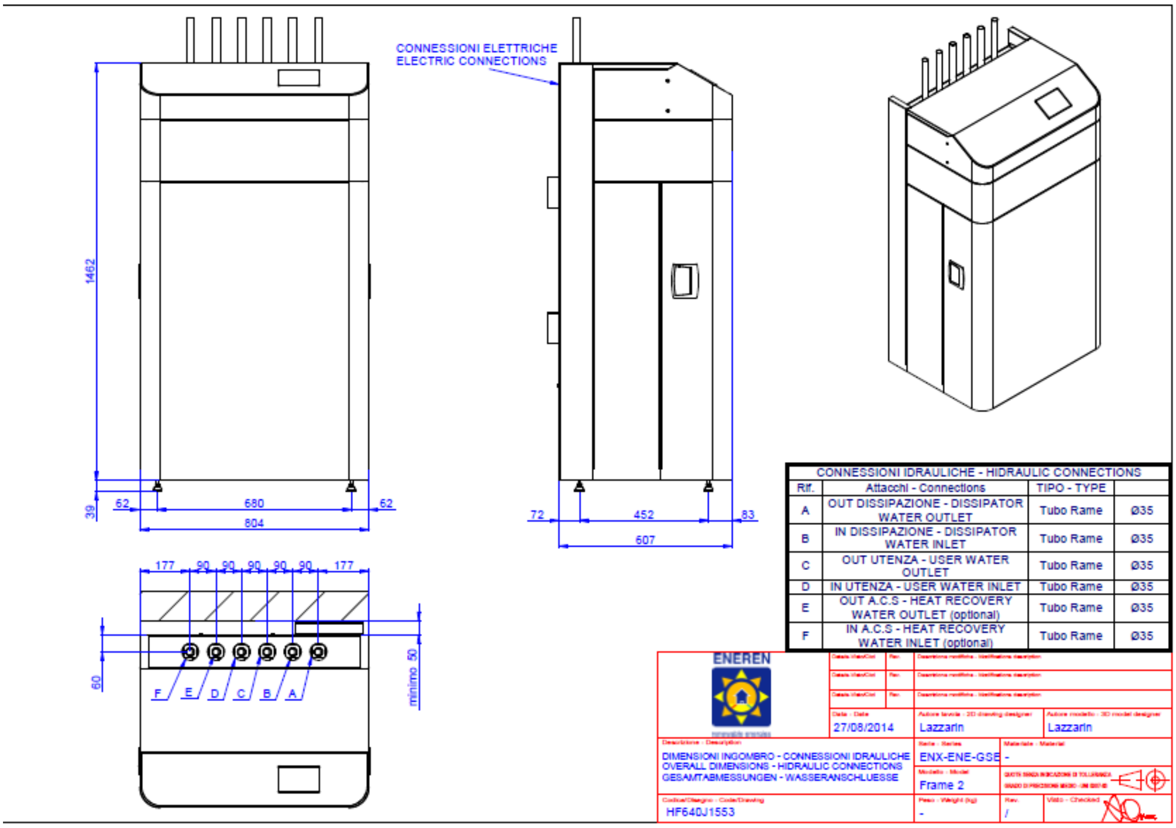

Figure 44 ENEREN Heat Pump Dimensions

The technical specifications provided by the supplier are reported in the following Tables.

Table 4 HP Performances, Scenario A

Heating@50/75°C;20/15°C;100%;		
Heating capacity	27.3	kW
Heating capacity [UNI14511]	27.3	kW
Water Flow user side	957	l/h
Water Pressure drops user side	<5	kPa
Water Flow source side	3067	l/h
Water Pressure drops source side	<5	kPa
Total Power input	10.0	kW
Total Power input [UNI14511]	10.0	kW
Total Absorbed Current	16.1	A
COP	2.73	
COP [UNI14511]	2.72	
SCOP High Temperature	4.20	
ERP Efficiency High Temperature	163.00	
ERP Efficiency Class High Temperature	A+++ / H.T. Heat Pump	

Table 5 HP Performances, Scenario B

Heating@50/75°C;40/35°C;100%;		
Heating capacity	46.3	kW
Heating capacity [UNI14511]	46.3	kW
Water Flow user side	1622	l/h
Water Pressure drops user side	<5	kPa
Water Flow source side	6391	l/h
Water Pressure drops source side	16	kPa
Total Power input	10.0	kW
Total Power input [UNI14511]	10.0	kW
Total Absorbed Current	16.1	A
COP	4.65	
COP [UNI14511]	4.61	
SCOP High Temperature	4.20	
ERP Efficiency High Temperature	163.00	
ERP Efficiency Class High Temperature	A+++ / H.T. Heat Pump	

Table 6 HP Performances, Scenario C

Heating@50/75°C;30/25°C;100%;		
Heating capacity	36.5	kW
Heating capacity [UNI14511]	36.5	kW
Water Flow user side	1280	l/h
Water Pressure drops user side	<5	kPa
Water Flow source side	4661	l/h
Water Pressure drops source side	9	kPa
Total Power input	10.0	kW
Total Power input [UNI14511]	10.0	kW
Total Absorbed Current	16.1	A
COP	3.62	
COP [UNI14511]	3.61	
SCOP High Temperature	4.20	
ERP Efficiency High Temperature	163.00	
ERP Efficiency Class High Temperature	A+++ / H.T. Heat Pump	

Table 7 ENVISION HP main characteristics

HP Main Characteristics		
Maximum absorbed current (FLA) [without options]	21	A
Start-up current (LRA) [without options]	118	A
Sound power level Lw (base unit)	74	db(A)
Sound pressure level Lp (base unit) @ 10 m EN3744	43	db(A)

Sound power level Lw (Low noise unit)	70	db(A)
Compressors/Circuits	1/1	
Power Supply	400 / 3+N / 50	
Refrigerant	R134a	
GWP	1430	
Oil Type	POE RL32-3MAF	
Oil Volume	3.4	l
Dimensions [LxDxH]	804x607x1462	mm
Weight without options	296	kg

2.1.1.3 Micro Gas Turbine

The presence of a micro Gas Turbine, in the context of ENVISION Project, is fundamental to provide electric power to both HP and the SPM. Furthermore, in relation to an increased need for thermal production by the Savona Campus management, supplementary heat production will be provided by the installed mGT.

The chosen size of the mGT consists of nominal electrical power of 100 kW and thermal power higher than 150 kW. In order to meet the ENVISION and installation site requirements, some specifications have been performed in advance of market research, resumed in the following lines.

The cogeneration system must be powered by methane gas at a pressure of about 60 mbar, it must therefore be equipped with an internal compressor integrated into the package. The thermal energy must be made available in the form of hot water, recovering the heat from the exhaust gases of the microturbine, at a temperature at least above 75°C. A nominal electrical efficiency of at least 29% and an overall efficiency of at least 80% is required. Considering the space available in the installation area, a service area of no more than 20 m^2 and a physically occupied area of no more than 3.5 m^2 with a maximum height of 2.5 m is required. Limited NOx and CO emissions are required with a limit of 15 ppmv. In relation to the residential environment, the noise level has to be compliant with a maximum permissible sound power level of 90 dBA measured according to ISO 9614-2:1996. The mGT will be installed in a room closed on two sides by a grating and with air intakes on the wall as reported in Figure 45.

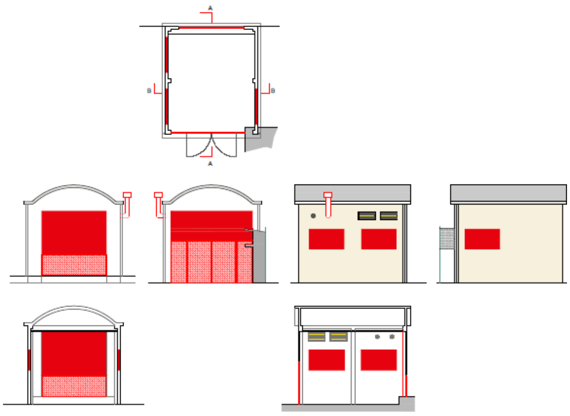

Figure 45 mGT installation building

Considering the room dedicated to the installation, the microturbine can be equipped for outdoor installation, with supply air intake directly from the room. In order to perform optimized management of the ENVISION energy-hub, the system must be able to be controlled remotely and must be able to operate in parallel with the electrical network. The partial load operation is an important aspect, therefore, a technical minimum not exceeding 50% of the nominal power is required.

The draw of the mGT system that will be installed in Savona is reported in Figure 46 and Figure 47.

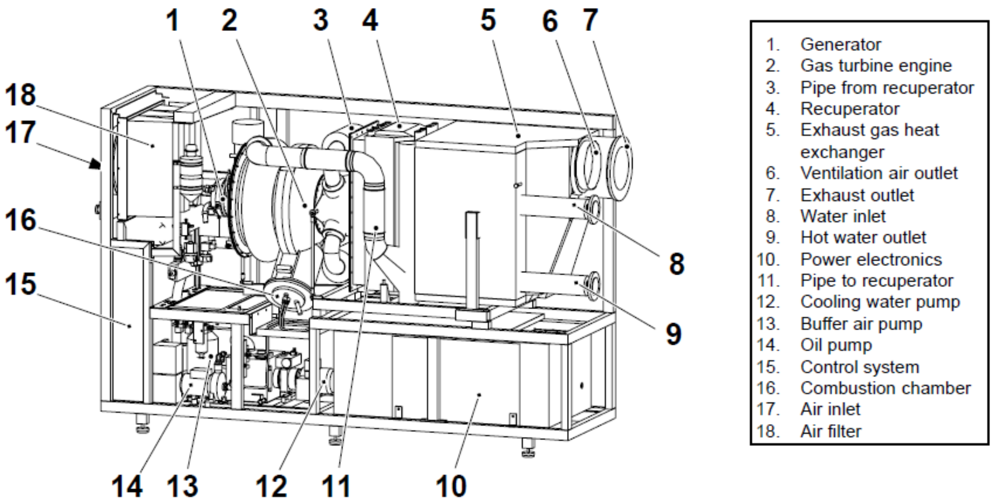

Figure 46 mGT draw

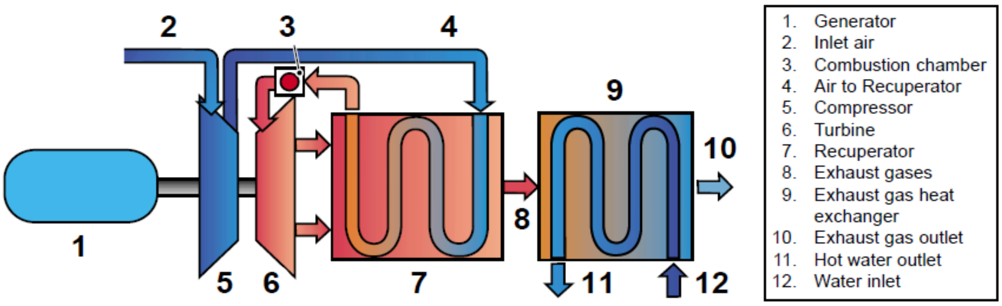

Figure 47 Operational scheme of considered mGT

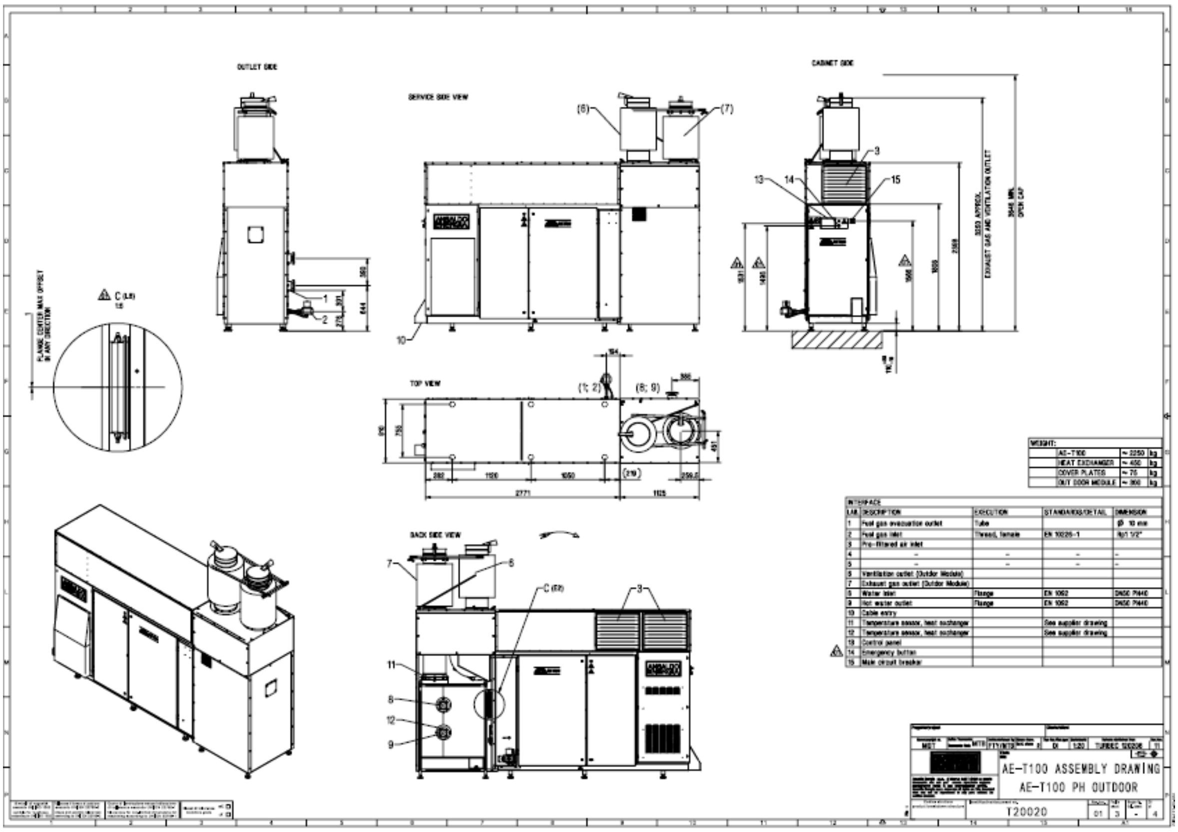

Figure 48 ENVISION mGT drawing

The main characteristics of the selected mGT unit are reported in the following Tables.

Table 8 Air intake characteristics

Air intake characteristics	
Air Inlet Temperature	from -10°C to 40 °C
Max air humidity	< 100%, without condensing
Air particle, max dimensions	1 µm
Max Air flow at 15 °C (process+cooling)	1.69 kg/s (1.38 m3/s)
Nominal air flow (process)	0.78 kg/s
Max air flow (process)	0.80 kg/s
Max pressure losses in inlet air duct (new prefilter)	< 180 Pa

Max pressure losses in inlet air duct (used prefilter)	< 320 Pa
Max temperature air flow	80 °C
Nominal temperature of exhaust gases	270 °C
Max temperature of exhaust gases	325 °C
Nominal exhaust gases flow	0.80 kg/s
Max exhaust gases flow	0.87 kg/s
Max pressure drop in outlet duct	250 Pa

Table 9 Heat recovery unit characteristics

Heat recovery unit characteristics	
Water side	
pH	6.5 ÷ 8.0
Max water pressure	1.6 MPa (g)
Max water flow	4 l/s
Min inlet water temperature	0 °C
Max inlet water temperature	150 °C
Water volume	25 l
Exhaust side	
Max exhaust gases temperature	325 °C

Table 10 Gas specifications

Gas specifications	
Fuel	Natural Gas
Pressure min/max	25 ÷ 100 mbar (g)
Temperature min/max	0 ÷ 50°C
Wobbe Index min/max	43 ÷ 55 MJ/Nm3
Max H2O content	150 ppmv
Max H2S content	5 mg/Nm3

Table 11 mGT Electrical characteristics

Electrical characteristics	
Nominal Voltage	400 VAC Tri-phase
Phases	3
Nominal frequency	50 Hz
Admissible frequency variations	-1.5
Synchronization	Automatic
Admissible voltage variations	-1.5
Nominale Power	100 kW, 120 KVA
Nominal current	144 A rms 100 kW, 400 V, cosϕ=1 178 A rms 100 kW, 400 V, cosϕ=0,81

Max current	203 A rms 100 kW, 340 V, cosf=0,83
Start-up current	25 A rms peak
Start-up power	15 kW peak

2.1.1.4 Thermal Storages

The Thermal Energy Storages (TES) installed are common water inertial storages. Their working principle is to keep constant the liquid volume, varying the energy stored in terms of liquid temperature. A temperature stratification occurs inside the storage.

TES is a system component used to store the thermal energy produced in excess by a generator and to return it to the user at any time it is required. They, therefore, allow to balance the energy demand and to deal with peak demands, in order to allow easier management of thermal generation. The simplest way to accumulate thermal energy is the heating (or cooling) of a solid or liquid body, rarely of a gas. The storage capacity of thermal energy by material or substance is expressed by its specific heat; in case the substance used to store heat is affected by a phase shift the storage capacity increases due to the contribution given by the latent heat. The most common substance used to store heat energy is water in the liquid state, while combinations of sodium nitrate and potassium nitrate are used in phase shift systems. Depending on the temperature reached by the fluid, storage systems can be divided into low, medium or high-temperature storage. The former does not exceed a temperature of 100°C and generally use water in the liquid state. Medium-temperature storage systems, up to 500°C, make use of molten salts and are used in solar power plants providing a reserve of energy to compensate for variations in the intensity of solar radiation. The high-temperature storage tanks, up to 1300°C, use ceramic material as a storage medium and are designed for specialized applications particularly related to the iron and steel industry. As concerns low-temperature storage tanks, they are generally steel tanks with insulating coating; in order to exploit as much as possible the natural water stratification, cold water is introduced from below and hot water is taken from above.

The storage tank used for ENVISION project is of the latter type, supplied by Di Camillo company. The installed capacity is **500 l**, the storage is represented in Figure 49.

Figure 49 500 litres Thermal Energy Storage in Savona Campus

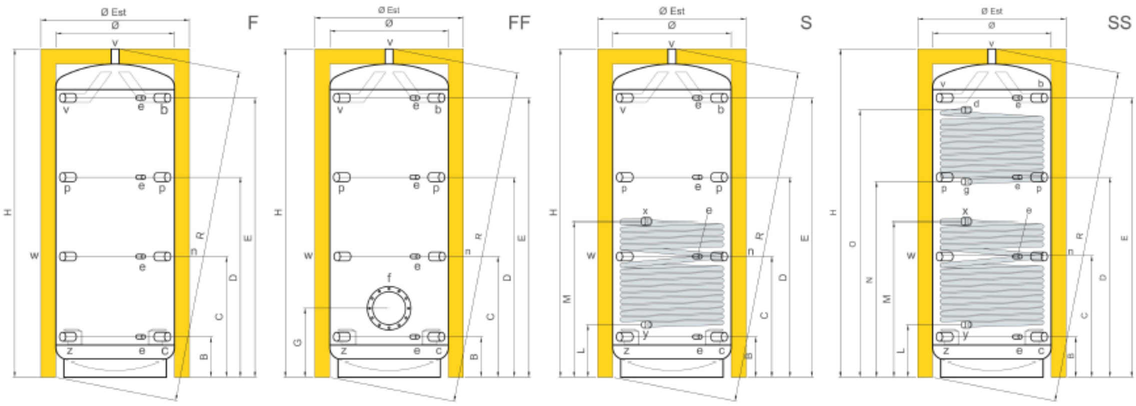

Figure 50 Inertial storage tank draw

Dimensioni (mm)				Quote (mm)										Serp (Mq)		Peso
LT	Ø	H	Ø Est	R	B	C	D	E	G	L	M	N	O	INF	SUP	Kg.
300	500	1565	600	1680	200	580	955	1335	-	280	800	900	1260	1.60	1.20	101
500	650	1650	750	1820	260	640	1015	1395	-	340	860	960	1320	2.00	1.80	143
800	790	1730	990	1790	270	650	1025	1405	460	350	870	975	1325	2.70	2.10	186
1000	790	2180	990	2230	270	810	1325	1855	460	350	1035	1295	1775	3.50	2.50	231
1250	950	2095	1150	2160	340	800	1265	1725	530	420	1020	1205	1645	3.80	3.00	265
1500	1000	2135	1200	2210	360	785	1285	1745	550	440	1100	1265	1665	4.50	3.20	288
2000	1100	2455	1300	2530	365	925	1495	2050	555	445	1085	1495	1975	4.80	4.00	386
2500	1200	2495	1400	2580	400	945	1490	2035	590	480	1080	1555	1955	5.00	4.00	420
3000	1250	2710	1450	2800	410	1020	1635	2245	600	490	1210	1765	2165	6.00	4.20	475
4000	1400	2820	1600	2920	470	1085	1695	2310	660	550	1270	1790	2230	7.00	5.00	653
5000	1600	2850	1800	2970	475	1085	1700	2310	665	555	1275	1830	2230	8.00	5.00	757

Figure 51 Inertial storage tank dimensions

For what concerns the intermediate storage, it is still needed to clarify some aspects with panels provider, but similar (or even smaller) tank is expected.

As mentioned, these storages are inertial. This typology contains heating water (not subject to hygiene quality regulations) and is commonly used in large systems or in systems for integration with heating. Inertial storage tanks in closed vessel circuits do not require special corrosion protection, have lower pressures and are not subject to scale deposits, as the system is only filled once with water. They are often made of carbon steel, have lower costs and a greater guarantee of durability. The heat exchange with the hot fluid is realized with an external tube or plate heat exchangers, this allows the exchange of higher power in reduced spaces and facilitates maintenance. As well, with regard to the integration, the technical water is taken from the tank and sent to the auxiliary source (boiler, heat pump). There are also inertial vessels intended only for the storage of domestic hot water; they are subjected to appropriate anti-corrosion treatments and must meet hygiene requirements.

2.1.1.5 Thermal Dissipators

Four thermal dissipators are installed in the Thermochemical Power Group (TPG) Laboratories and supplied by Alfa Laval. They are composed of a shell and tube heat exchanger and variable speed fans, controlled by inverter, which allow modifying the cooling power and therefore the thermal power consumed. These components, in fact, are used precisely in order to simulate a thermal user as could be, for example, the heating system of a building, for an overall capacity of **300 kWth**. The thermal dissipation system is reported in Figure 52.

Figure 52 Savona Campus Laboratories thermal dissipators

In this section, the technologies included in the ENVISION Southern demosite have been presented. Figure 53 shows a rendering of the final aspect expected for the demosite developed with SketchUp software.

Figure 53 ENVISION Southern Demosite rendering

2.2 System modelling

With the aim of performing a detailed design of the ENVISION system and, furthermore, to define a control strategy based on a Model Predictive Control approach, mathematical models of the main components of the Southern Demosite have been computed. In the following sections, a detailed description of solar façade panels and Heat Pump is provided; while concerning the mGT, considering the important background of the author research group, it has been used a simplified state-space model developed in previous activities. All the models are developed in Matlab Simulink ambient.

2.2.1 Solar façade panels model

The aim of solar façade panels model is to relate the external ambient conditions (such as ambient temperature, solar radiation and wind velocity) with a thermal output. This conversion from solar radiation to thermal power strictly depends on the colour chosen for the panels, since that to each colour is related a different absorption property. Three colours of uncovered façade panels have been investigated for Savona Campus demo (white, red and black). The presented model, validated by SEAC (partner of ENVISION Consortium), is based on experimental coefficients.

The governing equation that relates to environmental parameters with solar panels heat production is reported below [46]:

$$\frac{Q_{panel}}{A_{panel}} = \eta_0 G - c_1 \left(T_{avg_{panel}} - T_{ambient}\right) \tag{4}$$

Where G is the solar radiation and c_1 is a specific experimental panel parameter.

Dividing all the members of the equation for G, the equation can be also rewritten considering the charts in Figure 54 where are reported the performances of the panels depending on their colour and technology. Panel 1, Panel 2 and Panel 3 refer to covered solar collectors, not considered in this analysis. Panel 4, Panel 5 and Panel 6 refer respectively to Black, Red and White uncovered panels, the one considered in this analysis.

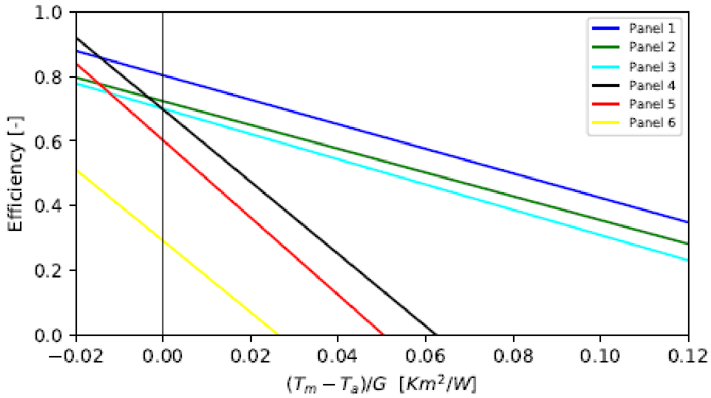

Figure 54 Façade panel performances curve

Furthermore, the η_0 efficiency is affected by the angle of incidence of solar radiation.

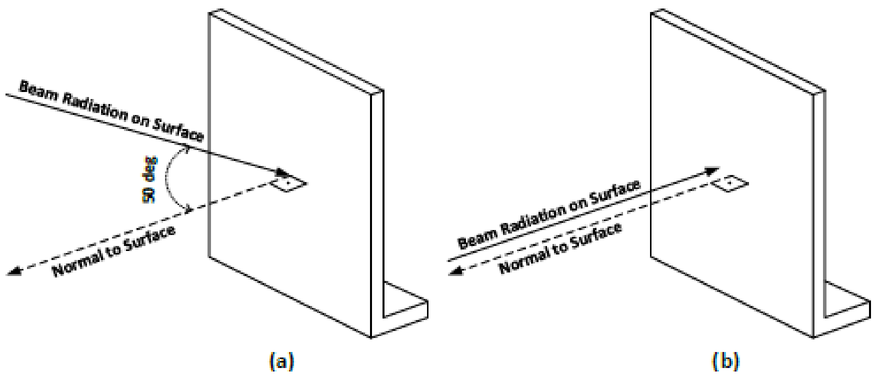

Figure 55 Incidence of solar radiation

The dependence of $\eta_0$to solar radiation, the incidence is reported in Figure 56, where not a really strong variation is foreseen for incidence lower than 50°C. Therefore, for simplification, this aspect has been neglected in the following steps; even because some incoherencies occurred in the highlighted area.

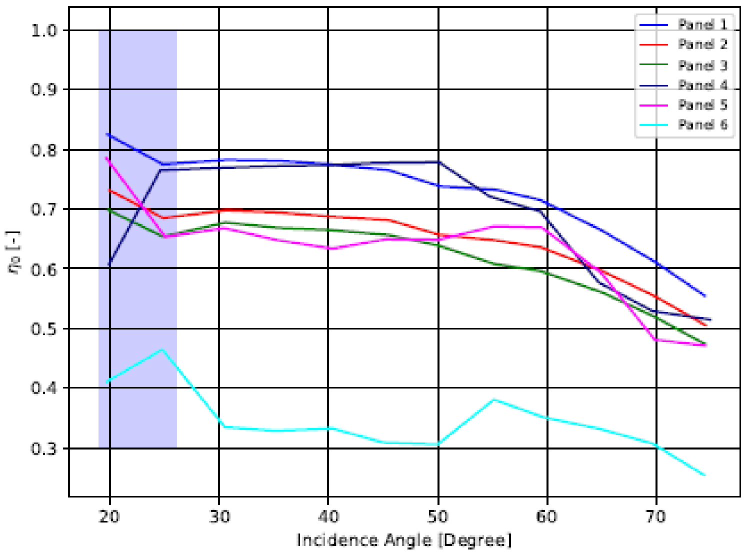

Figure 56 η_0 dependence on incidence angle

Therefore, basing on this curve it is possible to estimate the efficiency and, known *G* also the thermal production of the panel.

Furthermore, some losses can be considered due to the presence of wind (significant for wind velocity higher than 2.5 m/s) and are calculated as follows:

$$Q_{lossesWind} = c_6 * u_{WindVelocity} * G * A_{panel} \tag{5}$$

The values of c_6 are listed in Table 12 for the three considered panels:

Table 12 Wind Thermal Losses coefficient [s/m]

White Uncovered Panel	0.036
Red Uncovered Panel	0.058
Black Uncovered Panel	0.093

Therefore, the actual thermal production for each panel is:

$$Q_{real} = Q_{panel} - Q_{lossesWind} \tag{6}$$

The dynamic behaviour of the thermal panel is calculated considering as a control volume, the liquid contained in the panel piping. Referring to the control volume highlighted in Figure 57, the energy equation for the solar façade panel is reported in (7).

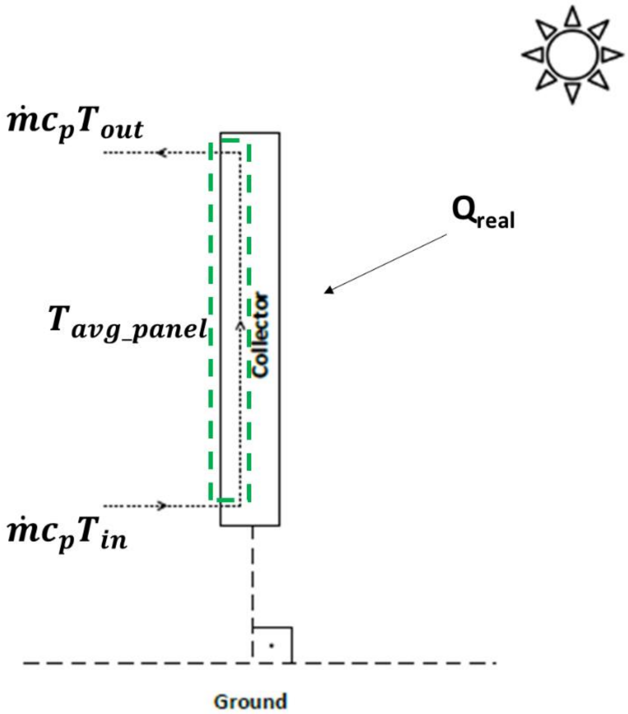

Figure 57 Solar Panel Control Volume

$$C\frac{dT_{avg_{panel}}}{dt} = Q_{real} + \dot{m}c_pT_{in} - \dot{m}c_pT_{out} \tag{7}$$

Where C is the thermal capacity. This value is provided by the façade panel supplier and depends on the colour of the panel considered. The values are reported in Table 13.

Table 13 Panel Thermal Capacity [kJ/K]

White Uncovered Panel	15.57
Red Uncovered Panel	17.63
Black Uncovered Panel	17.50

Considering that:

$$T_{avg_{panel}} = \frac{(T_{in} + T_{out})}{2} \tag{8}$$

Substituting (8) in (7) and solving the differential equation it is possible to calculate the outlet temperature from the panel considering the dynamics of the system.

The results of the validated model, developed by SEAC, are reported in Figure 58, Figure 59 and Figure 60.

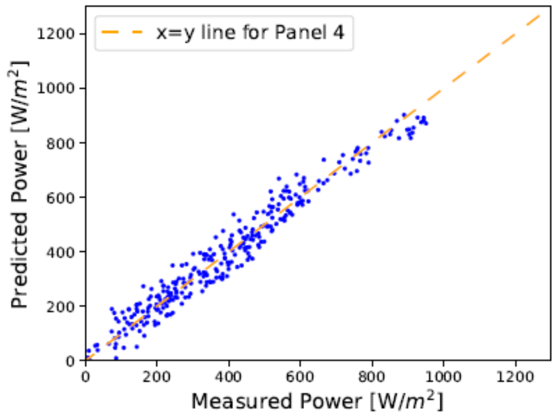

Figure 58 Black Uncovered Panel parity plot

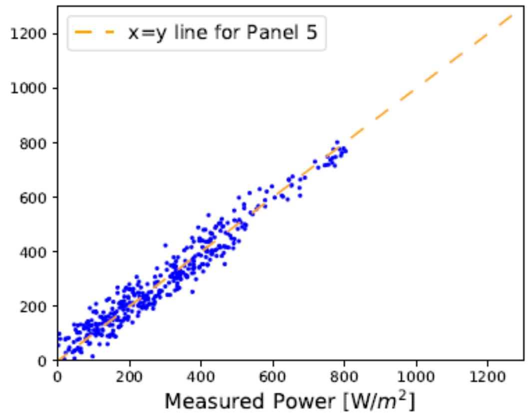

Figure 59 Red Uncovered Panel parity plot

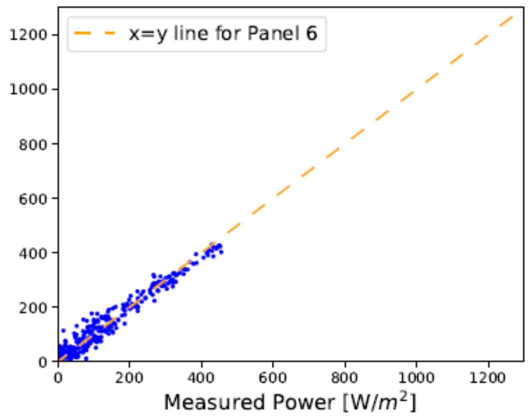

Figure 60 White Uncovered Panel parity plot

2.2.2 Heat Pump model

The second model implemented is a Heat Pump model. This HP works in interaction with the solar façade panels and the District Heating Network; therefore, a significative pressure gap between evaporator and condenser is required. The modelling of an HP system requires the modelling of all its four main components: two heat exchangers (condenser and evaporator), a compressor and an expansion valve. Furthermore, control is needed in order to guarantee the required temperature on the outlet user side (connection to DHN).

In a preliminary phase, a simplified model has been developed. Then, foreseeing the chance of an on-field validation, a more detailed model has been developed and initially validated on another Heat Pump system, installed in Savona Campus.

A brief description of these two models is presented in the next sections.

2.2.2.1 Simplified HP model

This model concerns only energy equations for dynamic calculations, assuming that those are the most relevant in the overall system behaviour. The selected working fluid is R1233zd(E) since seems the most performant for the considered temperature range [47]. The main assumption of this model consists into considering the outlet of condenser and evaporator on the saturation line, automatically, without the need for lamination valve control.

Figure 61 and Figure 62 represent schematically the operation of the considered HP.

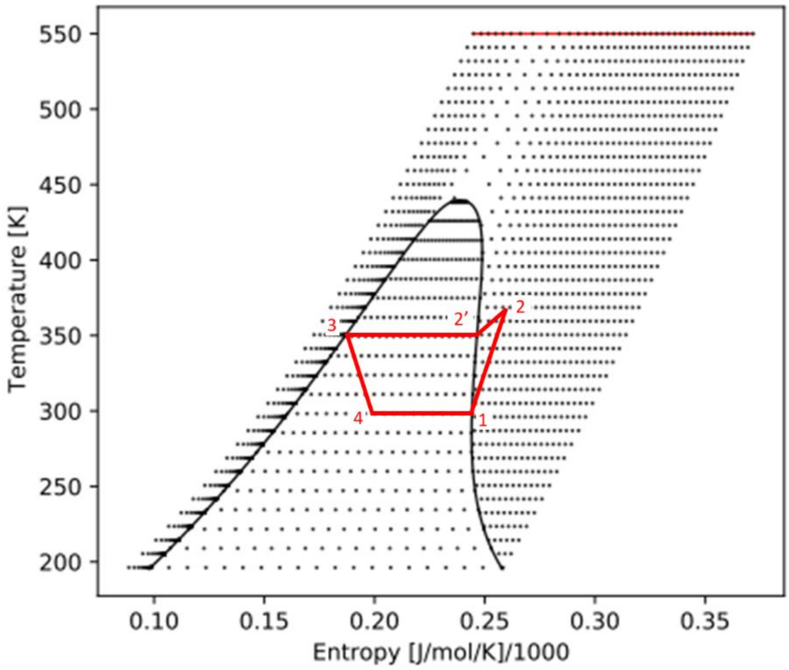

Figure 61 HP cycle on R1233zd(E) T-s diagram

1-2: compression of the working fluid to the higher-pressure level.

2-2': superheated gas cooling

2'-3: working fluid condensation, reaching saturated liquid conditions (x=0)

3-4: iso-enthalpic expansion

4-1: evaporation, reaching saturated vapour conditions (x=1)

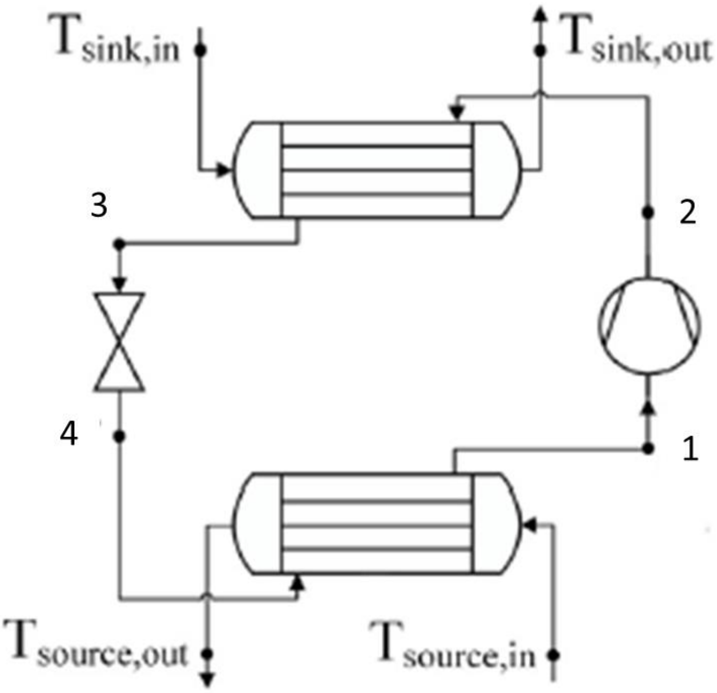

Figure 62 HP scheme

Where:

$T_{source,in}$ is the temperature from the panels [K]

$T_{source,out}$ is the return temperature to the panels [K]

$T_{sink,in}$ is the return temperature from the DHN [K]

$T_{sink,out}$ is the outlet temperature to the DHN [K] (required at 75-80°C).

In order to properly consider the working fluid properties, REFPROP tool has been adopted [48].

A dedicated description of the equations implemented for each component is below reported.

- **<u>Evaporator:</u>** In this component, the energy equation is calculated in a dynamic approach. Considering that this transformation occurs in a two-phase status for the working fluid, the calculated evaporation temperature is directly linked to the evaporation pressure through the use of fluid properties calculations by REFPROP. The energy equation, the equilibrium between the two fluids, is used to calculate the $T_{source,out}$ and is here reported:

$$\dot{m}_{source} c_{p_{source}} \left(T_{source,out} - T_{source,in}\right) = \dot{m}_{workingFluid} (h_4 - h_1) \qquad (9)$$

Where h_1 is obtained with REFPROP considering that point 1 belongs to the saturated vapour line, therefore once known the evaporation temperature is known, while h_4 is input from the expansion valve.
The dynamic approach is used to calculate the variation of the evaporator temperature and pressure.

$$C\frac{dT_{eva}}{dt} = UADelta_{TML,Eva} + \dot{m}_{workingFluid}(h_4 - h_1) \quad (10)$$

Where:

$$Delta_{TML,Eva} = \frac{(T_{source,in} - T_{eva}) - (T_{source,out} - T_{eva})}{\ln(\,(T_{source,in} - T_{eva})/(T_{source,out} - T_{eva}))} \quad (11)$$

The characteristics of the evaporator heat exchanger are reported in Table 14.

Table 14 Evaporator Characteristics [49]

Thermal Capacity C	52.8 kJ/K
Heat Exchange Area A	1 m^2
Global Heat Exchange Coefficient U	1000 W/(m^2K)

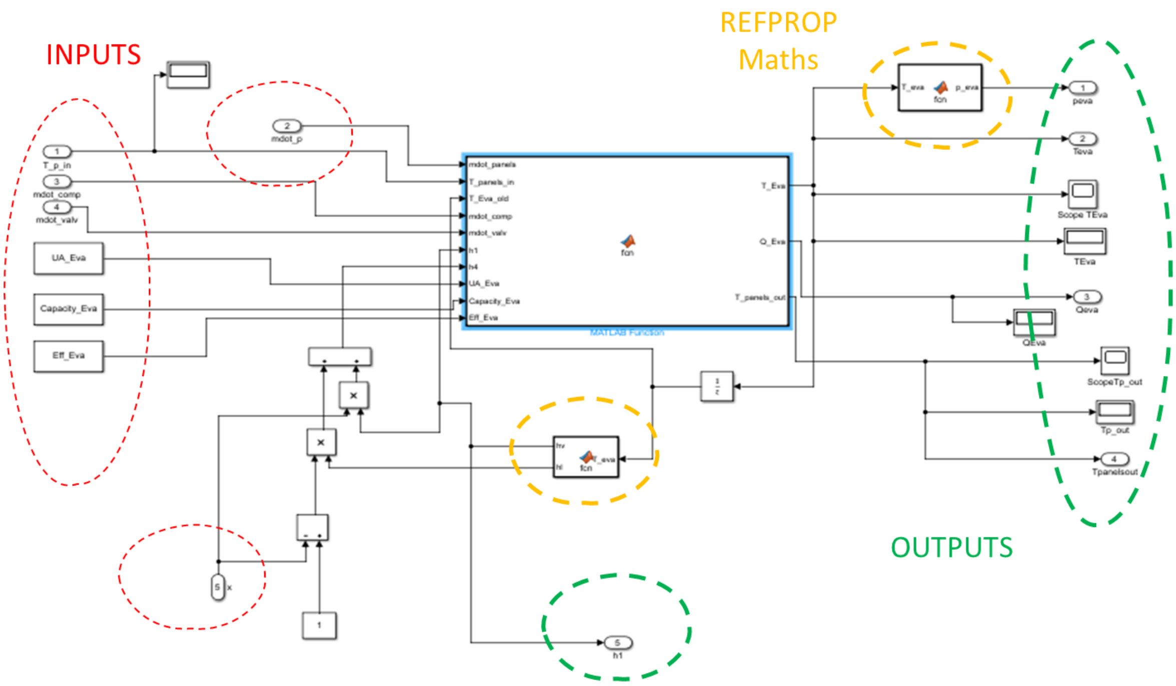

Figure 63 Evaporator Simulink Model

- **Compressor:** This component is responsible for the mass flow regulation in the HP. A controller on its rotational speed is therefore integrated, with the aim of guaranteeing the temperature required by the DHN.

  The main input of the component is the pressure gain needed and, therefore, the pressures from evaporator and condenser. The outputs are the outlet temperature from the compressor, that depends on compressor efficiency, and the working fluid mass flow rate.

  The compressor efficiency, in this simplified model, has been set as a constant value of 80%. Therefore, the outlet compressor temperature is calculated starting from the outlet enthalpy calculation:

$$h_2 = h_1 + \frac{h_{2s} - h_1}{\eta_{comp}} \tag{12}$$

  Where h_{2s}, the isentropic outlet enthalpy, is calculated with REFPROP referring to point 1 known conditions and the condenser pressure.

  REFPROP is then used to calculate the outlet temperature, knowing the condition of pressure and enthalpy in point 2.

  The mass flow rate $\dot{m}_{workingFluid}$ is then obtained referring to the compressor map reported in Figure 64. The pressure ratio $\beta = \frac{p_{cond}}{p_{eva}}$ is known, while the rotational speed is defined by the control system: with these two inputs, the mass flow rate is then obtained starting from the volumetric one, thanks to REFPROP density calculations.

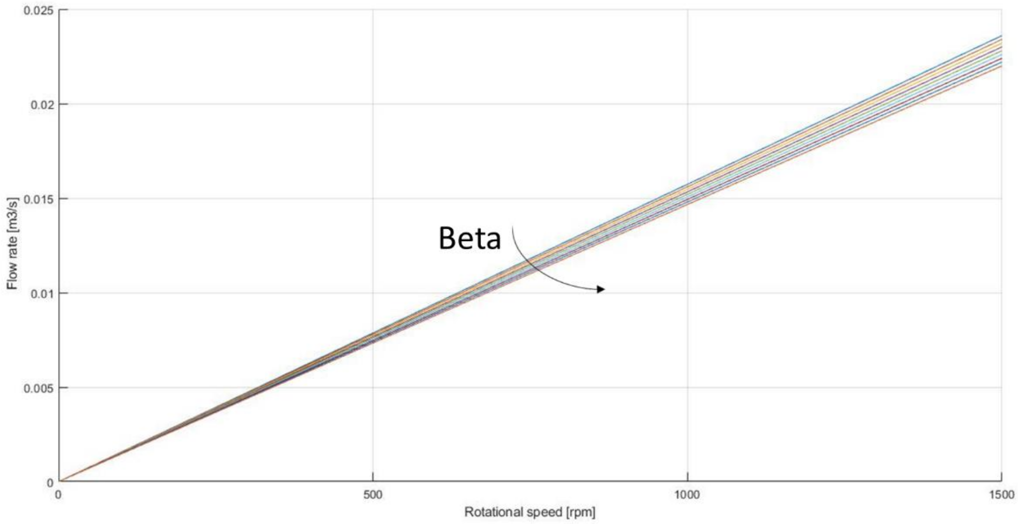

Figure 64 Compressor map

  The delay is then determined considering two characteristic delays: a first-order delay of 10 s and a downtime delay of 1 s [49].

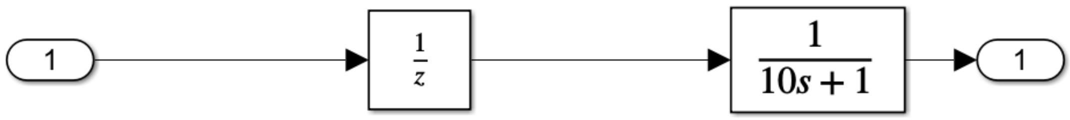

Figure 65 Compressor delays

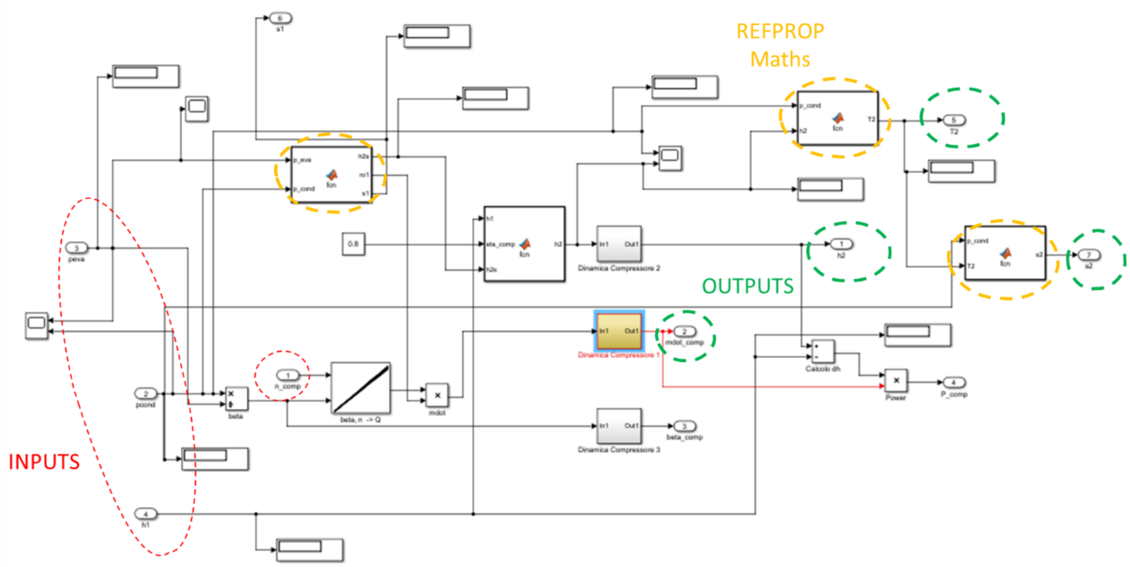

Figure 66 Compressor Simulink Model

- **Condenser:** The approach used for the condenser is similar to the one developed for the evaporator, with the addition of the superheated portion of heat exchange. The aim of this component is to calculate the outlet temperature of the sink side (DHN supply) and the dynamic of the condensing pressure.
  To do that the analysis can be divided into two sections. The first related to the phase changing is (2'-3) and the second that is related to the superheated vapour cooling (2-2').
  The equation of energy for the phase changing portion is used for the calculation of the intermediate outlet sink temperature $T'_{sink,out}$ (corresponding to the saturated vapour for the HP working fluid):

$$\dot{m}_{sink} c_{p_{sink}} \left(T'_{sink,out} - T_{sink,in} \right) = \dot{m}_{workingFluid} \left(h_{2'} - h_3 \right) \quad (13)$$

  Where $h_{2'}$ and h_3 are calculated with REFPROP, since respectively in vapour and liquid saturation state.
  The sink mass flow rate is then heated again in the superheated portion of the heat exchange (2-2'). In order to obtain the actual outlet temperature of the sink $T_{sink,out}$, the following equation is implemented:

$$\dot{m}_{sink} c_{p_{sink}} \left(T_{sink,out} - T'_{sink,out}\right) = \dot{m}_{workingFluid}(h_2 - h_{2'}) \tag{14}$$

In the end, with the aim of calculating the temperature (and therefore) pressure variations in the condenser, a dynamic calculation is developed only referring to the phase changing region:

$$C \frac{dT_{cond}}{dt} = UADelta_{TML,Cond} + \dot{m}_{workingFluid}(h_{2'} - h_3) \tag{15}$$

Where:

$$Delta_{TML,Cond} = \frac{\left(T_{cond} - T_{sink,in}\right) - \left(T_{cond} - T'_{sink,out}\right)}{\ln((T_{cond} - T_{sink,in})/(T_{cond} - T'_{sink,out}))} \tag{16}$$

The characteristics of the condenser heat exchanger are reported in Table 14.

Table 15 Condenser Characteristics [49]

Thermal Capacity C	55.4 kJ/K
Heat Exchange Area A	1 m^2
Global Heat Exchange Coefficient U	1500 W/(m^2K)

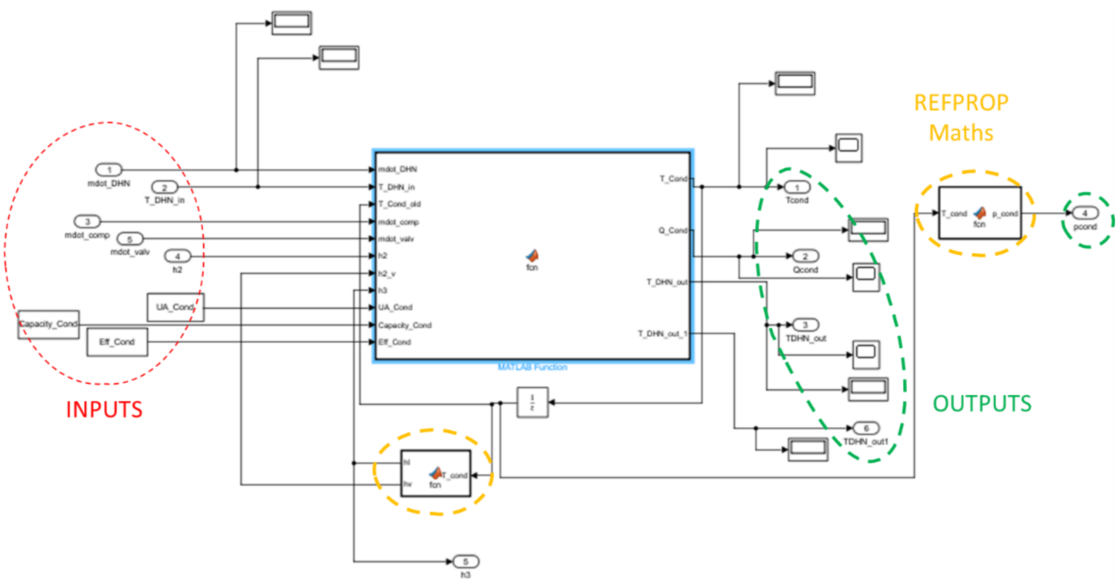

Figure 67 Condenser Simulink model

- **<u>Expansion valve:</u>** The aim of this component is to close the circuit through an isenthalpic lamination. Therefore, once that is known the enthalpy in the outlet of the condenser h_3, the same enthalpy is given to point 4 (inlet of evaporator, h_4). Furthermore, since that enthalpy and pressure are known, the vapour content can be calculated with REFPROP.

A delay is then defined in order to estimate the dynamic of the system as reported in a first-order delay of 20 s and a downtime delay of 1 s [49].

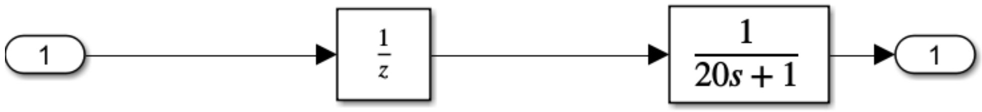

Figure 68 Expansion valve delays

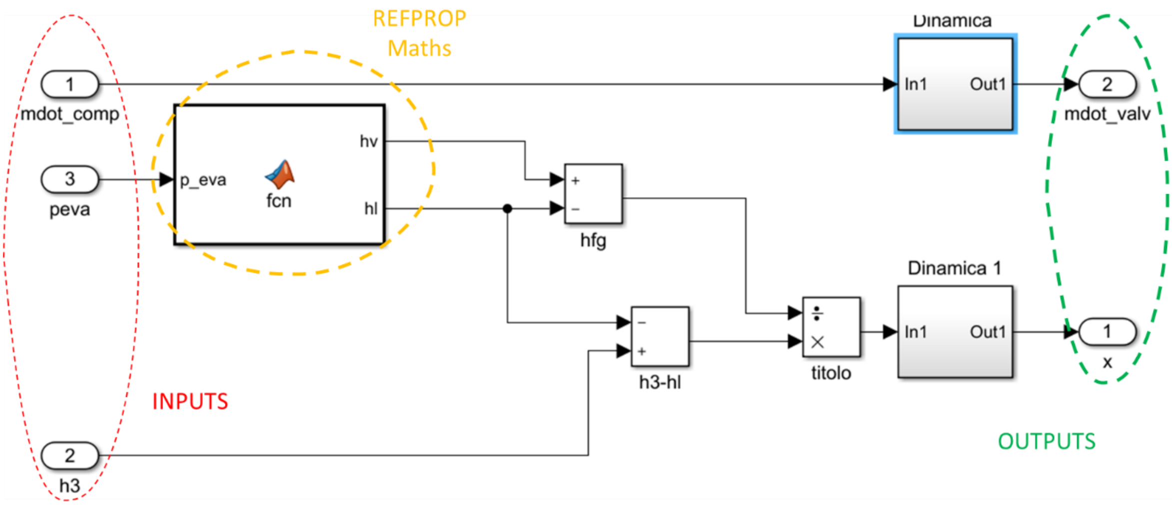

Figure 69 Expansion valve Simulink Model

- <u>**Control system:**</u> As stated before, there is the need to properly manage and control the system in order to provide the required temperature to the sink (80° C). To do that, the mass flow rate is regulated via the compressor rotational speed.
  With this aim, a PI controller has been implemented using the dedicated Simulink tool, the coefficients that guarantee a proper and stable system management are reported in Table 16.

Table 16 PI control coefficients

Proportional coefficient	154.81
Integral coefficient	17.51

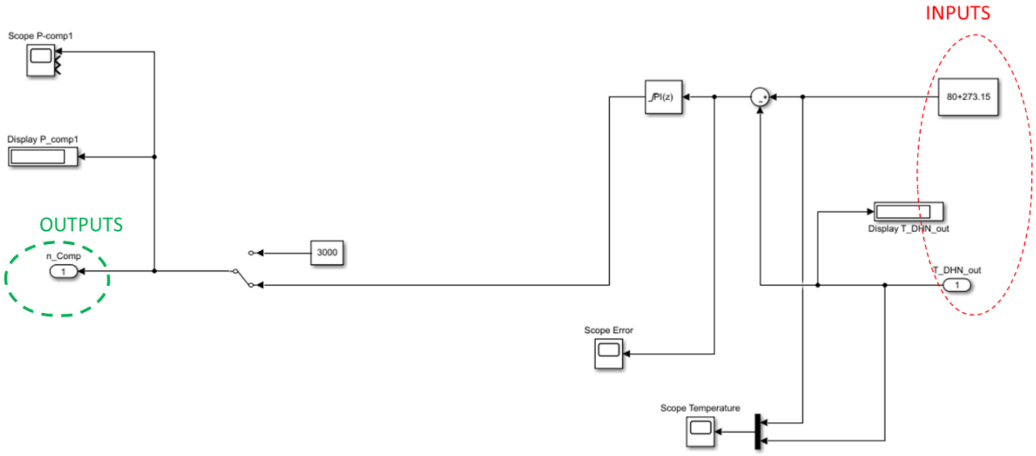

Figure 70 Control system Simulink model

All the mentioned components are properly interconnected, resulting in the overall HP system modelling represented in Figure 71.

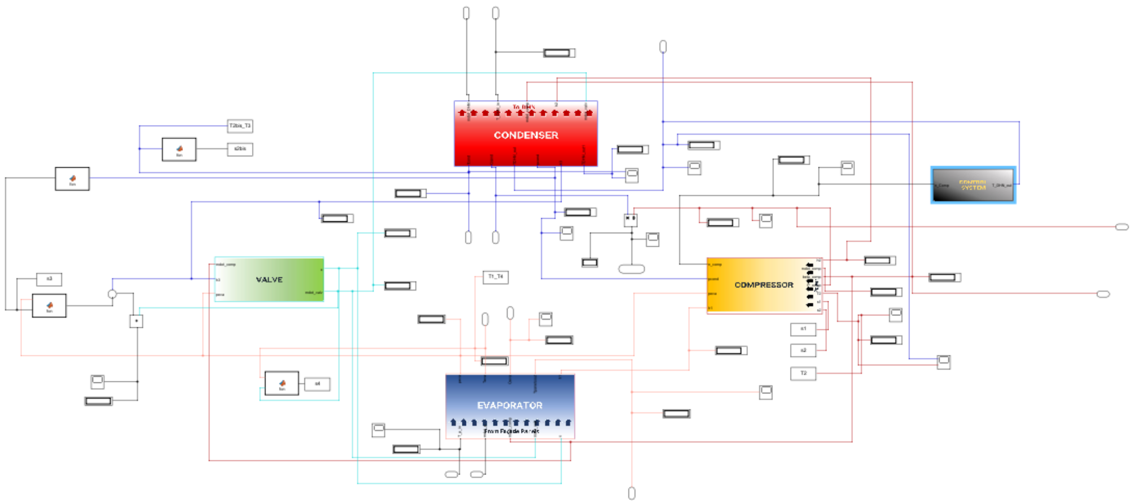

Figure 71 HP simplified Simulink model

2.2.2.2 Detailed approach for HP modelling: a brief description

Within the context of another H2020 project (Pump-Heat), where the author's research group is involved, a Heat Pump is installed and therefore a more detailed HP model has been developed with the chance of providing a static validation. Although this HP has a different configuration from the one related to the ENVISION project, the modelling approach can be adapted also on the ENVISION HP foreseeing the chance of an on-field validation. In the considered conditions, the HP works in a temperature range of -10 °C (evaporator side) and 25 °C (condenser side). The working fluid chosen for this configuration is R600.

The main development obtained with this approach is related to the heat exchangers. The moving boundary approach has been adopted [50] [51].

With this approach, it is assumed that in a region (with variable-length λ) of the heat

exchanger occur two-phases conditions. The length of λ varies depending on the operative conditions of the heat exchanger.
A brief description of this approach is provided with the example of a condenser.

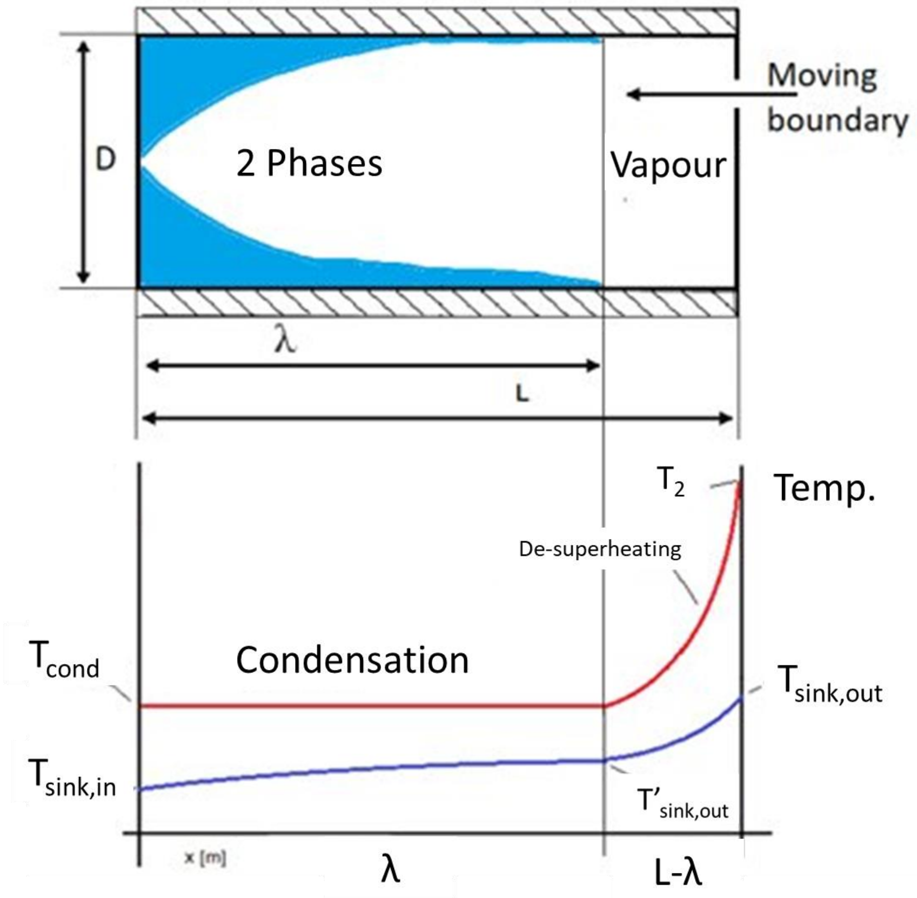

Figure 72 Moving boundary approach for HP Condenser

The calculation model is based on a system of equations that to be solved need to start from a first guess. The solutions obtained from the set of equations are then applied in the dynamic solution. A schematic description of this calculation is reported in Figure 73.

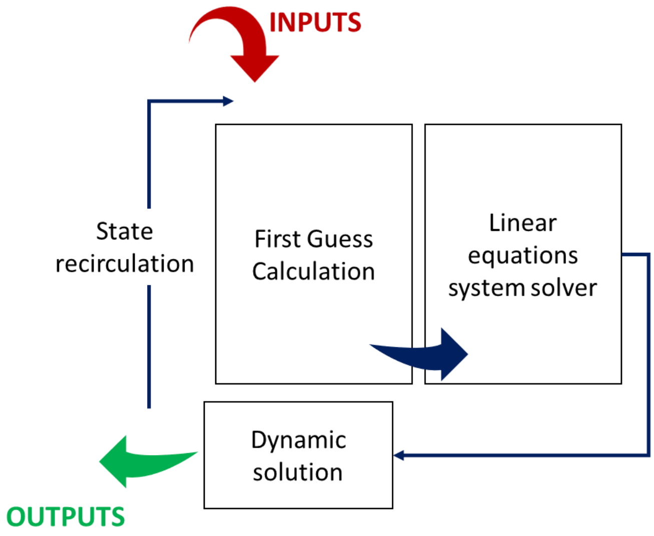

Figure 73 Calculation scheme for Heat Exchanger in a moving boundary approach

Applying the scheme presented in Figure 73 to the condenser the inputs of the system are:

$T_{sink,in}$ [K]: sink side, inlet temperature in the condenser;

$\dot{m}_{sink}$ [kg/s]: sink side, mass flow rate;

$c_{p_{sink}}$ [J/(kgK)]: sink side, specific heat;

h_2 [J/kg]: inlet condenser enthalpy, HP side;

T_2 [K]: inlet condenser temperature, HP side;

$\dot{m}_{working\ fluid}$ [kg/s]: HP working fluid mass flow rate.

The characteristic parameters of the heat exchanger, provided by the manufacturer, are:

L [m]: condenser length;

D [m]: condenser height;

U_s [W/(m^{2}K)]: global heat exchange coefficient, in the vapour region;

U_b [W/(m^{2}K)]: global heat exchange coefficient, in the two-phase region.

Therefore, the first guess calculation is reported in Table 17, where in blue are reported the unknown variables.

Table 17 First guess set of equations

$\dot{Q}_{b,w} = \dot{m}_{workingfluid}\,(h_{2'} - h_3)$	(17)
$\dot{Q}_s = \dot{m}_{workingfluid}\,(h_2 - h_{2'})$	(18)
$T'_{sink,out} = T_{sink,in} + \dfrac{\dot{Q}_{b,w}}{\dot{m}_{sink}\;c_{p,sink}}$	(19)
$T_{sink,out} = T'_{sink,out} + \dfrac{\dot{Q}_s}{\dot{m}_{sink}\;c_{p,sink}}$	(20)
$\lambda = L\left[1 - \left(\dfrac{\dot{Q}_s}{\dot{Q}_{b,w} + \dot{Q}_s}\right)\right]$	(21)

The first guess solutions obtained from Table 17, are then implemented in the system of equations presented in Table 18 and solved using the Trust-region-dogleg algorithm, where in blue are highlighted the final unknown variables.

Table 18 Equations system for condenser solution

$$\begin{cases} \dot{Q}_s = \dot{m}_{sink}\;c_{p,sink}\left(T_{sink,out} - T'_{sink,out}\right) \\ \dot{Q}_s = \dot{m}_{workingfluid}\,(h_2 - h_{2'}) \\ \dot{Q}_s = U_s\,(L - \lambda)\,D\,\dfrac{\left(T_2 - T_{sink,out}\right) - \left(T_{cond} - T'_{sink,out}\right)}{\ln\dfrac{\left(T_2 - T_{sink,out}\right)}{\left(T_{cond} - T'_{sink,out}\right)}} \\ \dot{Q}_{b,w} = \dot{m}_{sink}\;c_{p,sink}\left(T'_{sink,out} - T_{sink,in}\right) \\ \dot{Q}_{b,w} = U_b\,\lambda\,D\,\dfrac{\left(T_{cond} - T'_{sink,out}\right) - \left(T_{cond} - T_{sink,in}\right)}{\ln\dfrac{\left(T_{cond} - T'_{sink,out}\right)}{\left(T_{cond} - T_{sink,in}\right)}} \end{cases}$$

$\dot{Q}_s$ [W]: Heat exchanged in de-superheating region

$\dot{Q}_{b,w}$ [W]: Heat exchanged in two-phases region

λ [m]: two-phases region length

The dynamic solution is then obtained, with the equations below.

$$\Delta T_{ml} = \frac{\left(T_{cond} - T'_{sink,out}\right) - \left(T_{cond} - T_{sink,in}\right)}{\ln \frac{T_{cond} - T'_{sink,out}}{T_{cond} - T_{sink,in}}} \tag{22}$$

$$\frac{dT_{cond}}{dt} = \frac{\dot{m}_{workingfluid}\,(h_{2'} - h_3) - U_b\,\lambda\,D\,\Delta T_{ml}}{Capacity_{cond,liquid} + Capacity_{cond,solid}} \tag{23}$$

The static validation of this model has been possible thanks to experimental data provided by the HP supplier, Mayekawa. The results obtained for this approach have shown a good fitting with the experimental ones, both at design and off-design points, as reported in Figure 74.

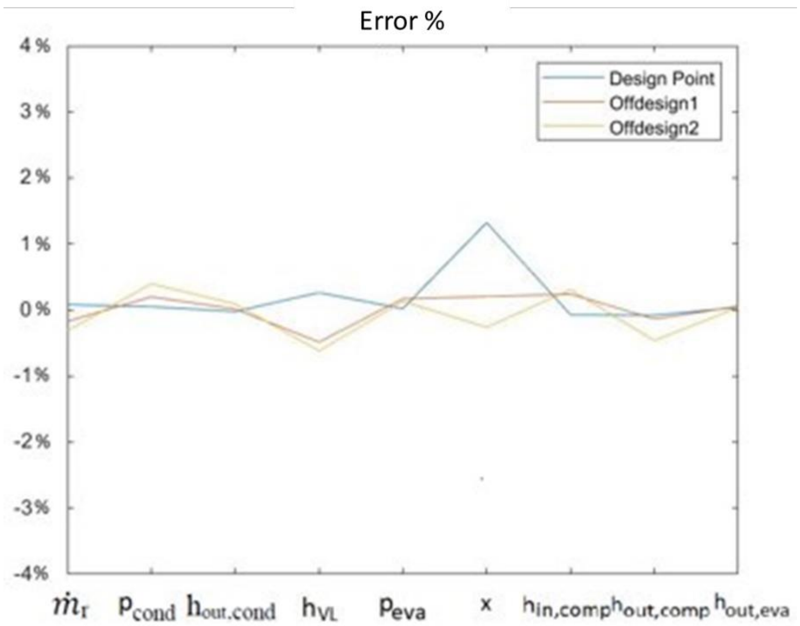

Figure 74 Error of main model parameters compared to the experimental data provided by Mayekawa

In order to match the results also in off-design operation, it has been needed to provide also a law for the variation of the different global heat exchange coefficients and also compressor efficiency. As a reference, here is reported below the estimated variation of U_b in comparison with a literature study on the variation of this coefficient [52], the two lines in Figure 75 show a close trend.

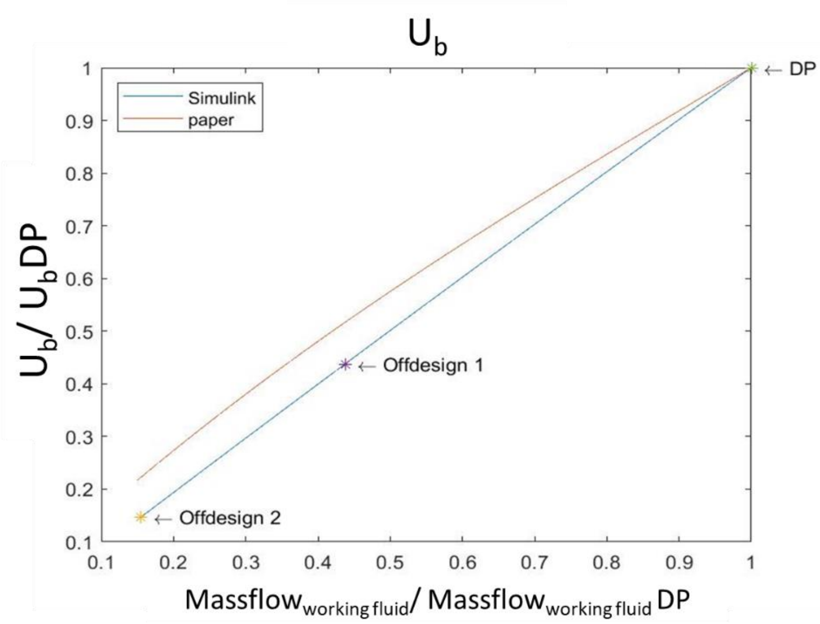

Figure 75 U_b coefficient comparison with a literature study

The complete dynamic validation of this model requires on-field activities that will be carried out by the author’s research group. Therefore, this can be just considered as a benchmark for the further validation also of the foreseen ENVISION HP installation.

Once defined and described the models of the ENVISION system, it is necessary to develop the optimization of the system both at hardware level (component sizing), and software level (control algorithm).

2.3 System configuration optimization

Before developing the management of the system, it is necessary to properly define the best configuration. To do that, at the first step, it is discussed in detail the best panel configurations, secondly, a thermo-economic evaluation is provided including also storages and sizing of the components.

2.3.1 Panel configuration

In order to properly define the configuration of the system, some evaluations have been carried out, considering both technical and economic aspects. The importance of the described models is also related to the evaluation of the best operational parameters of the solar façade panels in coupling with the Heat Pump. The considered parameters are the interconnection between the panels (series or parallel) and the mass flow rate through the panels. It is worth to specify that the series connection consists of single branches (i.e. White-Red-Black in series), interconnected in parallel each other, as reported in Figure 76. Considering the available building surface, 24 panels (for the size of 2x1 m) are estimated (8 for each colour).

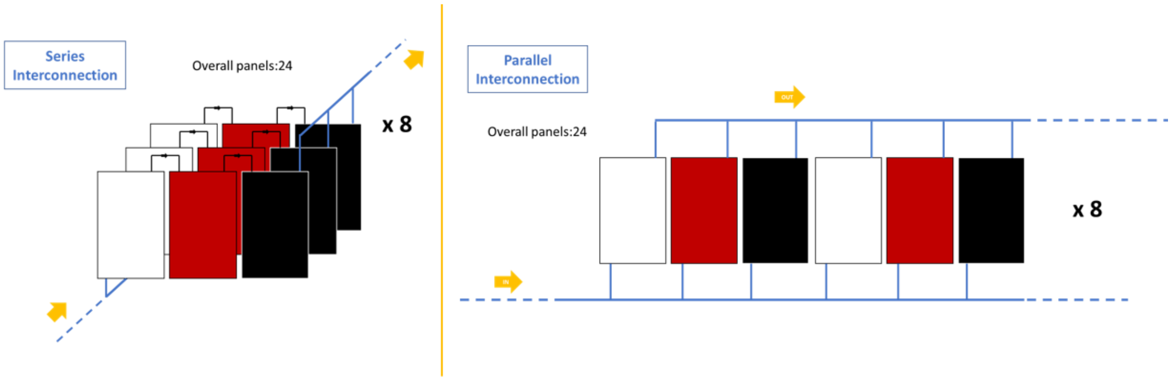

Figure 76 Series or parallel Panels interconnection

One of the most critical aspects for coupling solar façade panels with a heat pump is to find the configuration that leads to the best overall system performance. Different schemes have been simulated varying the mass flow rate through the single panels (min: 0.01 kg/s, max: 0.05 kg/s as available in the literature for the thermal and PV thermal panels [53], [54]) and the series or parallel panels configuration. The tests have been performed assuming a constant heat demand by the DHN at the fixed temperature of 75°C, this aspect allows to minimize the influence of other parameters focusing on the impact of façade panels on HP performances. The compressor power absorption of the HP is the only term of significant consumption in the system. In this scenario, the parameter that allows the evaluation of the system is the COP (Coefficient Of Performance) i.e. the index of efficiency of the HP, defined as $COP = \frac{Q_{cond}}{P_{el}}$. Having set as constant the heat demand, the only terms affecting the COP is the electric consumption of the HP. The best configuration of the system is the one that leads to lowest consumptions and, therefore, highest COP.

In add:

$$Q_{cond} = P_{el} + Q_{eva} \tag{24}$$

Where Q_{cond} is the heat demand and Q_{eva} the heat provided by the panels. Therefore, the maximization of heat produced by the panels guarantees the best performances of the system. Simulations for different scenarios have been performed in Matlab Simulink environment considering two representative solar days for cold and hot season. The results of these simulations are reported in Figure 77 and Figure 78.

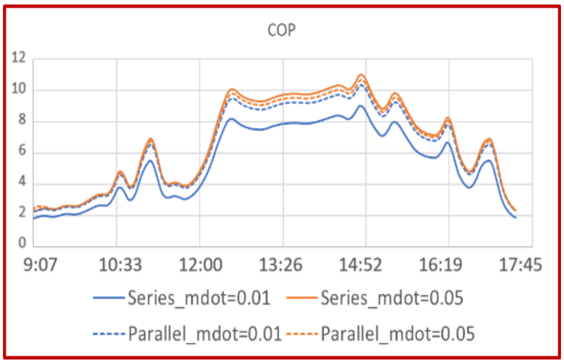

Figure 77 COP for different configurations in hot season

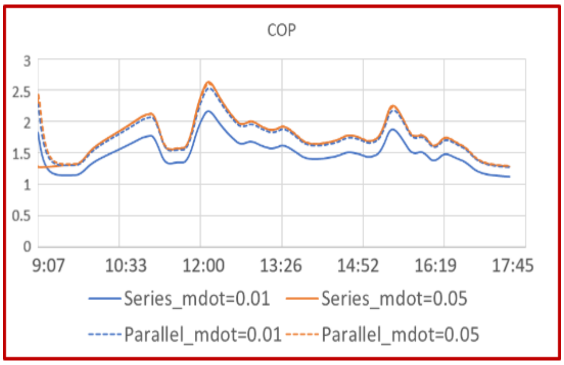

Figure 78 COP for different configurations in cold season

As evident, the performances of the HP are definitely higher in the summer conditions, where the panels perform better thanks to the significant solar radiation. For what concerns the impact of the studied configurations on the system performances, as it can be seen in Figure 77 and Figure 78 the highest COP values are reached for the interconnection in series with the max value of mass flow rate trough the panels. Indeed, the heat provided by the panels is given as a result of temperature and mass flow rate; increasing the mass flow rate the temperature in the outlet of the panels decreases. On the other hand, an increasing of mass flow rate leads to higher temperature in return at the inlet of façade panels circuit: this aspect leads to a lower panel efficiency. The parallel configuration on one side guarantees a higher overall value for the mass flow rates (single panel mass flow rate x 24 panels), but on the other side does not lead to high temperatures as the series configuration does (see Figure 79 for the example of summer conditions). Therefore, it can be concluded that the most exploitation of solar panels is possible with the configuration in series, maximizing the panel mass flow rate.

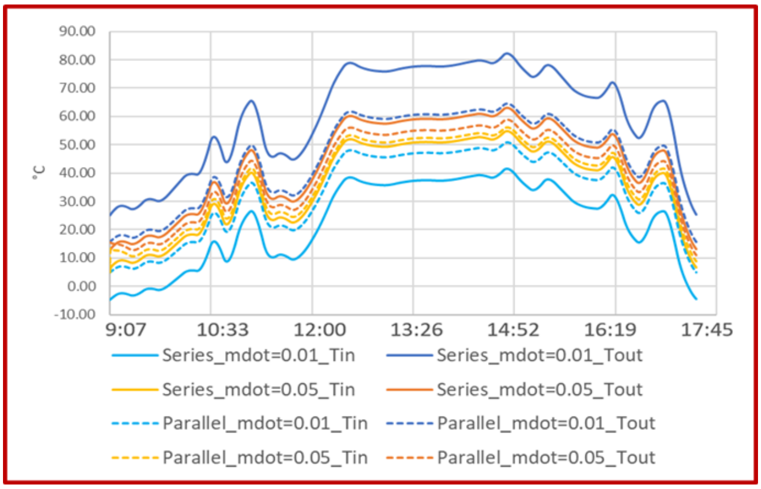

Figure 79 Inlet and Outlet temperature for the panels in different configurations

As an example of the proper operation of the PI control implemented in the HP model, with the aim of providing constant temperature to the DHN (80 °C), the temperature of the mass flow provided to the user by the HP is reported in Figure 80.

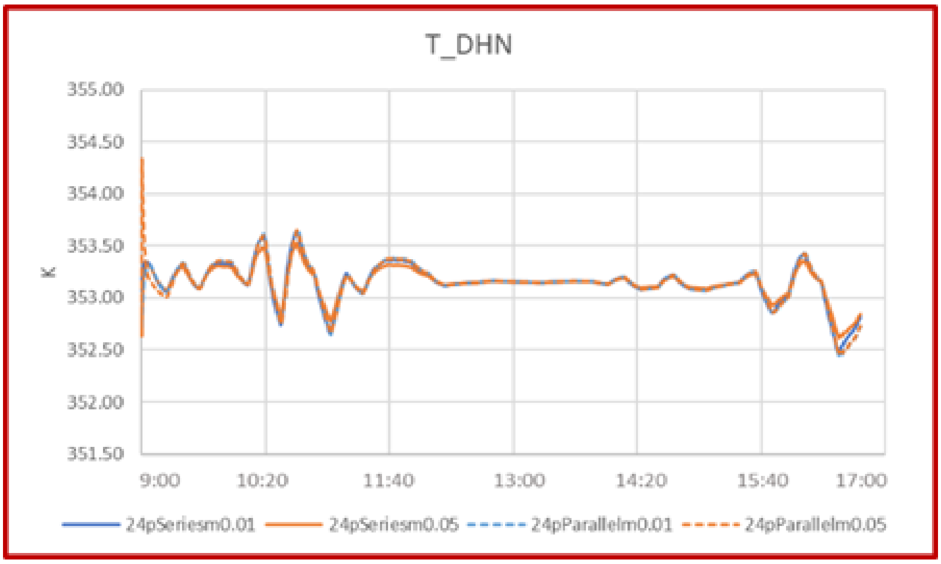

Figure 80 DHN Inlet temperature

2.3.2 System sizing

In this section, a detailed parametric analysis is performed focusing on the impact on the system of the choice of storage dimensions and the number of panels installed. Is therefore important to understand in detail how to properly design the heat source for a Heat Pump. In this section. At this stage, many solar thermal façade panels are considered as heat providers for the Heat Pump evaporator. In between inertial storage is installed in order to mitigate the strong fluctuations due to solar panels that can compromise the proper operation of the Heat Pump.

The layout of the system analysed is reported in Figure 81. Considering the scenario of Northern Europe for what concerns solar radiation and thermal demands (since represents the most challenging condition), a Heat Pump able to cover the thermal demand of 20 apartments, for a size of 52 m^2 each, is considered. The evaporator of this heat pump is supplied by solar façade panels interfaced with a Thermal Energy Storage (TES).

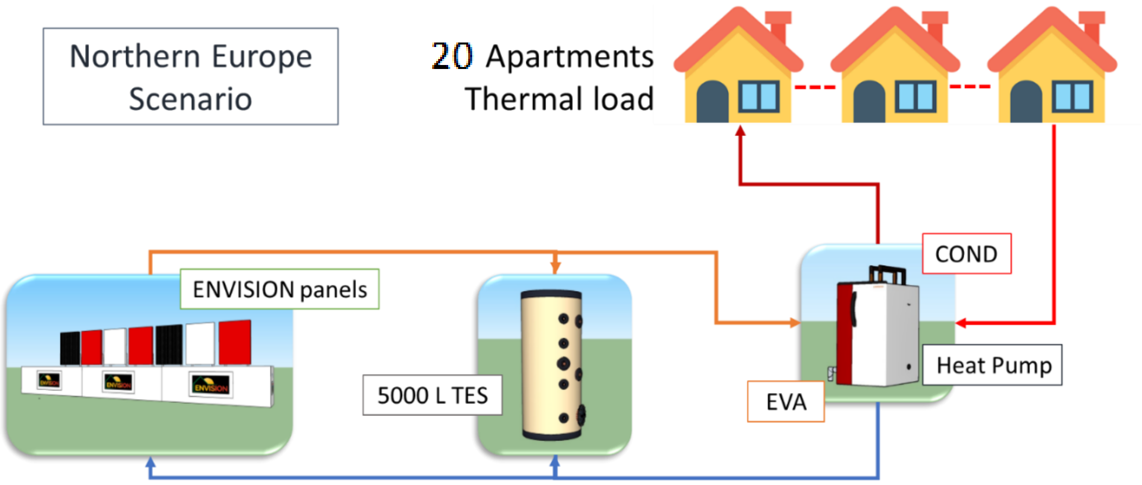

Figure 81 Simulated Layout

In the next section, it will be described the model and the environment used to perform the following analysis and results that considers both energetic and economic aspects.

2.3.2.1 Overall system model brief description

The model is developed in Matlab Simulink ambient, as reported in Figure 82. It consists of three main components: the solar façade panels (described previously, yellow area), the intermediate inertial TES (obtained from precedent activities [55], grey area) and the heat pump (described previously, orange area). The blue area represents the principle of TES management in order to maintain much stable as possible the water flow temperature seen by the evaporator. More in detail, if the temperature in the outlet of the solar thermal panels is higher than the average temperature inside the TES, the heat feeds the TES from the top, while the HP is supplied with the bottomer part of TES ("Charge phase"); on the other hand, when the outlet temperature from the panels is lower than the TES average, the flow from the panels feeds the bottom part of TES and the HP is supplied with the topper ("Discharge phase").

The Heat Pump has a PI control that aims to guarantee the setpoint temperature in the water outlet of the condenser (80°C). The thermal demand is regulated by changing the water mass flow rate through the HP condenser. In this context, the heat demand considers both DHW and space heating for 20 small apartments (52 m^2) as provided by BAM (member of ENVISION consortium) during their data collection campaign in previous. Considering a façade surface of around 52 m^2 per apartment, it has been decided to cover around the 17% of the available surfaces with façade panels (90 panels) or the 8% (45 panels).

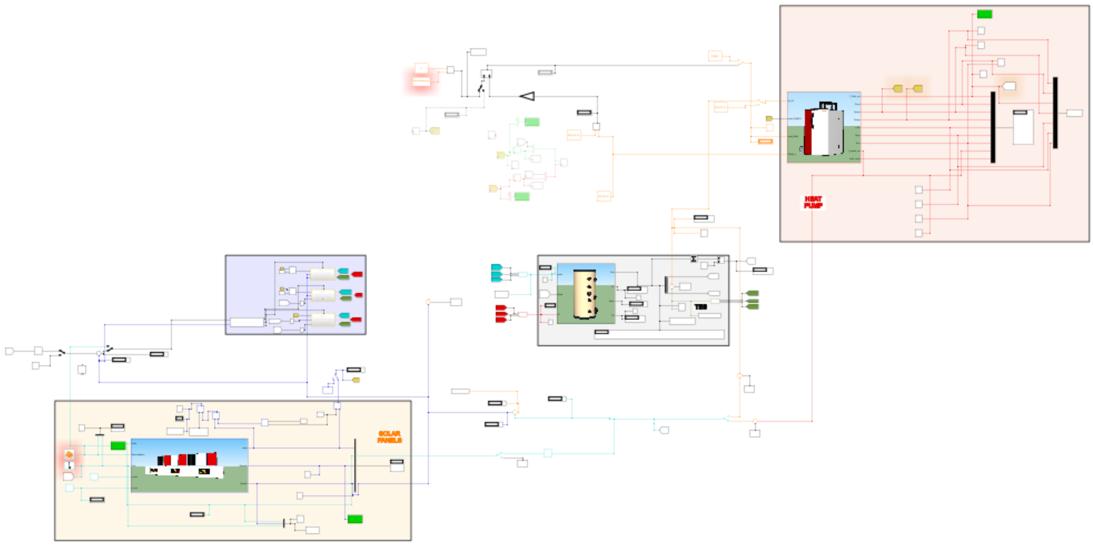

Figure 82 Matlab Simulink Model Layout

The inertial TES is considered with a size of three 5000L; the use of six 5000L TES will be also simulated in order to understand the impact of the TES size on the system behaviour. The higher TES capacity will, surely, increase the stability of the heat pump operation. This analysis is needed to understand the actual impact of this increase, remembering that large TES requires a lot of space to be installed.

2.3.2.2 Simulations and Results

Different scenarios have been simulated considering both winter and summer weather conditions on a daily base. As explained in the previous chapter, the main parameters are the number of panels and the number of 5000L TES. Therefore, the simulated configurations are reported in Table 19.

Table 19 Simulated scenarios

	90 Panels	45 Panels
3x 5000 l TES	Case A	Case B
6x 5000 l TES	Case C	Case D

The thermal demand for the 20 apartments, provided by BAM, is reported for a winter day in Figure 83. This demand refers to both space heating and domestic hot water (DHW). Moving to the summer period (no data available by BAM), it has been used the same trendline, but the demand has been conservatively set to 60% of the winter one.

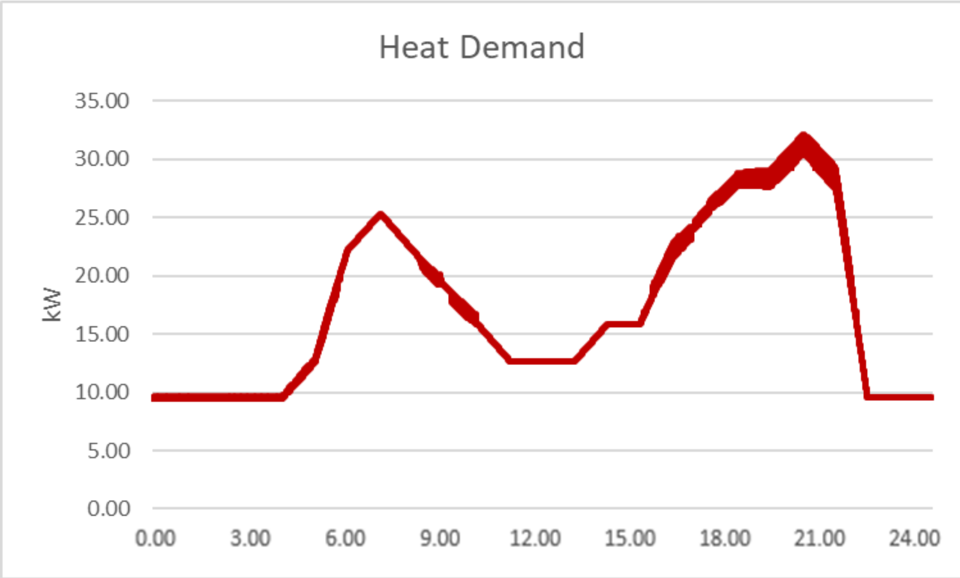

Figure 83 Thermal demand for 20 apartments of 52 m²

One of the main aspects to be considered in this analysis is the behaviour of the Heat pump, that it can be strongly affected by temperature fluctuations on the evaporator side.

- **Winter scenario**

Initially focusing on the winter period, Figure 84 shows the standard deviation of the water inlet temperature in HP's evaporator for the different configurations.

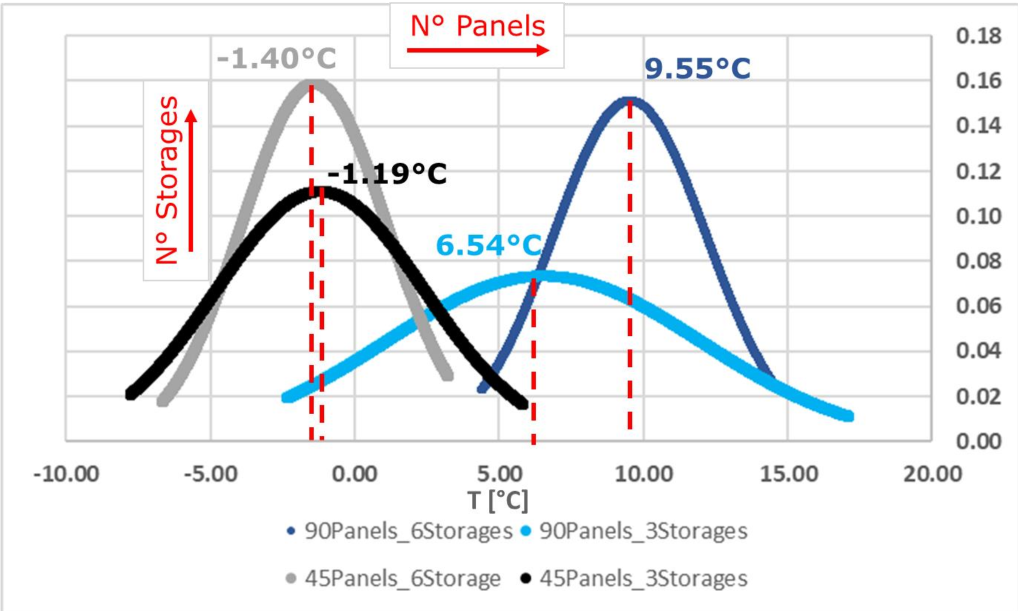

Figure 84 Temperature deviation of water inlet of HP's evaporator (Winter)

It is possible to underline that the higher number of panels leads to higher temperature on the evaporator side, since more heat is provided to the heat pump evaporator. This aspect leads to better efficiencies for what concerns the Heat Pump. Indeed the

Coefficient Of Performance (COP) increases when the temperature difference among evaporator and condenser gets lower (see Figure 85). Since that in this application, the condenser temperature is almost constant (fixed water outlet temperature due to DHN), an increase of evaporator temperature guarantees significantly higher COP. Generally speaking, the temperatures reached with 45 panels are not really interesting to justify the installation, while moving to 90 panels (around 17% of façade coverage) the results are more interesting.

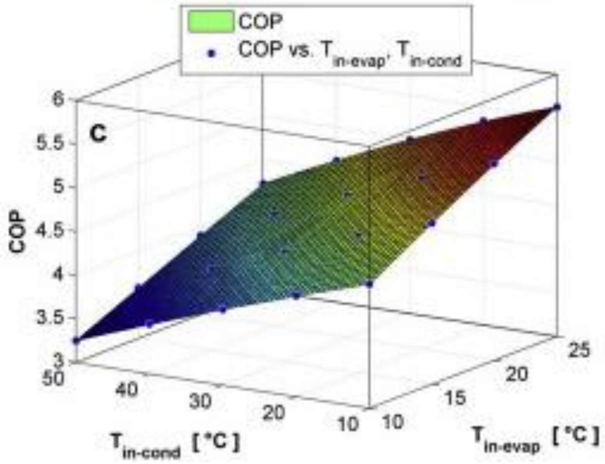

Figure 85 Heat Pump COP variation with temperatures [56]

Furthermore, it is worth considering the TES impact on system behaviour. Looking at the aim of having the temperature much constant as possible on the evaporator inlet, as expected higher TES volumes guarantee a better normal distribution.
In order to analyse deeply the impact of the proposed configuration on the system, it is worth to focus also on the economic aspects, summarized in Table 20.

In particular the cost of electricity has been set to a value of 0.30 €/kWh as an average value for EU-28 and conservative for a Netherlands scenario [57]. The cost for the ENVISION solar façade panels is estimated on a value of 250 €/m^2 as indicated by EMERGO (the ENVISON partner responsible of panels construction and supply) with a lifetime expected of 10 years.
The capital cost related to the storage system is obtained from previous works and activities developed by the author's research group, where a value of 250 €/ton of capacity is considered [58].
In order to estimate properly the potential on the environmental aspect provided by the use of ENVISION technologies, the CO_2 emissions related to the use of Netherland National Electric Grid are considered as a baseline, with a value of 618 g/kWh [59].

Table 20 Economic and environmental assessment (Winter)

WINTER	90Panels_6Storages	90Panels_3Storages	45Panels_6Storages	45Panels_3Storages
Daily th production [kWh]	418.81	410.99	418.79	418.75
Tot el consumption [kWh]	192.90	194.33	219.76	218.93
COP avg	2.17	2.11	1.91	1.91
Daily el cost [€] (Price 0.3 €/kWh)	57.87 €	58.30 €	65.93 €	65.68 €
Panels cost [€] (Price 250 €/m2)	45,000.00 €	45,000.00 €	22,500.00 €	22,500.00 €
Daily Panels cost [€] (10 years life)	12.33 €	12.33 €	6.16 €	6.16 €
HP cost [€]	6,000.00 €	6,000.00 €	6,000.00 €	6,000.00 €
HP Daily cost [€] (10 years life)	1.64 €	1.64 €	1.64 €	1.64 €
Storage cost [€] (125 €/t)	3,750.00 €	1,875.00 €	3,750.00 €	1,875.00 €
Daily Storage cost [€]	1.03	0.51	1.03	0.51
Daily total cost [€]	**72.87**	**72.79**	**74.76**	**74.00**
Daily CO2 Emissions [kg] (618 g/kWh Netherlands Grid)	**119.21**	**120.10**	**135.81**	**135.30**

One of the most interesting values reported in Table 20 is the average COP on a daily base. As mentioned before, a larger coverage of façade surfaces with thermal solar panels leads to higher COP, while different TES sizes do not significantly affect this parameter. The electricity consumption is mainly due to the HP electrical demand (used for running its compressor) while just a small part is linked to the façade panels recirculation pump: the higher COP and the lower the electric consumption. Under a pure economic point of view, the electricity daily cost represents the main voice of cost on a daily basis.
Focusing on other economic aspects, it is worth noting that the actual daily cost of façade panels represents a significant portion of the overall costs, considering a lifetime of 10 years. HP and TES cover a small part of the total daily costs. Therefore, moving to the overall daily cost it can be noted that these costs can be reduced by increasing the solar field size; indeed the benefit that they provide in terms of electricity consumption reduction is much higher than the increase of capital cost linked to the larger number of panels installed. At the same time, a reduction in electric consumption leads also to lower CO_2 emissions with a positive impact on the environment. Considering an average on a daily base, there is no impact of the thermal storage size on the energetic performance. Furthermore, adding the fact of TES low cost, also under the economical point of view, it is possible to assume that the TES size does not affect significantly the thermo-economic analysis. In the end, the main comments on the TES size can be extrapolated from the results presented in Figure 84.

- **Summer scenario**

Considering now the summer scenario, better performances are expected by the system since the combination of lower heat demand and higher solar radiation represents an optimum condition for system operation. Figure 86 shows the deviation of the water temperature at the inlet of HP's evaporator. It is immediate to notice that this time, the available temperatures are significantly much higher than the one experimented during the winter period.

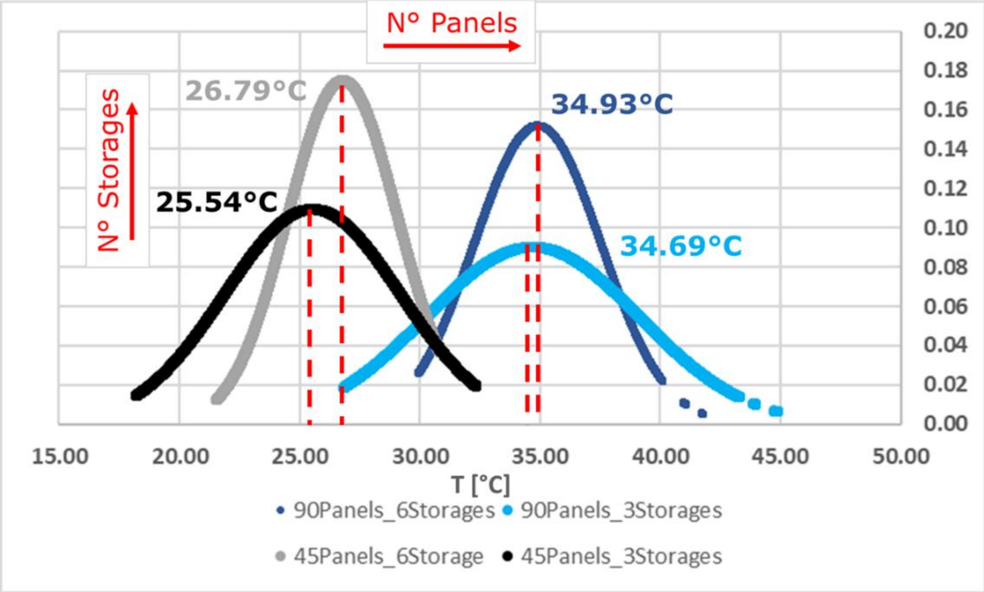

Figure 86 Temperature deviation of water inlet of HP's evaporator (Summer)

The chance to have a bigger storage guarantees more constant temperature and therefore a more stable operation of the HP. The water outlet in HP's condenser is still set to 80°C, therefore having the high temperatures shown in Figure 86 leads to high COP and more performant system management. The thermo-economic performances are resumed in Table 21.

Table 21 Economic and environmental assessment (Summer)

SUMMER	90Panels_6Storages	90Panels_3Storages	45Panels_6Storages	45Panels_3Storages
Daily th production [kWh]	245.49	251.01	250.98	250.90
Tot el consumption [kWh]	72.13	74.25	85.52	86.79
COP avg	3.40	3.38	2.93	2.89
Daily el cost [€] (Price 0.3 €/kWh)	21.64 €	22.27 €	25.66 €	26.04 €
Panels cost [€] (Price 250 €/m2)	45,000.00 €	45,000.00 €	22,500.00 €	22,500.00 €
Daily Panels cost [€] (10 years life)	12.33 €	12.33 €	6.16 €	6.16 €
HP cost [€]	6,000.00 €	6,000.00 €	6,000.00 €	6,000.00 €
HP Daily cost [€] (10 years life)	1.64 €	1.64 €	1.64 €	1.64 €
Storage cost [€] (125 €/t)	3,750.00 €	1,875.00 €	3,750.00 €	1,875.00 €
Daily Storage cost [€]	1.03	0.51	1.03	0.51
Daily total cost [€]	**36.64**	**36.76**	**34.49**	**34.36**
Daily CO2 Emissions [kg] (618 g/kWh Netherlands Grid)	**44.58**	**45.88**	**52.85**	**53.64**

As expected, the COP is higher than the one obtained in the winter period. Focusing on the daily costs, the lower heat demand combined with the higher COP leads to a significant reduction in terms of electricity cost; therefore, during the summer period the portion of daily costs related to façade panels increases. In fact, looking at the total daily costs, the thermodynamic benefits provided by the installation of a greater number of panels (lower electricity costs) are not compensated by the higher capital costs of the panels. On the other hand, focusing on environmental aspects, the chance of having higher COP values and better system efficiency, thanks to the installation of a larger number of panels, leads to lower emissions.

In order to have a better comprehension of the obtained results, it is easier to compare them with the “state of the art” technology for heat production: a gas boiler. Therefore a comparison considering a characteristic day on a yearly basis (6 months of winter and 6 months of summer are considered in order to make the elaboration easier) it has been performed between ENVISION Technologies (Table 22) and boiler (Table 23). For the boiler solution the following assumptions are provided: the cost of natural gas for residential users has a value of 0.078 €/kWh [60]; the boiler cost is fixed at a value of 6000 € [61] (similar to HP cost), while the related emissions are calculated based on a reference value of 60 g/MJ [62].

Table 22 Yearly Economic and environmental assessment

YEAR	90Panels_6Storages	90Panels_3Storages	45Panels_6Storages	45Panels_3Storages
Daily th production [kWh]	332.15	331.00	334.89	334.82
Tot el consumption [kWh]	132.52	134.29	152.64	152.86
COP avg	2.79	2.75	2.42	2.40
Daily el cost [€] (Price 0.3 €/kWh)	39.75 €	40.29 €	45.79 €	45.86 €
Panels cost [€] (Price 250 €/m2)	45,000.00 €	45,000.00 €	22,500.00 €	22,500.00 €
Daily Panels cost [€] (10 years life)	12.33 €	12.33 €	6.16 €	6.16 €
Storage cost [€] (125 €/t)	3,750.00 €	1,875.00 €	3,750.00 €	1,875.00 €
Daily Storage cost [€]	1.03	0.51	1.03	0.51
HP Cost [€]	6,000.00 €	6,000.00 €	6,000.00 €	6,000.00 €
Daily HP cost [€]	1.64 €	1.64 €	1.64 €	1.64 €
Daily total cost [€]	**54.75 €**	**54.77 €**	**54.63 €**	**54.18 €**
Daily CO2 Emissions [kg] (618 g/kWh Netherlands Grid)	**81.89**	**82.99**	**94.33**	**94.47**

Moving to a daily analysis based on a yearly average, it can be noticed that the costs of the four different configurations are pretty much the same; this is due to the combination of the different aspects explained separately in the specific sections (for winter and summer period). Since one of the most relevant goals of ENVISION is the reduction of emissions, moving towards sustainable and positive energy buildings, the results collected in Table 22 suggest that a large number of installed panels guarantees better performances of the system and therefore lower emissions. In add, since these emissions are considered referring to the Netherlands Electric Grid, the possible use of photovoltaic or other renewable systems could further reduce the emissions. In the end, the solution considered for the next evaluations is the one with 90 panels and 6 TES: the high number of panels guarantees low emissions, the larger size of TES guarantees more stable operation of the HP.

Table 23 Thermo economic results for boiler

Boiler Year	
Daily Gas cost [€] (Netherlands 0.078€/kWh)	32.65 €
Boiler cost [€]	6,000.00 €
Daily Boiler cost [€] (10years life)	1.64 €
Daily Total cost [€]	**34.30 €**
Daily CO2 Emissions [kg] (60 g/MJ)	**90.42**

Therefore, comparing the chosen solution with the boiler one it is immediately perceptible that, as expected, the state of the art is more economic than the innovative solution. This aspect is mainly linked to the high daily cost of electricity (only the electricity cost is higher than the total daily cost for the boiler scenario). Generally speaking, the main voices of cost are related to the panels and electricity, see Figure 87.

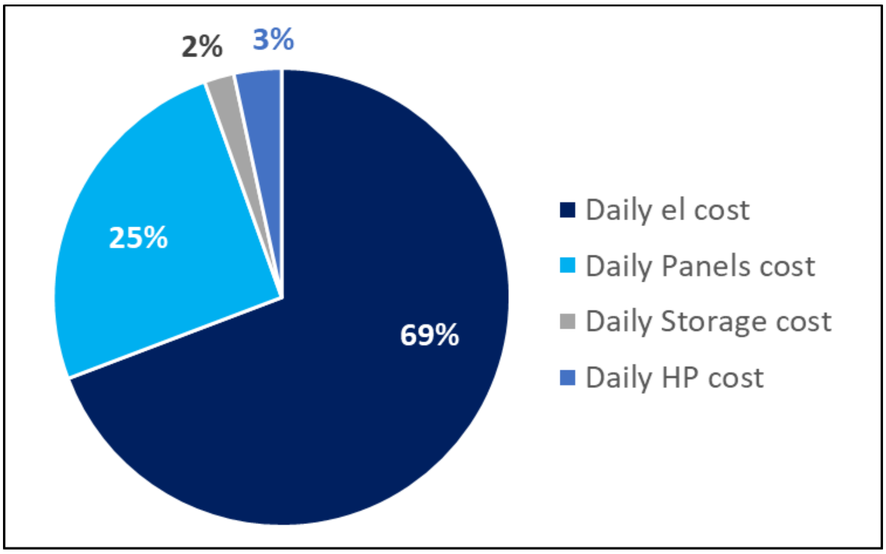

Figure 87 Split daily costs of ENVISION solution on a yearly base

In this sense, an attempt to reduce solar façade panels cost (or increase their lifetime) could permit a larger installation of them (considering the chance to have additional space for their installation) without increasing the total costs (especially considering the summer scenario). If this improvement could be possible, there is a chance to reduce drastically the electricity consumptions (and therefore costs) becoming competitive under the economic point of view with the boiler solution. For what concerns the environmental point of view, the use of ENVISION technologies can guarantee a reduction of around 10% of CO_2 emissions. As stated before, the possible introduction of PV panels or an increase in the use of façade thermal panels could lead to even lower emissions.

2.4 Control strategy development

ENVISION aims to reach a high readiness level of the technologies developed within the project. To do that, it is important to develop a management system able to maximize the performance and potential of the considered technologies. The management at District Level is analysed considering also the installation of ENVISION technologies inside District Heating Networks (DHNs) or Smart Grids (SGs). The aspect that mostly affects the impact of ENVISION in the current energetic scenario is the one related to the environment, therefore guarantee low emissions will be a priority in the evaluation of the best management of the system. On the other hand, considering the will to have wide dissemination of the proposed technologies, the economic aspect cannot be neglected to develop robust and significant system management.

Before having a detailed analysis of the management of the ENVISION system, it is worth to provide a brief description of the state of the art of DHNs and SG in order to understand better the environment where these technologies take place.

Analysing the state of the art, Europe is one of the leading places on Earth for what concerns the development of DHNs (especially Northern Europe) with more than 6000 different systems installed [63]. The use of distributed generation and DHNs allows an increase of efficiencies and energy savings: indeed, it is possible to reduce thermal losses thanks to local consumption. Furthermore, the flexibility in the management leads to higher efficiencies and therefore primary energy savings. District heating represents a promising solution for supplying heat to numerous consumers, especially in urban areas with a high density of users. Additionally, district heating is a suitable platform for integrating low carbon technologies like heat pumps on a large scale, renewable energy sources and thermal energy storage to improve the general efficiency and to minimize greenhouse gas emissions. District heating, indeed, can integrate renewable energy through heat pumps (such as geothermal and solar thermal energy), waste heat, energy from municipal waste and thermal energy storage; all of which increase the flexibility of the systems. The DHN differs in terms of working temperature and technologies for heat generation. Conventional DHNs consist of a main centralized unit that provides thermal energy to all the users connected to the DHN; nowadays the need to increase the penetration of renewable energy in the energy mix is leading to wider use of distributed generation. Figure 88 summarizes the technologies and the respective temperature available in the DHN.

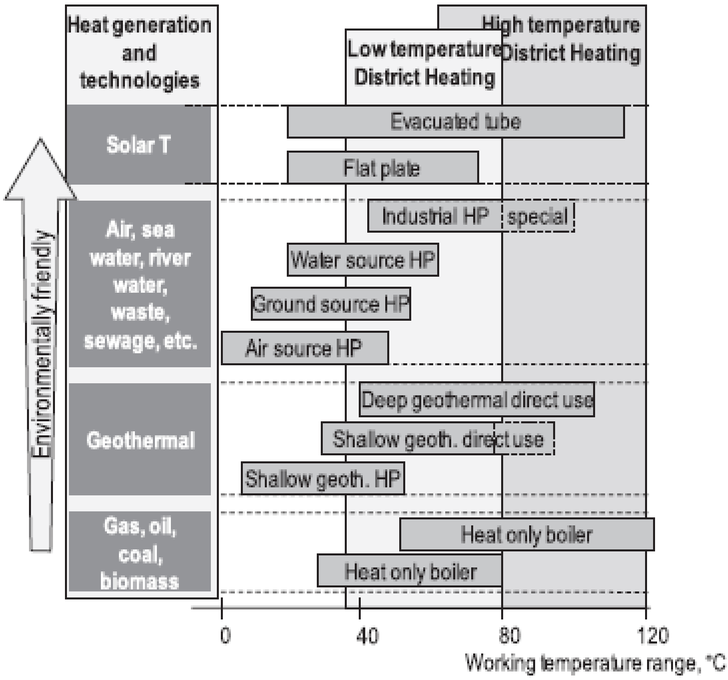

Figure 88 Overview of district heating temperature range due to heat generation technologies and sources [64]

Low-temperature district heating networks can operate with supply line water temperatures between 50-55 °C or 60-70 °C and return line water temperatures of 25 °C to 40 °C, meeting the heating requirements for space heating and domestic hot water in residential or public buildings. Lower temperatures in district heating networks lead to lower distribution losses, higher integration possibilities for heat pumps, lower electricity supply and an improvement in heat storage possibilities. ENVISION project works in the direction of increasing the available building surface to harvest energy to be converted in thermal or electrical power. These heating systems need to be coupled with a Heat Pump in order to reach the required temperatures by the DHN. In this sense, this analysis takes into account the use of heat harvesting systems for the building façade coupled with an HP, working as a temperature booster. Considering also the more and more interest in Smart Grids, solutions taking into account also the presence of Combined Heat and Power (CHP) units are evaluated. This analysis is also necessary considering that the ENVISION Southern demo site will take place in Savona Campus, in interconnection with Smart Poly-generation Micro Grid (SPM). The EU encourages CHP as an efficient energy production technology since offers high efficiency in heat and electricity generation with lower emissions than with separate processes.

Focusing on the integration of Heat Pumps in DHNs different aspects have to be taken into account, Figure 89 summarizes the most relevant parameters to be considered to properly design a heat generation unit in a DHN. The selection of a suitable heat pump arrangement for a given district heating system depends on three main technical features: the heat source for the heat pump, the technology of the heat pump to be applied and the profile of the heating requirement.

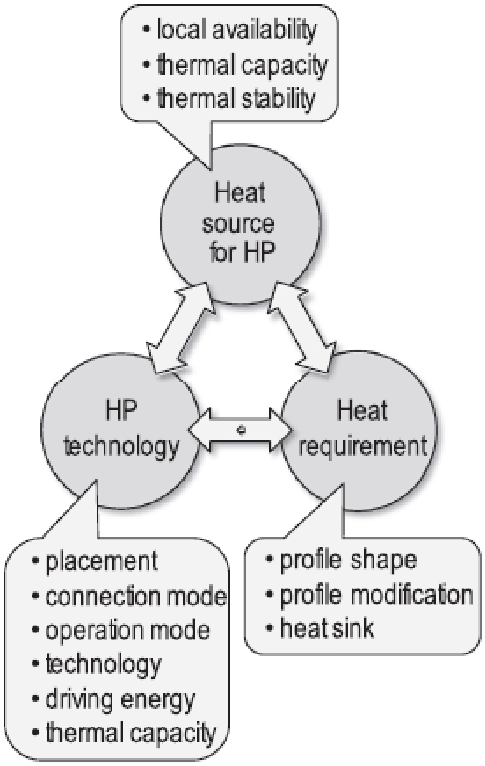

Figure 89 Technical triangle for HP integration into DHN [64]

The heat sources available for the heat pump, heat pump technology and the heating requirement of the application are key points to be considered in heat pump integration into a district heating system.

During the heat pump design process, it is essential to indicate which components of the technical triangle can be adjusted and what are the suitable arrangements for efficient functionality of the DHN. It is worth noting that the components in the technical triangle can be redefined depending on the choice of heat pump technology for the given system. In some cases, it is necessary to modify components of the future system. According to the technical triangle, there are many options such as a reduction in heating requirement (e.g. through improved thermal insulation the buildings), a connection of heat pump units with other heat sources (e.g. conventional energy sources for maximum load, renewable energy sources, etc.) and feeding the heat pump by renewable energy sources (e.g. PV, hydro, wind). The heat source can be enlarged (e.g. additional geothermal boreholes) or diversified (two or more heat sources), etc. Figure 90 shows four different examples of the dimensioning of an HP integrated with a DHN.

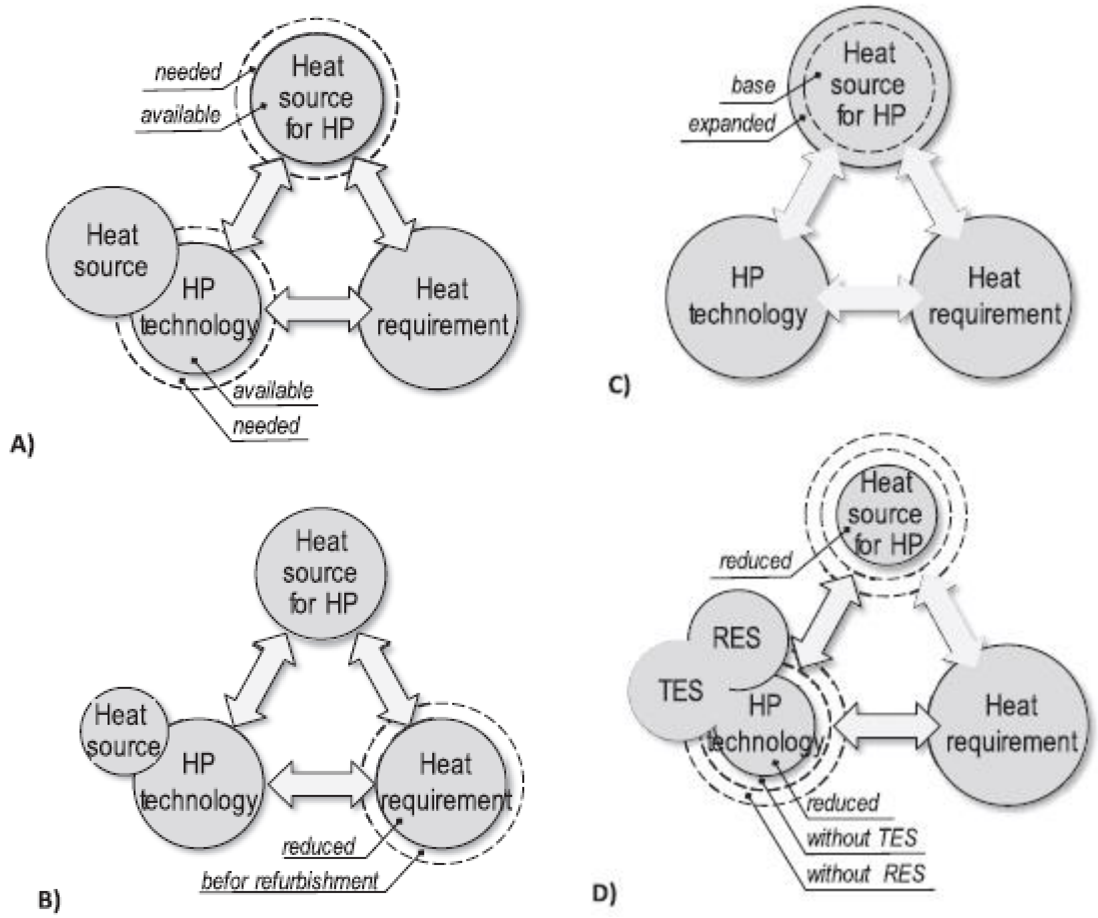

Figure 90 Technical triangle in four different scenarios [64]

In the case where the capacity of the heat source for the heat pump is limited and, therefore, the HP cannot provide the required heat, some possible solutions are reported in Figure 90. Figure 90 (A) reports a scenario where this issue is solved by adding a new heat source to supply the HP; if the added heat source is still not sufficient to cover the heat requirements, the solution provided in Figure 90 (B) uses a building refurbishment in order to decrease the demand. In Figure 90 (C) the same issue is solved by an expansion of the original heat source (e.g. more solar thermal panels). Figure 90 (D) shows the case of a small HP inside a DHN, to supply the heat requirement, it occurs the use of Renewable Energy Sources (RES) and Thermal Energy Storages (TES) also connected to the same DHN. The use of seasonal TES could be significant in order to be completely independent of traditional heat sources (HS), as shown in Figure 91.

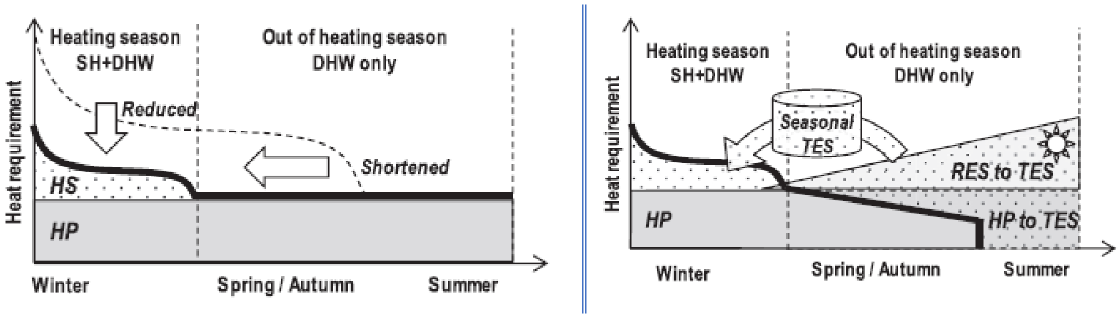

Figure 91 Traditional Heat coverage (on the Left) considering building refurbishment and Innovative management (on the right) considering the use of only innovative energy sources [64]

With this configuration is, therefore, possible to store the heat produced by HP and other RES in the Seasonal TES and use this heat during the winter period when the heat demand is higher. Depending on the DHN generation and other parameters, there are several possible interconnections between the HP and the DHN as reported in Figure 92.

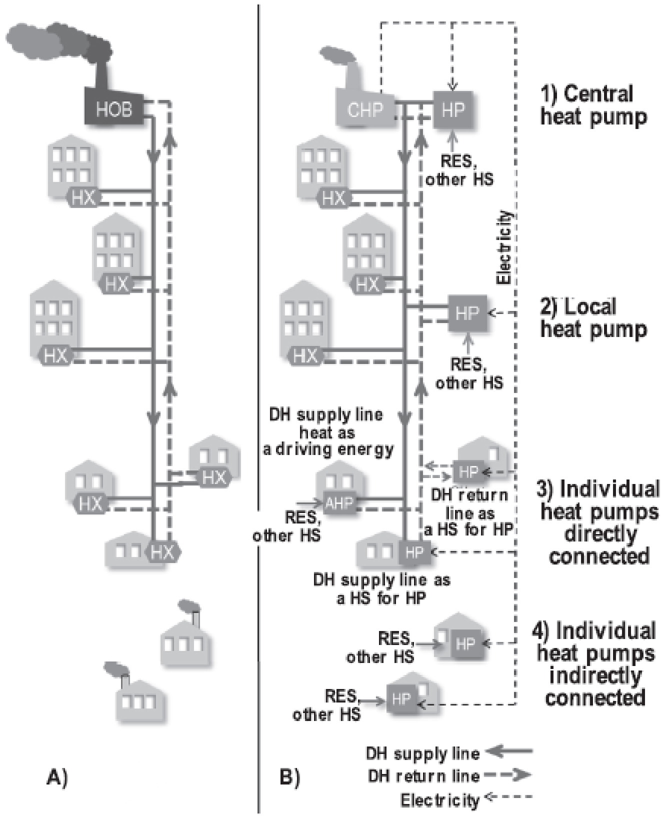

Figure 92 Schemes for: (A) traditional fossil fuel-based DH and (B) heat pump placement options in advanced DH [64]

The local heat pump can have a high or medium thermal capacity and it is placed near to a locally available heat source, connected directly to the DHN supply line, while small individual HPs can be directly connected to return line of DHN or indirectly connected just because of the use of the electricity provided by the central CHP unit. It has to be noted that the interconnection of HP to the DHN return line can be quite complicated for what concerns already existing DHNs. This means big changes in the system, locally it is necessary to install a heat exchanger in the DHN return pipe or change the connection to local substations, these solutions lead to consequent high investment costs.

The first part of this section focuses on the development of the management ad district level of different technologies interconnected to a DHN or a Smart Poly-generation grid. The analysis performed in the previous section acts as an input for this one, that is focused on the system management that minimizes costs. The tool used to perform this analysis is W-ECoMP, a software developed by TPG (Thermochemical Power Group, http://www.tpg.unige.it/TPG/), a research department of the University of Genoa.

2.4.1 W-ECoMP Description

W-ECoMP (Web-based Economic Cogeneration Modular Program) is a modular and flexible software tool, which aims at the thermo-economic, time-dependent analysis and optimization of energy systems, including off-design conditions.

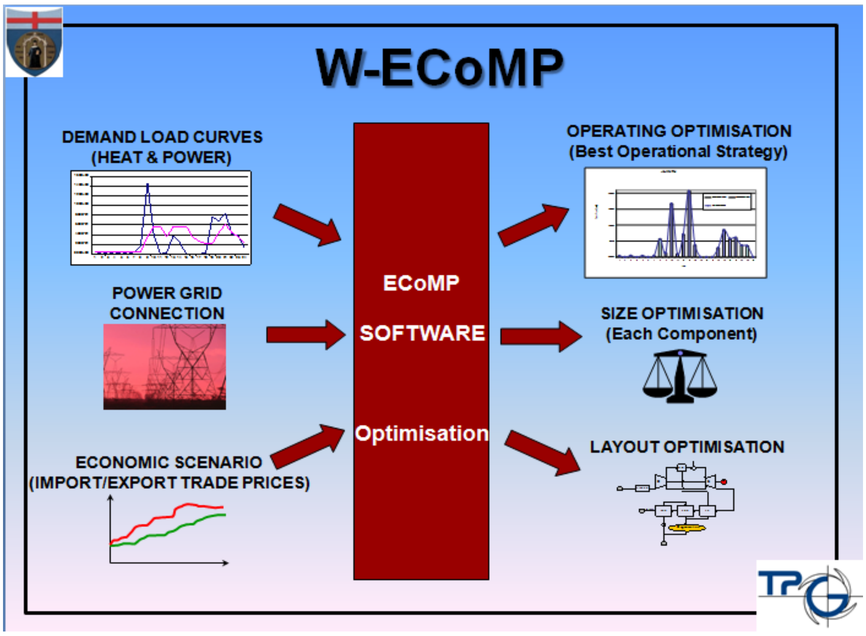

Figure 93 W-ECoMP description

W-ECoMP is characterized by a modular approach and a user-friendly interface, which allows the user to build complex system configurations in a short time. This approach maintains the flexibility and extendibility of the library of components. Each component is described by three subroutines which define mass and energy flows, off-design performance curves, variable and capital costs. The determination of cost functions for the different modules is based on the contribution provided by TPG's industrial partners over the last few years and by reference to literature data. Cost functions are constantly updated. In order to increase the analysis consistency, energy systems are simulated through specific performance curves that fit experimental/calculated data describing the off-design behaviour of each component in the library (see Figure 94).

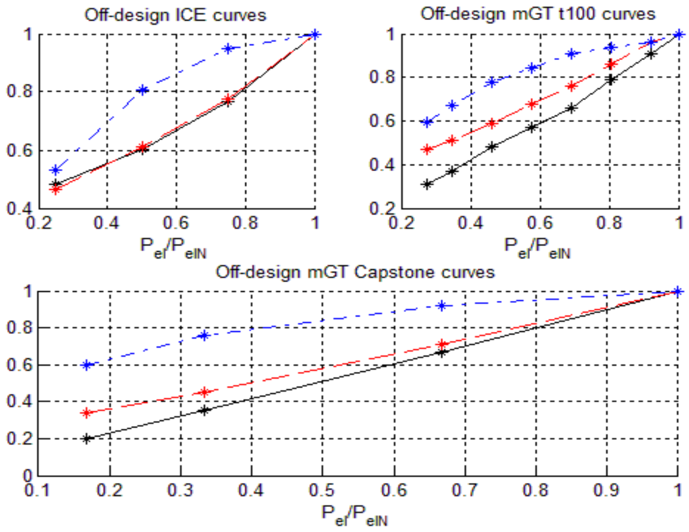

Figure 94 Example of off-design curves in W-ECoMP

The modular structure of the software allows users to combine the single components in order to analyse a wide typology of plants (such as residential users, power plant, poly-generative smart grids). In addition, the analysis of the same plant can be performed considering different economic scenarios, investigating the influence of one or more parameters variation on the global performances of the energy system. One of the most important features of W-ECoMP is the possibility of performing the thermo-economic analysis at two different hierarchical levels, to optimize respectively:

- the operating strategy for existing energy systems (low level)
- the size of one or more components during the plant design (high level)

Capital and variable costs are considered for system size optimization, while only variable costs are considered to optimize the operating strategy of existing energy systems. In the design optimization, the size of each component is evaluated together with its capital cost. The evaluation of the optimal operating strategy is then carried out at the lower level of optimization according to the actual energy load demands (i.e. electricity, heating and cooling energy). The objective function is usually selected as the total costs/revenues balance within the plant operating life.

2.4.2 District cases management

Considering the scenario of a developed DHN, where it is possible to control and manage all the distributed technologies in order to properly satisfy the total demand, it has been necessary to evaluate how the different systems can be managed on a district scale. In order to provide a clearer vision of these aspects, the case of Smart Grids (thermal and electrical demand and production on a district scale) and the case of DHN (only thermal demand on a district scale) are considered separately. The analysis is performed using W-ECoMP software.

2.4.2.1 *Case with CHP units (Smart Grids)*

In smart grids, both electric and thermal power is produced, distributed and consumed within the same network, with the main objective to create a neutral (or a positive) energy hub that includes all the users inside the smart grid.

In relation to what it will be implemented in Southern-Demo site within ENVISION project, in this analysis of a smart grid, are considered different small energy hubs consisting of a CHP unit (mGT) and Heat Pump. Figure 95 shows the plant layout analyzed in this section.

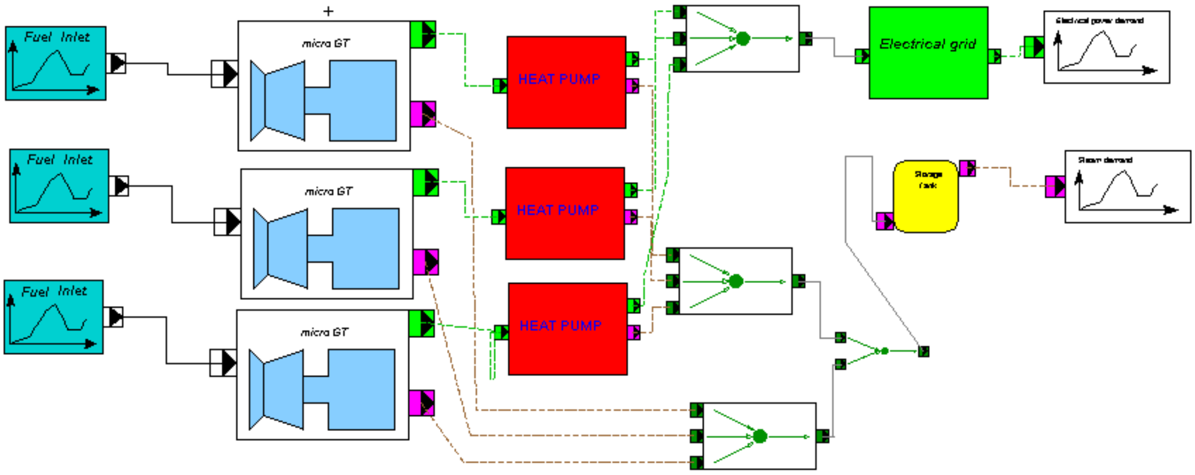

Figure 95 Smart-grid configuration on W-ECoMP

At this stage, the smart grid is considered to be composed of three energy hubs. The CHP units can supply the electric power needed by the heat pump with which every mGT is coupled. The electric power in excess is then delivered to the smart grid users. For what concerns the thermal aspect, the heat produced by mGT and HP are merged and provided to the DHN. A centralized storage tank is installed in order to guarantee good management of the system, creating independence between thermal and electric aspects. The installed heat pumps have different sizes, furthermore, each heat pump is equipped with a different number of panels. This aspect is reflected on the HP’s COP, that varies depending on the number of panels installed. The values of COP are obtained and scaled from the developed analysis in section 2.3.2. The CHP units that are considered in this phase are micro Gas Turbines with a size of 30 kW and an electrical efficiency around the 30%, while the CHP efficiency is up to 90% [65].

Table 24 and Table 25 summarize the main properties of the system installed in the considered smart grid.

Table 24 Heat Pumps properties

	Size	COP Winter	COP Summer
HP 1	9.5 kWe	2.1	3.4
HP 2	16 kWe	1.9	3.0
HP 3	7.5 kWe	2.0	3.15

Table 25 CHP unit properties

	Size	%Eff
mGT 1	30 kWe	30%
mGT 2	30 kWe	30%
mGT3	30kWe	30%

Compliant with the present discussion, the performances of the system will be evaluated in the winter and summer scenario. Therefore, the COP of the Heat Pumps is different depending on the season and the façade panel performances. The variations of the COP during the day are simulated changing the ambient temperature in the input data of W-ECoMP, since the tool is not able to perform a calculation with the detail level of the MATLAB Simulink model. Anyway, it has to be noticed that the presence of an intermediate TES leads to stable HP operations, therefore little COP changes during the day are expected (neglecting the off-design COP variations).

The thermal load has similar trends to what have been proposed in Figure 83 but scaled in relation to the higher system size of this analysis.
The electrical loads used are obtained from the trendlines reported in Table 26. The absolute value is then scaled down, in order to be compliant with the size of the technologies installed in the considered energy hub.

Table 26 Trendlines for electric loads used on summer (top) and winter (bottom) [66]

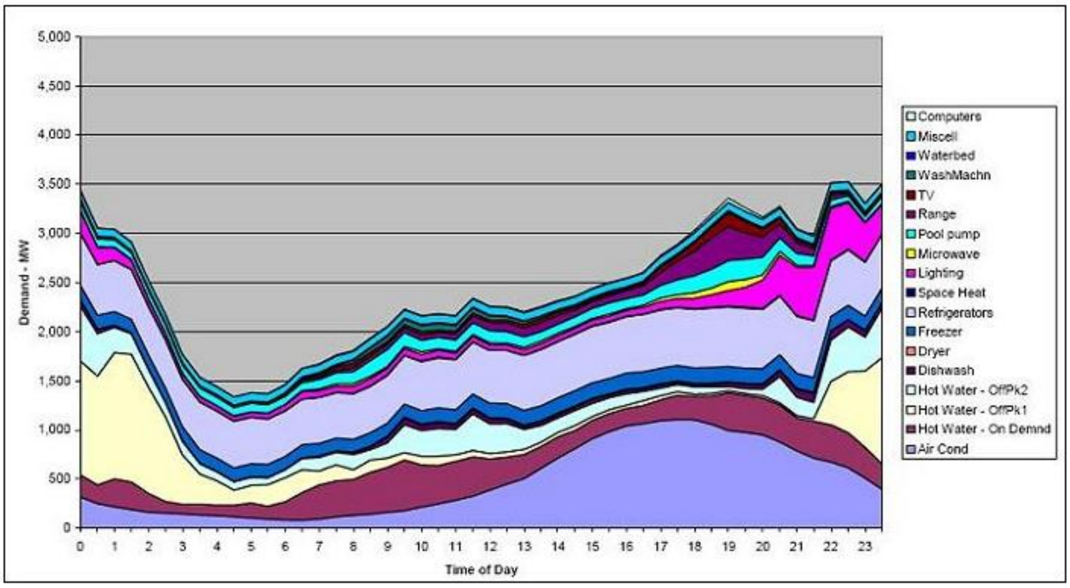

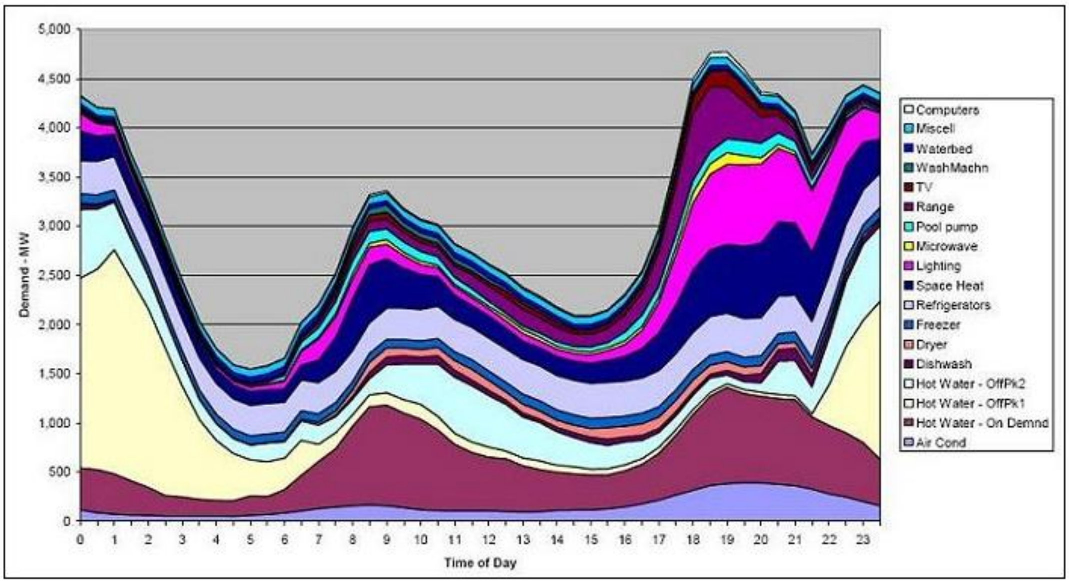

- **<u>Winter scenario</u>**

The initial focus will be on the winter scenario. Considering a smart poly-generation grid, the proportion between electric and thermal demand is fundamental in terms of system management. For a winter scenario, the proportion between thermal and electric demand is quite high. Therefore, in order to satisfy both demands, the use of CHP units could be promising since their rate of production thermal/electric is compliant with the demand one. Figure 96 and Figure 97 show the management proposed by W-ECoMP algorithm, electrical and thermal respectively.

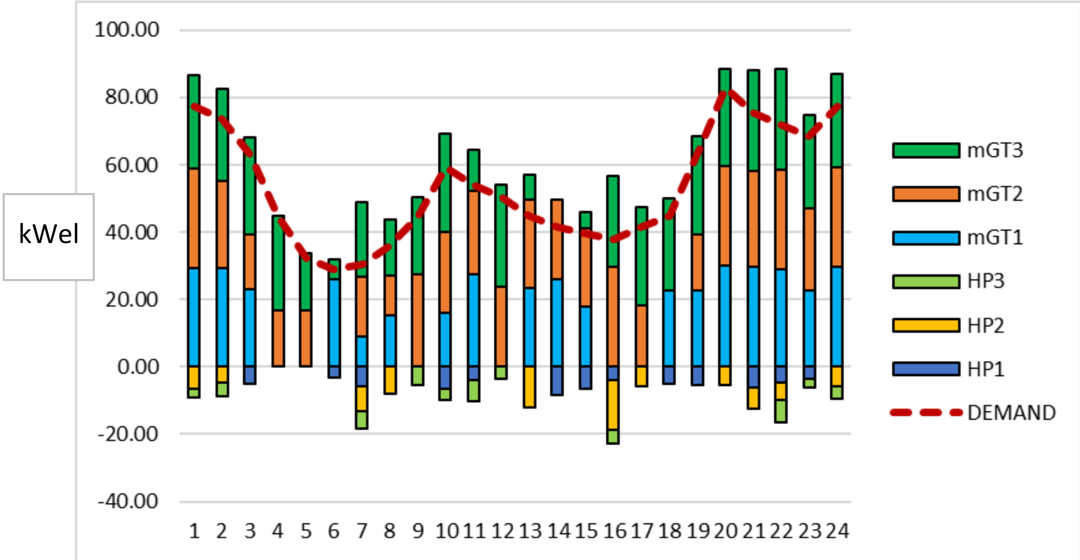

Figure 96 Smart Grid Electric management in a winter scenario

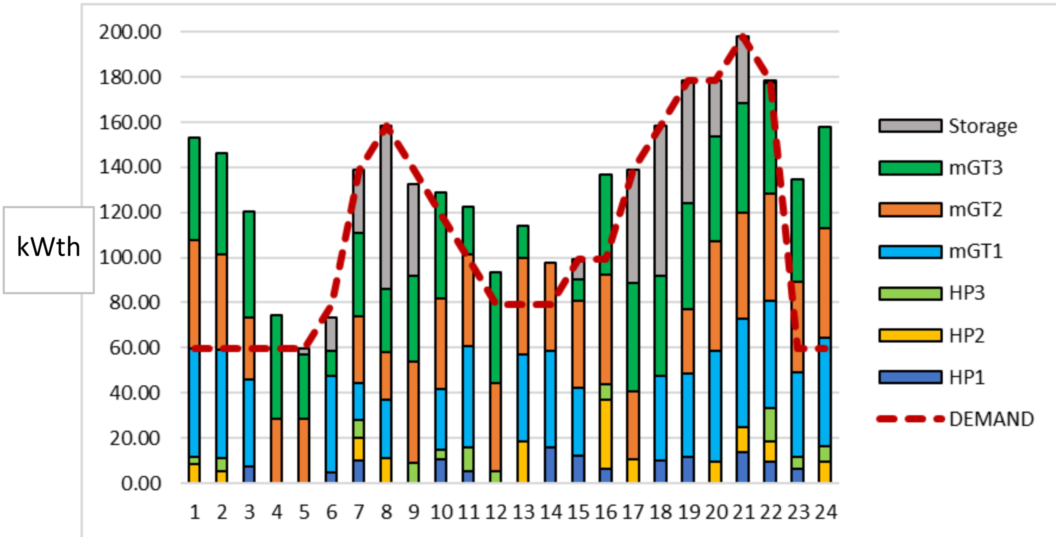

Figure 97 Smart Grid Thermal management in a winter scenario

Considering the absence of batteries and the will to create an energy-neutral smart grid, the system is managed in order to follow the electrical demand while thermal follows. In this context, the mGTs are strongly used, while the HPs are used to produce even more thermal energy. Indeed, the use of heat pumps guarantees the production of thermal energy thanks to the more use mGTs. Furthermore, the chance of using the mGT close to their design point leads to better performances. In the end, the presence of HPs has many different benefits on this kind of system.
The storage is used in order to decouple the thermal and the electrical demand by storing the thermal demand in excess, produced when the electric demand leads to an intensive thermal production (during the night).
The intense use of mGTs is confirmed in Figure 98, where it can be seen that most

of the time the machines are used over 80% of their design power. As confirmed in Table 27.

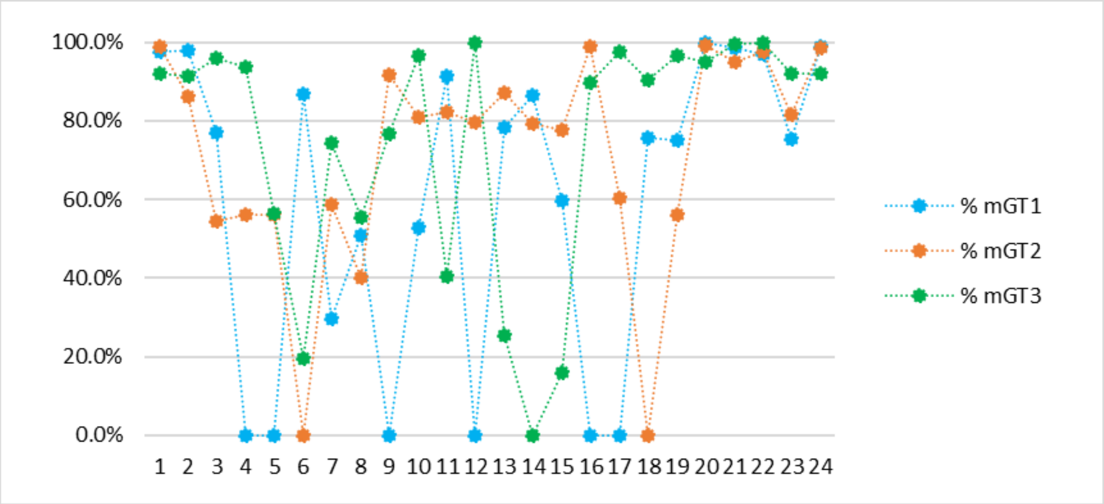

Figure 98 mGTs partial load in a winter scenario

On the other hand, heat pumps are mostly managed to satisfy thermal demand. Therefore they are used a bit more in partial load. It has to be considered that, since the 3 mGTs are the same, the main discretionary factor for their use is related to the HP more efficient in the considered period. The choice of this best Heat Pump will lead to the choice of mGT use.

Table 27 Percentage of time spent by each mGT in a certain working condition, winter scenario

	mGT1	mGT2	mGT3
On-Design	38%	50%	63%
Turned Off	25%	8%	4%
Partial Load	38%	42%	33%

Figure 99 shows the COP of the HPs during the operation purposed by W-ECoMP algorithm. Considering their COP at the design point, it is evident that they work most of the time in partial load since the COP values in Figure 99 are quite lower than the design point ones (reported in Table 24).

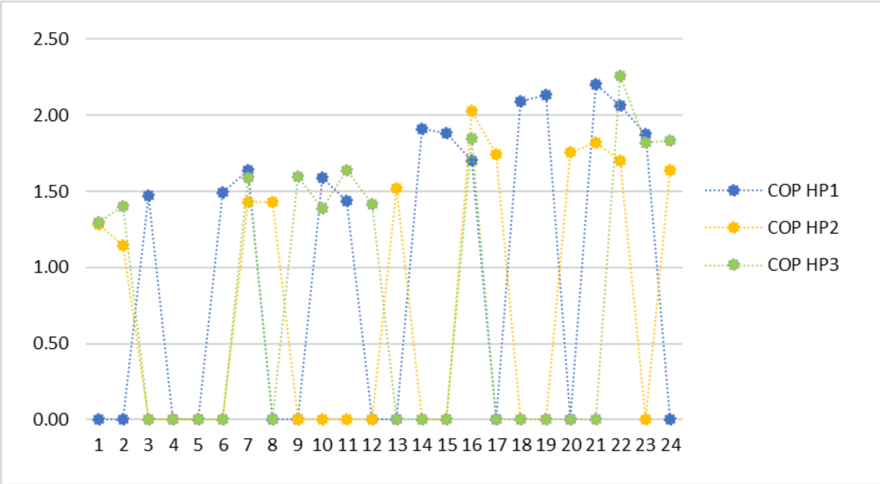

Figure 99 COP of Heat Pumps in a winter scenario

- **<u>Summer scenario</u>**

In this case, the summer scenario is affected by lower thermal demand and even lower electrical demand. In this sense, the use of HP is more substantial than the winter period. The presence of HPs guarantees an increase in electrical demand and, therefore, the use of mGTs. Figure 100 and Figure 101 show the system management proposed by W-ECoMP algorithm.

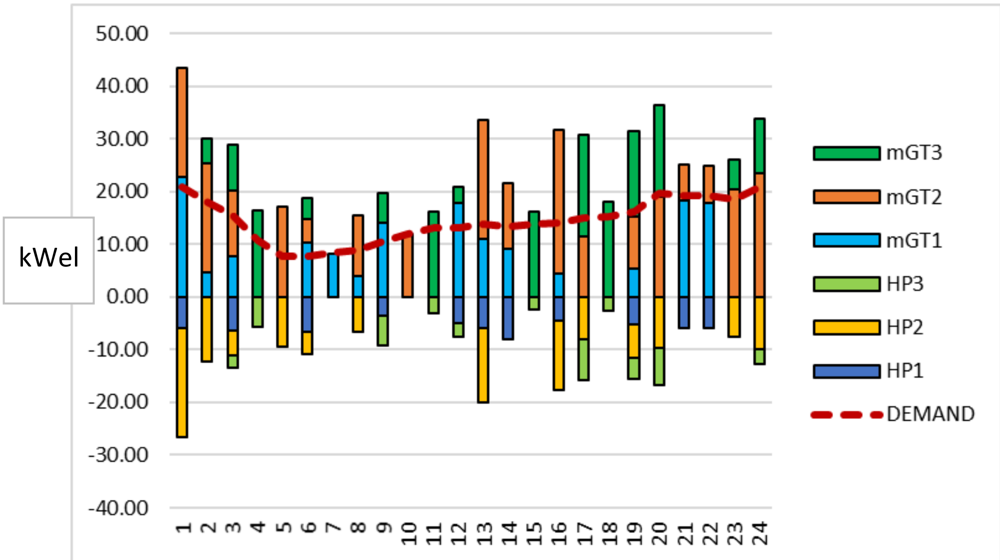

Figure 100 Smart Grid Electric management in a summer scenario

Considering the low electric demand, the mGTs have to work at partial load. Therefore, also the thermal production is not always sufficient to satisfy the heat demand. This issue, especially in periods with significantly low electric demand, can be solved by introducing the use of heat pumps. The use of heat pumps and mGTs, combined with thermal storage, allows guaranteeing a proper satisfaction of both demands.

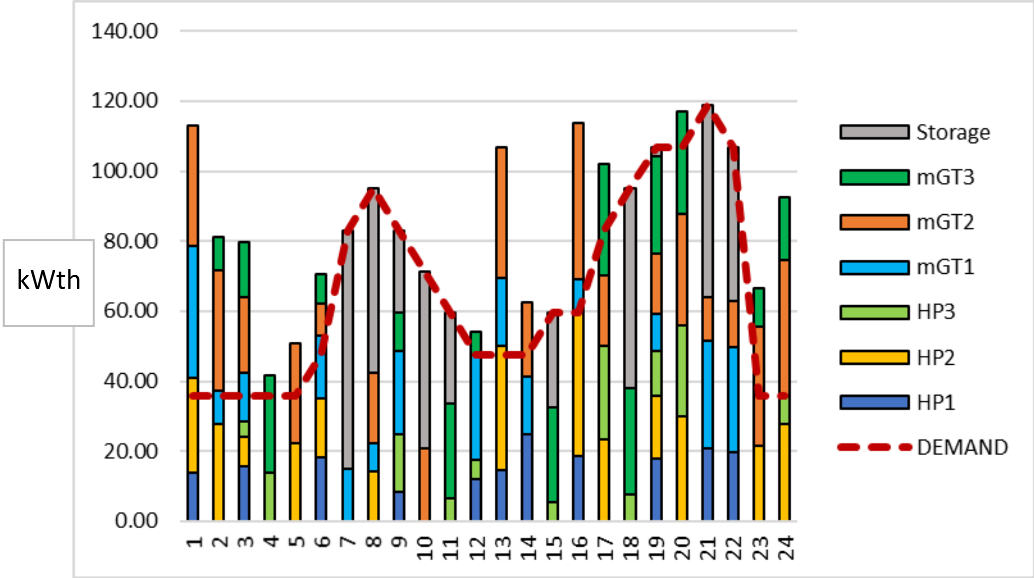

Figure 101 Smart Grid thermal management in a summer scenario

As stated before, Figure 102 shows that the mGTs works mainly at partial load since the low electrical demand, as summarized in Table 28. It can be seen that sometimes different mGTs are used at strong partial load. This aspect could seem not advantageous in terms of system efficiency. On the other hand, considering also the thermal aspect, in this period it could be not sufficient the use of only one heat pump. Therefore, two different mGTs has to be used to supply the respective heat pumps for the necessary heat production. A significative example of this assertion is period 20, where the only use of one mGT could be sufficient to satisfy the electric demand, but in order to satisfy also the thermal demand, 2 heat pumps are needed. The use of these 2 heat pumps requires the use of two different mGT at partial load.

Table 28 Percentage of time spent by each mGT in a certain working condition, summer scenario

	mGT1	mGT2	mGT3
On-Design	0%	4%	0%
Turned Off	42%	29%	42%
Partial Load	58%	67%	58%

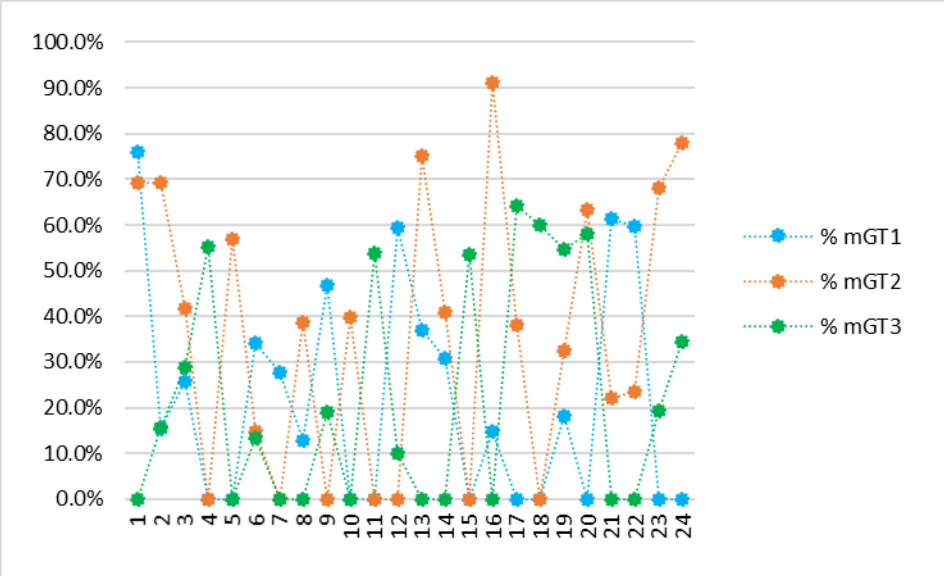

Figure 102 mGT partial load in a summer scenario

What has been stated previously is confirmed by Figure 103 where, focusing on period 20, it is possible to notice that the Heat Pumps are really close to their design point since that are working with high COP (also a bit higher than the design point due to the light positive impact of small hourly temperature variation).

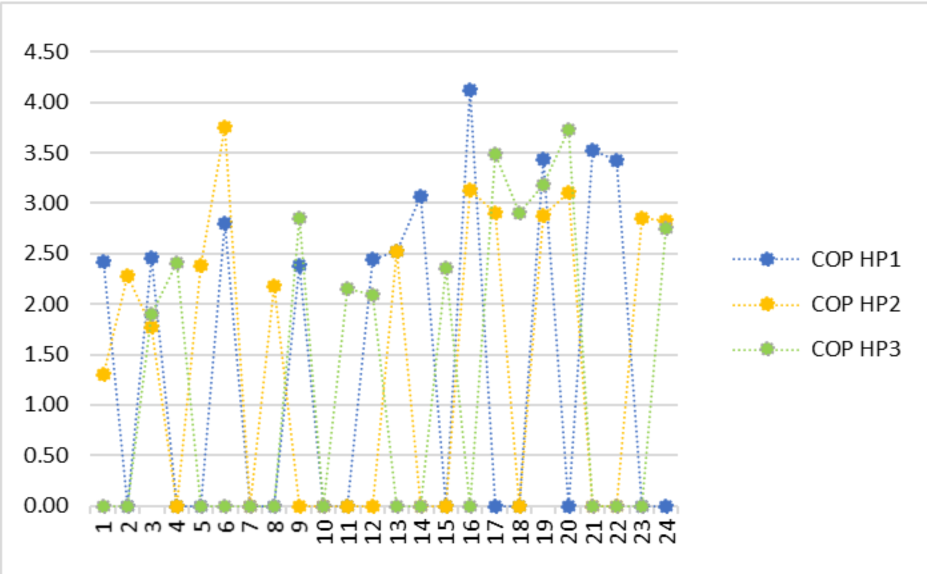

Figure 103 COP of Heat Pumps in a summer scenario

In conclusion, it can be stated that there are huge differences in the winter and summer management of a poly-generative smart grid. These differences are mainly related to the strong changes in terms of energy demand depending on the season.

Furthermore, the use of Heat Pumps (considering their ENVISION configuration) it is strongly encouraged by their higher COP.

For what concerns the storage typology, in this phase it has been considered common thermal storage in order to guarantee flexibility to the system management. This choice is compliant with the system currently present in Savona Campus. It is worth noting that the choice of the storage (especially in terms of dimensions e.g. seasonal, weekly, daily,…) could have a significative impact on the management of this kind of system. With this scope, a more detailed analysis will be developed in activities carried out by other consortium partners, where particular attention will be also referred to the analysis of seasonal storages understanding if they can be compliant with ENVISION technologies and goals.

2.4.2.2 Case with only Heat producers (District Heating Networks)

The analysis of a DHN is developed considering three different Heat Pumps with different sizes and configuration, all connected to the same DHN. Once that the demand of the whole DHN is known, the management of these HPs will be evaluated in order to minimize cost and maximize the system efficiency, guaranteeing the demand-supply.

The system layout is presented in Figure 104. It has to be noted that the presence of an electrical grid and electric demand is required to make the model run, but with a proper setup of the model, it is considered only the thermal aspect.

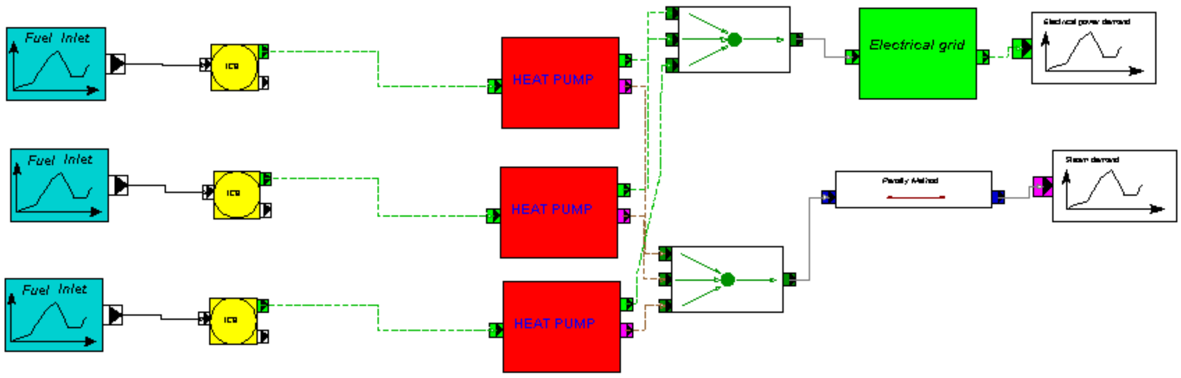

Figure 104 DHN configuration on W-ECoMP

The heat pumps are designed with different sizes, furthermore, each heat pump is equipped with a different number of panels. This aspect is reflected on the HP's COP, that varies depending on the number of panels installed. In Table 29 are summarized the properties of the different HPs. The inputs related to the COP are related to the presence of façade solar panels, proportional to the HP size. The highest the COP and the larger number of panels are installed. The input data are extrapolated from the Matlab Simulink analysis presented in section 2.3.2.

Table 29 Heat Pump properties

	Size	COP Winter	COP Summer
HP 1	9.5 kWe	2.1	3.4
HP 2	16 kWe	1.9	3.0
HP 3	7.5 kWe	2.0	3.15

Even in this case, two characteristic days for winter and summer period are considered. Therefore, COP values of the Heat Pumps are different depending on the considered scenario, due to the different behaviour of the façade panel system. The demand is related to common users connected in a DHN, the absolute values are set in compliance with the installed thermal power of the system.

- **Winter scenario**

Initially, the focus will be on the winter scenario. This scenario is the one related to the higher thermal demand and also the low performances of façade panels. In this sense, this period is a kind of "worst-case" considering the yearly basis analysis of the system. The three heat pumps are managed in order to satisfy the thermal demand, minimizing the operational costs. The results of the obtained management are reported in Figure 105.

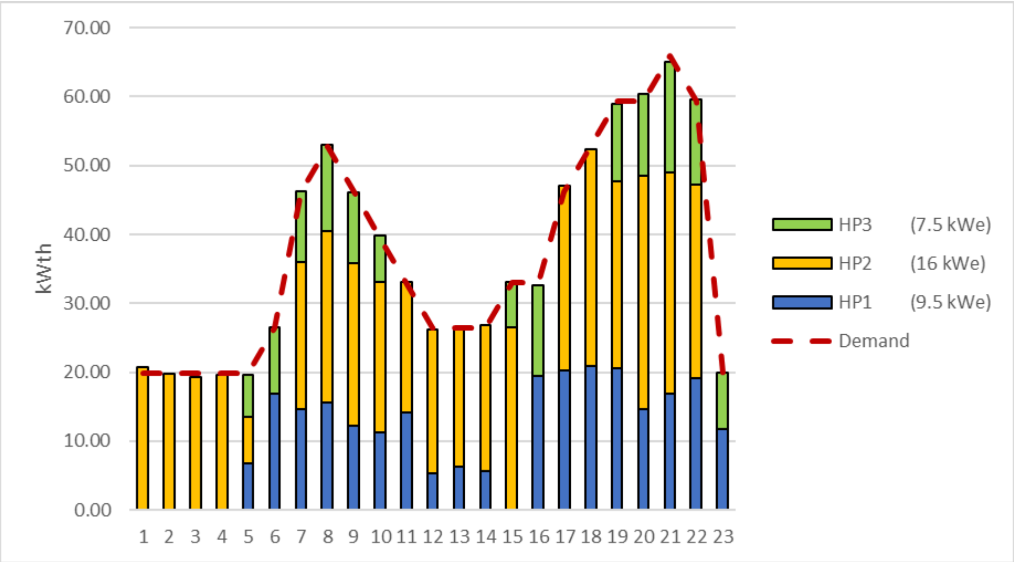

Figure 105 DHN management in a winter scenario

The performances of the heat pump are affected by its off-design curves in terms of partial loads. The variation of ambient temperature is used to emulate the changes of façade panels performances affecting the HP's COP in terms of evaporator temperature variation.

It is evident to see that, despite its lower efficiency, the HP2 is the most used because of its size. Indeed, use at a partial load of the Heat Pump leads to lower efficiencies. In this sense, most of the time is convenient to use as much as possible only one Heat Pump (even if with low COP) because the use of many of that at partial load is less efficient. The COP of the different heat pumps is then reported in Figure 106 and can be compared with the partial load chart of the HPs. It can be noted that neglecting the small effect of ambient conditions on façade panels and T_{eva} (mitigated by the presence of the intermediate storage tanks), the COP curves have similar behaviour to the partial load ones (Figure 107). It is worth noting that the partial load is considered in terms of electric power, moving from the design point.

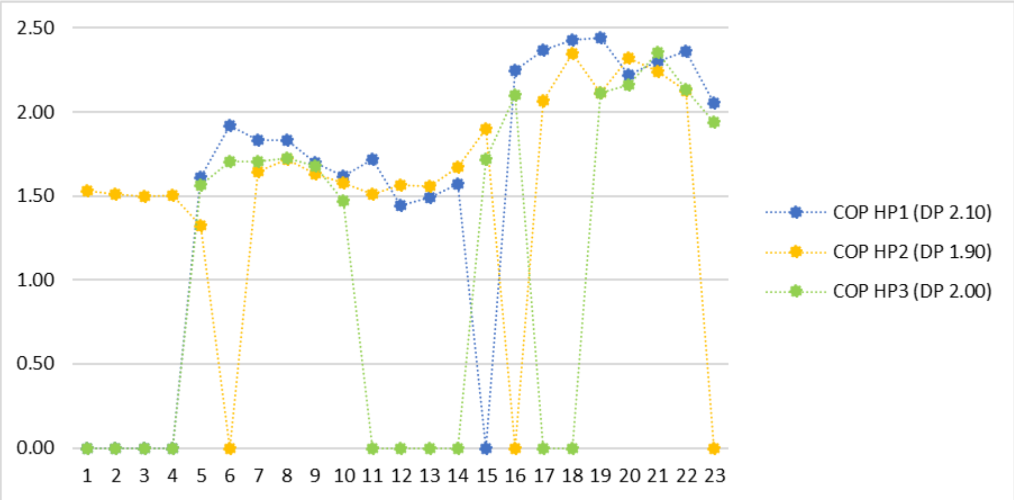

Figure 106 COP on a daily basis in a winter scenario

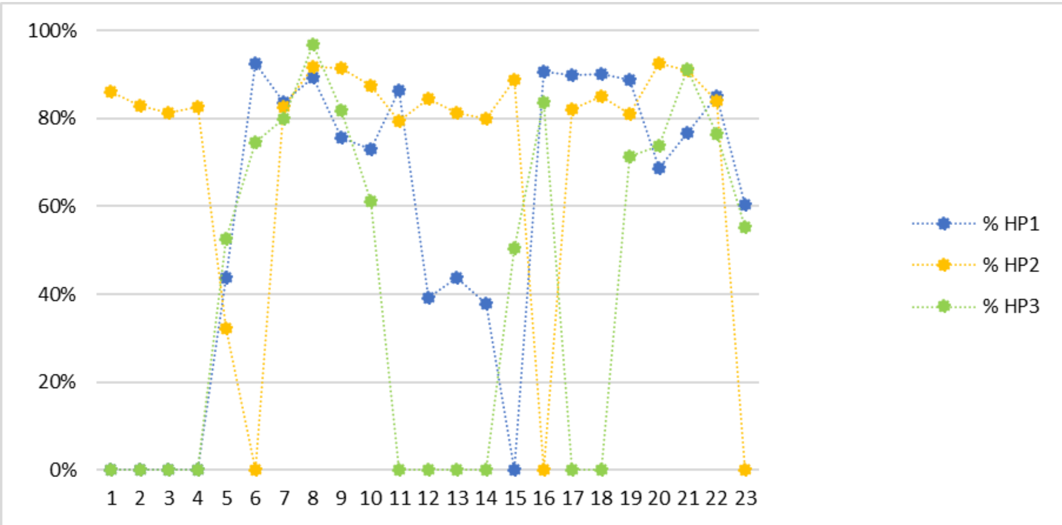

Figure 107 Heat Pumps partial load on a daily basis in a winter scenario

As shown in Figure 107, the minimum off-design for the HPs is around 30%; therefore under this limit, the machine is forced to switch off. The analysis of the previous figures shows that the HP with the lower COP is forced to work most as possible close to its design point, in order to do not decrease too much its efficiency. When necessary, the HP1 is the one mostly used at partial load since starts from a higher COP at the design point. Generally speaking, when the demand requires the use of all the installed HPs, it is convenient to operate with a light partialization for every machine. The use in the design point (max power) of one HP will lead to a stronger partial load of the others and, therefore, significantly lower COP.

- **Summer scenario**

Moving now to the summer scenario, it can be expected a context where the performances of the Heat Pumps are better; on the other hand, a lower heat demand could lead to stronger partial load. In this sense, the management of the district requires attention, monitoring both the demand side and environmental side (solar radiation, outdoor temperature) for every single cluster.

Figure 108 shows the management of the DHN proposed by the genetic algorithm implemented in W-ECoMP. It can be immediately noticed the absence of the HP2. Indeed, this heat pump is the one characterized by the lower COP; meanwhile, the lower thermal demand could be easily satisfied just with the use of the other two Heat Pumps. Then, the HP2 can be switched off during the summer period.

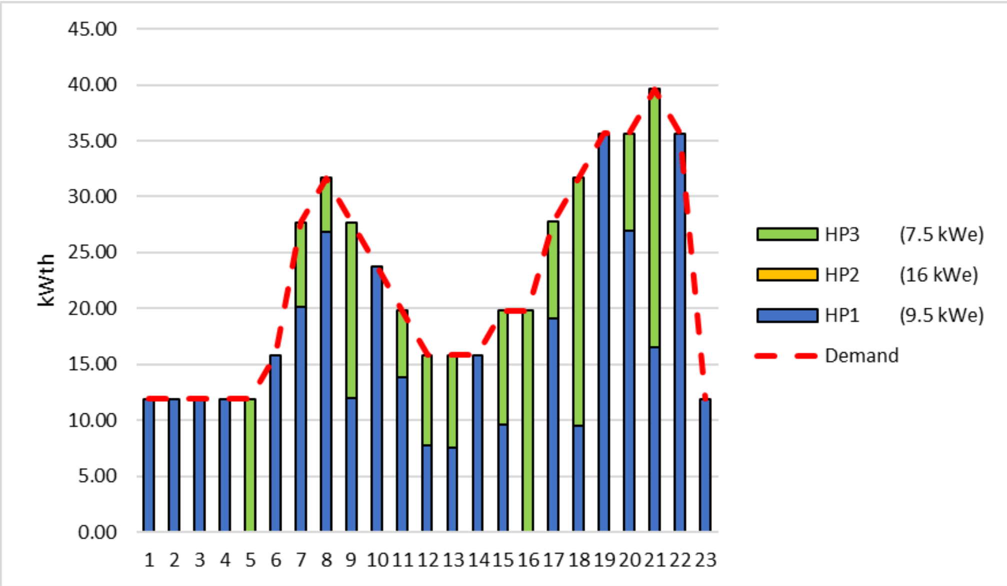

Figure 108 DHN management in a summer scenario

In this sense, the management of the summer period is easier. The two heat pumps are regulated in order to be used as much as possible, making them work as much close as possible to their design point. In the case when only one heat pump is not enough to satisfy the heat demand, both heat pumps are partialized in order to guarantee an overall higher efficiency for the system. The thermal capacity of the heat pumps is strongly related to the COP, therefore once established the compressor size, the thermal capacity increases with COP. This is why, in particularly advantageous periods, the HP1 is able to produce around 35 kWth. Figure 109 and Figure 110 shows the heat pumps performances with the proposed management.

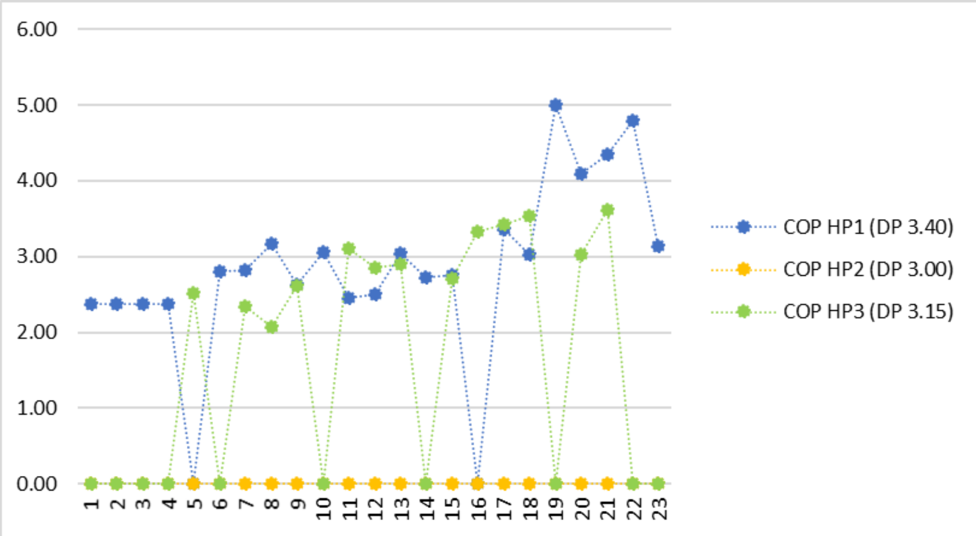

Figure 109 COP on a daily basis in summer scenario

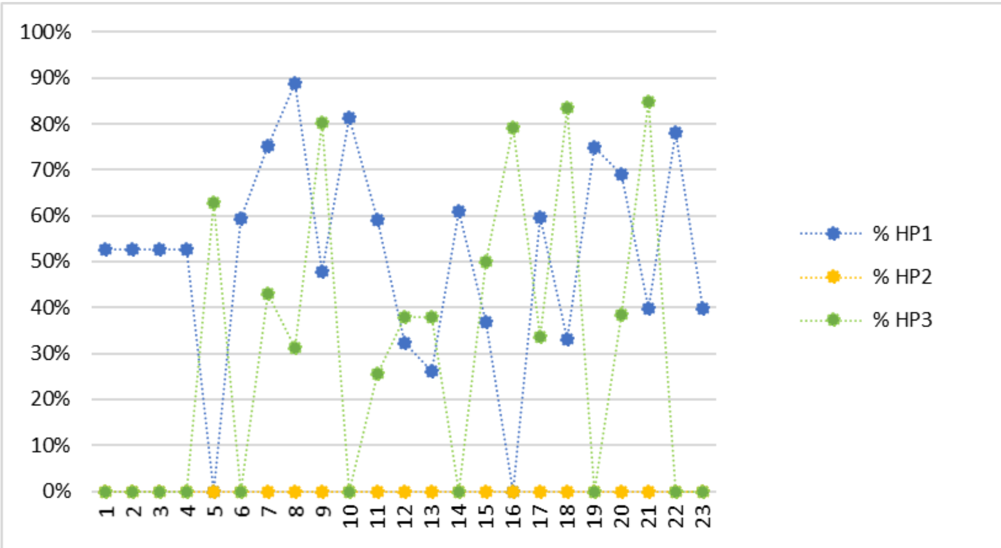

Figure 110 Heat Pumps partial load on a daily basis in summer scenario

It is worth considering that the partial load curves are related to the use of the compressor. Also in this case, the management of the system guarantees partial loads higher than 30%. Meanwhile the increased heat capacity, due to higher COP in summer conditions, allows satisfying the thermal demand without working at full operation with one HP.

For a general overview, it is worth considering that the lower efficiency occurring at partial load can be limited by using variable compressor displacement via the de-activation of one or more cylinders. In this way a more flat off-design performance curve can be obtained and, contemporary, it is possible to push at a lower level the minimum off-design point.

One of the most important observations that are needed talking about "centralized" DHN management is the electric cost related to the HPs supply. Indeed, in this case, considering that each HP belongs to a certain single user, the thermal demand is managed globally on the whole DHN, but the electric load will be supplied locally. In this sense, the much intense use of a single HP, despite another, will lead to higher electric costs in charge of this penalized single user. In order to solve this issue, there are two possible ways to be actuated in the design phase of the DHN:

- Every single HP unit has to be the same. In this way, installing a "standardized" heating module, it will be possible to do not penalize anyone of them. Indeed, a daily rotation in the use of each HP will guarantee on the weekly (and therefore monthly and yearly) basis the same use of all the HP installed in the DHN (same electric consumption).

- Share equally among the different users the electricity costs linked to HP use. This approach is needed in the case of HPs with different size. To reach this aim it is necessary to install a dedicated electricity consumption meter for each HP able to monitor the electricity supply for the different HPs and, then, share in a proportionally and agreed way this total amount.

2.4.3 Single system analysis

The system layout simulated in this section is similar to the one that will be installed in Savona Campus and consists of a single energy-hub installed inside a smart grid. The aim of this activity is to define, generically, the best practises that occurs in the management of this kind of systems. As described in the previous sections, the energy hub consists of a CHP unit (100 kWe micro-Gas Turbine) that supplies both heat (to DHN) and electricity (supplying both HP sand smart grid). The HP (10 kWe), as shown in the previous chapter uses as a heat source on the evaporator side the thermal energy produced by ENVISION's solar façade panels. A water thermal storage tank (for this simulation considered with a capacity of 9 tons) is also installed in order to guarantee more degrees of freedom in the system management decoupling the electric and the thermal demand. Figure 111 shows the layout on W-ECoMP of the considered application. Since that inside the software is not possible to set the heat sources for the heat pump, the main input and indicators for the heat pump are the one obtained from the analysis performed with Matlab Simulink in the previous chapter. The chosen configuration is the one with 90 Panels and 6x5000 L storages. The Heat Pump COP is defined considering the results obtained from the detailed analysis performed in section 2.3.2, for both summer and winter scenario. The variations of the COP during the day are simulated changing the ambient temperature in the input data of W-ECoMP, since the tool is not able to perform a calculation with the detail level of the previous one. Anyway, it has to be noticed that the presence of an intermediate TES leads to stable HP operations, therefore little COP changes during the day are expected (neglecting the off-design COP variations).

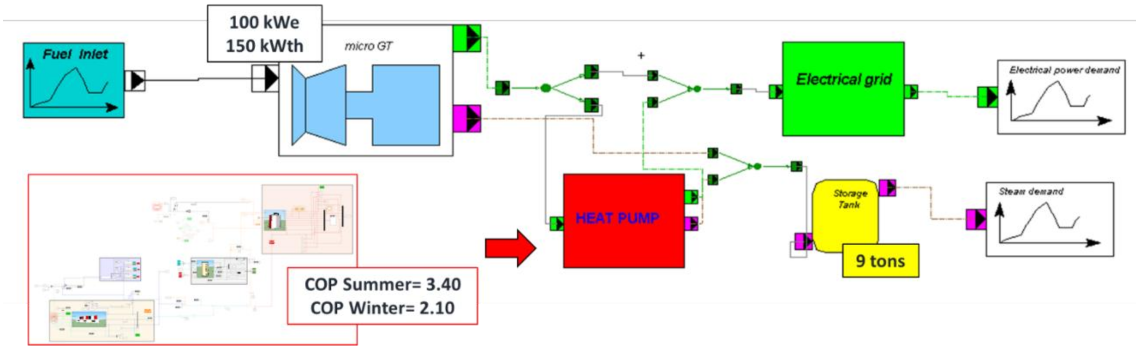

Figure 111 W-ECoMP simulation layout

The energy loads are primary inputs for the systems. Several buildings are considered in these simulations, following the trendline of the data provided by BAM for what concerns the heat demand, as reported in Figure 83. Same approach has been used for what concerns the electric load, following the trends proposed in Table 26.
It is worth underlining that the Southern Demo, located in Savona, gives also the chance to test different loads thanks to the programmable load emulator installed in the University of Genoa laboratories at Savona Campus.

In this section are presented the results obtained through the simulations developed using W-ECoMP. The tool suggests the management linked to the lower costs in terms both of capital and operation costs. The management will be firstly reported on a daily basis for winter and summer conditions, then an analysis focused on the economic aspect will be developed on a yearly basis.

- **Winter scenario**

The results for the optimized system management obtained in the winter scenario are reported in Figure 112 and Figure 113.

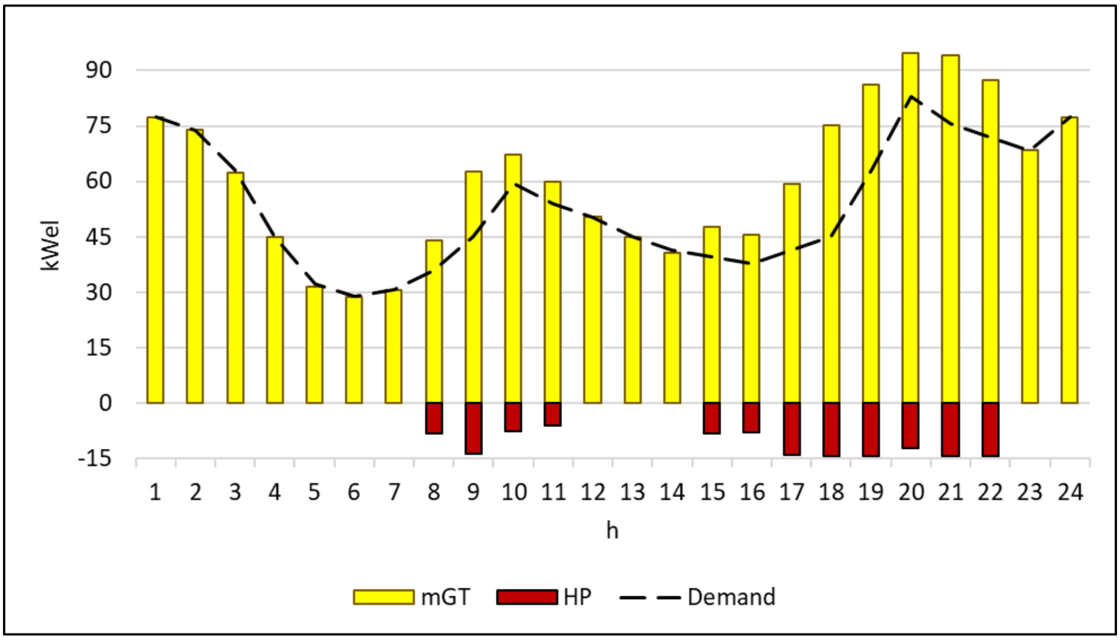

Figure 112 Electric management in a characteristic winter day

Since that no batteries are installed in the system, the micro Gas Turbine (mGT) is managed in order to cover the demand considering also the supply of the HP. The HP is regulated looking at the thermal demand, considering also its use when the COP is higher.

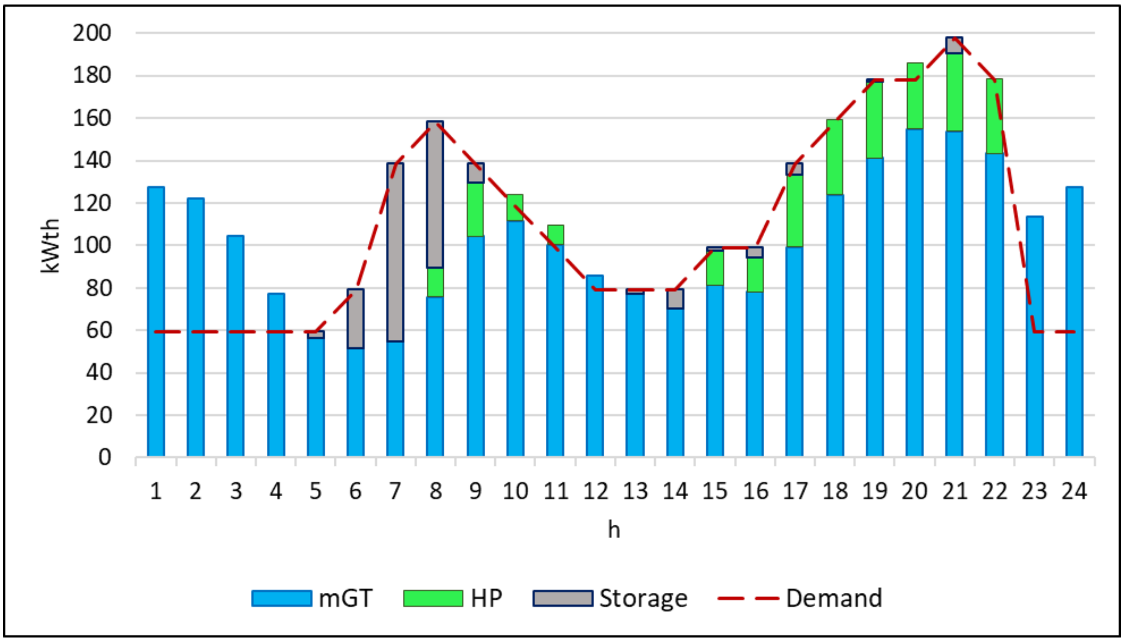

Figure 113 Thermal management in a characteristic winter day

The storage is needed to store the excess of thermal energy produced by the mGT following the electric load. Its use is fundamental to guarantee proper management of the system considering both demands. The HP is useful since leads to a double thermal management increase; in fact, in addition to the HP produced heat, it has to be considered also the additive portion of thermal energy produced by the mGT to supply the HP electrical demand. In this sense, the presence of HPs guarantees good flexibility in the management of both demands. Furthermore, it is worth considering that HP can be used as power-to-heat technology in case of PV panel presence. Indeed, during hours where the power produced by PV panels is not needed, it can be considered the use of this power to supply an HP producing heat. This heat, if not required, could be anyway stored more easily than electric energy that requires batteries (more expensive and complex systems).

Figure 114 shows the state of charge of TES used as a buffer in the management of thermal and electric demand.

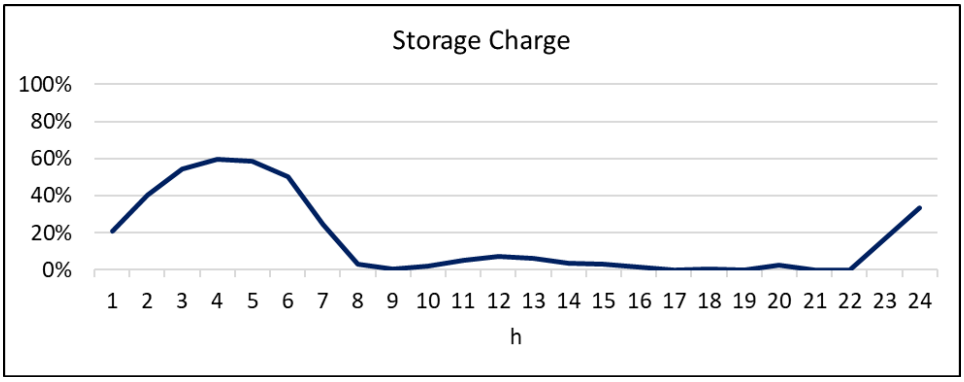

Figure 114 Storage daily usage on the winter scenario

The currently used storage system shows a size probably over the real necessities of this configuration. Therefore, smaller storage can be considered, even if as stated before, the economic impact of thermal storage is almost negligible in this application. The main limits on TES size are mostly related to space limitations.

- **Summer scenario**

Moving to the summer scenario, the management strategy suggested by W-ECoMP is similar to the winter one, where the main goal is to follow the electrical demand (as no electric storages are present). Respecting the proportion between winter and summer presented by the trendlines in Table 26, the values of electrical demand for summer period have been proportionally reduced moving from the winter one. This aspect, looking at Figure 115, leads to periods when the electrical demand is lower than the minimum mGT off-design. Furthermore, the heat demand does not suggest the use of mGT coupled with HP. In this case the only solution is to feed the HP using the grid, in orer to properly track both electric and thermal demand.

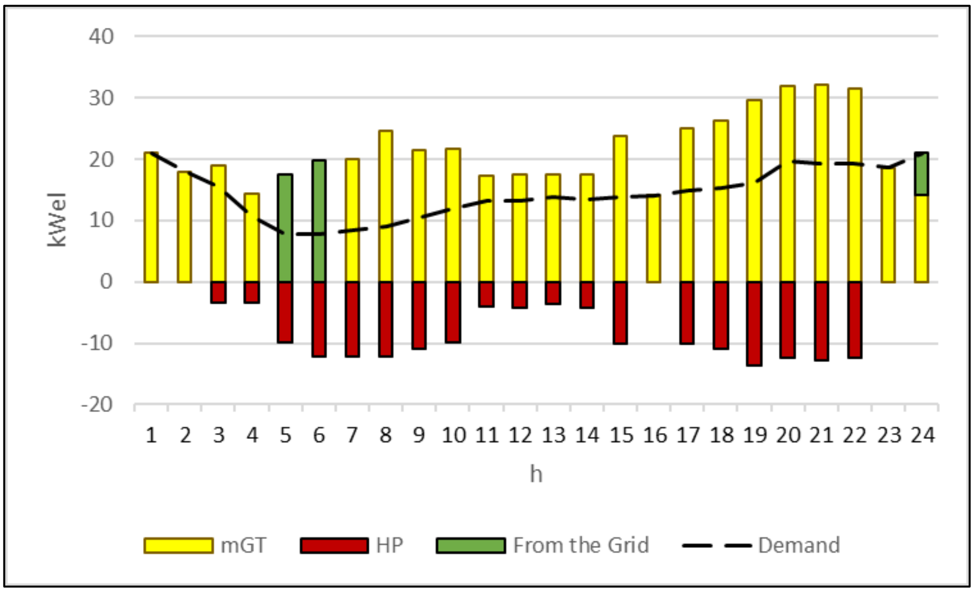

Figure 115 Electric management in a characteristic summer day

Therefore, in this condition, it is necessary supplying the system purchasing electricity from grid in order to cover the electric demand. The chance of having the Heat Pump allows using more significantly the mGT and therefore with higher efficiency (closer to design point). This aspect is also visible looking at the thermal management in Figure 116.

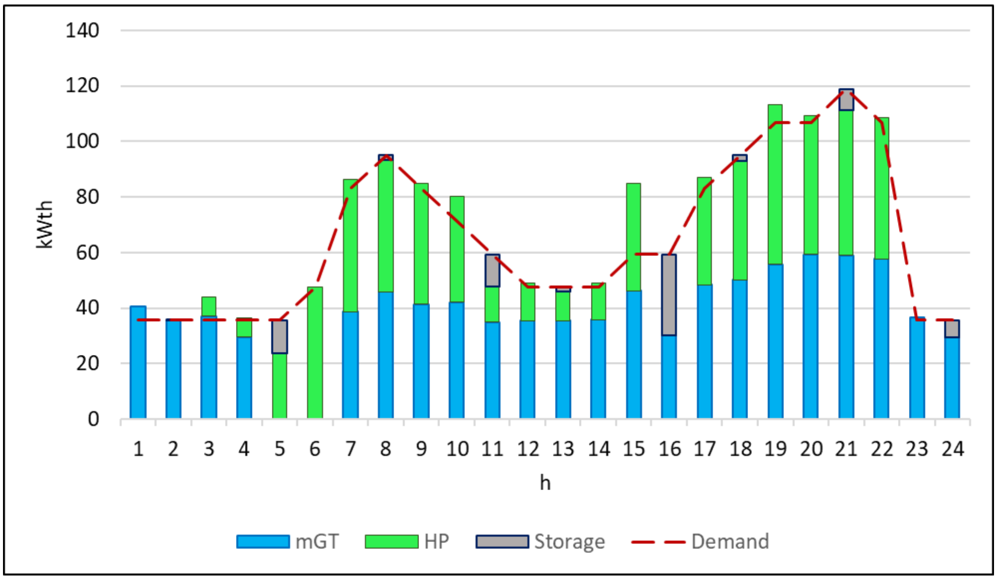

Figure 116 Thermal management in a characteristic summer day

The summer scenario shows a larger use of the Heat Pump (in green) than what occurs in the winter scenario. This aspect is linked to the chance of using more the mGT (increasing the actual electricity demand of mGT) but also because, in summer period, the COP of the Heat Pump is higher as result of the more intense solar radiation on the façade panels.

The TES state of charge, reported in Figure 117, confirms that the selected size of the storage is significantly higher than the needs. The flexibility given by the use of Heat Pump in terms of a proper management of both loads leads to a lower necessity of TES.

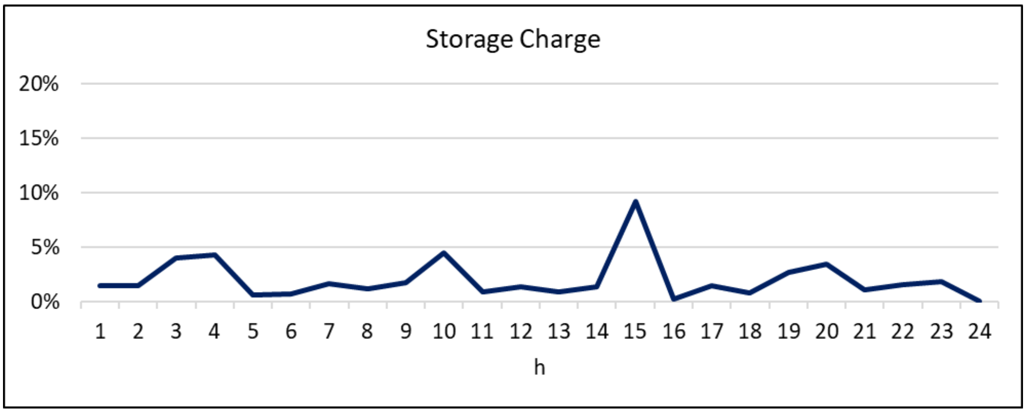

Figure 117 Storage daily usage on the summer scenario

The described scenario could be completely different in case of PV panels installation for HP supply. In that case the HP is strongly related to solar radiation, therefore its use is particularly significant in periods with high solar radiation (large thermal power from the panels and large electricity production from PV). Then, TES could be used to store the intense heat production from the HP, especially in periods with low thermal demand.

2.4.3.1 Increased electric demand case study

From the results obtained before, it seems that the electric demand covered by the considered energy hub can be increased. In fact, considering an increase of the electric demand it could be possible to avoid minimum off the design and use more continuously the mGT at max power (where its efficiency is higher).

Starting from the **winter scenario**, from Figure 118 it is possible to notice that the mGT is strongly used because of the higher electricity demand. This aspect, considering also its CHP operation leads to a really little use of the HP. The HP is indeed used to cover the heat demand only when the heat provided by the mGT (and the storage system loaded by mGT) is not sufficient.

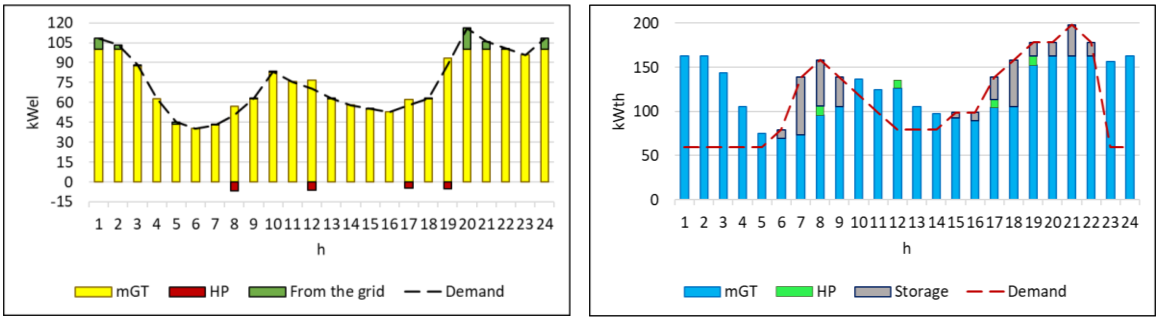

Figure 118 Electrical (left) and thermal (right) management in a winter scenario

It is worth underlining the use of the HP at noon. Even if its use is not immediately necessary to cover the heat demand, the HP is anyway turned ON since its COP is higher. The heat in excess is stored, but it has been produced at high efficiency (higher HP's COP due to particularly hot conditions). In addition, it can be considered that the demand is higher than the mGT size (100 kWe), in this case, it is necessary to occur at the grid to completely satisfy the demand.

Moving to the **summer scenario** it is possible to see that, this time, the mGT can work permanently over its minimum off-design. Therefore, there is no need to supply electricity from the grid. Furthermore, thanks to the presence of HP, the real demand that the mGT has to cover is higher, therefore its efficiency is increased.

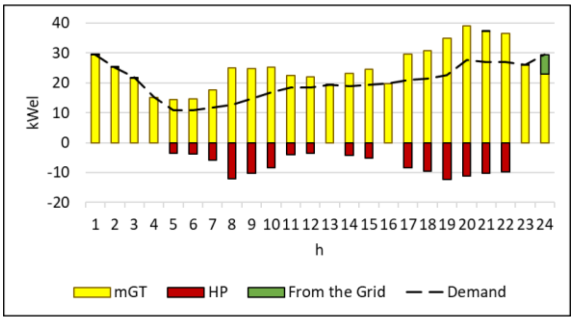

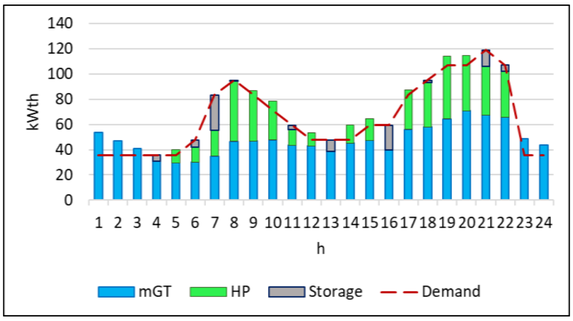

Figure 119 Electrical (left) and thermal (right) management in a summer scenario

The summer scenario, thanks to the good performances of façade panels, guarantees high COP for the HP. Therefore, the HP is significantly more used. Also, in this case, it can be noticed that, due to the absence of electrical energy storage, the management is focused on following the electrical demand, minimizing the costs related to grid purchasing. On the other hand, the presence of TES and HP allows having more degrees of freedom in the management of both demands.

2.4.3.2 Economic analysis

The economic analysis is important in order to evaluate the costs and the performances of the management proposed by W-ECoMP in comparison also with standard applications. The comparison is done in terms of Levelized Cost Of Electricity (LCOE) and Levelized Cost Of Heat (LCOH). The analysis is made on a yearly base, considering 6 months of summer and 6 months of winter. Figure 120 shows a detail of the performances in terms of energy demand, energy production and the costs related to the fuel consumption (0.92 €/kg of Natural Gas). As expected, the costs related to the winter scenario are more significant since energy production is higher if compared with the summer one.

Winter (6 months)				
El produced [MWh]	El demand [MWh]	Th produced [MWh]	Th demand [MWh]	Thermal dissipations [MWh]
240.92	234.55	499.33	476.98	22.35
		Cons. fuel [ton]	Fuel Costs [€]	**Total Costs [€]**
		91.74	84,404.0	**84,820.3**
Summer (6 months)				
El produced [MWh]	El demand [MWh]	Th produced [MWh]	Th demand [MWh]	Thermal dissipations [MWh]
59.62	63.29	286.19	286.19	0.00
		Cons. fuel [ton]	Fuel Costs [€]	**Total Costs [€]**
		65.57	60,325.4	**61,562.7**
TOTAL (year)				
El produced [MWh]	El demand [MWh]	Th produced [MWh]	Th demand [MWh]	Thermal dissipations [MWh]
300.54	297.84	785.52	763.17	22.35
		Cons. fuel [ton]	Fuel Costs [€]	**Total Costs [€]**
		157.31	144,729.4	**146,383.0**

Figure 120 Yearly operational costs detail

In order to analyse more in detail the different costs of this energy hub, interconnected to a smart grid, Figure 121 summarizes all the involved costs used for the calculations of LCOH and LCOE defined as follows:

$$LCOH = \frac{\sum_i (CapitalCosts_i + O\&M_i + FuelCosts_i)}{\sum_i (ThProduction_i)}$$

$$LCOE = \frac{\sum_i (CapitalCosts_i + O\&M_i + FuelCosts_i)}{\sum_i (ElProduction_i)}$$

Where i is referred to the years of the lifecycle.

The capital costs have to be considered specifically if are related to thermal or electricity costs. In the case of a CHP unit such the mGT, since its main goal is to produce electricity, its capital cost is mainly attributed to LCOE (70%). Anyway, in order to use the heat from the mGT exhaust, a recuperator is needed: its cost is considered in the LCOH evaluation. Solar façade panels and TES are, as well, part of the capital costs related to LCOH. For what concerns the fuel costs, they are only related to the Natural Gas consumption of the CHP unit. Considering that, over its thermal production, part of its electricity production is used to supply the HP, around 70% of the fuel costs are considered in the LCOH calculation. The global lifecycle of this system is considered to be 10 years.

Cost mGT	[€]	140,000.00 €
Cost mGT recuperator	[€]	40,000.00 €
Cost HP	[€]	6,000.00 €
Cost Solar Panels	[€]	45,000.00 €
Cost Storages	[€]	5,000.00 €
Years	[anni]	10
CI annual el	[€]	14,000.00 €
C O&M annual el	[€]	1,400.00 €
C fuel annual el	[€]	57,891.77 €
CI annuali th	[€]	9,600.00 €
C O&M annual th	[€]	960.00 €
C fuel annual th	[€]	86,837.65 €
El energy produced	[MWh]	300.5
Th energy produced	[MWh]	785.5
LCOH	**[€/MWh]**	**124.0**
LCOE	**[€/MWh]**	**243.86**

Figure 121 Voice of cost for LCOE and LCOH calculations

The obtained LCOH value is quite promising if compared with standard solar plants (LCOH= 149 €/MWh [67]). The LCOE, on the other hand, is quite high if compared with standard mGT applications (LCOE= 120 €/MWh [68]). This is mainly due to the strong partial load of mGT related to the limited electric load. This scenario leads to a not completely use of the mGT that has the highest costs.

Considering the scenario with higher electric demand (see Figure 122), the calculation of the LCOE gets lower. In this sense, it has to be considered to use as much as possible the most expensive component (mGT) in order to properly depreciate its cost.

LCOH	**[€/MWh]**	**126.6**
LCOE	**[€/MWh]**	**193.01**

Figure 122 LCOH and LCOE for the scenario with higher electric demand

Considering the overall energy produced and the total costs, the levelized cost of energy can be calculated. Depending on the considered electricity load supplied by the ENVISION system, the calculated value ranges between 180 and 190 $/MWh. As reported in ***Figure 123***, this value is quite high if compared with the American Scenario taken as a comparison, it is also worth noting that the cost of panels could decrease in the next future through a full industrialization process.

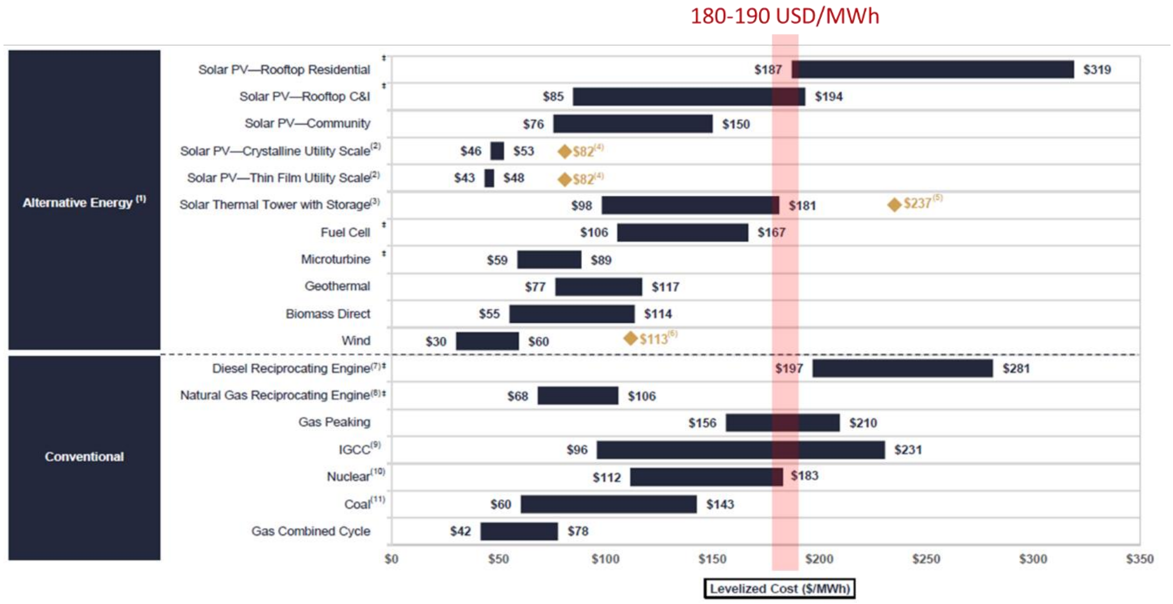

Figure 123 Levelized cost of energy for ENVISION system compared to alternative and conventional energy systems [69]

2.4.4 Control algorithm for the Savona Demosite

This section is focused on the algorithm that will be implemented in ENVISION Southern-Demosite. The control scheme that will be utilized for the considered application is a Model Predictive Control (MPC). This kind of control will be generally described in a preliminary section in order to understand the potential and also possible drawbacks of this choice; then a dedicated section will be focused on how this control architecture will be set and designed in order to match the Southern-Demosite needs.

2.4.4.1 MPC General Description

The MPC is a control-based architecture that utilizes an explicit model to predict the future response of a system. This is achieved by a prediction horizon based on preceding and future actuator commands. Implemented for many applications, the application of MPC in the field of the smart grid has risen consistently in the last decade [70].

Model Predictive Controls depend on dynamic models of the process, most of the time linear empirical models derived from system identification. MPC refers to a class of computer control algorithms that use an explicit mathematical model to predict future system behaviour. At each control interval, the MPC operates to optimize the future response of the plant by computing a sequence of future manipulated variable regulations, over the predicted horizon. Then, only the first input of the optimal sequence of control elaborated is delivered into the system. The entire calculation is repeated at subsequent intervals of control. Originally MPC has been developed to meet the specialized control needs of power plants and petroleum refineries, while, it can now be found in a wide variety of application areas [71]. Traditional feedback controllers operate, in response to a variation, by regulating control action in the output setpoint of a system, while MPC is a method that focuses on constructing controllers that can adjust the control operation before a variation in the output setpoint actually occurs. Combining traditional feedback operation with this predictive ability, the controller can operate smooth adjustments that are closer to the optimal control action values.

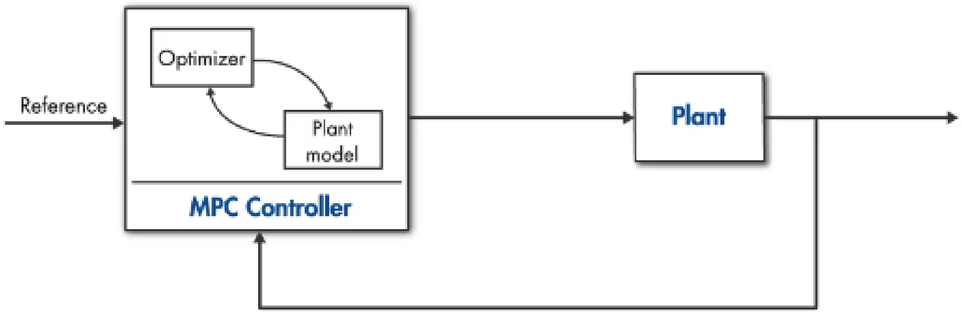

Figure 124 MPC Controller Scheme

As Figure 124 shows, an MPC is a MIMO (Multi Input Multi Output) control algorithm that uses a model of the system to predict the future behaviour of the system. A cost function minimization is applied to find the best control action driving the predicted output close to the reference. In the end, it can be stated that MPC implements the best control actions that come from a minimization process involving a defined cost function. During the process of minimization of the cost function, the system has to respect fixed constraints such as technical specifications (e.g. minimum off-design). Figure 125 reports a schematic description of the concept that stands behind MPC operation.

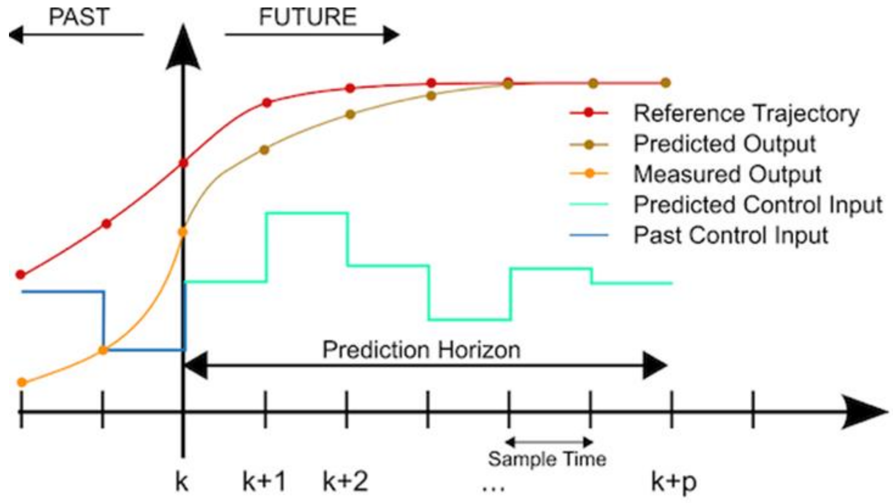

Figure 125 MPC Concept description

The model implemented inside the MPC, predicts the output of the plant depending on the manipulated variables. In order to guarantee that the output is close enough to the reference over the prediction horizon, an optimizer is used for minimizing the *J* cost function. Therefore, the MPC provides the sequence of manipulated variables that guarantees the minimization of *J*, but only the first action will be actually implemented (the first in the sequences of manipulated variable). Then the plant moves to the next time step, where it is possible that the real plant output is different from what has been predicted by the MPC at the previous timestep: this can be due by some unmeasured disturbance. At this point, the MPC process begins again for this new time step.

In detail, the **Prediction Horizon** represents the number of samples in the future where the MPC predicts the plant output. At the instant *k*, the MPC controller predicts the plant output along the period k + Np. The choice of the prediction horizon affects the control behaviour; in this sense, longer prediction horizons guarantee more robust, stable but slower control behaviours. In particular, short Prediction Horizon reduces the length of time during which the MPC controller predicts the system outputs. In this case, the MPC works more like a traditional feedback controller. Differently, a long Prediction Horizon increases the predictive ability of the MPC controller, but the performances get poorer due to extra calculations.

The **Control Horizon**, instead, represents the number of samples within the Prediction Horizon where the MPC controller can affect the control action. The main point of the optimization problem is to compute a new control input vector, u_k, to be feed to the system, and taking into consideration process constraints. A short control horizon means more carefully changes in the control action. A long control horizon means more aggressive changes in the control action.

The main drawback of MPC is that a **plant model**, for example, a model which describes the input to output behaviour of the system, is needed. This model requires an easy form in order to guarantee lean calculations (ideally linear models) and should produce accurate predictions based on easily identifiable parameters. In practice, usually, simply data-driven linear models are used. Considering that the most employed systems are a steady-state estimation, fast transient response and mid-range response, the best solution is the simplest model that gives accurate enough predictions, namely the capture of transient behaviour (shape of response) in a range of 10-20% error that is acceptable due to feedback. For all these reasons, the model assumed for MPC is a discrete state-space model as reported below:

$$\begin{cases} x_{k+1} = Ax_k + Bu_k \\ y_k = Cx_k + Du_k \end{cases} \qquad (25)$$

Where x, u, y denote respectively the state, input and output variables.

As explained before, in order to properly operate the control, a **cost function** minimization process occurs. The cost function J is reported below.

$$J = \sum_{i=1}^{N} w_{y_i}(r_i - y_i)^2 + \sum_{i=1}^{N} w_{u_i}\Delta u_i^2 \qquad (26)$$

Where:

y_i : i th controlled variable

r_i : i th reference variable

u_i : i th manipulated variable

w_{yi} : weighting coefficient reflecting the relative importance of y_i

w_{ui} : weighting coefficient penalizing relative changes in u_i

N: prediction horizon

So the basic problem is to solve:

$$\frac{\partial J}{\partial u} = 0 \qquad (27)$$

Finding the set of u that guarantees the minimization of the problem, as reported in

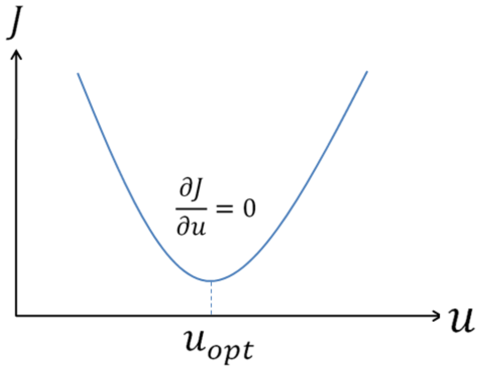

Figure 126 Optimization problem solution

The choice of weights strongly affects the control performances. It is, therefore, possible to prioritize the respect of the setpoint tracking or to smooth changes of manipulated variables. Depending on the relative values given to these weights it is possible to have different behaviour of the control; the most the importance of w_{yi} the quickest, but nervous, the control behaviour.

All physical systems have constraints. There are physical constraints like actuator limits and safety constraints like temperature and pressure limits. Finally, there are performance constraints like overshoot.

In MPC constraints are defined for the outputs and for the inputs and their variations:

$$y_{min} \leq y \leq y_{max} \quad (28)$$
$$u_{min} \leq u \leq u_{max} \quad (29)$$
$$\Delta u_{min} \leq \Delta u \leq \Delta u_{max} \quad (30)$$

An optimal control system is only optimal if it satisfies constraints. MPC embeds constraints into the optimization, while most control strategies (e.g. PID) implement constraints as an afterthought (saturation, overshoot).

Model Predictive Control is often used in addition to traditional control like PID (Proportional Integrative Derivative). In large plants, MPC is used in addition to traditional PID and it isn’t a replacement of them. MPC is used as an overall system, while PID controllers are used as single-loop controllers. MPC is a more advanced method of process control used for MIMO systems, while PID handles only a Single Input and a Single Output (SISO). The models used in MPC are usually intended to represent the behaviour of complex dynamic systems. The additional complexity of the MPC control algorithm is not particularly suitable for the control of simple systems, which are well regulated by PID controllers. Typical dynamic peculiarities that are difficult for PID controllers are often referred to large time delays and high-order dynamics. Another advantage of MPC is that cross-coupling in

MIMO systems are taken into account in an optimal way. MPC is a simple method for controlling MIMO systems.

2.4.4.2 Preliminary ENVISION MPC

In a preliminary phase, before an actual on-field control test campaign, basic control of mGT and Heat Pump, in order to cover the electrical and thermal loads in the best way respecting the intrinsic limitations of the system, has been developed. The setpoints are given by the loads uploaded in Matlab Simulink representing two days for the hot and cold season. The controller gives as output the electrical power required from the mGT (P_mGT) and the heat required from the HP (Q_cond) through a predictive calculation developed on a state-space system (representing the real model) implemented inside the controller. Figure 127 reports the simplified state-space model implemented inside the MPC, representing the HP.

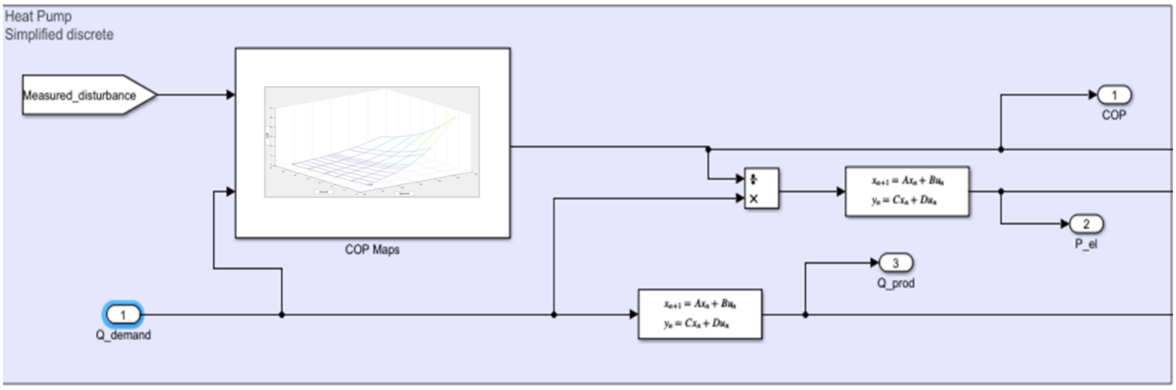

Figure 127 HP state-space model for MPC

The inputs of the model are the thermal demand (here reported as Q_demand) and the temperature from the panels, actually a measured disturbance for the system. These two parameters are inserted in COP maps, in order to estimate the COP of the HP in the expected conditions. The main outputs of the system are then, the electric consumption of the HP (reported as P_el) and the actual Heat Pump thermal production (reported as Q_prod). The COP is also reported as a monitored parameter of the HP performances.

The matrixes of the HP states model are reported below and obtained from the linearization of the simplified model described in 2.2.2.1:

$$A_{HP} = \begin{bmatrix} 0.998 & 0 \\ 0 & 0.998 \end{bmatrix}$$

$$B_{HP} = \begin{bmatrix} 0 & -0.0023 \\ 0 & 0.1 \end{bmatrix}$$

$$C_{HP} = \begin{bmatrix} -0.0025 & 0 \\ 0 & 0.0025 \end{bmatrix}$$

$$D_{HP} = \begin{bmatrix} 0 & 0 \\ 0 & 0 \end{bmatrix}$$

The mGT state-space model, indeed, is reported in Figure 128.

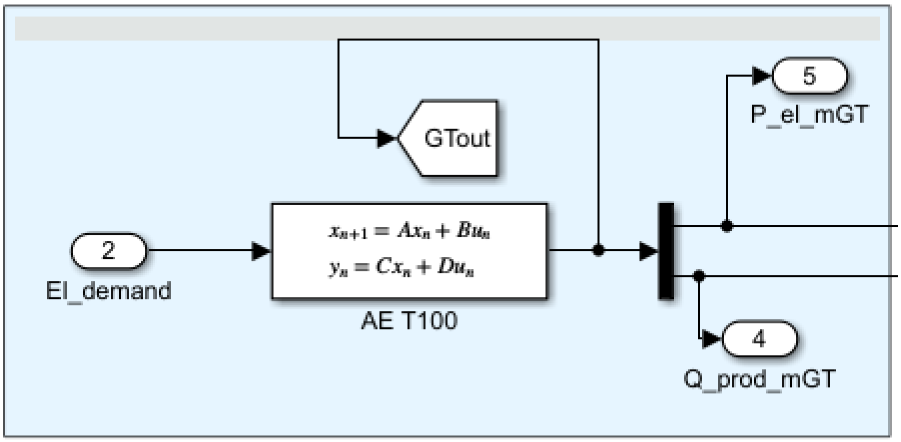

Figure 128 mGT state-space model

The input for this model is the electric demand (reported as El_demand), while the outputs are the thermal and electrical production, respectively reported as P_el_mGT and Q_prod_mGT.
From previous activities of the author's research group, it has been possible to obtain the values for characteristic matrixes of the mGT state-space model, below presented.

$$A_{mGT} = \begin{bmatrix} 0.88 & 0 \\ 0.16 & 0.90 \end{bmatrix}$$

$$B_{mGT} = \begin{bmatrix} 0.12 \\ 0 \end{bmatrix}$$

$$C_{mGT} = \begin{bmatrix} 1 & 0 \\ 0 & 1 \end{bmatrix}$$

$$D_{mGT} = \begin{bmatrix} 0 \\ 0 \end{bmatrix}$$

The MPC regulates the heat provided by the heat pump acting on the mass flow rate from the DHN, while the PI control inside the HP guarantees the desired outlet temperature. The temperature from the façade panels circuit (T_outPanels) is implemented as a measured disturbance since it is a parameter that affects the HP performances (namely the COP) without that it can be controlled by the MPC. The MPC implemented is schematically reported in Figure 129.

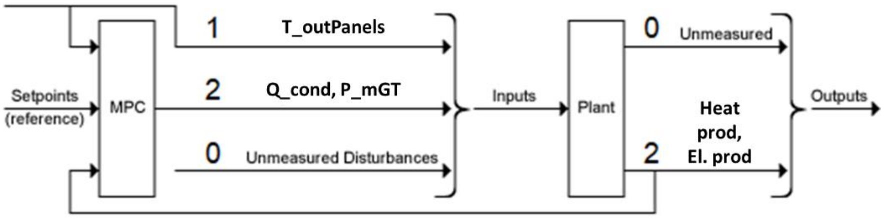

Figure 129 Case study MPC structure

Where Q_cond is the actual thermal demand for the HP and P_mGT is the actual electric demand for the mGT. These two variables are the manipulated variables by the control system (u_i), while the outputs of the system (y_i) are represented by the overall thermal and electric production. The setpoints are represented by the energy loads.

The MPC has been implemented using Matlab Simulink MPC Toolbox that, with its user-friendly interface, allows an easier setting of the weights. The relevance of thermal loads has been considered more significant than the electrical one since that in this configuration no thermal storages are considered. Therefore, the MPC weights have been tuned in respect of these system requirements, by using Matlab Simulink MPC Toolbox.

The main constraints and setting for the developed MPC are reported in Table 30.

Table 30 Preliminary MPC parameters

Sample time	0.1
Predicted Horizon	100
Control Horizon	2
y_{min}, y_{max} thermal	-
y_{min}, y_{max} electric	-
u_{min}, u_{max} mGT	20, 100 kWel
u_{min}, u_{max} HP	2, 20 kWth
$\Delta u_{min}, \Delta u_{max}$ mGT	-10, +10
$\Delta u_{min}, \Delta u_{max}$ HP	-
w_u mGT	3.52
w_u HP	3.52
w_y thermal demand	0.068
w_y electric demand	0.028

It is worth noting that, considering the quite fast maths behind this model, the use of a small sample time does not lead to long calculations. The main constraints are related to the employed machine size for both mGT and HP, it is worth noting that at this phase a cautelative value of 20 kWth for the HP has been considered since that an evaluation on the field of the HP performances has been possible. Variations in time are mainly limited to mGT since its higher inertia.

The results obtained for the summer period are reported as a significative example. This period, indeed, is the period where the façade panels are supposed to have a stronger impact on the system.

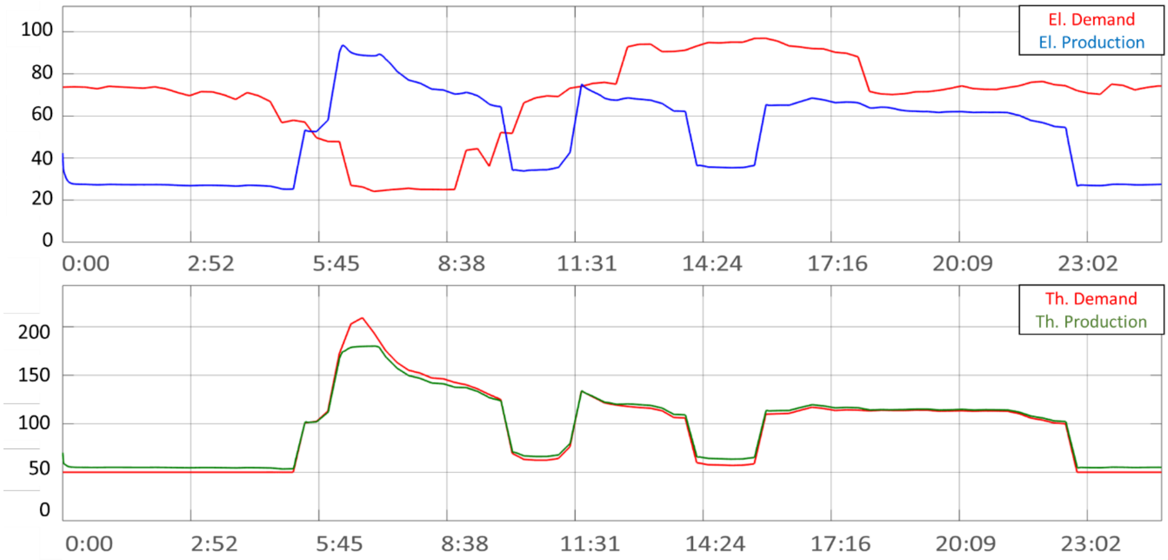

Figure 130 Electric (top) and thermal (bottom) system management

Figure 130 shows that, in compliance with the set weights, the thermal demand is well covered and privileged respect to the electric one. Furthermore, it is worth considering that the installed thermal capacity is not sufficient to guarantee a complete tracking of the thermal demand in the early morning peak. Indeed, as Figure 131 confirms, the system manipulated variables in that period reach their maximum constraints. This aspect, connected to the not really accurate tracking of the electric demand, suggest a need for thermal storage.

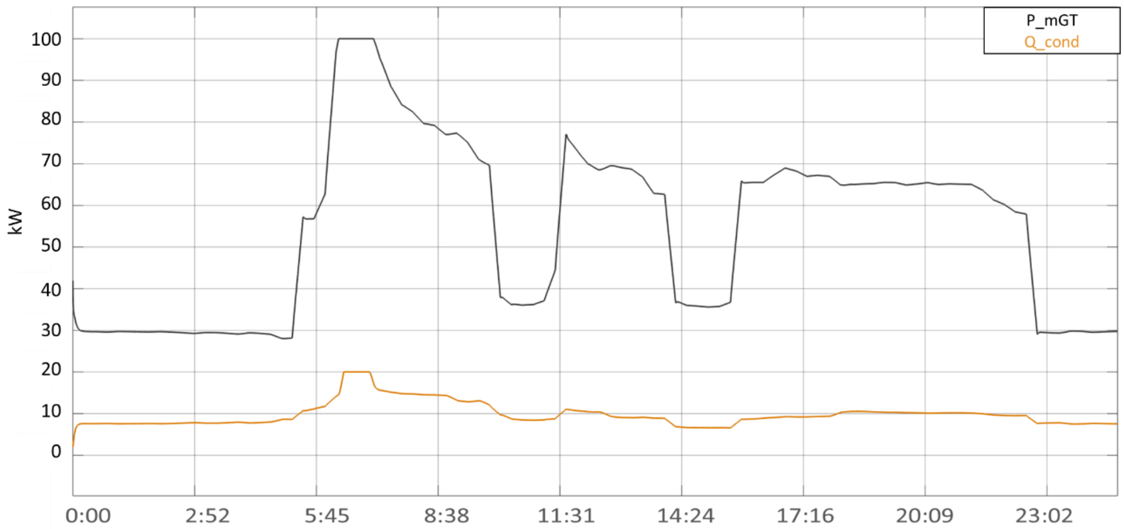

Figure 131 MPC controlled variables

Considering the variables manipulated by the system, some slight differences can occur moving to the operation of the actual system. Figure 132, indeed, shows the real thermal production for both mGT and HP. At this control stage, it has not been implemented any particular priority to the use of mGT or HP, therefore the thermal demand is equally split between the HP and mGT depending on their max size selected for this application.

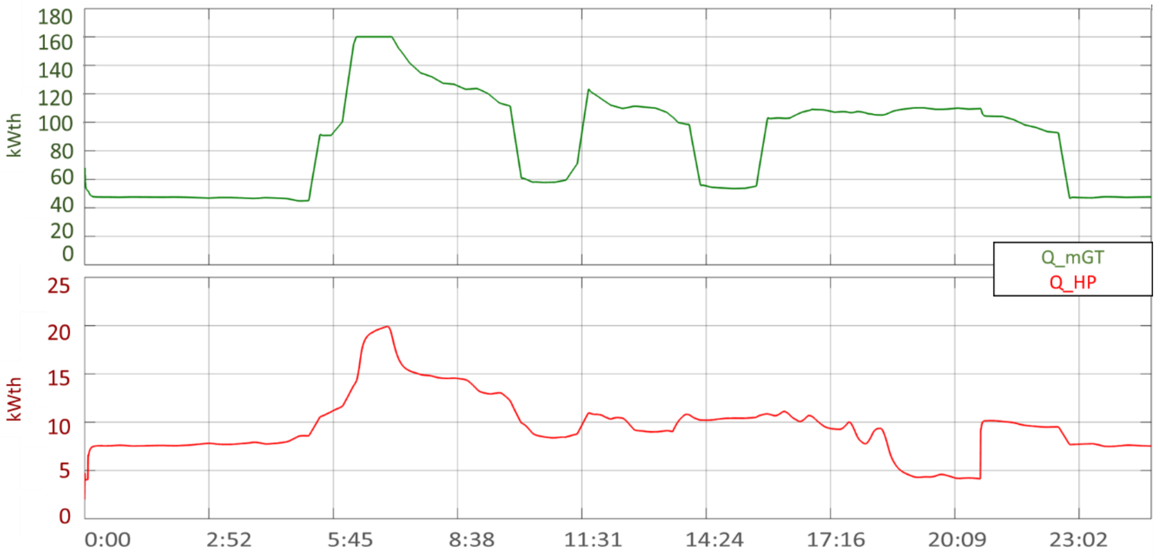

Figure 132 HP and mGT actual thermal production

This preliminary control suggests the need for improvements, in order to be able to analyse more in detail the actual system that will be installed in Savona Campus. To do that, some upgrades have been developed, in order to be implemented, tested and tuned during the experimental campaign, where data will be available and collectable.

2.4.4.3 ENVISION MPC upgrades for experimental campaign

In the context of ENVISION, it will be necessary to implement a more detailed control, able to manage also economic aspects and not just a load tracking. In order to reach this ambitious goal, it is necessary to upgrade the developed MPC, building an advanced MPC. This advanced MPC takes care of system economics, together with energetic aspects. The proper management of this system is particularly useful considering the interface of an "ENVISION system" with a DHN, having the chance of buying or selling both thermal and electricity to their associate grids.

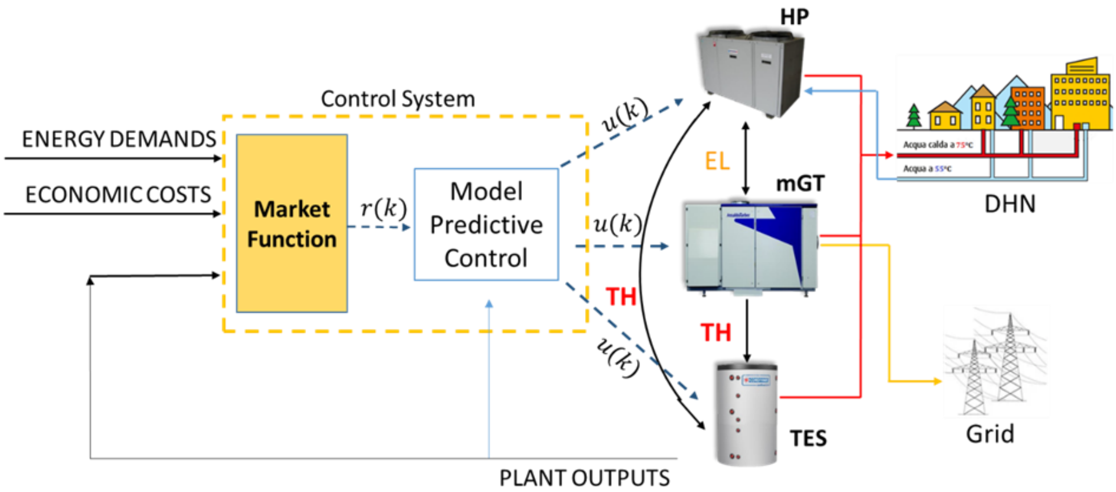

Figure 133 Advanced MPC description for ENVISION system

This advanced control requires the implementation of an additional block, in charge of calculating the variable cost of the system via a so-called market function. This market function is then given as an input to the actual MPC that will manage the system considering also the minimization of this additional input, as reported in the layout of Figure 134.

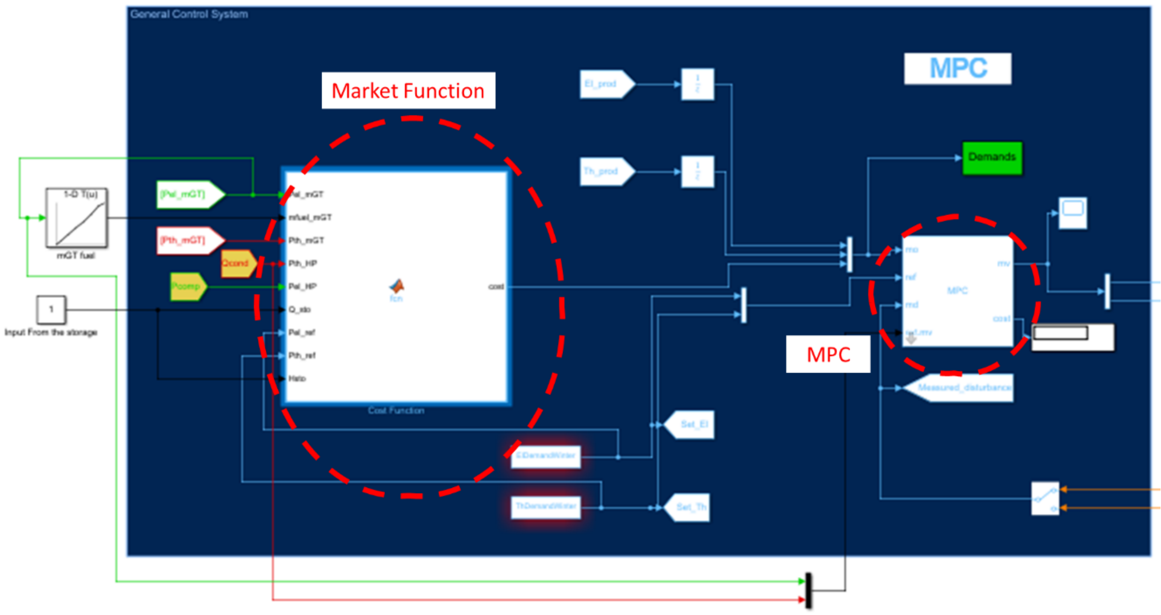

Figure 134 ENVISION advanced MPC layout in Matlab Simulink

With this upgrade, the MPC will be able to consider also economic aspects tanks to an additional cost function. The first step (Market Function) generates a new input to be minimized for the following MPC controller. No models are present inside this first step and its flexibility helps to manage different problems. Considering the ENVISION context, where a poly-generative smart grid is present, the point is to find the best compromise between economics and demand-supply.

The market function C implemented in the first step of the control system is one reported below:

$$C = c_{F_i} m_{F_i} + c_{El.Grid_i} P_{El.Grid_i} + c_{Th.DHN_i} P_{Th.DHN_i} - c_{El.Sell_i} P_{El.Sell_i} - c_{Th.Sell_i} P_{Th.Sell_i} \pm c_{TES_i} P_{TES_i} \tag{31}$$

Where c_i are the costs related to the ith period. These costs are related to the fuel consumption, to the electrical and thermal purchasing (from Grid and DHN), to the selling price of thermal and electrical power and to the TES charging or discharging process. In order to maintain the chance of having good system flexibility, the Storage charging process will be privileged when close to the empty state, while the discharging process is privileged when the Storage is almost full.

Thanks to the implementation of this market function, it will be possible to have an optimized control that focuses not only on the tracking of thermal and electrical demand, but that considers an optimization in terms of costs and, therefore, efficiency. Thanks to this approach it will be also possible to improve the environmental aspects moving towards more green management of the system, implementing also costs related to system emissions. It is worth to underline even in this phase, that the DHN temperature of 75°C is guaranteed by the PID control implemented inside the HP model. For what concerns the mGT, this condition is guaranteed intrinsically by the machine specifications.

In order to tune and set up properly this advanced control system, a properly validated model is needed. Therefore, the developed model of the plant, presented in section 2.2 has to be validated during the on-field campaign once that the installation of ENVISION components will be completed, especially for what concerns the prototypal Heat Pump. These validated models will be then used to properly emulate the plant behaviour, while a state-space model derived from the complete model will be implemented inside the MPC. After the finalization of the detailed definition of all the controller component, a detailed tuning of the control system will be performed, both at software and plant level, using as a guideline the results obtained from the W-ECoMP analysis presented in the previous sections.

Since that represents a reference, it is really important to know the thermal and electrical demand profile in advance, giving to the MPC the chance to optimize the cost function over the prediction period. In this sense, the idea is to have in advance, from the central management of the Smart Grid the indication of the loads that they will expect to be satisfied by ENVISION machines in the next day. These profiles will be used as a reference for the control of the plant via MPC. Some little adjustments could be implemented in real-time.

2.5 Preliminary test campaign

In order to properly install the technologies included in the final Southern Demo, some renovation works are needed at Savona Campus. The pandemic of COVID-19 has caused some little delay in the bureaucratic procedure for the permit to start the work. In this sense, it is expected the beginning of the work at the beginning of 2021, having the site ready for the first half of 2021.

In the meanwhile, some preliminary evaluations of panel performances have been done installing four panels in Savona Campus as shown in Figure 135.

Figure 135 Preliminary Demo at Savona

Two panels are connected in series and two in parallel in order to understand which configuration performs better. To do that, sensors have been installed evaluating the temperatures and mass flow rate. The layout of the preliminary demosite is reported in Figure 136.

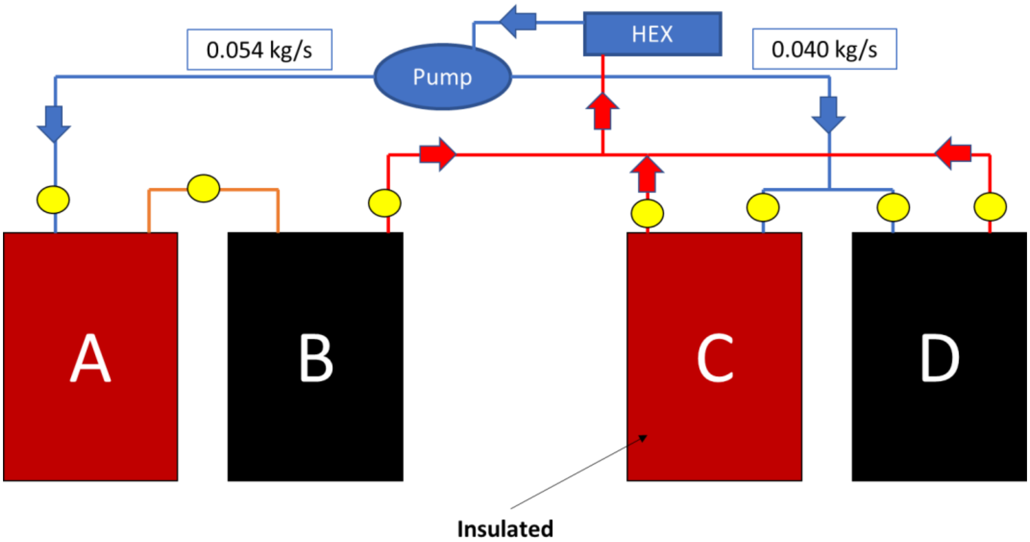

Figure 136 PreDemo layout

Where in yellow are reported the sensors used for the monitoring of the system temperatures. The selected sensor probes are PT 100, a detailed view of the sensors installed is reported in Figure 137.

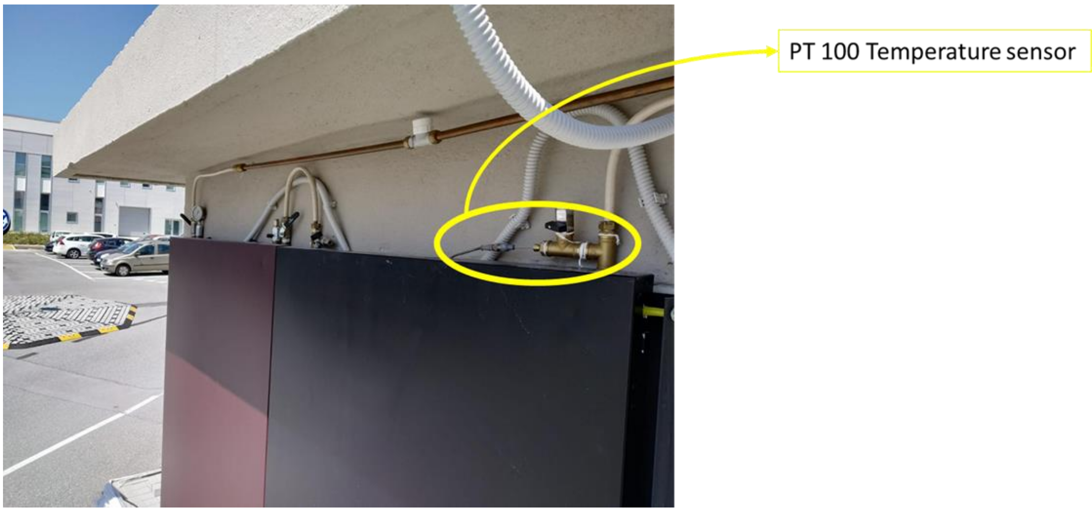

Figure 137 Temperature sensors detail

The heat capacity of the installed system is quite small; therefore, it has been decided to dissipate the heat produced in ambient via a forced ventilation small heat exchanger. Furthermore, the different performance between a panel with insulation on the back, and a standard panel has been evaluated.

The first main positive feedbacks from the test-rig activities refer to the easy installation technique and the low weight of the panel. On the other side, in terms of an actual residential installation, with high TRL, an improvement in terms of aesthetic it has to be considered. Indeed, since the piping and hydraulic system results quite voluminous, a properly coverage of these components could guarantee a better aesthetic impact.

It is also worth noting that, at this preliminary phase, it has been decided to evaluate the impact of insulation in the back of the panels in order to avoid thermal dissipations. During the development of ENVISION façade panels, the suppliers proposed to do not insulate the panels in order to enhance the heat exchange area with the external air, in order to guarantee an heat absorption from the external ambient, even in case of zero solar radiation. In this configuration, the connected HP could be then considered kind of air-to-water HP. The performances of insulated or not insulated panels will be therefore one of the main results of this preliminary test campaign.

The main interesting results are reported in the following lines. It can be noticed that the working temperature of the solar panels are quite high, therefore, considering the efficiency curves presented in Figure 54, the expected efficiency of the panel in this application is limited. In order to improve the efficiency of the solar panels, a higher thermal load should be connected to the panels. At this stage, the aim was to test the panels at high temperatures, since are a requirement in order to properly manage the ENVISION system in interconnection to the Savona Campus DHN.

The first results reported are referred to data acquisition in a summer morning, August. During this period, the Savona Campus was closed, therefore it has not been possible to acquire their solar radiation measurements. In order to solve this issue, data provided by SOLCAST has been used as a reference for this period [72]. The environmental data provided by SOLCAST are reported in Figure 138, where wind conditions, solar radiation and ambient temperatures are shown.

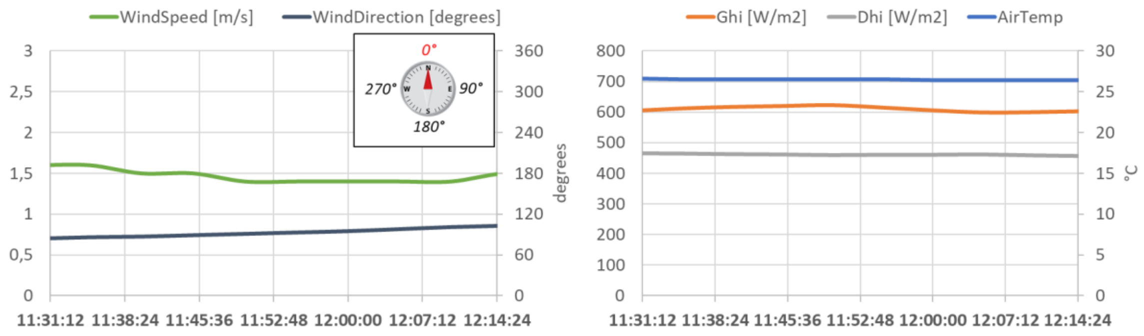

Figure 138 Ambient conditions for morning August day by SOLCAST

Figure 139 shows the inlet and outlet temperature of the panels during data acquisition in a summer morning. As highlighted in yellow, in some periods, where the solar radiation decreases (mainly due to cloud presence), the outlet temperature of the panels gets equal or lower than the inlet one. This condition means that the panel is dissipating more heat than the one absorbed by the solar radiation.

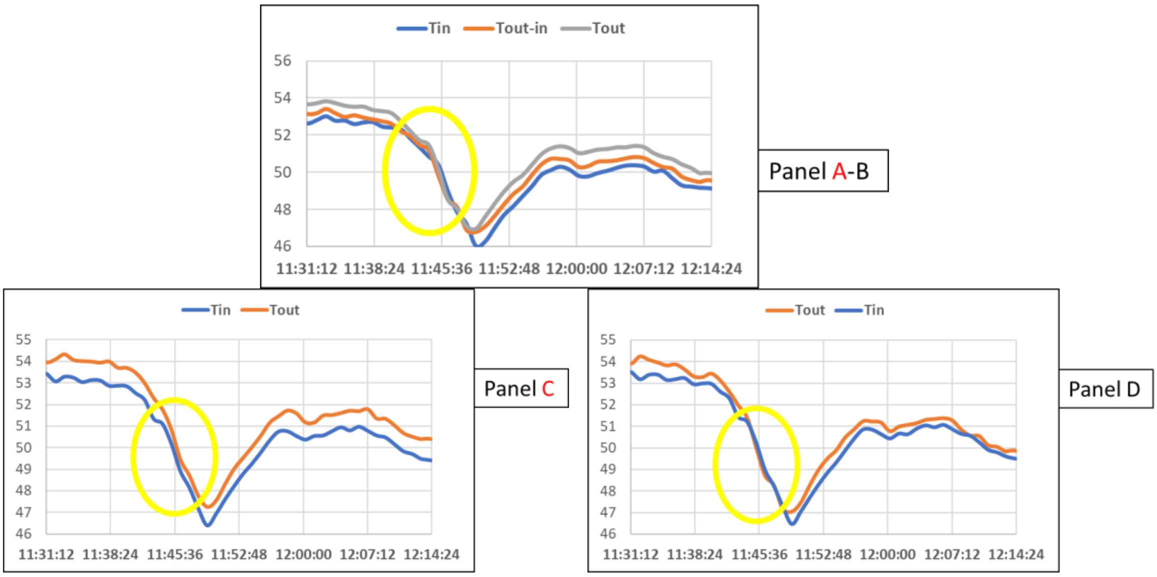

Figure 139 Temperature trends for the panels during August morning

Anyway, looking at the performances of the insulated panel (Panel C), the presence of insulating material on the back of the panel allows a minimization of the cited thermal dissipations. Therefore, the outlet temperature of the panels still remains higher than the inlet one. The cited aspects in terms of temperature are confirmed by the results shown in Figure 140, where the heat produced by the panels is reported.

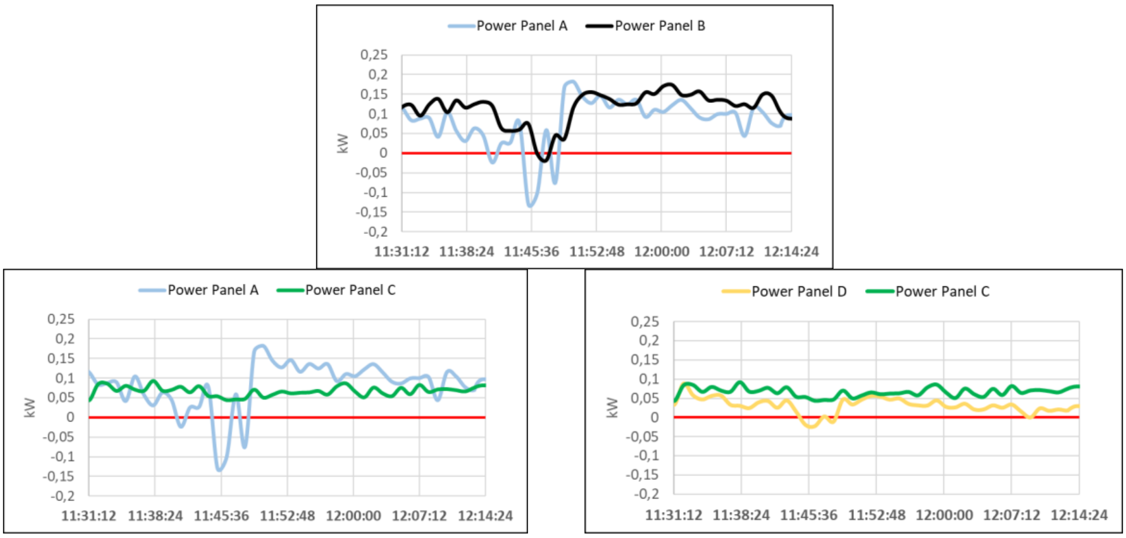

Figure 140 Heat produced by ENVISION panels, August morning

It is worth to underline that the insulated panel has more constant behaviour, allowing to avoid thermal dissipations in ambient when the temperature in the panels is higher than the ambient one. Generally speaking, it can be considered that, for a South-East oriented façade, each panel (around 2 m^2 of surface) produces not more than 200 Wth at the temperature of 50°C.

In addition, considering the series-parallel configuration, the experimental data confirms what has been performed by model simulations in section 2.3.1. The panels installed in parallel configuration (C-D) seem to perform worse than the series ones (A-B). Anyway, it is worth noting that this evaluation could be also affected by different shadowing occurring on the two different sides of the façade.

Analysing the conditions in the afternoon of the same day, from the values provided by SOLCAST and reported in Figure 141, it is highlighted a decrease of solar radiation moving to the late afternoon hours.

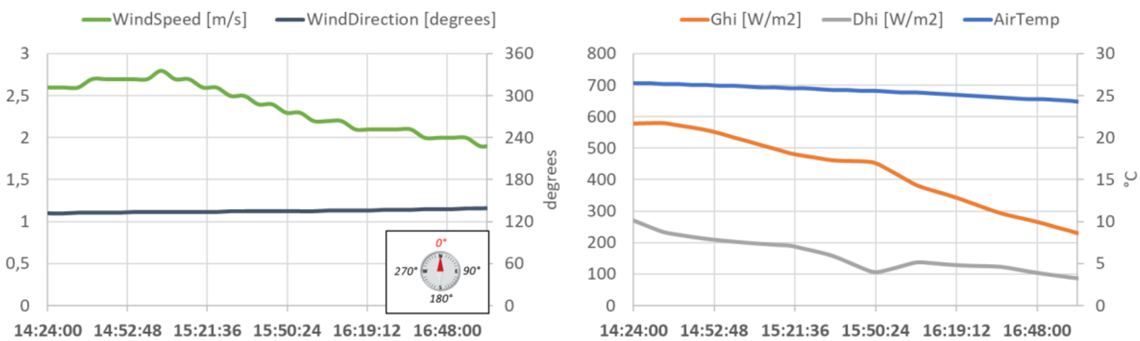

Figure 141 Ambient conditions for afternoon August day by SOLCAST

This aspect is reflected in a decrease of panels temperature, moving from 50°C to almost 35°C, as reported by Figure 142.

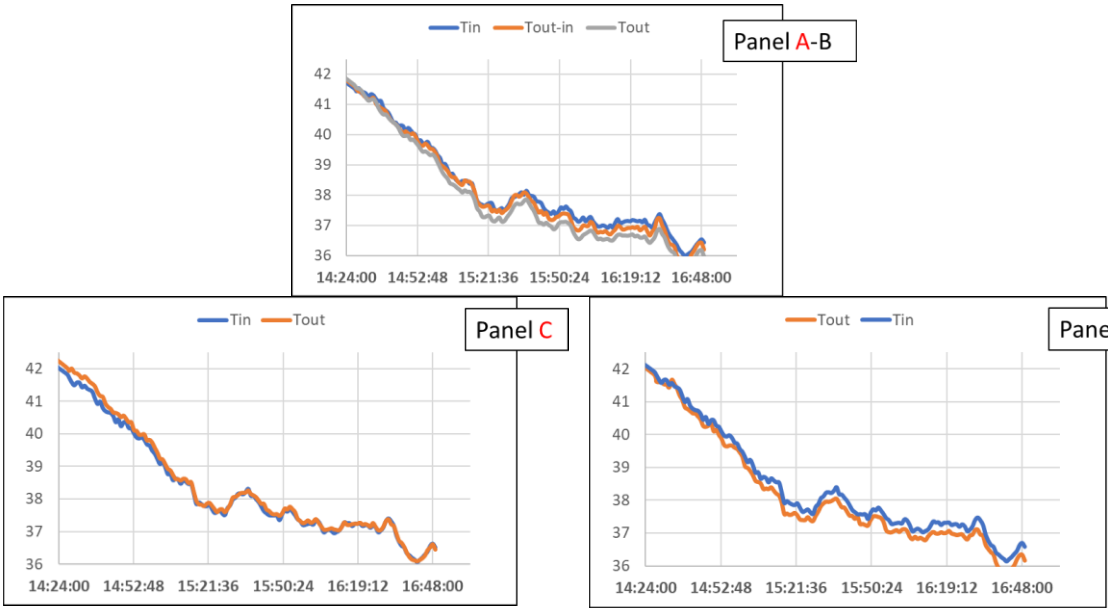

Figure 142 Temperature trends for the panels during August afternoon

Furthermore, the only panel that is still able to produce heat is the insulated one (Panel C), while the others, with outlet temperatures lower than input ones, perform thermal dissipation. This aspect can be confirmed looking at the heat production, reported in Figure 143, where only the green line (related to Panel C) still maintain a positive heat production. The lower solar radiation, reported by SOLCAST data, is anyway converted in lower heat production also by Panel C.

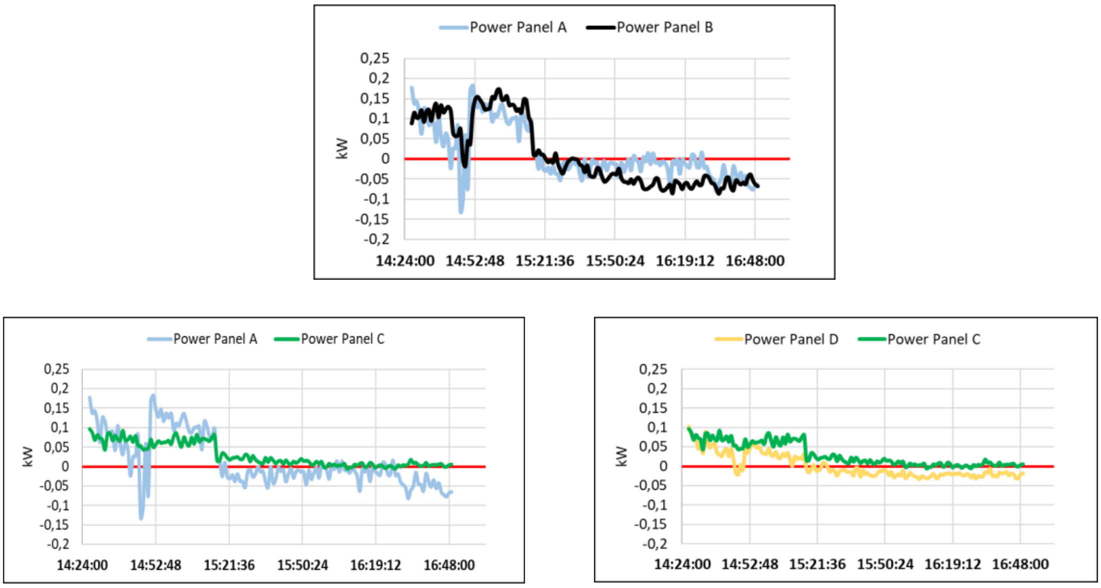

Figure 143 Heat produced by ENVISION panels, August afternoon

After the detailed description of the two different periods developed for an August day, a global daily analysis is provided for September. In this month, it has been possible to have access to the solar radiation data collected by Savona Campus (Figure 144).

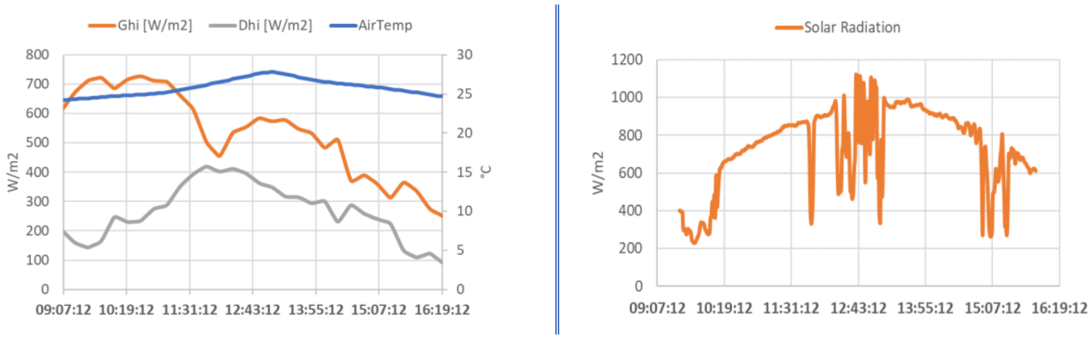

Figure 144 Daily Ambient conditions for September, SOLCAST data (left), Savona Campus data (right)

It is worth underlining that some differences are present comparting the data mathematically estimated by SOLCAST, and the actual data collected by Savona Campus. In this specific period, the calculations provided by SOLCAST underestimate the solar radiation.

The collected data from the experimental campaign are then reported in Figure 145.

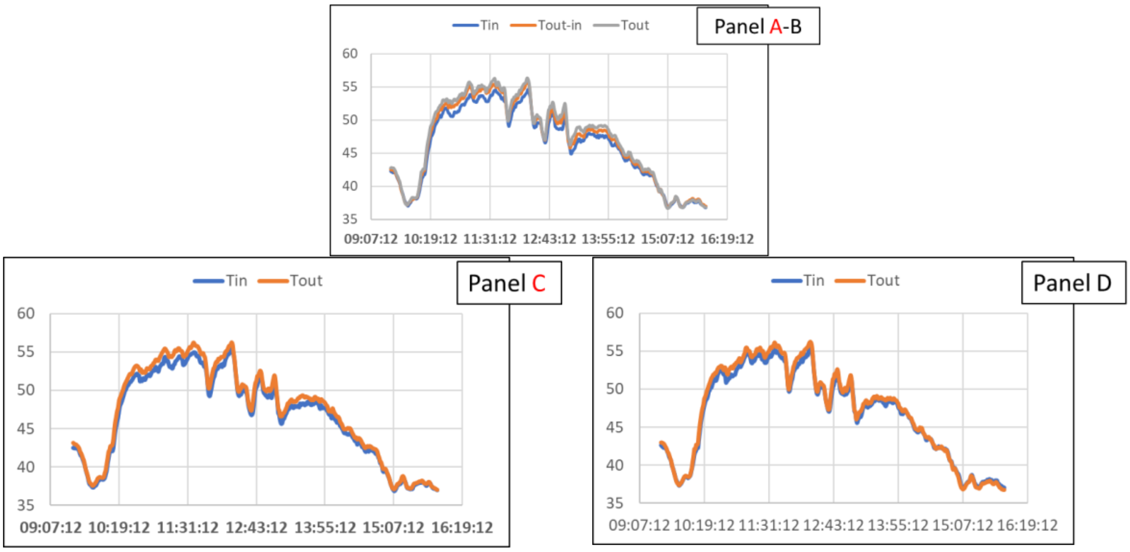

Figure 145 Temperature trends for the panels September day

The provided general overview shows that the panels, depending on the variation of solar radiation, work with temperatures varying between 35 and 55 °C.

For what concerns the heat production, Figure 146 shows the collected data and elaborated data.

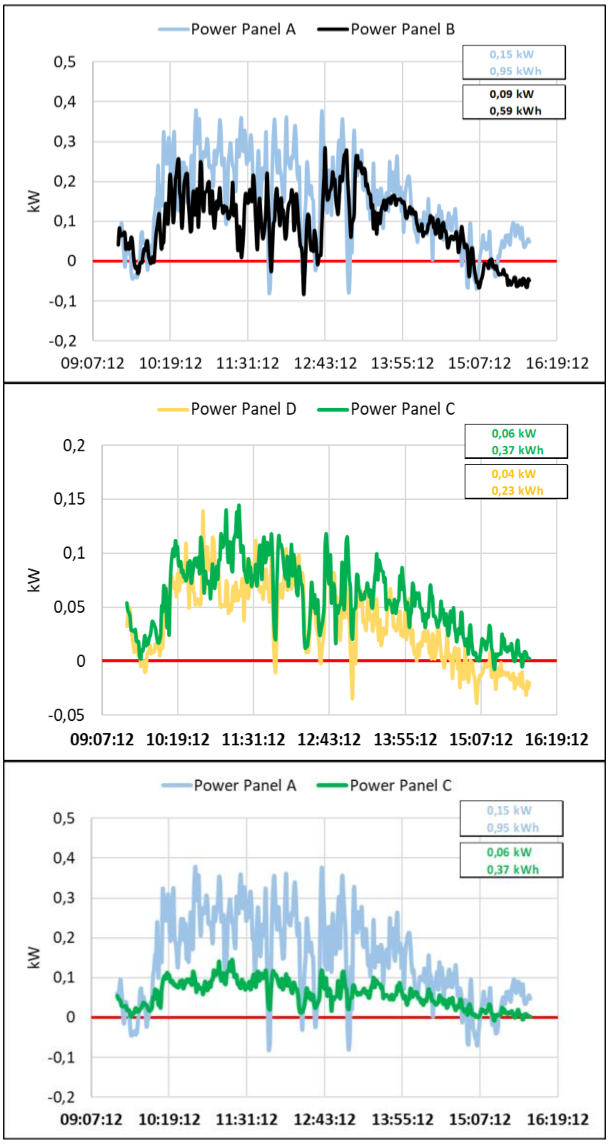

Figure 146 Daily monitoring of panels heat production in September

Due to on-site shadowing, beginning from the first hours of the afternoon, the heat production decreases significantly. This aspect has a relevant impact on the performance of the panels. The insulated panel (Panel C) avoids thermal dissipations also in the late afternoon, while the others are more affected by solar radiation changes. On the other hand, comparing the two red panels installed (Panel A and Panel C), the panel A performs better because of the two aspects mentioned above: series interconnection and less shadowing on that side of the building. In order to evaluate the harvesting performances of the system and not only the pure quantities of heat produced, the efficiency of the panels is calculated based on the following equation:

$$Efficiency = \frac{Panel\ Heat\ Power}{SolarRadiation * PanelArea} \quad (32)$$

The results are then reported in Table 31.

Table 31 Panels efficiency

Panel	Average Daily Efficiency	Peak Efficiency
A	10%	28%
B	5%	24%
C	4%	9%
D	2%	10%

Comparing the efficiencies of the two panels on the western side of the façade (Panel A and Panel B) they present higher efficiency than the ones on the eastern side (Panel C and Panel D). This aspect confirms what has been stated previously regarding the series interconnection benefits but also the better radiation conditions on the western side of the façade.

For what concerns a comparison between black and red panels, interesting conclusions can be made. Looking at the series interconnection, since the black represents the second member of the scheme, higher temperatures are expected in its inlet and therefore lower efficiencies. Therefore, despite the black colour, in the same conditions, guarantees higher efficiency; the different working temperature due to the series interconnection decrease its efficiency if compared with the red one.

Moving on the parallel interconnection, the inlet temperature of the two panels is the same; in this case, then, higher efficiencies are expected for the panel with the most performant colour (black, Panel D). Nonetheless, the presence of insulating material on the back of the red panel (Panel C) guarantees better performances, with an average efficiency higher than what has been measured for the black one.

3 A maritime application of Distributed Generation

As reported in Figure 18, transport is one of the most energy-demanding sectors in Europe. In this sense, the need to pollutant emission limitations requires a significant effort for re-thinking an innovative way for the production of energy in this context. In order to apply the benefits of Distributed Generation in transport, the only sector where DG is applicable is represented by maritime applications, thanks to the large volumes and consumptions. In the world of transportation, the maritime sector has been able to evolve steadily, showing its competitiveness to transportation systems introduced in global trade in more recent times. Modern ships have progressed in terms of efficiency and safety, allowing for a reduction in the time required to travel along intercontinental routes.

Compared to alternative transport systems (road, rail, air), shipping is more efficient and allows for the cost-effective transport of goods of all kinds in large volumes to major trade destinations around the world. With 11 billion tons of goods transported by sea in 2018 [73], the maritime sector has reconfirmed its essential role in the world market, accounting for about 90 per cent of global trade [74]. Figure 147 shows the relevant results obtained in terms of emissions by the maritime sector when compared with other sectors.

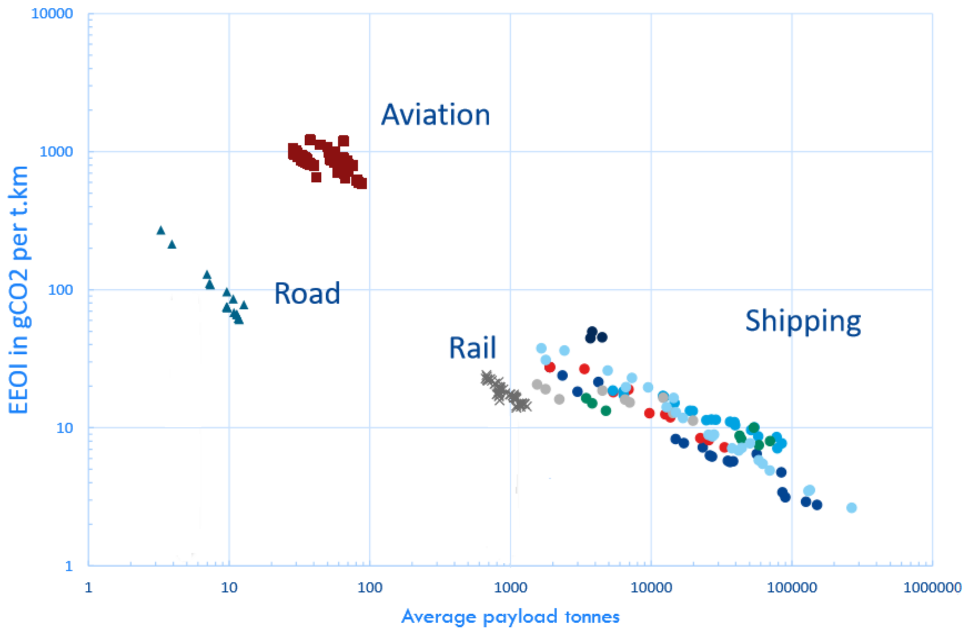

Figure 147 Transport sectors comparison [75]

The world marine fleet is mainly equipped with marine diesel engines, whose qualities are well suited to the maritime application. In particular: their insensitivity to ship movements and resistance to the marine environment makes them reliable systems; furthermore, they are efficient and easy to maintain. The durability of their components makes diesel engines long-life systems and thanks to their good power density it is possible to save precious space on board. At the same time, Internal Combustion Engines are characterised by the good response to load variations and their contained operating costs. With the gradual introduction of technologies such as exhaust gas turbocharging and the common-rail system, these engines have evolved over time and have become the most widely used solution in marine applications, leaving sporadic and specific fields of application to steam turbines, gas turbines and nuclear power plants.

The maritime sector refers to the International Maritime Organisation (IMO), a United Nations body that regulates maritime traffic through a series of regulations that promote safe and environmentally friendly transport by sea. The task of ensuring that these regulations are observed is delegated to governments and local institutions.

Figure 148 IMO Logo

Recently, public opinion and authorities have become more responsive to environmental issues. In a scenario where industrial realities are optimizing their processes to reduce their impact on the environment, the maritime sector has started to take similar measures in order to maintain its competitiveness in the face of alternative transport systems. The IMO Congress on pollution prevention (known as MARPOL, standing for Maritime Pollution) is the main body that regulates ship-related emissions. The MARPOL Annex VI document, which became effective in 2005, was created to limit SOx and NOx emissions globally [73]; previously agreed limits were revised in 2008 and introduced in 2010 [74]. In recent times, geographical areas known as Emission Control Areas (ECAs) have been defined, where only vessels that comply with even more stringent emission limits, also established by MARPOL Annex VI, are allowed to navigate. Figure 149 shows the current and potential ECAs.

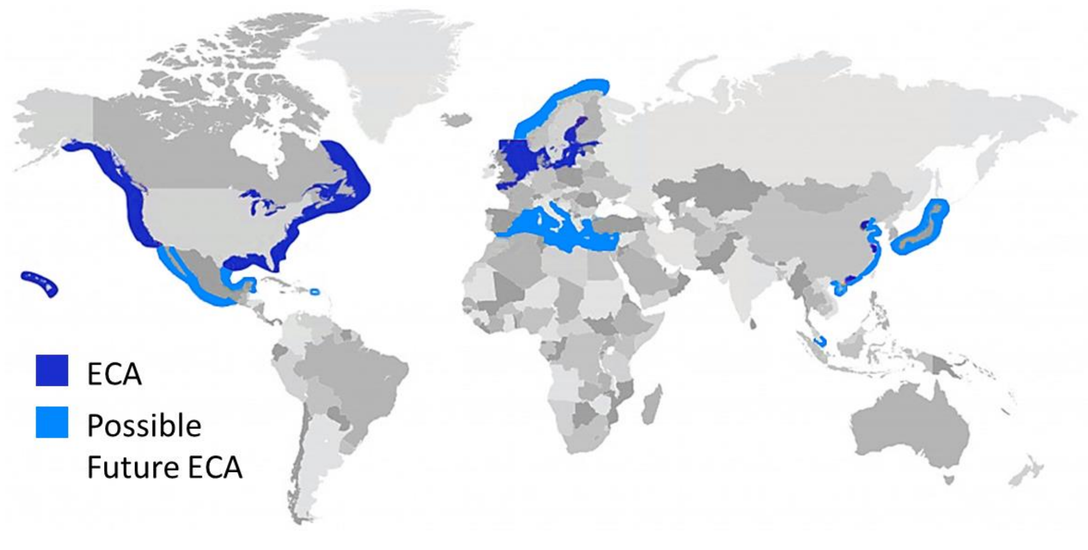

Figure 149 ECAs and potential ECAs [76]

The following are the restrictions currently in place to reduce SOx and NOx emissions. On January 1, 2020, the maximum globally permitted sulphur content in marine propulsion fuels was reduced from 3.5% by mass to 0.5% by mass. In SECAs (Sulphur Emission Control Areas), the sulphur content allowed in fuels from January 1, 2015 cannot exceed 0.1% by mass: vessels can navigate in these regions if they use sulphur-reduced fuels or are equipped with the appropriate exhaust after-treatment systems (scrubbers) [73]. SECAs already established involve the Baltic Sea, the North Sea, the U.S. and Canadian coasts, the seas around Puerto Rico and the U.S. Virgin Islands [76].

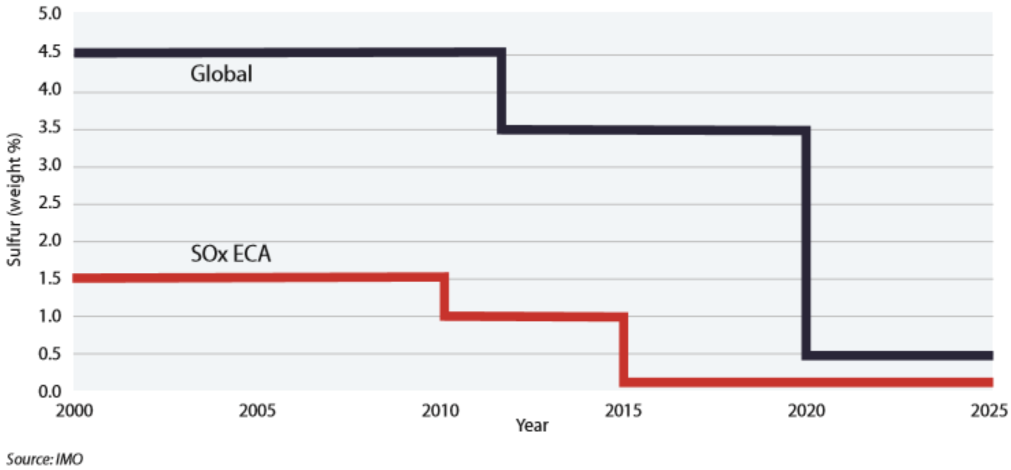

Figure 150 SOx limitations [73]

MARPOL Annex VI sets limits for nitrogen oxides emitted by marine diesel engines over 130 kW [73]; these limits depend on the engine speed and the date of ship construction. Manufacturers now refer to the IMO Tier II regulations, which apply to vessels constructed after January 1, 2011. If the vessel crosses a NECA (NOx-Emission Control Areas) zone, it is necessary to comply with the more stringent IMO Tier III regulations, which apply to ship constructed after January 1, 2016. Currently, NECA zones established worldwide include the North American coast, the waters of Puerto Rico, and the U.S. Virgin Islands.

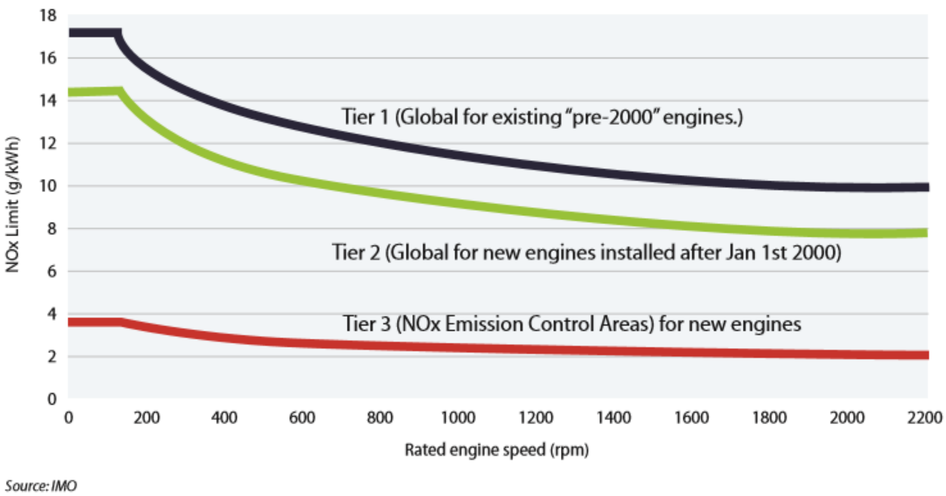

Figure 151 NOx limitations [73]

The reduction of SOx and NOx emissions is proceeding in parallel with the adoption of new policies aimed at reducing greenhouse gas emissions. To measure CO_2 emissions associated with international ship traffic, the IMO has commissioned three data collection campaigns:

- The first study, conducted in 2000, estimated that ship traffic in 1996 contributed 1.8% of anthropogenic CO_2 emissions.
- From the results of the second study, published in 2009, carbon dioxide emissions in 2007 came to 880 million tons, accounting for 2.7% of CO_2 emissions from human activity.
- The third study, conducted in 2014, updated the estimations made by the previous emissions study, raising them to 885 million tons of CO_2 (representing 2.8 per cent of annual anthropogenic emissions); the third study also estimated emissions of 796 million tons of CO_2 in 2012, representing 2.2% of carbon dioxide emissions from human activity.

In 2011, MARPOL Annex VI was updated by including new requirements for ship energy efficiency: the Shipping Energy Efficiency Management Plan (SEEMP) and the Energy Efficiency Design Index (EEDI) are measures that came into force in 2013 with the aim of optimizing the operational profile and design of commercial ships to increase their carrying capacity [74]. This constitutes the first step taken by the maritime industry towards lowering carbon-based emissions.

In April 2018, the IMO approved a preliminary plan setting new targets for reducing GHG emissions that, considering also the expected increase of vessels in the future, aims to:

- reduce CO_2 output per unit of work by at least 40% by 2030;
- reduce CO_2 output per work unit by at least 70% by 2050;
- halve total carbon dioxide emissions by 2050 in respect of 2008 measurements.

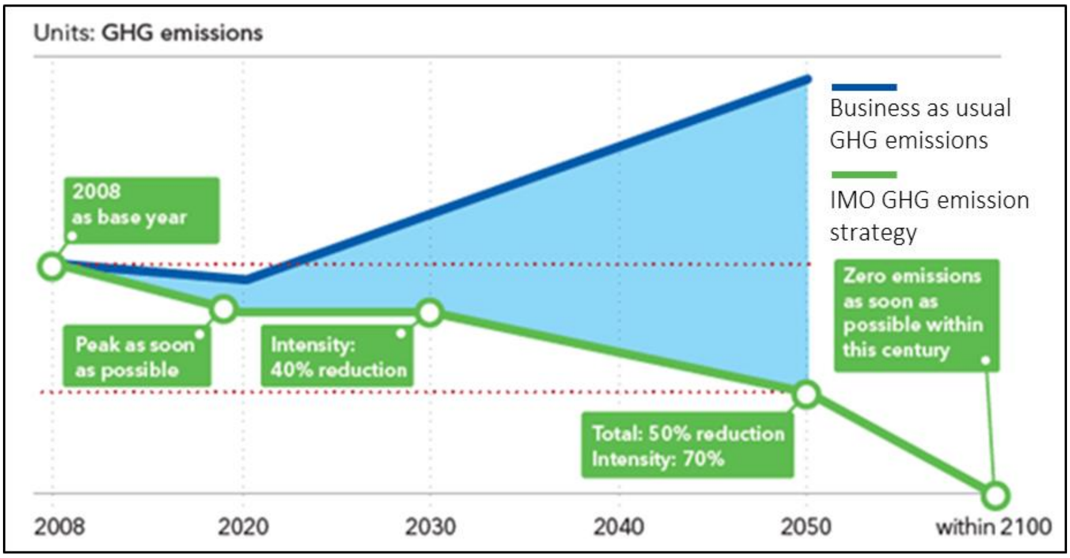

Figure 152 CO_2 emissions limitation trend by IMO regulations [74]

3.1 GEI Project

In the described scenario, Fincantieri funded the GEI project (Generazione Elettrica Innovativa) in collaboration with CNR (Centro Nazionale Ricerche) and University of Genoa [77]. This project is focused on the development of innovative solutions for the generation, distribution and management of energy onboard ship via the application distributed generation approach. The aim of this project is to guarantee the optimization of energy efficiency and environmental sustainability, maximizing the payload and increasing the reliability of the energy system.

The selected vessel for this activity is the Royal Princess cruise ship.

Figure 153 Royal Princess cruise ship

The main characteristics of the selected vessels are resumed in Table 32.

Table 32 Royal Princess main characteristics

Overall Length	330.01 m
Beam waterline	38.4 m
Overall Beam	47 m
Draught	8.5 m
Gross tonnage	142’714
Capacity	3600 passengers
Passenger lower beds	3560
Overall beds	4200
Cruise speed	22 kn
Max speed	22.9 kn
Safe return to port speed	7 kn

MS Royal Princess is a cruise ship operating for the ship owning company Princess Cruise and is the third ship to sail for the company under this name. The ship was built by Fincantieri S.p.A at its shipyard in Monfalcone, Italy. Princess Cruise ordered the Royal Princess unit, as well as its sister Royal Princess on February 17, 2010, and the final contract was signed on May 4, 2010. The hull was launched in August 2012 and the ship was delivered to the

owner company in spring 2013.
The vessel has a large number of decks, most of which are accessible to the ship's paying passengers; it also offers a wide variety of on-board services for leisure and entertainment purposes. As required by safety regulations, the Royal Princess ship is divided longitudinally into Main Vertical Zones (MVZ), based on SOLAS fire requirements. As regards the ship under analysis, the seven MVZs identified by the progressive numbering 1-7 starting from the bow have been considered. For the sake of completeness, MVZ 0 is also mentioned, located at the extreme bow, which was not considered for the study of distributed electrical generation. Vertically, the ship is developed on a total of 19 decks from the building line. Passenger cabins are mostly located on the high decks, as are public spaces dedicated to hotel services. Crew quarters and technical rooms are mainly located on the lower decks, with engine rooms located aft.
The integrated electric propulsion system consists primarily of the following parts:

- Diesel generator sets, in an adequate number and size to meet the required performance of the propulsion and all ship and operational services;
- Integrated command and control system of the platform for unmanned engine rooms;
- Auxiliary systems to propulsion (water, oil, fuel, compressed air, hydraulic) complete with pipes, valves and accessories;
- Engine apparatus room ventilation systems;
- Two fixed blade propellers driven by electric motors;
- Three transverse bow thrusters with variable pitch driven by electric motors;
- Three transverse aft propellers, driven by electric motors;
- Two main electric propulsion panels.

Entering into the specifics (see Table 33), the unit currently has installed on board 4 Diesel engines produced by Wartsila (Model: 2 x 12V46F and 2 x 14v46F), with a total installed power of the ship is 62400 kW. The propulsion is entrusted with to 2 electric motors built by VEM for SAM Electronics connected to fixed-pitch propellers, for a total energy requirement of 18000 kW per axis.

Table 33 Engines on board

Diesel Engine Wartsila 12V46F	2 x 14.4 MW
Diesel Engine Wartsila 14V46F	2 x 16.8 MW
Total Diesel Generators	62.4 MW
Electric motors SAM Electronics	2 x 18 MW
Total Electric propulsion	36 MW

The analysis of the vessel energy consumptions, provided by Fincantieri, suggests that the size of the distributed generation units will have as reference power from a maximum of about 7.5 MW to a minimum of 4 MW (considering medium and low voltage users for Hotel Services). The difference is given by the presence or absence of the air conditioning system among the services to be provided. Other configurations can be considered between these two scenarios.

In order to supply this load with distributed generation, according to with the electrical scheme developed (reported in Figure 154), it has been decided to install nine modules of 800 kWe and distributed as reported in Table 34.

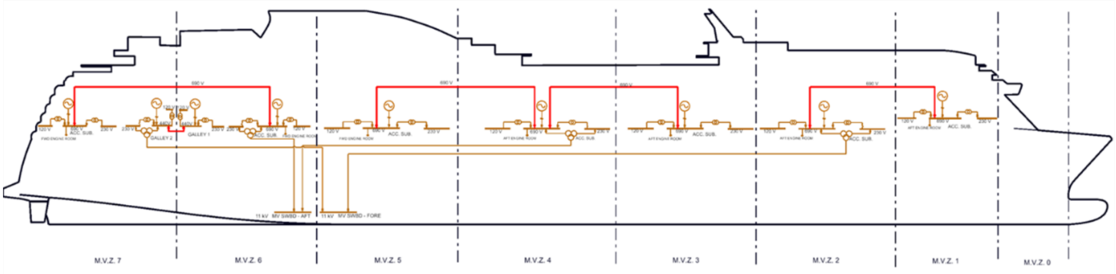

Figure 154 Electrical scheme for DG on board

Table 34 Units distribution on board

MVZ 1	800 kW
MVZ 2	800 kW
MVZ 3	800 kW
MVZ 4	800 kW
MVZ 5	800 kW
MVZ 6	2 x 800 kW
MVZ 7	2 x 800 kW

With the aim of producing both thermal and electrical power in a distributed generation approach, the considered technologies are: micro Gas Turbine fuelled by Liquid Natural Gas (LNG) and PEM Fuel Cells fuelled by Hydrogen.

The analysis of these technologies, considering the mentioned application, has to take into account energetic and economic aspects but also footprint and weights. Indeed, in the case of maritime application, the minimization of occupied volumes is fundamental in order to guarantee room for the payload; furthermore, huge weights lead to intensive fuel consumptions.

3.1.1 Micro Gas Turbine with LNG

The first of the different solutions proposed in this analysis relies on a system of gas-fired micro-turbines, installed in varying numbers in each MVZ, for the entire Distributed Electric Generation (GED) of the hotel services. The microturbines are fed directly by LNG, without any preliminary treatment (e.g. reforming). One of the main advantages in the use of this configuration is the flexibility of the plant as it is able to modulate well the load curve of the energy required by the hotel services and it is possible to track the peaks of this demand with a very fast response of the generation system. This leads to a saving of weight since there is no need for energy accumulators, such as battery packs. In addition, the small size of the turbines themselves and their low weight/generated power ratio allows a more flexible installation even in small spaces. The main disadvantage of this type of installation is the high demand for combustion air and cooling air required by the individual turbines, which results in ventilation and exhaust ducts of significant size: it is, therefore, necessary to carefully evaluate the positioning of the system on board the ship. It should be noted that distributed generation will supply only the utilities connected at low voltage (690V and below) while the utilities connected at high voltage (11kV) or linked to non-hotel services will be supplied by the dual-fuel diesel engines installed on board.

3.1.1.1 mGT description

Determined the size of the electrical generation units, it is necessary to choose among the products on the market the most suitable for the installation needs. The choice has fallen on the 800 kW Capstone microturbine, model C800S powered by LNG. The turbine in question is composed of 4 elements of 200 kW each combined within a single container of 65.3 m3 volume, with a length of 7.5 m, 3.0 m wide and 2.9 m high. The weight is 14100 kg with an electrical efficiency of 33%. The technical specifications have been collected in Table 35 [78].

Table 35 mGT Capstone 800s technical specifications

Capstone C800S		
Nominal Power	kW	800
Nominal efficiency	-	0.33
Exhaust temperature	°C	280
Exhaust mass flow rate	kg/s	5.300
	Sm^3/s	4.402
Air flow rate	kg/s	5.249
	Sm^3/s	4.360
Overall energy production (180 hours)	MWh	144
Weight	ton	14.10
Width	m	3.00
Length	m	7.50
Height	m	2.90
Area	m^2	22.50
Volume	m^3	65.25

For the sizing of the LNG storage tanks intended for hotel services, the same autonomy of 180 hours (7.5 days) has been chosen as assumed for the propulsion units. The basic idea is to have separate tanks from those intended for propulsion for a question of availability of the plants, compatibly with the available volumes on board the ship. The LNG consumption of each of the 9 microturbines is 230 g/kWh and therefore the gas requirement for 9 units totalling 7.2 MW was 637.7 m3 for 180 hours of continuous operation. Table 36 summarizes the data used and the calculations made for sizing.

Table 36 LNG tanks dimensioning

Capstone C800S	
Consumptions [g/kWh]	230
Single unit power [kW]	800
Overall Power [kW]	7200
Autonomy [kg]	298080
Density [kg/m^3]	467.4
Total LNG volume x 9 mGTs [m3]	**637.7**

3.1.1.2 Storage system description

The technology currently available for the construction of adequate LNG storage tanks allows for several different solutions. Usually, they are double-membrane tanks with efficient insulation obtained in different ways, but basically, the gas is stored already in a liquid phase at a very low temperature and lower than its evaporation point. Despite the efficient insulation of the tanks, they are not able to keep the gas entirely liquefied, but a certain amount of heat can pass through the membrane causing an increase in the internal pressure of the tank which in turn favours the evaporation of a part of the gas. This phenomenon is commonly called "boil off" and requires a dedicated recovery and treatment plant. In fact, to allow optimal management of the internal pressure of the tank, the boil-off steam must be extracted from the tank and used directly or liquefied again and reintroduced inside. This phenomenon cannot be completely eliminated with current technology, but only reduced in its frequency by using pressurized tanks with different geometric shapes.
The challenges that current technology faces for LNG storage and transport are:

- the low temperatures required, which in turn require:
    - special construction materials such as stainless steel and aluminium;
    - special types of insulation;
    - special provisions to avoid shrinkage of the case.
- the ease of combustion, the volatility of the gas and the related safety measures to be taken;
- the large volumes of the crate;
- the location on board of the LNG containers.

Usually, the tanks intended for LNG are classified into two different types:

- **Membrane crates**: They are tanks that make the best use of the space available, but in addition to the primary containment membrane made up of the tank itself, they also require a complete secondary membrane to prevent any gas leakage. Therefore, they have a nitrogen containment system and gas detectors located in each insulated space. A schematic of a membrane-type enclosure is shown in Figure 155. They present benefits like a greater volume of LNG stored via a reliable technology; furthermore, the LNG bunkering takes place at very low temperatures and this allows a higher energy per m^3 of gas loaded. On the other hand, this kind of storage has a high frequency of boil-off and need for adequate treatment plant with annexed high production costs [79].

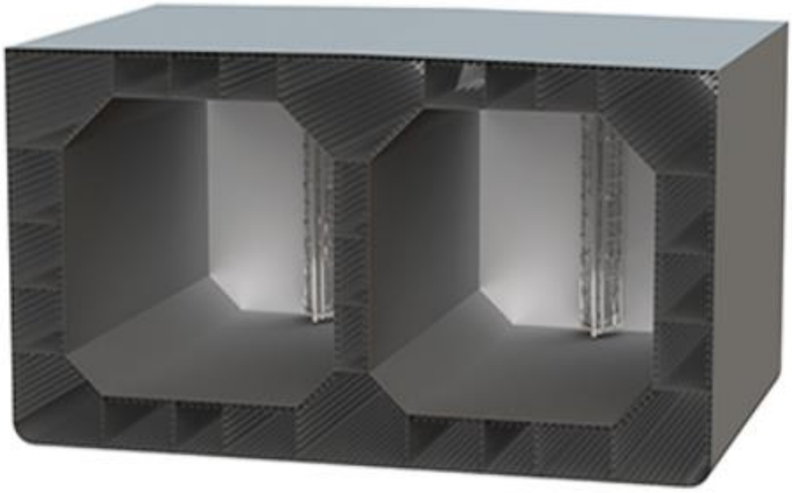

Figure 155 Membrane LNG tank

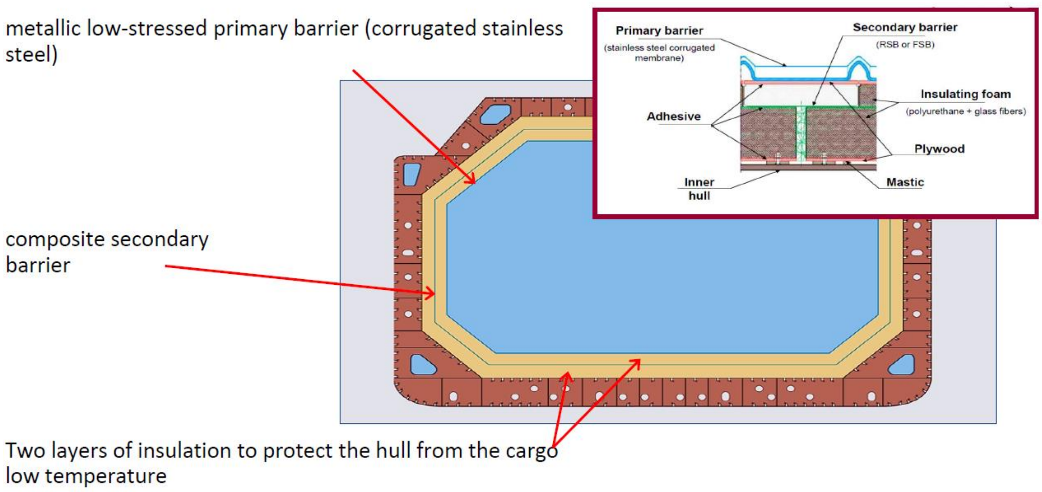

Figure 156 Membrane LNG tank description

Membrane tanks are structural, i.e. they contribute to the strength of the ship, on the contrary, the so-called "independent tanks" are not structural elements but are completely independent of the structures of the ship and are inserted inside them. The design of the LNG tanks for propulsion is inspired by the design of the holds of gas tankers now commonly used for the transport of liquefied gas.

- **Independent tanks**: they can be divided into three categories, namely Type A, B and C. The latter is the most common type of tank in LNG-fuelled vessels. Type C tanks have a cylindrical shape and are the only ones that allow high internal pressures to be reached, up to a maximum of 20 bar. They operate typically at around 5 bar, allowing the gas to be sent directly into combustion engines without the use of dedicated pumps. They can be installed both in the horizontal and vertical position and both types are subjected to accurate testing of fatigue strength. They do not require secondary protection like the other types of tanks described, as they have the typical structure of concentric shells: they consist of an inner vessel containing the liquefied gas installed inside a second outer vessel to prevent leakage. The two casings are made of austenitic stainless steel, while the space between the two shells is insulated either with insulating materials, such as perlite or kept under vacuum. They present many advantages since representing standard storage, they allow an increase of pressure without the need for special external containment systems; furthermore, they have excellent insulating properties and guarantee an easy installation to bunk. On the other hand, they are very space demanding for their installation [79].
  They are produced in cylindrical or bilobed form, depending on space requirements and placement on board. The valve system and the pressure and temperature control system must be placed inside a suitably insulated and insulated "pre-tank" room that must be added to the occupied volume as it is directly connected to the box itself. In Figure 157 is represented a scheme of cylindrical Type C case with relative pre-tank.

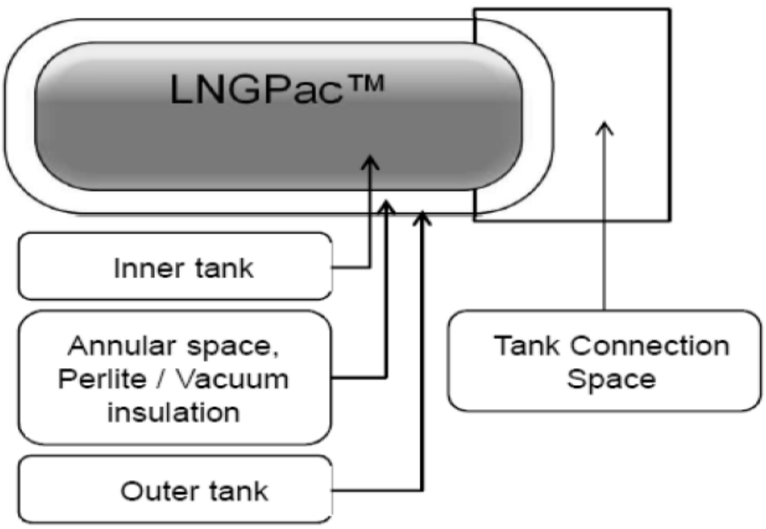

Figure 157 Type C LNG tank layout

Figure 158 illustrates a section of bilobed Type C tank; it can be considered as formed two cylindrical type cases connected on their longest side [80].

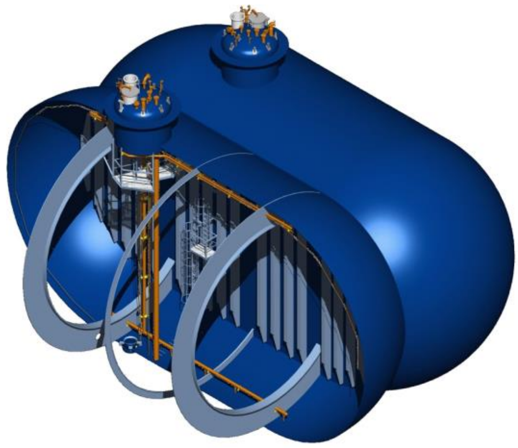

Figure 158 Bi-lobed LNG Tank Type C

Considering the use of Type C tank, the 637.7 m3 of liquefied gas needed to supply the distributed generation for 180 hours must be placed inside 3 bilobed boxes with the following dimensions: 14 m in length, 6.4 m in total width and 3.2 m in height (1.6 m is the size of the cylinder radius).

3.1.2 PEM Fuel Cells with Hydrogen

The second proposed configuration sets the stage for a future evolution away from the systems traditionally used in power generation on board ships [81] [82] [83]. Fuel cell (FC) technology is considered one of the most promising technologies for the production of electrical energy because of the large number of possible applications and because it has the energy and environmental characteristics that make its use advantageous. Fuel Cells allow converting the chemical energy contained in a fuel directly into electrical energy by exploiting the electrochemical reaction that takes place inside them. This involves a series of advantages that involve different aspects:

- Fuel cell system is independent of the intermediate thermodynamic transformation and consequently from the relative constraints characterizing the thermodynamic cycle of Carnot. This would allow obtaining a conversion efficiency theoretically higher than those of conventional thermal machines.
- The purely electrochemical nature of the transformation allows the elimination of moving elements (except for auxiliaries) and this translates into a reduction of noise and vibrations produced by the system, to the benefit of passenger comfort.
- Electrical energy is produced by reacting oxygen contained in the air with fuel, typically hydrogen, obtaining electricity and water as products.
- The chemical nature of the conversion allows the reduction or elimination of NOx, SOx, CO_2 and particulate matter (PM) emissions. From the point of

view of eco-sustainability, the advantage offered is substantial, especially when compared with current Diesel engines.

- The efficiency of the cells is not very sensitive to variations in electrical load and is independent of the installed power.

3.1.2.1 PEMFC description

A brief description of Fuel Cells typologies and characteristics has been provided in section 1.2.2.2. From this analysis, it can be summarized that, among all the available Fuel Cell technologies, low-temperature PEM Fuel Cells can be considered the most suitable and reliable for short term use in a maritime application; representing the most developed, efficient and least costly to produce and maintain technology. PEMFCs have already been used in numerous automotive applications, as well as on the German passenger ship Alsterwasser (96 kW module) and the German 212A class submarines (multiple modules of 30 to 50 kW each). PEMFCs use carbon-based electrodes on which a catalyst consisting of platinum or its alloys is dispersed. The electrolyte is a humidified polymeric membrane with high proton conductivity, which acts as an electrical insulator but at the same time allows the passage of only hydrogen ions (H+). The operating temperature must be between 60°C and 100°C, as higher temperatures would not allow keeping the polymeric membrane humid, preventing its proper functioning. In the specific case of PEMFCs hydrogen (H) and oxygen (O) are reacted to produce water (H_2O) heat and electricity. The produced water is exhausted at the cathode together with the excess air. Compared to other types of fuel cells, PEMs have a number of advantages such as high power-to-weight ratio, low operating temperature, reduced start-up time (minutes), the relative simplicity of construction, low requirements on the materials used in its structure, absence of corrosion problems and discrete durability over time. The low operating temperature is a benefit in terms of installation, safety and transport, but at the same time, it is a source of some disadvantages, such as poor tolerance to the presence of CO in the fuel (allowed content <10ppm) and difficult thermal integration between fuel treatment system and stack. The efficiency of this system is between 0.5 and 0.6 with the possibility of recovering heat from the produced water, even if it can be considered a low-value heat due to the low operating temperatures. A schematic of the operation of a low-temperature PEMFC is shown in Figure 159.

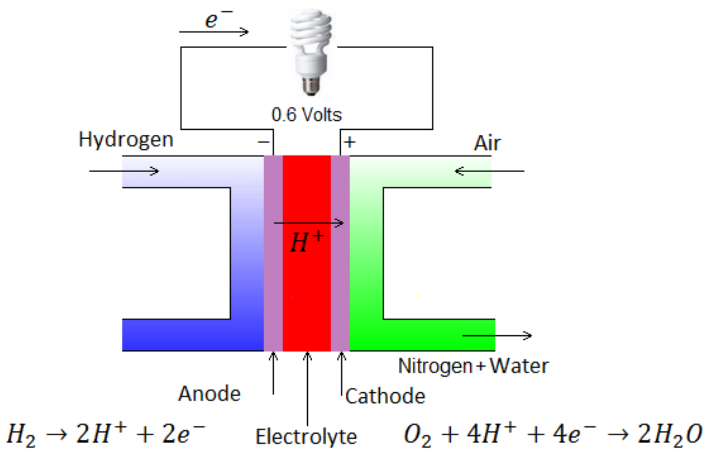

Figure 159 PEMFC schematic of the operation

PEMFCs are composed of an anode, where the oxidation of hydrogen occurs, and a cathode where the reduction of oxygen occurs. Physically, these two elements are assembled to form the so-called MEA (Membrane Electrode Assembly). In the stack, the MEA assembly is arranged between two bipolar plates, except for the first and last cells in which the external plate is in contact with a single electrode. The bipolar plates have several functions [84]: provide electrical connections between cells, distribute the gaseous flow of fuel and oxidizer to the single electrodes uniformly, remove water produced by the reaction and allow effective heat dissipation. The bipolar plate consists of a single material on which the gas channels are machined, usually monolithic graphite, or carbon resins or metal-impregnated graphite. Figure 160 shows the assembly diagram of a stack.

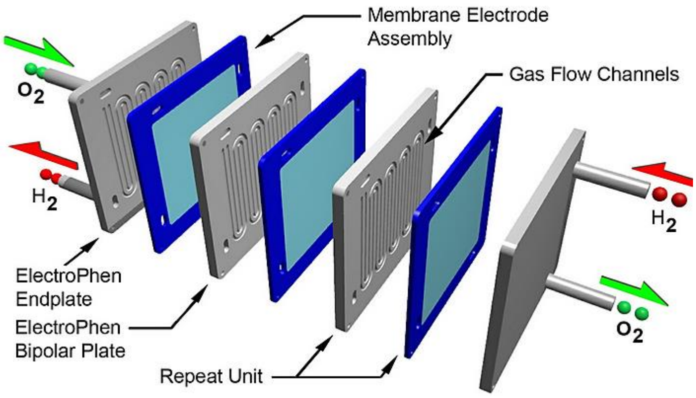

Figure 160 Structure of a PEMFC Stack

If an alternative fuel to hydrogen is to be used in this type of cell, it must be previously converted before entering the anode. For hydrocarbons, this implies the use of a separate reformer and a system of pre- and post-production filters that complicate necessarily the entire electrical generation system making it less competitive for a maritime application. In the latter case, the Fuel Cells not only produce water as a waste substance but also carbon dioxide (CO_2) as a result of the reforming action to which the fossil fuel must be subjected. The only way to overcome this problem is the direct loading of hydrogen into the tank. Therefore, considering the need to provide a promising and efficient solution for the maritime application, in this analysis it is considered only the application of PEMFC directly fuelled by Hydrogen, without the need of a reforming process, as reported in Figure 161.

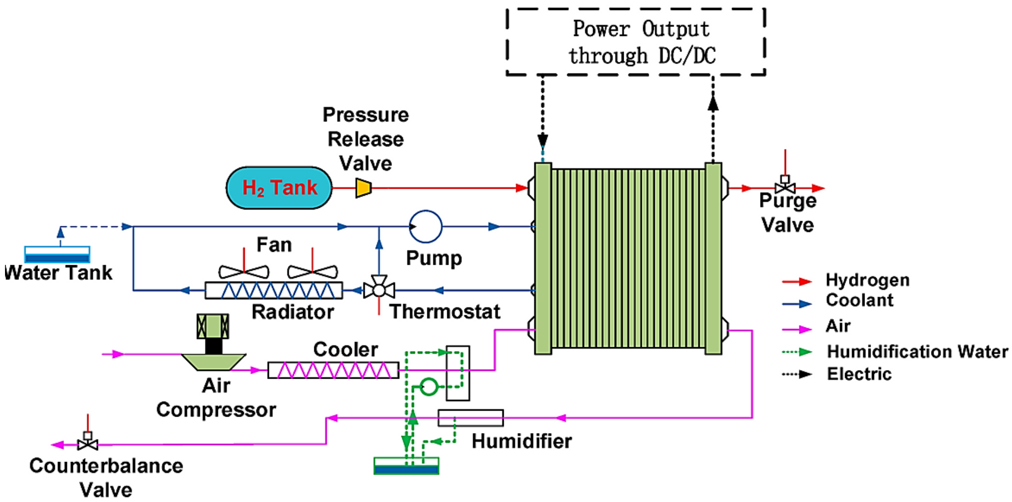

Figure 161 PEMFC fuelled by H_2 layout

The distributed generation to be implemented on board the Royal Princess requires 800 kWe generating units in each MVZ 1 to 5 and 1.6 MWe units (2 x 800 kWe) in MVZ 6 and 7 in order to also cover the electrical load required by the on-board kitchens. For what has been described in the previous paragraphs, when we consider Fuel Cell module we refer both to the generation system that uses single stacks connected together to obtain large powers, and to all the auxiliaries that ensure its correct functioning and adequate safety conditions. These elements are all placed inside a container of variable size according to the total power of the module itself and constitutes a complete generation unit to which inputs and outputs are connected.

After analyzing the proposals of Fuel Cell modules currently available on the market, the 1 MWe system produced by Hydrogenics has been chosen [85]. Considering the high modularity of the fuel cells systems, the values reported in the Hydrogenics datasheet have been scaled down to an 800 kWe system, as needed in the considered application. The obtained values are reported in Table 37.

Table 37 800 kWe PEMFC specifications

Hydrogenics 800 kWe PEMFC		
Nominal Power	kW	800
Nominal efficiency	-	0.45
Water Production	kg/h	503.3
Hydrogen supply	kg/h	53.3
Air flow rate	kg/s	1.06
Specific H_2 consumption	g/kWh	66.7
Weight	ton	21.6
Width	m	9.8
Length	m	4.9
Height	m	2.90
Area	m^2	48
Volume	m^3	139.3

With reference to the efficiency value in Table 37 some clarifications should be made. The value indicated in the brochure is the peak efficiency, quite different from the one at the point where the cell produces the maximum power. To better understand this concept, it can be useful to analyze Figure 162.

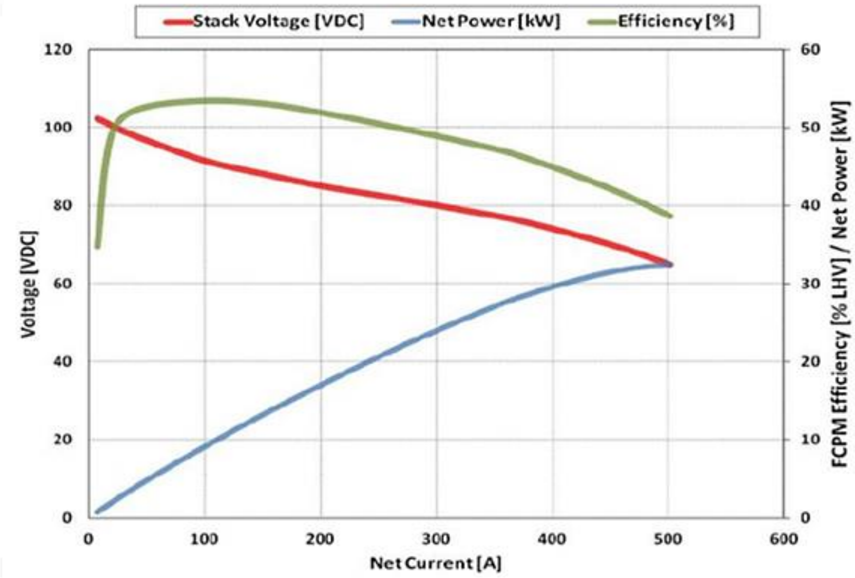

Figure 162 PEM Hydrogenics HD 30 characteristic curve [86]

This figure shows the characteristic curve of the Hydrogenics HD 30 cell: the 800 kW cell considered in the analysis consists of an assembly of a various number of 30 kW stacks. Therefore, the considerations made on this cell, are valid in the same way for the 800 kW module used in this study. Figure 162 shows the cell voltage, net power and system efficiency as a function of the current flowing through the cell. It can be seen that the peak value of the efficiency is around 55%, at a point where the cell develops about 10 kW of power. Moving instead to the point where the cell develops its rated power (30 kW), the efficiency drops to a value of 45%, used in this first phase of the study and included in Table 37. This value is not particularly high if compared with the levels of efficiency achieved to date by this technology. However, it should be noted that the Hydrogenics fuel cell works at high current densities, which allows greater compactness of the plant, at the expense of a decrease in efficiency and therefore an increase in fuel consumption. Taking into account the naval application of this machine, and the consequent need to minimize overall dimensions, it was therefore decided to opt for this cell. The PEMFC Hydrogenics represents in fact a good compromise between size and efficiency for our application.

On the basis of the data collected in Table 37, it is also possible to calculate that each single Fuel Cell module of 800 kWe nominal power requires about 9600 kg of H_2 for 180 hours of continuous operation. The total amount of H_2 required by the 9 units installed on board is therefore 86.4 tons. Considering storing hydrogen in a liquid state, the density of the fluid is 70.2 kg/m^3, and therefore the total volume of liquefied hydrogen required by the system is about 1230 m^3. Each PEMFC requires about 136.7 m^3 of Liquid H_2.

3.1.2.2 Storage system description

The choice of using a Liquid H_2 (LH_2) storage system represents the first alternative to the common and voluminous pressurized cylinders, using the liquefaction of the gas and subsequent physical containment within suitable containers. The density of liquid hydrogen (LH_2) at ambient pressure and liquefaction temperature of about -253 °C (20° K) is 70.2 Kg/m^3. For the maintenance of such low temperatures are used cryogenic tanks with a double wall, insulated with perlite and equipped with a cavity inside which is made the vacuum. The structure itself is not very different from that of the Type C tanks used for LNG storage, but the operation of the tank is similar to that of a highly engineered thermos: the insulation is not perfect and there are heat flows through the insulation directed towards the external environment. This causes the formation of boil-off gas and a consequent increase of the internal pressure of the crate: in order to bring the pressure values back under safety levels it is necessary to expel the gas in the atmosphere or to convey it inside a system to be reused. It should be noted that heat loss is less relevant for large tanks. Typical tanks of this type are produced by Linde and shown in Figure 163. Despite these complications, nowadays liquid cryogenic hydrogen storage is the most widely used technology for the transport of large quantities of LH_2 (thousands of kg) with low boil-off losses and that satisfies the requirements in terms of density, dimensions and weight. Installing such technology on board naval units involves greater complexity of the fluid distribution system, refuelling system and higher associated costs. It should be kept in mind that the energy cost of liquefaction (which is not carried out on board but in land-based plants) is also considerable and corresponds to about 30% of the energy content of the fuel itself and that the ratio between the weight of the tank (tare) and the volume of liquid hydrogen (net weight) is about 10 [87].

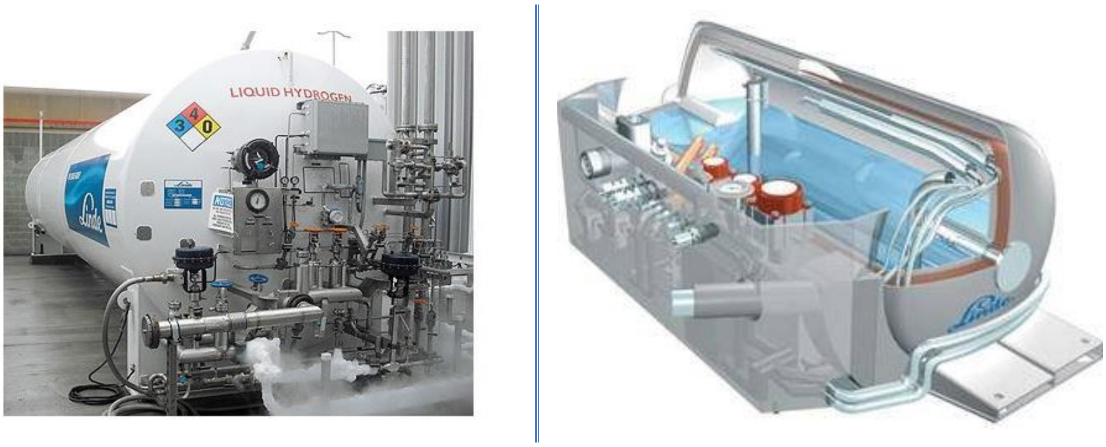

Figure 163 Linde cryogenic Hydrogen tank

After these considerations, the choice has fallen on cryogenic storage as it turns out to be the most mature and proven technology for the transport of large volumes of hydrogen.

Assuming a location of hydrogen tanks in a single MVZ but in two rooms independent of each other to maintain the redundancy of the power system, it was still necessary to assume a number of tanks that were chosen equal to 8 cylindrical cryogenic tanks with the dimensions of L = 9 m and D = 4.8 m that allow the transport of about 162.7 m^3 each. The dimensions shown are to be intended as net, that is, they consider only the volume of hydrogen required, however, during installation on board it is necessary to consider an additional and not negligible thickness related to the structure of the crate itself. The total volume of liquid hydrogen embarked with the methods just described is equal to 1302 m^3, slightly higher than what is actually required because the tank must not remain completely empty but must still contain a minimum amount of liquefied hydrogen to maintain a stable internal temperature.

Assuming instead a distributed solution in which a tank feeds a single PEMFC fuel cell with a nominal 800 kW, 9 cryogenic tanks are required, each containing 136.8 m^3 of liquefied hydrogen necessary to ensure 180 hours of continuous operation of the FC. Assuming the use of cylindrical Type C tanks, the hydrogen will be placed inside containers 9 m long and 4.5 m in diameter, for an effective volume of 143 m^3. The weight of the stored hydrogen is 10038 kg while the total weight of the full crate is 100380 kg (considering a gross weight/volume LH_2 ratio of 10).

It is worth considering that, the use of Hydrogen on board requires detailed evaluation in terms of risk management. Currently, there are no regulations to be used as a reference, therefore a detailed analysis of risk has been developed in a dedicated section of the work on GEI project [88], with the aim of creating guidelines in the regulation and application of this innovative solution on board vessels.

3.1.3 Systems comparison at steady-state level

Once that the technologies have been described and analysed, it is fundamental to provide a comparison at a steady state level in order to have a preliminary idea of which could be the most performant solution. The required performances refer to good energetic performances and, therefore, low emissions; but also to economic aspects in order to guarantee good replicability of the analysed solutions. Furthermore, considering the maritime application, limited dimensions are significantly important in order to maximize the payload; therefore also a comparison in terms of dimensions and weight becomes necessary in this scenario.

3.1.3.1 Dimensions comparison

Firstly, a comparative analysis will be carried out in terms of volumes and weights occupied by the different technologies involved. In a naval application, where space management is one of the most relevant problems, it is interesting to evaluate the possibility of having a compact system that saves space that could be used to increase possible economic gains (e.g. passenger cabins). Table 38 summarizes the results of a comparison between the various technologies and storage systems taken into consideration. The table shows, for the various technologies, the overall dimensions for each of the single components required in order to have a total size of 800 kWe for each MVZ. Since, for two of the seven MVZs, it was assumed to install a power of 1600 kW, the total number of 800 kW zones actually present on the ship is nine. In this sense, weights and dimensions are calculated for each MVZ and also for the whole ship. The analysis of this table shows that the mGT solution appears to be the most compact technology in terms of volume and weight. The heaviest solution is the one that foresees the use of PEM with liquid hydrogen directly stored on the ship. It should be noted that this fact is in contrast to the characteristics of the system. In fact, the higher efficiency of a PEM, compared to an mGT, allows the use of a lower quantity of fuel consumed (and therefore stored) for the same energy production. In addition, the direct use of stored hydrogen, having an LHV (referred to the unit of mass) greater than natural gas, allows a lower amount of fuel in terms of weight (for the same energy required). However, the largest portion of the weight for this solution lies in the weight of the tank, net of its contents. LNG tanks, on the other hand, turn out to be lighter in which it is estimated that the weight in kg of the tank can be approximately equal to the volume in m3 of LNG stored inside it. It should be noted that the estimated tank volume represents the gross volume of the system, including auxiliaries, and was calculated by taking into account the diameter and total length data. For extensiveness, the solution with hydrogen storage in cylinders at a pressure of 500 bar is also reported. Cylinders of 16.5 kg of hydrogen each with a weight of 730 kg and a volume of 1270 l were considered as a reference [89]. It is possible to highlight how this solution involves weights and volumes significantly higher than other technological solutions. In this sense, the study of this solution, already strongly penalizing in terms of overall dimensions, will not be further investigated.

The same conclusion can be done for the solution considering the use of PEMFC with LNG by using a reforming unit. In this case, issues relating the store of Hydrogen on board can be solved, but an additional component (the reformer [90]) is needed with associated additional costs, volumes and weights. Therefore, taking into account the significative overall volumes and weights required, also this technology has not been analysed in detail within this study.

Table 38 Volumes and weights comparison

		Single Unit Area	Single Unit Volume	Single Unit Weight	n° units per MVZ	Total Area per MVZ	Total Volume per MVZ	Total Weight per MVZ	Overall Area (9x 800kW MVZs)	Overall Volume (9x 800kW MVZs)	Overall Weight (9x 800kW MVZs)
		[m²]	[m³]	[ton]	-	[m²]	[m³]	[ton]	[m²]	[m³]	[ton]
PEMFC + Reformer con LNG	FC (800kW)	47.59	139.44	21,60	1	165	460	151,2	1481	4142	1361
	Reformer	30	75	24	2						
	LNG Tank	56,92	170,77	81,64	1						
PEMFC + LH2	FC (800kW)	47.59	139.44	21.60	1	128	282	122	1152	2542	1098
	H_2 Liquid Tank	45.58	143	100.38	1						
PEMFC + Compressed H2	FC (800kW)	47,59	139,44	21.60	1	295	881	457.2	2654	7933	4115
	H_2 500 bar tank	0.42	1.27	0.73	582						
mGT + LNG	mGT (800kW)	22.50	65.25	14.10	1	52.4	160.8	85.7	471.3	1447.41	771
	LNG tank	89.6	286.72	214.8	1/3 considering 3 overall tanks in the cruise						

3.1.3.2 Efficiency comparison

In general, it should also be properly reported and analyzed how the various technologies are more or less advantageous from the point of view of energy efficiency, taking into account the processes that, in some cases, involve the treatment of fuel (Reforming).

Table 8.11 shows the efficiencies of the various solutions taken into consideration [78] [85] [90]. It can be seen that, although the PEM has an electrical efficiency of about 45%, its use in combination with the reformer involves a significant decrease in efficiency up to a value of 28%. This fact leads to the preference for the solution with mGTs as, in addition to higher system efficiency, taking into account what has been shown in the previous section, the overall dimensions are considerably reduced compared to the option of the PEM with Reformer. Reasoning purely in terms of efficiency, it is clear that the most interesting solution is a system with Fuel Cells powered by hydrogen (in add, the use of liquid hydrogen storages despite the compressed one guarantee volumes optimization). Therefore, also under this analysis, the most promising solutions for on board maritime application are represented by PEMFC with hydrogen and mGT with LNG.

Table 39 Efficiency comparison

		Power production per unit	Fuel consumption for 1 week per unit	Fuel	n° units per MVZ	Net Power per MVZ	Energy production in 180h per MVZ	Specific Consumption	Overall Net power	Fuel Energy available	Overall system efficiency
		[kW]	[kg]	-	-	[kW]	[kWh]	[kg/kWh]	[kW]	[kWh]	-
PEMFC + Reformer con LNG	PEMFC	800	9600	H2	1	776	139680	0.275	6984	506140	27.6%
	Reformer	-12	19204	LNG	2						
	LNG Tank	-	-	-							
PEMFC + H_2	PEMFC	800	9600.00	H2	1	800	144000	0.067	7200	320000	45.0 %
	LH_2 Tank	-	-	-							
mGT	mGT	800	33112.80	LNG	1	800	144000	0.230	7200	436353	33.0%

3.1.3.3 Economic comparison

In the end, considering the desired replicability of the solutions analysed, economic feasibility becomes a relevant aspect. In order to perform the economic comparison, it is important listing the different cost and price hypothesis. The LNG fuel cost has been estimated to be 8 USD/MMBtu [91], equivalent to 0.023 €/kWh; while for liquid hydrogen, used in the direct application in PEMFC, the cost was estimated to be 2.50 USD/kg [92], equivalent to 0.064 €/kWh. The capital costs of the various systems have been based on the TPG research group background experiences and data available in the literature. Regarding the PEMFC, its cost is estimated at 3418 €/kW [93]; while the reformer has a cost of 2500 USD/kg of H_2 produced, equivalent to 2137 €/kg of H_2 produced [94]. In contrast, the Capstone microturbine considered has a cost of 1020 €/kW. On the other hand, the evaluation of tank costs has been more difficult. Not many data are easily available, especially for the sizes of the tanks considered in this study. However, with appropriate references [95], we estimated the cost of an LNG tank at 1000 USD/m^3 of stored Liquid Natural Gas, equal to 0.144 €/kWh of stored LNG. While for liquid hydrogen tanks, a study by TIAX provided a value of 3 USD/kW of stored hydrogen [96]. The economic evaluation is done in terms of operating costs and fixed costs, i.e., the capital costs of purchasing the necessary equipment. As a term of comparison, the use of Marine Fuel Oil (hereinafter MFO) is considered as State of the Art (SoA). The choice of MFO derives from its compliance with the actual constraints in terms of emissions imposed by the regulations during stops in port. The cost of this fuel is about 589 USD/ton of MFO [97]. Analyzing the data in Table 40, it is worth noting that the solution with PEMFCs seems not very cost-effective due to the high cost of PEMFC (Capex) and of liquid hydrogen (operating costs). The use of mGTs, instead, could be strongly considered also from the economic point of view as it allows to reduce significantly the capital costs, and in part also the operative ones, compared to the alternative technologies studied.

In Table 40 for completeness, it is also reported the economic evaluation of PEMFC application with the reformer. Also under the economic point of view, this solution is not very performant because of the need for purchasing two reformers for fuel treatment (capital costs).

Table 40 Economic comparison

		Power production per unit	Weekly fuel cost per MVZ	Single unit CAPEX	Fuel	n° units per MVZ	SoA Fuel consumption	SoA Weekly fuel cost per MVZ	Economic gain (in comparison to SoA) per MVZ	Total CAPEX per MVZ
		[kW]	[€]	[€]	-	-	[kg]	[€]	[€]	[€]
PEMFC + Reformer con LNG	FC	800	-	2735043	H2	1	24652	12410	599	5’628’690
	Reformer	-12	11812	1373846	LNG	2				
	LNG Tank	-	-	145954	-	1				
PEMFC+LH_2	FC	800	22974	2735043	H2	1	25414	17514	-5461	3’555’556
	LH_2 Tank	-	-	820513	-	1				
mGT + LNG	mGT	800	10183	816000	LNG	1	25414	17514	7331	946’351
	LNG Tank	-	-	130351	-	1				

Within this economic analysis, it is important to take also into account the lifetime of the considered technologies. Estimating that the lifecycle of the considered cruise ship could be 20 years, the impact of the installed technologies' lifetime is rather relevant. Market data estimate a maximum lifecycle for Fuel Cells of around 5 years, while for an mGT a lifetime of around 10 years can be estimated. Therefore, the capital costs of these machines will be repeated several times over the life of the ship.

All the different considerations proposed are summarized in the chart presented in Figure 164 where, considering a discount rate equal to 2% (average eurozone value in from 2015) [98], the economic management of the various solutions is estimated in the case of continuous use at full load of all the generation units along the overall cruise ship life cycle (20 years).

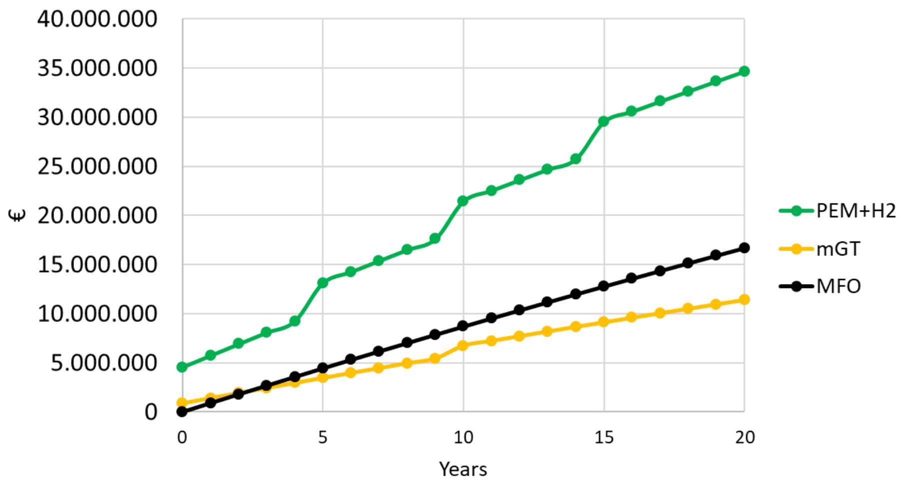

Figure 164 Economic analysis of the two main solutions in comparison with SoA (MFO with ICE)

Since there is no energy selling, all the curves of Figure 164 have a positive slope (no economic gains). Therefore, the solutions are evaluated on the basis of the economic savings of the various technologies compared to the exclusive use of the engine. Analysing the chart, it can be observed that only the microturbine solution appears to be competitive in economic terms, as it combines low management costs with a low capital cost; in fact, these management costs appear to be even more advantageous than using the motor with MFO (see the positive value in Table 40, column "*Economic gain (in comparison to SoA) per MVZ*"). The solution that foresees the combined use of PEM requires high capital costs which, associated with the short lifecycle of the Fuel Cells, impose a strong penalty from the economic point of view. Furthermore, the direct use of hydrogen with PEMFC involves additional high operational costs, due to the costly fuel. In order to compare the different investments, it is also interesting to determine the Levelized Cost Of Electricity (LCOE) parameter, already mentioned in section 2.4.3.2, and defined as follows [99]:

$$LCOE = \frac{\sum_i (CapitalCosts_i + O\&M_i + FuelCosts_i)}{\sum_i (ElProduction_i)}$$

The LCOE is a very easy method for comparing the unit costs of different power generation technologies over their entire economic life cycle or over a specified period of time. In the case analysed, taking into account the assumptions previously stated, the best value of LCOE is obtained in the solution with gas microturbines and is equal to about 0.092 €/kWh, as reported in Table 41.

Table 41 LCOE evaluation for the studied technologies

	PEMFC+H2	mGT
LCOE [€/kWh]	0.269	0.092

Detailed economic analysis must, however, also take into account the space occupied by the various technological solutions because, on a vessel, the space occupied has its own economic value since it could otherwise be used for passenger cabins or other consumer destinations that allow an economic return in the management of the entire naval system.

3.1.4 Time-variant analysis

As part of a time-varying analysis, it is necessary to analyse the thermal and electrical load trends, in order to be able to establish the operating regime of the various generators. Unfortunately, actual data on energy loads of the vessel in question are not available, and also in the literature, there is a scarcity of data collected for scenarios comparable to the one analysed here. It should be noted that the electrical load taken into account is exclusively related to Hotel services, as the use of distributed generation technologies in GEI project aims to satisfy these loads in order to have a management of the ship system in port (without propulsion) with low emissions. From the thermal point of view, the same Hotel services are considered. Therefore, the thermal demand necessary for hotel services, drinking water and air conditioning will be evaluated. On the basis of the experience gained by Fincantieri and the processing of some available data, an electrical load has been created in which there are nights with low load, days with a higher load (more pronounced in the case of days of navigation as the entire number of passengers is present on board) and accentuated peaks at mealtimes, due to intensive use of kitchens. The electrical and thermal loads vary according to the external environment. For this reason, two load profiles have been created: one for a hot external environment and one for a cold external environment (similar to summer and winter conditions in a Mediterranean area). Referring to the thermal load, no data or estimations have been available from Fincantieri's experience. Therefore, in agreement with them, it has been assumed that this load can be considered proportional to the electrical load for the two different environmental conditions.

The Royal Princess, at the moment, is used for weekly cruises where no more than two consecutive days of sailing are scheduled. Therefore, the week of study consists of a maximum of two consecutive days of navigation. Initially, a profile was created in compliance with the values indicated by the EB (Energy Balance) provided by Fincantieri. However, it is well known that the EB is a very conservative estimate compared to the real consumption data that are then actually recorded on the ships. The values included in the EB are inclusive of many voices that, within this study focused exclusively on hotel load, may be neglected. In this way, the load profiles are obtained strictly considering the demand for hotel services, excluding ancillary services to the engine room as they are provided by other systems. The obtained load profiles for the overall cruise ship are reported in Table 42.

Table 42 Thermal and Electrical load profile for warm and cold external ambient, overall cruise ship

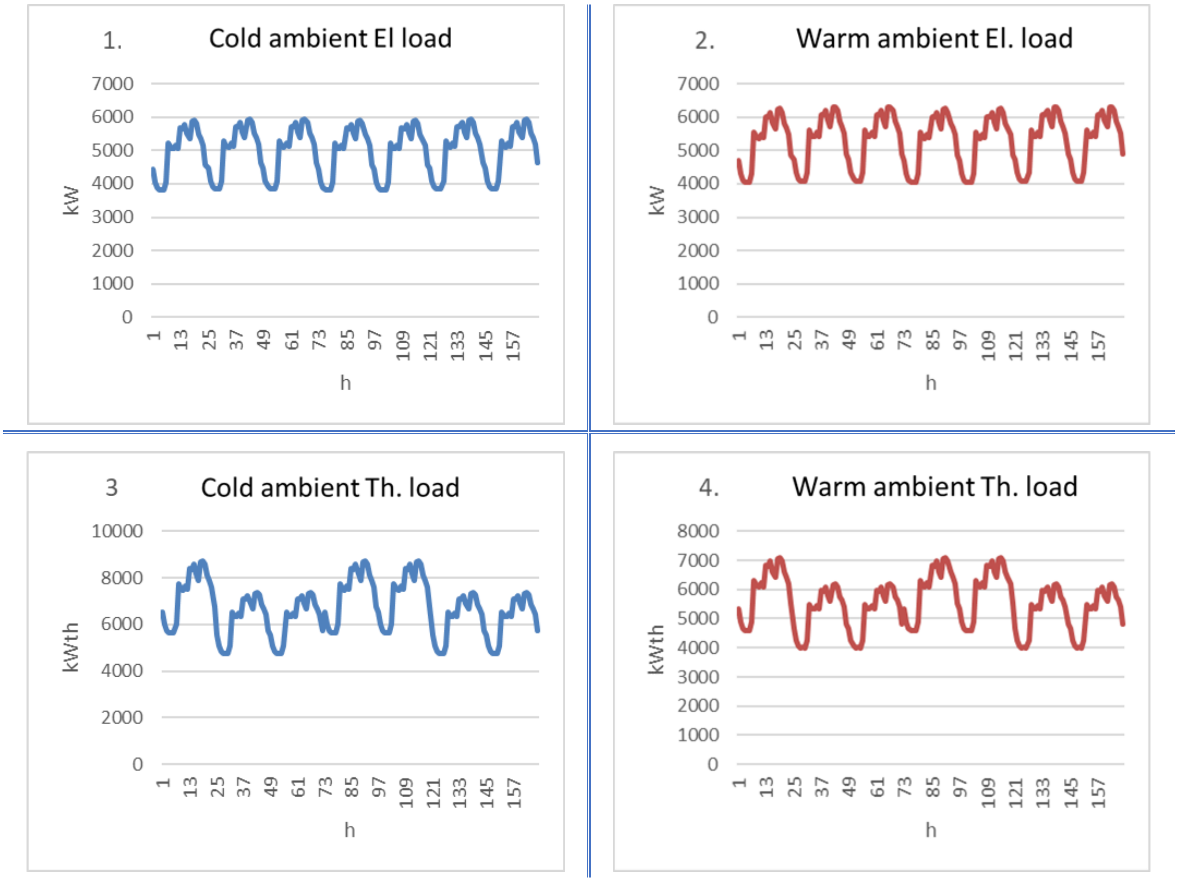

Given the choice of the electrical architecture, which requires some MVZs to be grouped together from the electrical point of view, it is necessary to construct load profiles suitable for the various groups of MVZs considered.

The first group consists of MVZ 1-2. The electrical hotel load of this group is mainly air conditioning, lighting and rooms. The same considerations can be made for the second group of MVZ (3-4-5) in which the distribution of the hotel electrical load is made on the same services considered in the first group of MVZ. The situation is different for the third and last group of MVZs (6-7). The hotel electric load in this group is, in fact, mainly made up of galleys. The galleys could assume different trends during the day compared to the hotel load generated for the other zonal groups; however, as it is not possible to have more accurate and truthful load profiles available, it has been decided to assume the same trend used for the other two groups of MVZ.

The thermal and electrical loads for the different group of MVZ, the so-called Zonal Group (hereinafter ZG), are reported below.

Table 43 Thermal and Electrical load profile for warm and cold external ambient, ZG 1

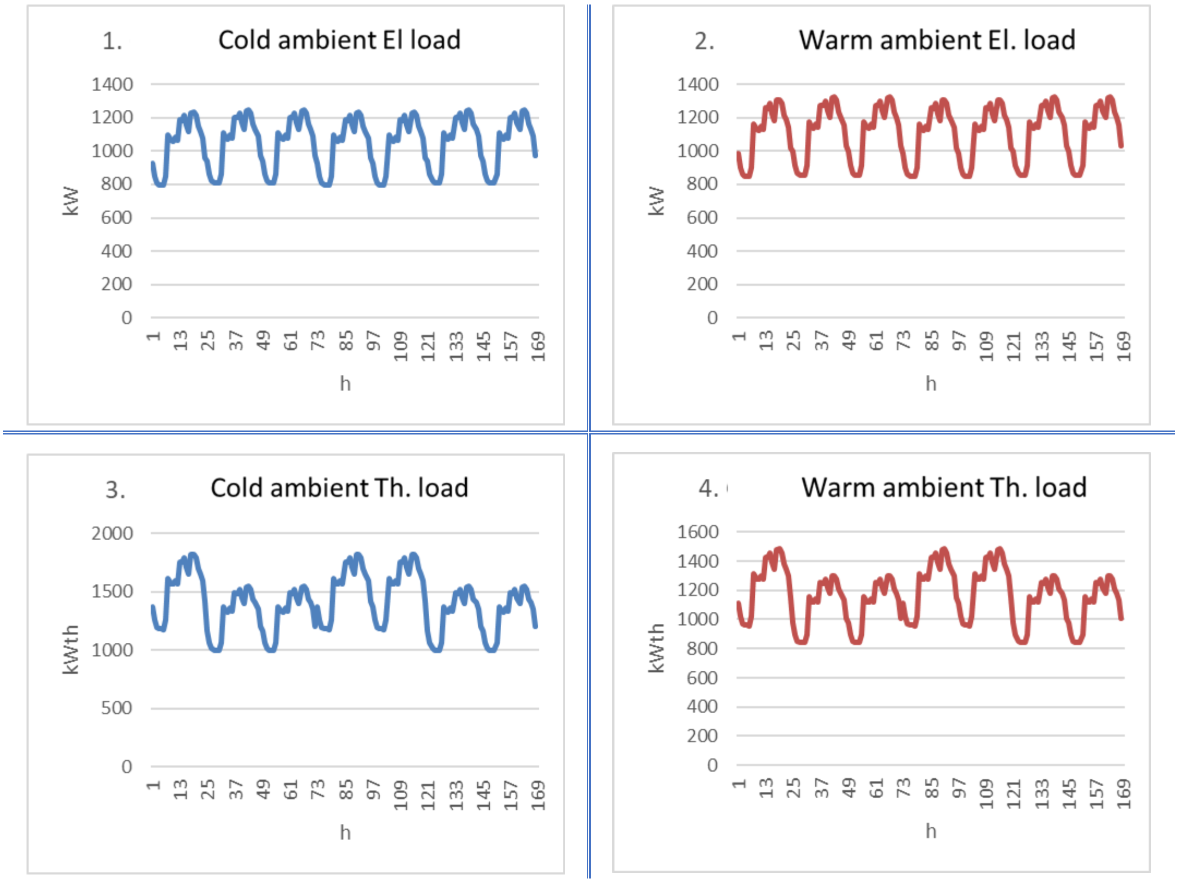

MVZ 1 and MVZ 2 consist the Zonal Group 1. In each of these MVZs, a cogeneration unit is installed with a size of 800 electrical kW, for a total of 1600 kW in the zonal group. Therefore, from Table 43 and the electrical peak value is 1325 kW. Then, it is evident that the installed power is sufficient to cover this load. On the other hand, from the thermal point of view, it will be necessary to analyse which technologies have a thermal efficiency that can cover the load. Particularly interesting is the cold ambient condition since a low electrical load is matched by a high thermal load.

Table 44 Thermal and Electrical load profile for warm and cold external ambient, ZG 2

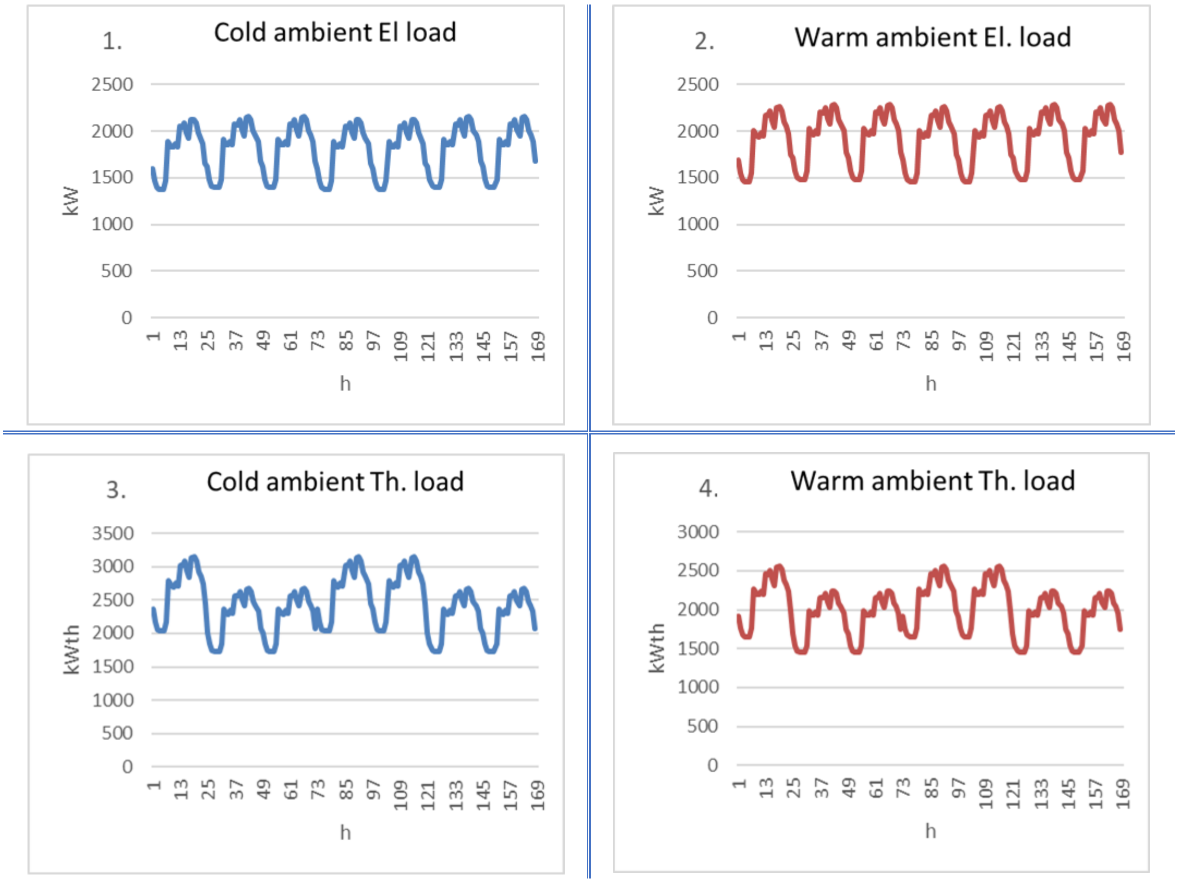

In ZG 2 are grouped MVZ 3, 4 and 5. For each of MVZ 3, 4, and 5, a cogeneration unit of 800 electric kW size is installed, for a total of 2400 electric kW in the zonal group. Also for this zonal group, considering that the highest electrical value is 2287 kW (with reference to the data in Table 44) it can be stated that the installed power is sufficient to cover the load taken into consideration. From the thermal point of view, the same considerations are made as for the ZG 1.

MVZ 6 and 7 (ZG 3) are the ones represented by the largest electrical load as they incorporate the galleys with their large electrical demand. In this sense, for each of the MVZs, two 800 kW cogeneration units have been installed, for a total of 3200 kW installed in the zonal group including MVZ 6 and 7. The highest value of the electricity demand is about 2712 kW (see Table 45), showing once again how the installed power is sufficient to cover the selected portion of electrical demand. As said before, from the thermal point of view it will be analysed through time-varying analysis how the various technologies are able to satisfy simultaneously electric and thermal demand.

Table 45 Thermal and Electrical load profile for warm and cold external ambient, ZG 3

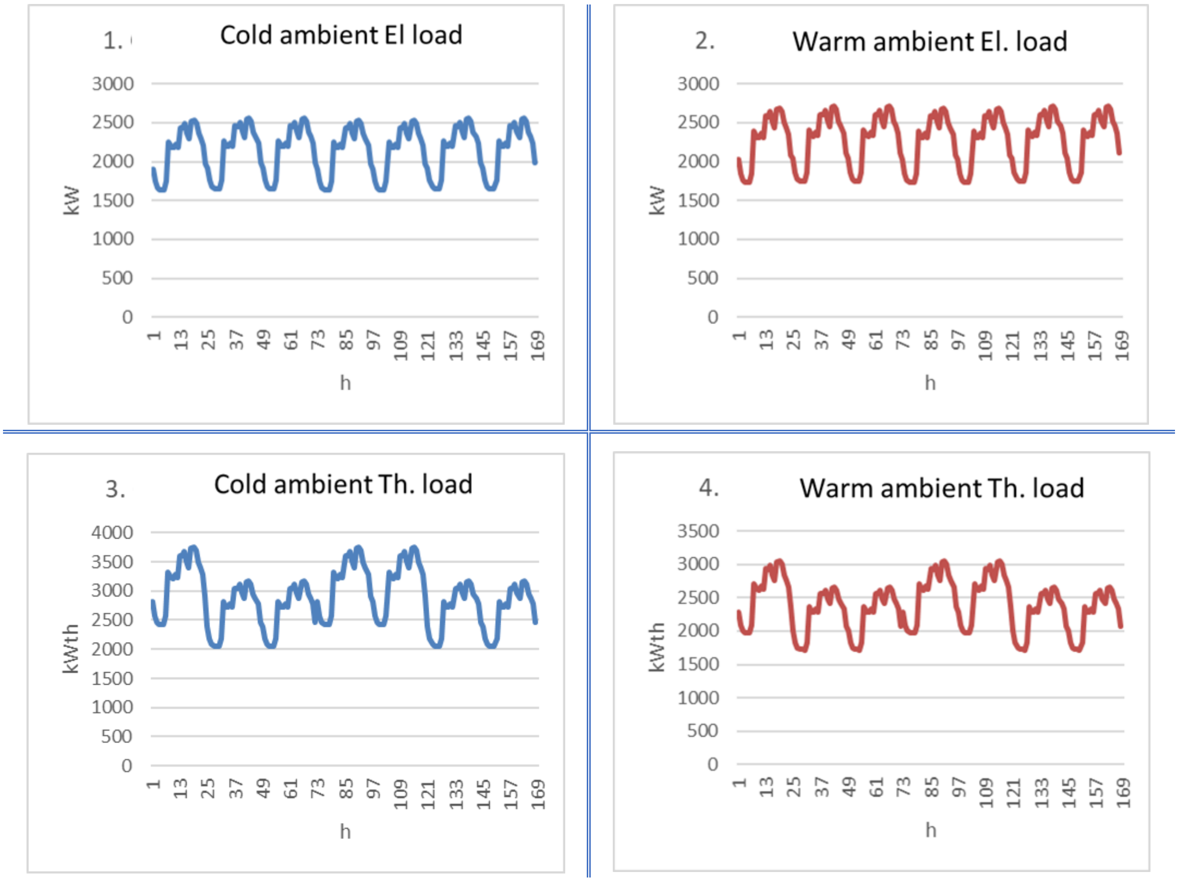

In this project, the time-variant analysis has been performed using W-ECoMP software. The same tool has been used within the ENVISION project, therefore for the description of W-ECoMP please refer to section 2.4.1.

Therefore, in the following sections, the results of the time-variant analysis via W-ECoMP for the two considered technologies are described in detail.

3.1.4.1 mGT with LNG configuration

The layout used for the distribution of the energy flows is reported in Figure 165, in particular, the scheme for the simulations of mGT configuration in W-ECoMP is described.

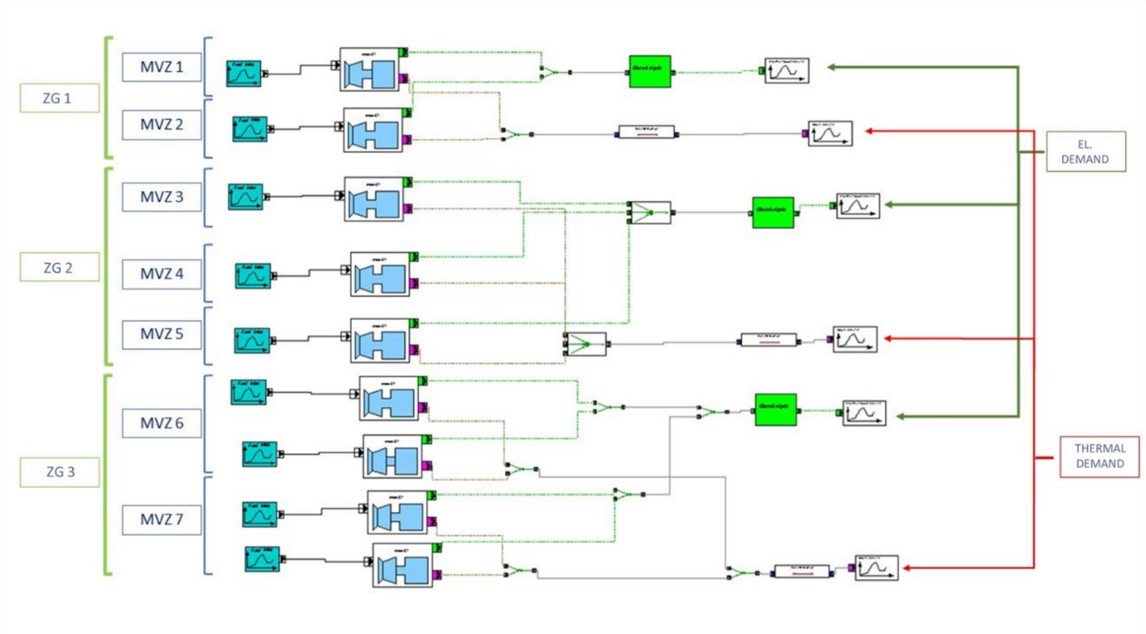

Figure 165 Energy system layout in W-ECoMP

The 7 different MVZs are aggregated into 3 Zonal Groups (ZGs) that independently meet the thermal and electrical requirements of the respective group. Zonal Group 1 will therefore aggregate MVZs 1 and 2; GZ 2 will include MVZs 3, 4 and 5 while GZ 3 groups MVZs 6 and 7 (each composed of 2 units of 800 kW). Initially, the electrical load has been prioritized so that the various cogeneration units are adjusted to cover the electrical demand without excessive imbalances.

Table 46 W-ECoMP input data for mGT simulations

Name:	microGT
Nominal Electrical Power [W]	800000.0
Nominal Electrical Efficiency	0.33
Fuel LHV (J/kg)	47000000
% off design Electrical Power	1.0
Fuel Cost [euro/kg]	0.30
Nominal Thermal Efficiency	0.498
fuel cost option	Fixed cost
% min off design	0.07
Operating and Maintenance Cost [euro/kWh]	0.0001
MGT TYPE	Capstone
INDCOST	Set your cost
mGT capital cost [euro]	816000

Name:	Electrical grid
Purchased electricity cost [euro/kWh]	0.10
Electricity selling price (grid) [euro/kWh]	0.00
Limit for grid purchasing [Wh]	1000
Electricity selling price (user) [euro/kWh]	0
Option for grid sale	Not allowed
Maximum El. excess without penalties [Wh]	1000
Maximum El. shortage without penalties [Wh]	1000
Index for electricity cost Rate	Fixed cost
PES evaluation option	Not active
PARAGUAY Option	Not active
Electricity selling price option	Fixed
TEE value [euro/TEE]	86.97
User purchasing price option	Fixed

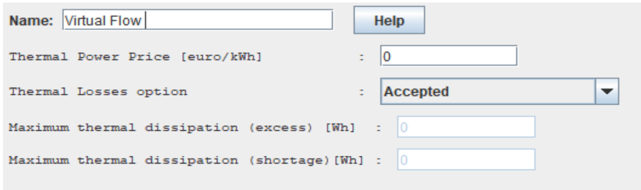

Table 46 shows the data that was entered into the code to set the various technical characteristics and costs. In particular, the significant data are the ones characteristic of the microturbine and those of management of the electrical and thermal network.

- **<u>Cold scenario</u>**

It has been decided to simulate initially the energy management of the ship considering the scenario of the cold external environment. In this scenario, the ratio between electrical and thermal demand is lower than in the case of the hot external environment. Despite the rather high thermal efficiency of the mGTs, it could still be more difficult to satisfy the thermal demand by following a control strategy of the type "thermal follows" (in which priority is given to the electrical load) in the cold scenario. Introducing the weekly load profiles in the software, it is carried out the simulation for every Zonal Group in order to verify which is the optimal management of the system that maximizes the efficiency of the system and therefore, minimizes the consumptions, with a consequent reduction of the management costs. In Table 8.19 the obtained results are shown, where it is reported for every zonal group the tracking of the electric and thermal loads by the various CHP units.

Table 47 Electrical and thermal management of mGTs in the three different ZGs

	MVZ 1-2 (ZG 1)
1	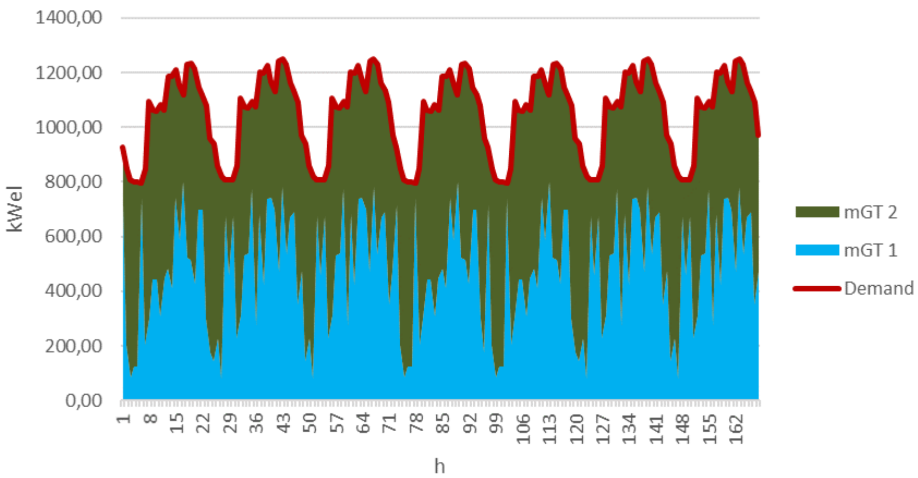 **Figure 166 ZG1 electrical management**

2

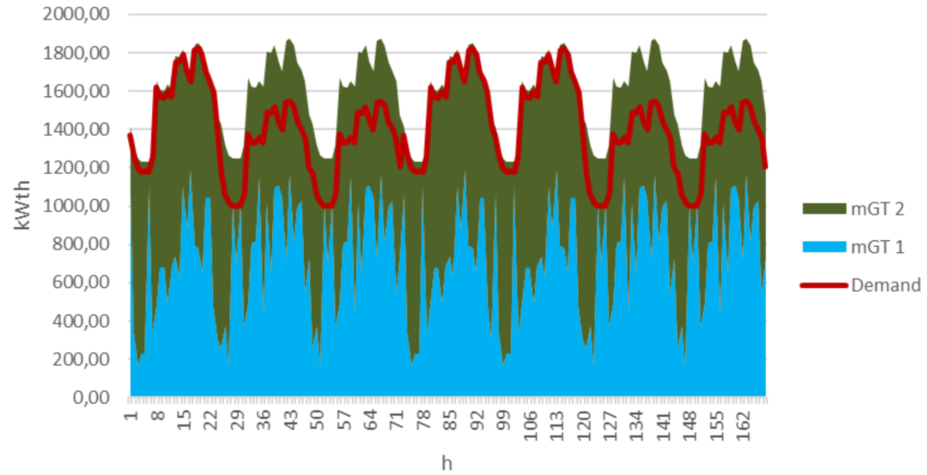

Figure 167 ZG1 Thermal management

MVZ 3-4-5 (ZG 2)

3

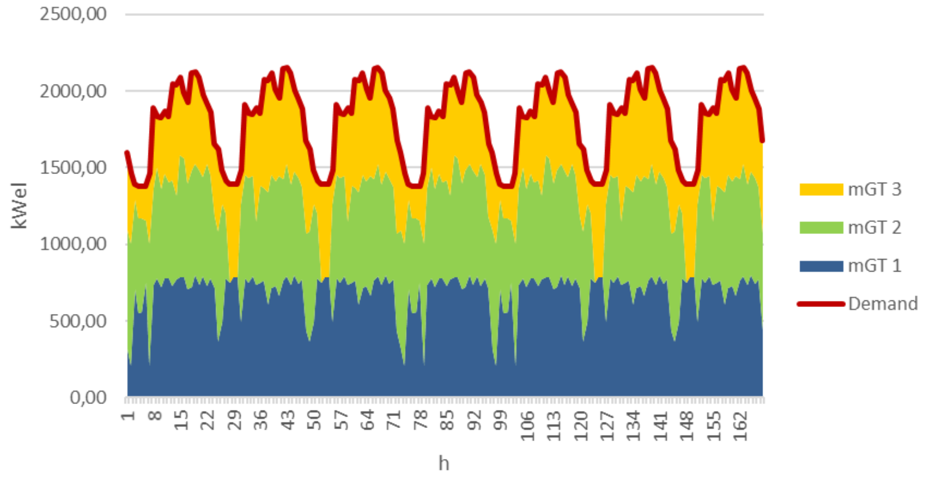

Figure 168 ZG2 Electrical management

4

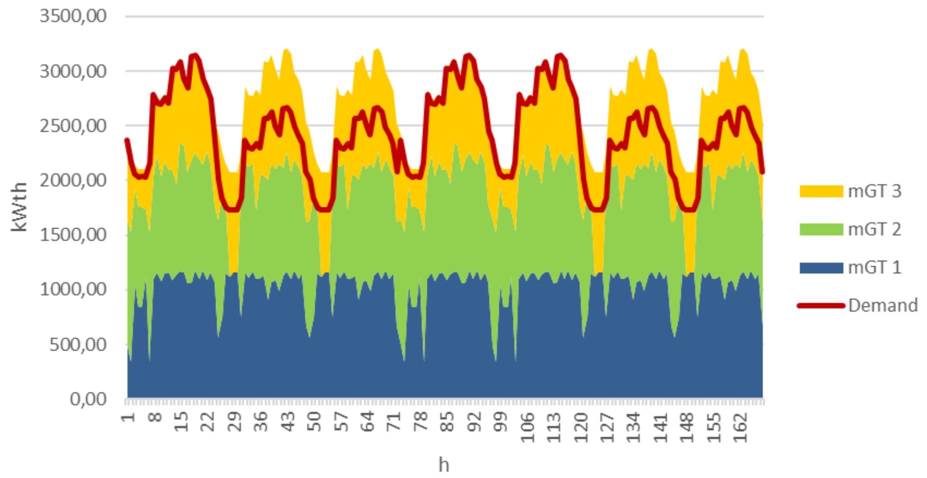

Figure 169 ZG2 Thermal management

<table>
<tr><th colspan="2">MVZ 6-7 (ZG 3)</th></tr>
<tr><td>5</td><td>
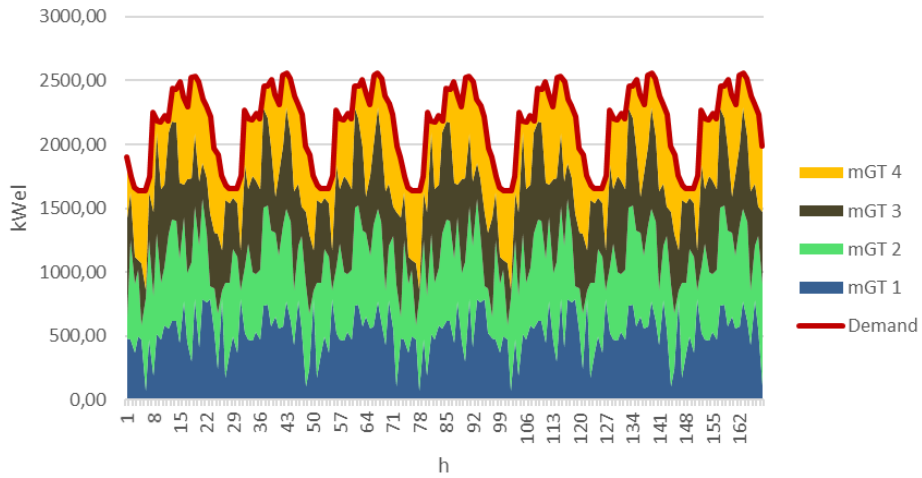

Figure 170 ZG3 Electrical management
</td></tr>
<tr><td>6</td><td>
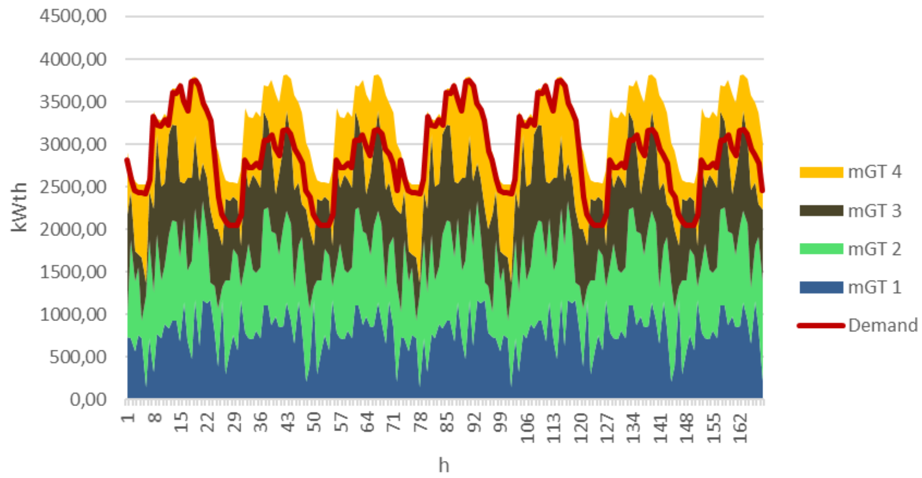

Figure 171 ZG3 Thermal management
</td></tr>
</table>

In a first analysis of the charts shown in Table 47 it can be seen that, in order to properly track the electrical demand profile, there is a need for thermal dissipation during the navigation period when the thermal demand is rather low. In this case, it will be verified if there is the possibility to supply an additional thermal demand to the one referred to the hotel load, or if the heat in excess should be dissipated externally (since that the installation of storage is not considered in order to avoid additional volumes and weights). In any case, it can be stated that the electrical and thermal demands of the hotel load are covered by the installed mGTs. It is important to underline that, in the case of mGT, it is preferable to avoid ON/OFF in order to mitigate a decrease in their lifetime. In this sense, Table 48 shows the number of ON/OFFs for the various mGTs on a monthly basis.

Table 48 mGT ON/OFFs on a monthly basis

MVZ 1-2 (ZG 1)	MVZ 3-4-5 (ZG 2)	MVZ 6-7 (ZG 3)
0-0	5-6-5	0-0-0-0

The cold ambient management provides for a rather limited number of start-ups and shutdowns, even if they are all concentrated on a single zonal group (ZG 2). The ON/OFFs are distributed quite uniformly among the three different installed machines in ZG, during the long-term management of the plant, it will be advisable to make a sort of "rotation" in the use of these mGTs. In this way, it is possible to increase the uniformity in the use of the machines, minimizing the request for maintenance interventions.

Going deeper into the analysis of the above charts, it is interesting to analyse at what percentage of load, and therefore with what efficiency, the optimization software drives the different microturbines to work. These data are reported in the graphs of Table 49 in relation to the hours of operation in a given operating condition.

Table 49 Partial Loads and efficiency of mGTs for each ZG in a cold ambient (in descending order)

MVZ 1-2 (ZG 1)

1

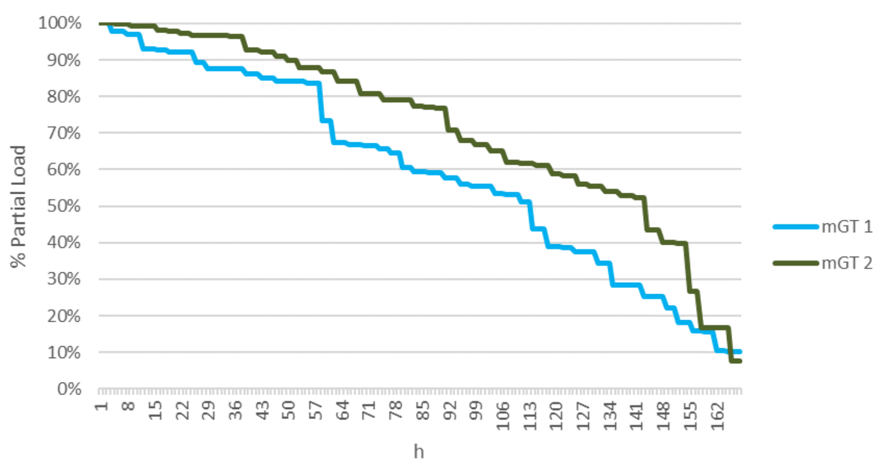

2

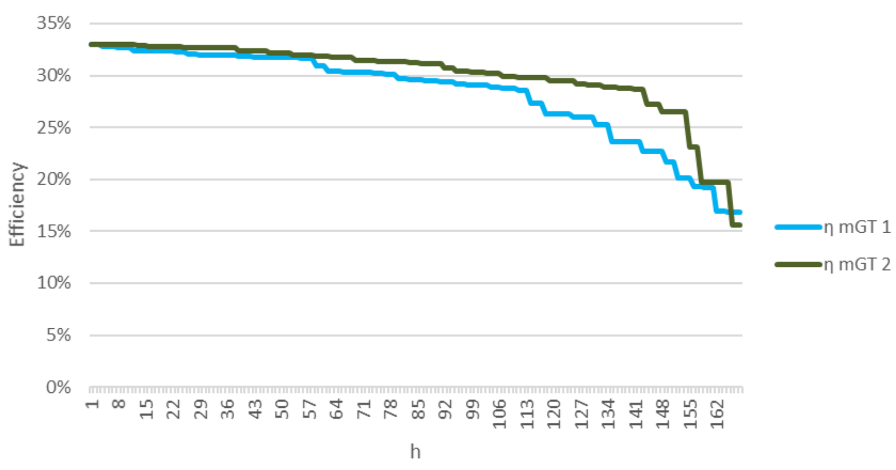

MVZ 3-4-5 (ZG 2)

3	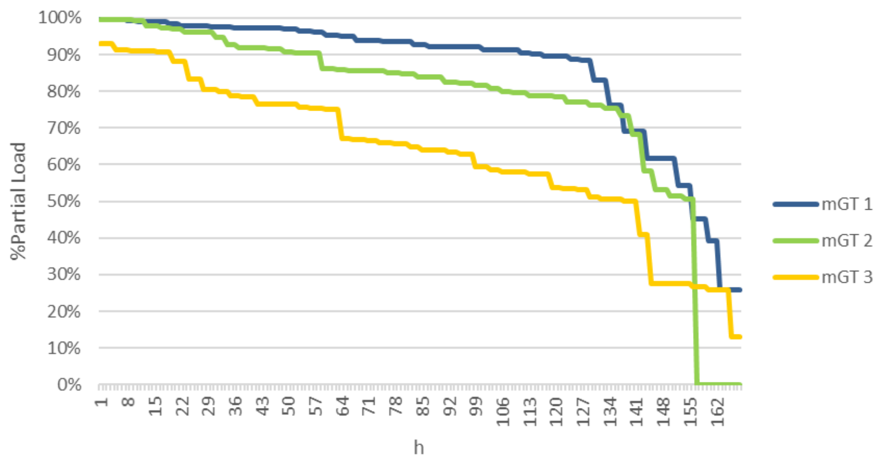
4	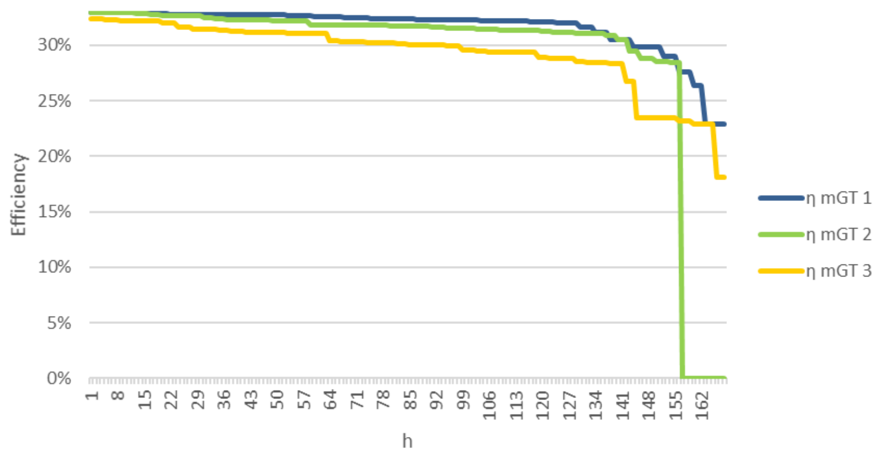
MVZ 6-7 (ZG 3)	
5	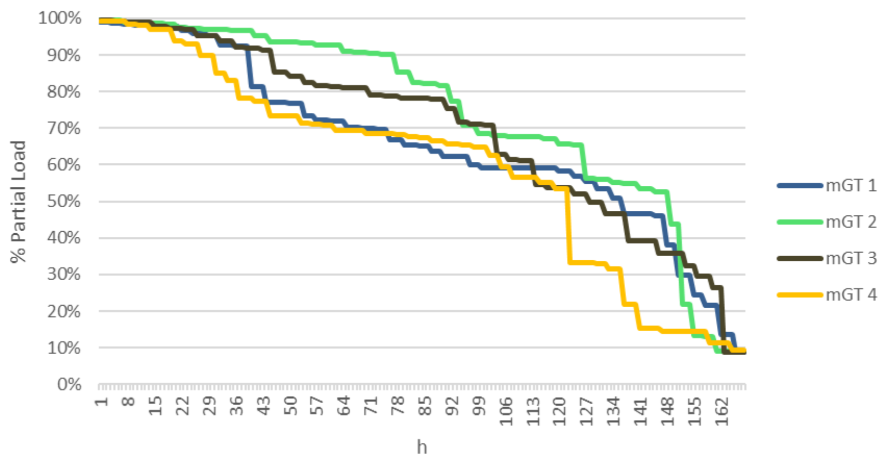

6	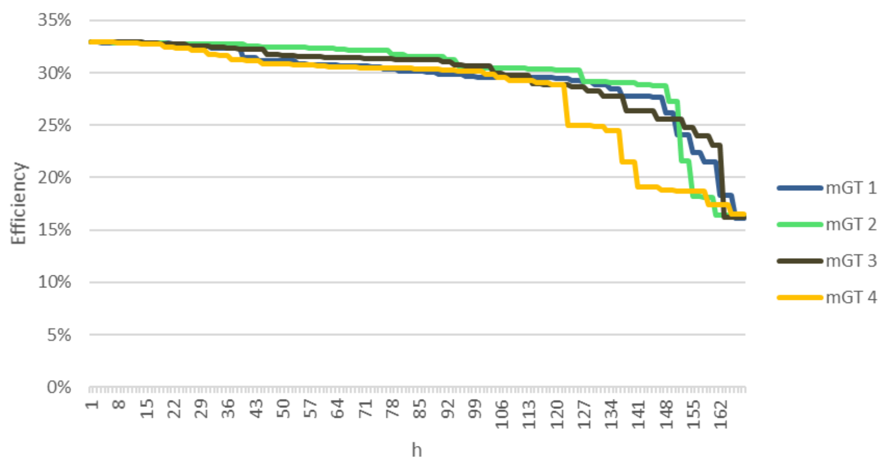

Analysing the data in Table 49, it emerges that the electrical load is never distributed proportionally among the various machines. In this sense, it becomes advisable also to carry out "rotation" between the different mGTs of every zonal group to the aim to a uniform of the use of them. Considering Zonal Group 1 (Figure 1 in Table 49) the management of the two units involves the use of mGT 2 mainly in a range between 95% and 40% while mGT 1 is used at slightly lower loads in order to track the electrical demand. Due to the quite flat conformation of the off-design curve of the mGT Capstone taken into consideration, both machines work mainly with efficiencies not lower than 25% (Figure 2 in Table 49).

Regarding Zonal Group 2, it can be seen that the mGT 1 of this group operates at rather high utilization rates, almost steadily above 60%, while the mGT 2 operates on a lower utilization range, with several valleys below 30% utilization (Figure 3 in Table 49). The management of mGT 3 involves shutdowns in order to avoid operations at low efficiency. In this situation it is more efficient to shut down one mGT, increasing the percentage of use of the other two that works with higher efficiency values (Figure 4 in Table 49). Zonal Group 3 is the one characterized by the highest loads, therefore the 4 machines installed in this zone work almost all the time with a load percentage greater than 40% with efficiencies greater than 25%. The mGT 4 in that group actually runs at lower percentages of use, with efficiencies around even 20% (Figure 5 and Figure 6 in Table 49). Thus, it is possible to state how in an outdoor cold environment scenario there is good coverage of electrical and thermal loads, with the focus on dissipating the excess thermal energy produced by the mGTs.

- **Warm scenario**

The analysis of the scenario in the warm outdoor environment leads to more intensive use of the various microturbines in order to cover the increased electrical load. At the same time, given the decrease in thermal load, the heat generation attached to the electrical production will lead to greater dissipation. To see in detail the behaviour of the various zonal groups, it is repeated, for this scenario, what has been done and reported in the case of the cold outdoor environment.

Table 50 Electrical and thermal management of mGTs in the three different ZGs in warm ambient

<table>
<tr><th colspan="2">MVZ 1-2 (ZG 1)</th></tr>
<tr><td>1</td><td>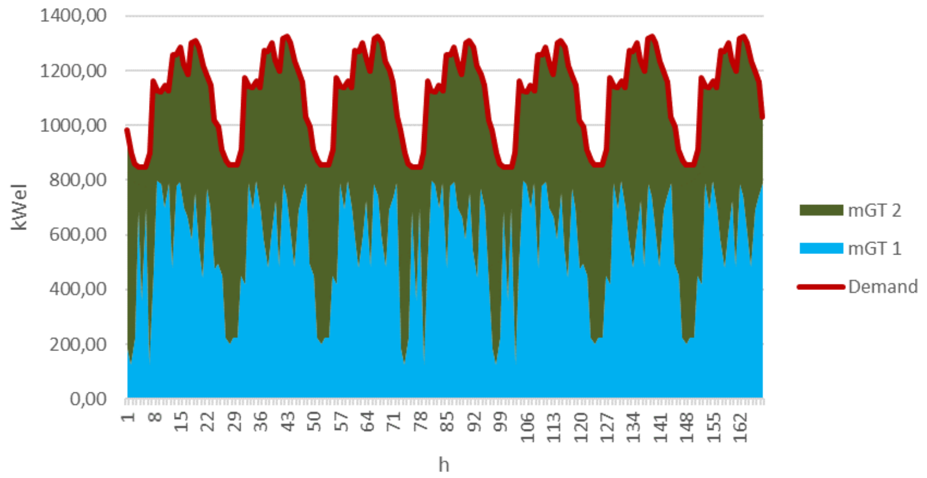

Figure 172 ZG 1 electrical management warm ambient</td></tr>
<tr><td>2</td><td>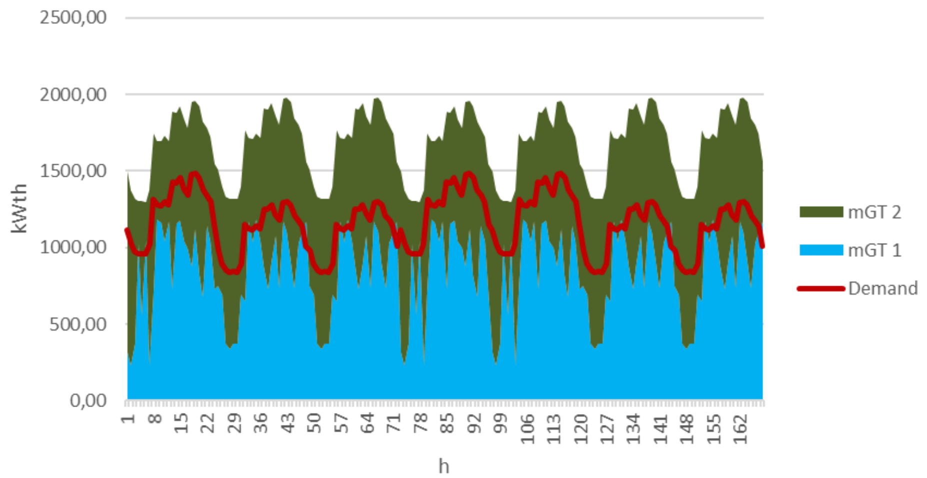

Figure 173 ZG 1 Thermal management warm ambient</td></tr>
<tr><th colspan="2">MVZ 3-4-5 (ZG 2)</th></tr>
</table>

3	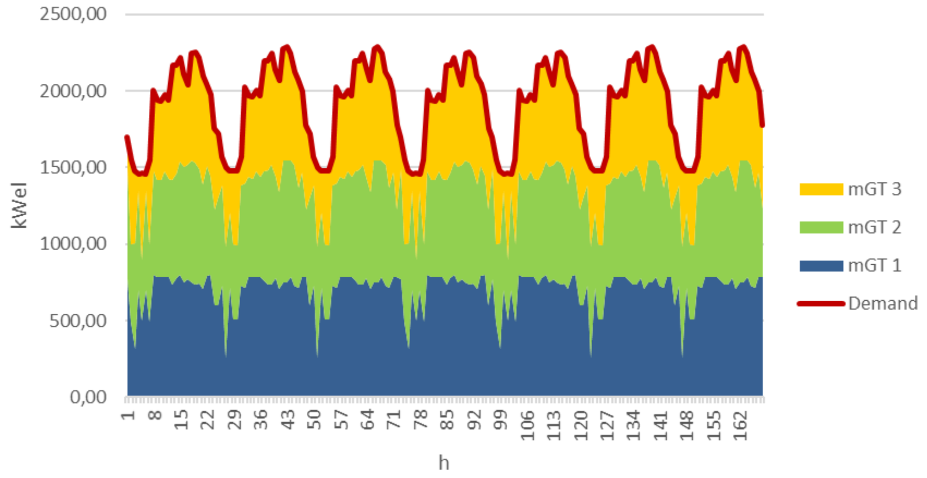 **Figure 174 ZG 2 Electrical management warm ambient**
4	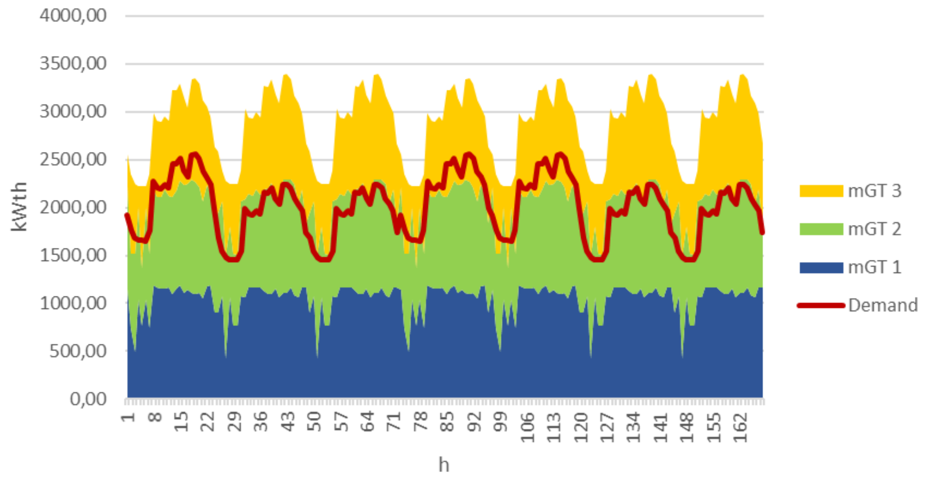 **Figure 175 ZG 2 Thermal management warm ambient**
MVZ 6-7 (ZG 3)	
5	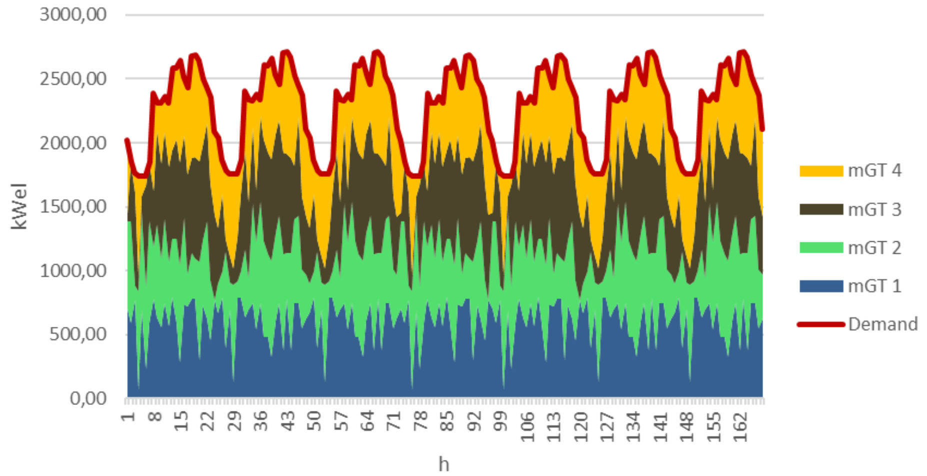 **Figure 176 ZG 3 Electrical management warm ambient**

6	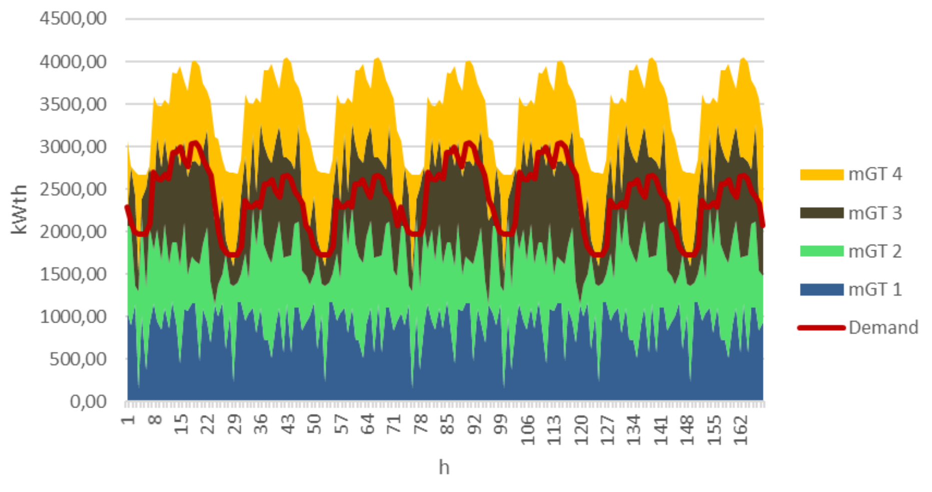 Figure 177 ZG 3 Thermal management warm ambient

Table 50 illustrates the system operation in a scenario with a warm outdoor environment. It can be noted that, even with these higher electrical loads, the size chosen for the machines is sufficient to meet the electrical demand. Regarding the thermal aspect, the thermal dissipations are, as anticipated, quite considerable.

It is interesting to evaluate the possible ON/OFF of the various machines during operation. The results are shown in Table 51.

Table 51 mGT ON/OFFs on a monthly basis, warm ambient

MVZ 1-2 (ZG 1)	MVZ 3-4-5 (ZG 2)	MVZ 6-7 (ZG 3)
0-0	0-0-0	9-9-9-9

In this scenario, given the type of electrical load more intense, there are more switches on and off for some machines. In particular, as far as zonal group 3 is concerned, ON/OFF are observed. It should be pointed out that the calculation code used already gives an economic "penalty" for each start-up and shutdown of a machine in terms of "artificial" maintenance costs that only affect system management. Therefore, in this circumstance, it is more convenient to switch some machines off and on rather than have the system work at lower efficiency rates. Obviously, as mentioned above, a "rotation" in the use of the various mGTs is advisable in order to have a uniform and less premature wear of the system.

Table 52 Partial Loads and efficiency of mGTs for each ZG in a warm ambient (in descending order)

MVZ 1-2 (ZG 1)

1

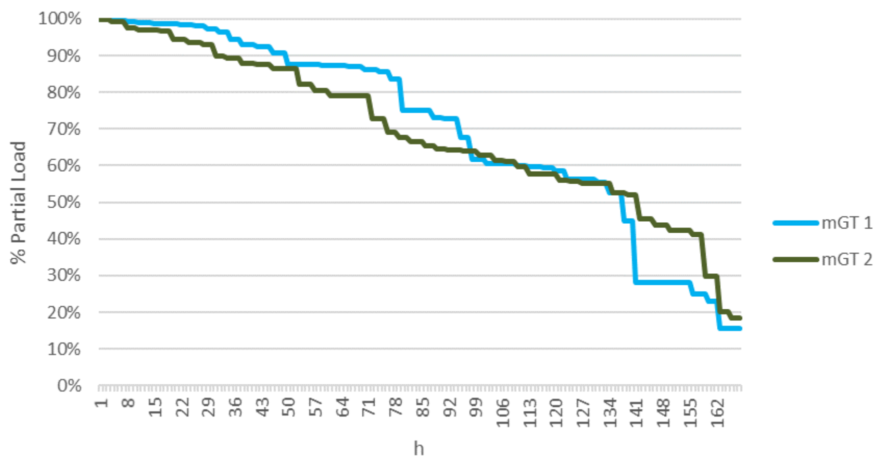

2

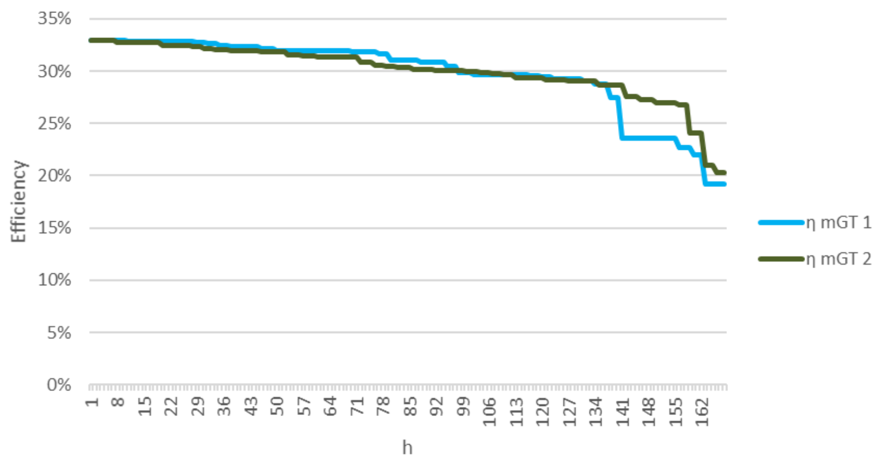

MVZ 3-4-5 (ZG 2)

3

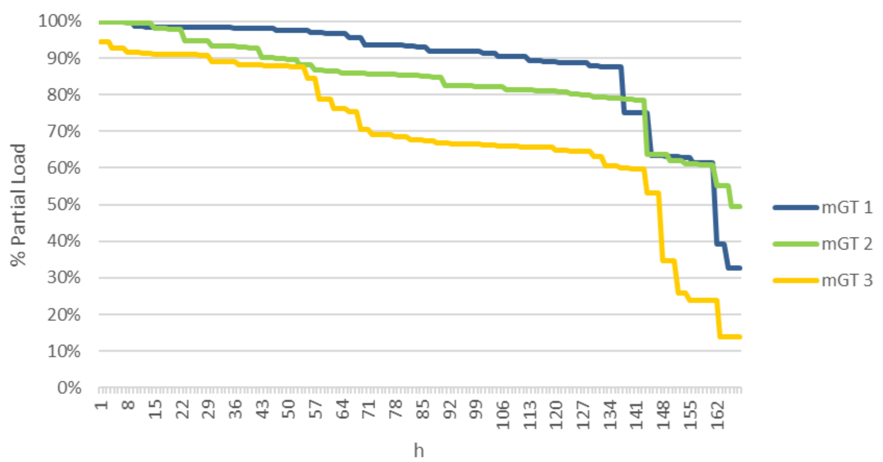

4	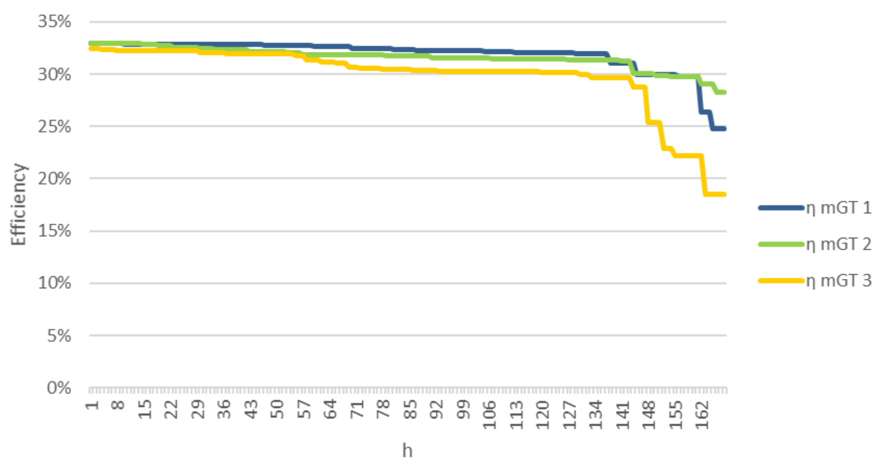
MVZ 6-7 (ZG 3)	
5	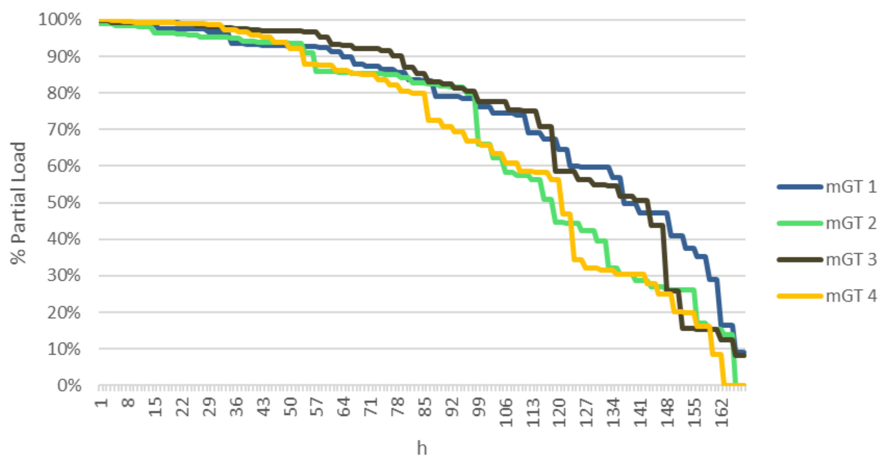
6	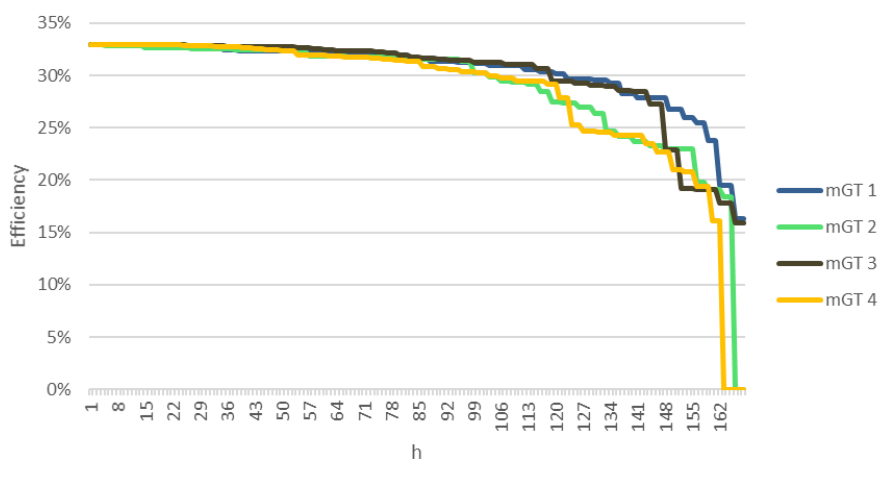

It is evident that, compared to the cold environment scenario, the percentages of use of the various microturbines are higher in the warm one, resulting in higher performance ranges. In the zonal group 1, the two mGTs work sharing the load in a uniform way, with an efficiency that is mainly over 25% (Figure 1 and Figure 2 of Table 52). The situation is even more pronounced for zonal group 2 (Figure 3 and Figure 4 of Table 52) where the various machines work with efficiencies around 30%, despite their load modulation, due to their rather flat off-design curve. Similar considerations can be performed for zonal group 3 (Figure 5 and Figure 6 of Table 52).

In order to evaluate the impact of the management proposed by W-ECoMP an economic analysis is performed. Table 53 reports the economic data used as a basis for this analysis.

Table 53 Economic data

Economic Hypothesis	
CO_2 Emissions cost [€/ton]	0
GNL cost [€/ton]	300
Discount rate	2%
Inflation	1%

It is worth noting that a slot has been inserted regarding the cost of CO_2 emissions. In fact, if a "carbon tax" was to be applied in some port areas, the economic impact of using a combustion system instead of a Fuel Cell would be quite significant depending on the value of this tax. At the moment no tax is applied in this direction, therefore this value is set as null.

Table 54 Cold ambient weekly costs per ZGs

Cold ambient (weekly)						
ZG 1	*El produced [MWh]*	*El demand [MWh]*	*Th produced [MWh]*	*Th demand [MWh]*	*CO_2 Emissions [ton]*	*Thermal dissipations [MWh]*
	176.41	176.41	267.01	236.55	122.27	30.45
	On/Off	*O&M [€]*	*Fuel cons [ton]*	*Fuel Costs [€]*	*CO_2 costs [€]*	***Total costs [€]***
	0	1,234.9	44.46	13,338.1	0.0	**14,573.0**
ZG 2	*El produced [MWh]*	*El demand [MWh]*	*Th produced [MWh]*	*Th demand [MWh]*	*CO_2 Emissions [ton]*	*Thermal dissipations [MWh]*
	304.33	304.33	456.17	408.07	204.61	48.10
	On/Off	*O&M [€]*	*Fuel cons [ton]*	*Fuel Costs [€]*	*CO_2 costs [€]*	***Total costs [€]***
	4	2,130.3	74.40	22,321.1	0.0	**24,451.4**

ZG 3	El produced [MWh]	El demand [MWh]	Th produced [MWh]	Th demand [MWh]	CO_2 Emissions [ton]	Thermal dissipations [MWh]
	361.66	361.66	546.52	485.04	249.09	61.48
	On/Off	O&M [€]	Fuel cons [ton]	Fuel Costs [€]	CO_2 costs [€]	**Total costs [€]**
	0	2,531.6	90.58	27,173.3	0.0	**29,705.0**

Table 55 Warm ambient weekly costs per ZGs

Warm Ambient (weekly)						
ZG 1	El produced [MWh]	El demand [MWh]	Th produced [MWh]	Th demand [MWh]	CO_2 Emissions [ton]	Thermal dissipations [MWh]
	187.14	187.14	282.21	195.73	128.39	86.48
	On/Off	O&M [€]	Fuel cons [ton]	Fuel Costs [€]	CO_2 costs [€]	**Total costs [€]**
	0	1,310.0	46.69	14,005.9	0.0	**15,315.9**
ZG 2	El produced [MWh]	El demand [MWh]	Th produced [MWh]	Th demand [MWh]	CO_2 Emissions [ton]	Thermal dissipations [MWh]
	322.83	322.84	482.98	337.65	215.60	145.33
	On/Off	O&M [€]	Fuel cons [ton]	Fuel Costs [€]	CO_2 costs [€]	**Total costs [€]**
	0	2,259.8	78.40	23,520.4	0.0	**25,780.2**
ZG 3	El produced [MWh]	El demand [MWh]	Th produced [MWh]	Th demand [MWh]	CO_2 Emissions [ton]	Thermal dissipations [MWh]
	383.66	383.66	577.23	401.32	260.59	175.91
	On/Off	O&M [€]	Fuel cons [ton]	Fuel Costs [€]	CO_2 costs [€]	**Total costs [€]**
	9	2,685.6	94.76	28,427.5	0.0	**31,113.1**

Comparing the data of Table 54 with those of Table 55 it can be observed how the greater demands lead to greater consumptions and, therefore, costs. However, it should be evinced how such an increase in the costs results rather contained considering that working to higher loads, the machines have efficiencies higher. Also the maintenance costs, proportional to the

use of the machines and therefore to the electrical energy produced, are slightly higher in the hot scenario than in the cold scenario. It should be considered that, at economic level, in this phase, the actual economic impact of the ON/OFF is not calculated, as it is already limited by the code and difficult to quantify numerically.
The study done on a weekly basis is now extended to the whole year, assuming that the ship is located half of the time in a hot scenario and the other in a cold one. The weeks in which it is estimated that the ship is used in a year are equal to 50 (25 for each scenario). In order to have a clear and immediate view of costs and consumption, the data for the whole cruise ship over the whole year are reported in the dedicated Table 56.

Table 56 Costs and fuel consumptions on a yearly basis for the whole cruise ship

Cruise Ship (annual)						
El produced [MWh]	*El demand [MWh]*	*Th produced [MWh]*	*Th demand [MWh]*	*CO_2 Emissions [ton]*	*NOx Emissions [ton]*	*Thermal dissipations [MWh]*
43,401	43,401	65,303	51,609	29,513	9.67	13,694
On/Off	*O&M [€]*	*Fuel cons [ton]*	*Fuel Costs [€]*	*CO_2 costs [€]*	*NOx costs [€]*	***Total costs [€]***
250	303,806	10,732	3,219,657	0	0	**3,523,464**

With the data in Table 56, we, therefore, have a direct and global evaluation of the system management costs in the case of using microturbine technology. On the basis of these values, it will be possible then to develop a more detailed economic analysis that takes into account the fixed costs, the lifetime of the system and the various aspects of savings with respect to the technology studied in the next section. It will also be important to evaluate the benefits and drawbacks of using innovative technologies with respect to the state of the art and the environmental regulations introduced.

3.1.4.2 PEMFC with Liquid Hydrogen

After the study of microturbines, we proceed with the analysis of Fuel Cells in order to make a comparative analysis in technical and economic. Also in this case the significant data have been set within the code in W-ECoMP. These values are reported in Table 57.

Table 57 W-ECoMP input data for mGT simulations

Name: Fuel Cell	
Nominal Electrical Power [W]	800000.0
Nominal Electrical Efficiency	0.45
Lower Heating Value [J/kg]	120000000
% off design Electrical Power	1.0
Fuel Cost [euro/kg]	2.14
Nominal Thermal Efficiency	0.3
CELL TYPE	PEMFC
Fuel cost type	Fixed cost
% MIN OFF DESIGN	0.0
INDCOST	Set your cost
Fuel cell capital cost [euro]	2735043
Operating and Maintenance Cost [euro/kWh]	0.012

Name: Electrical grid	
Purchased electricity cost [euro/kWh]	0.10
Electricity selling price (grid) [euro/kWh]	0.00
Limit for grid purchasing [Wh]	2000
Electricity selling price (user) [euro/kWh]	0
Option for grid sale	Not allowed
Maximum El. excess without penalties [Wh]	1200
Maximum El. shortage without penalties [Wh]	1200
Index for electricity cost Rate	Fixed cost
PES evaluation option	Not active
PARAGUAY Option	Not active
Electricity selling price option	Fixed
TEE value [euro/TEE]	86.97
User purchasing price option	Fixed

Name: Virtual Flow	
Thermal Power Price [euro/kWh]	0
Thermal Losses option	Accepted
Maximum thermal dissipation (excess) [Wh]	0
Maximum thermal dissipation (shortage) [Wh]	0

- <u>**Cold scenario**</u>

Also in this case the study is divided by first analyzing the effect of the cold external environment, then the one in the hot external environment will be developed. It should be noted that the PEM Fuel Cells present rather low thermal efficiencies, therefore it could be possible not to meet the thermal load by following a "thermal-following" control approach. This situation could result particularly problematic in the context of cold external environment management, where the ratio between electrical load and thermal load is lower. The priority of this study remains, however, to satisfy the electrical demand, so in this phase, we will focus exclusively on the possibility of following the electrical load. Possible solutions to satisfy both loads will be presented later. With the same profiles of weekly load used previously it is performed the simulation for every Zonal Group in order to find the management of the system able to maximize the efficiency of the system reducing consumptions, emissions and costs.

In Table 8.30 the obtained results are reported, where it is shown for every Zonal Group the electric and thermal load supply by the various cogenerative units.

Table 58 Electrical and thermal management of PEMFCs in the three different ZGs in cold ambient

MVZ 1-2 (ZG 1)

1

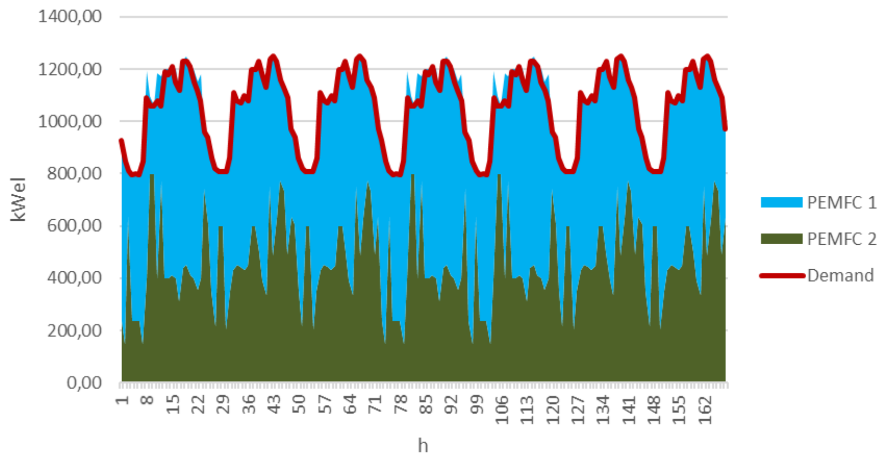

Figure 178 ZG 1 Electric management cold ambient

2

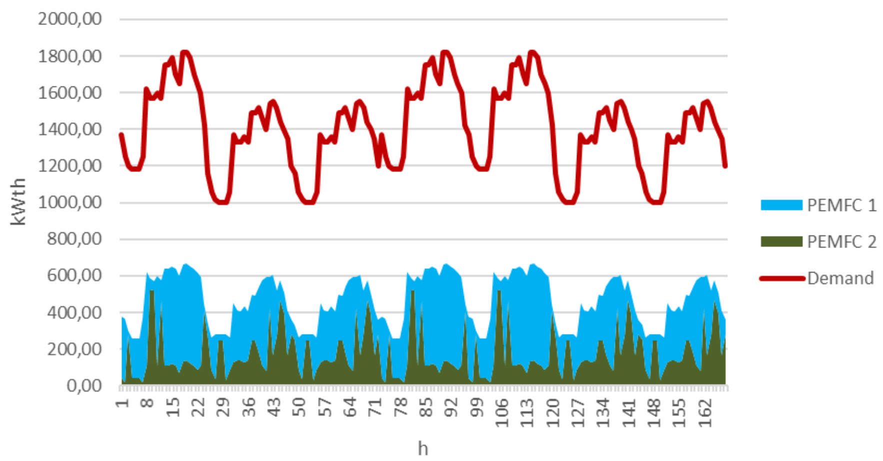

Figure 179 ZG 1 Thermal management cold ambient

MVZ 3-4-5 (ZG 2)

3

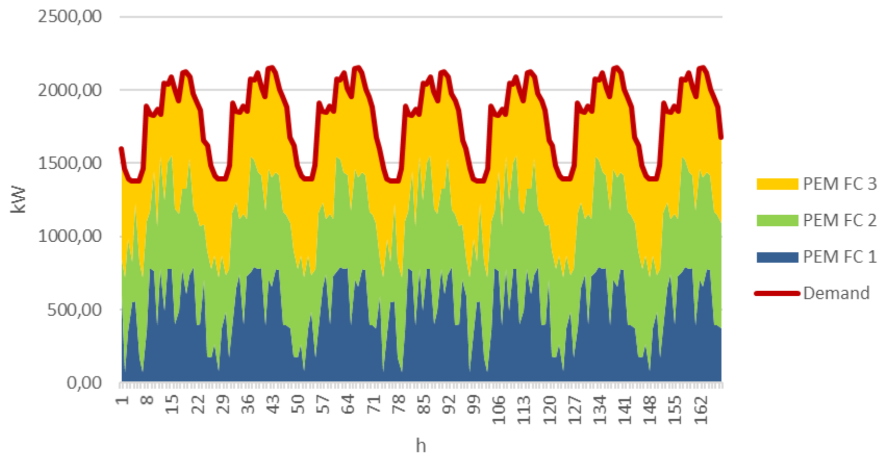

Figure 180 ZG 2 Electric management cold ambient

4

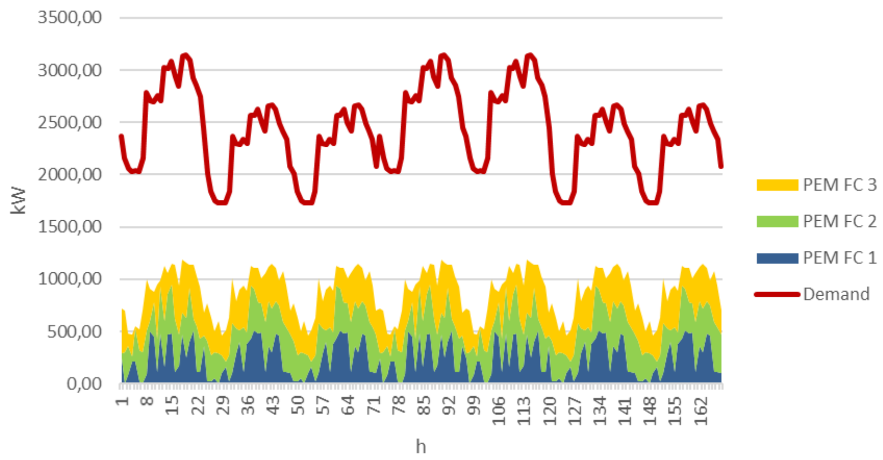

Figure 181 ZG 2 Thermal management cold ambient

MVZ 6-7 (ZG 3)

5

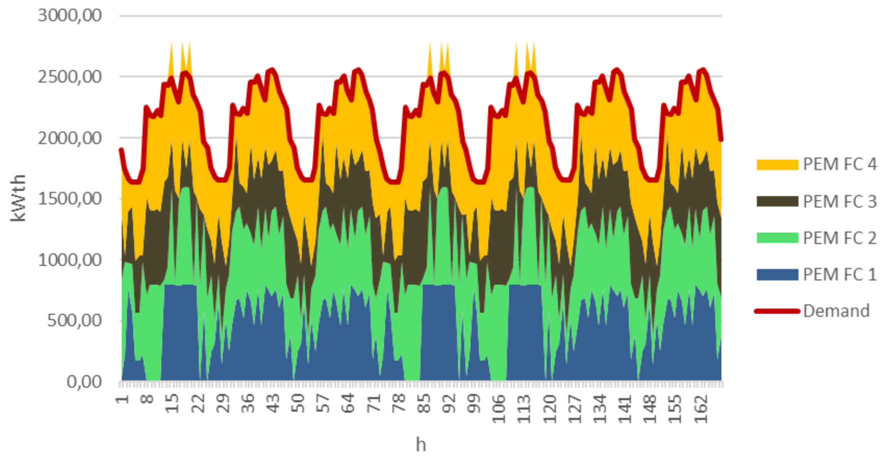

Figure 182 ZG 3 Electric management cold ambient

6

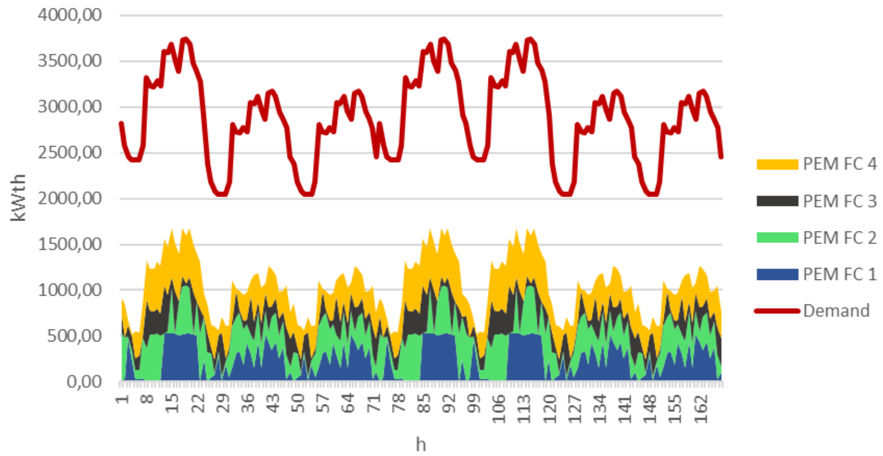

Figure 183 Thermal management cold ambient

As initially anticipated, from the charts in Table 58 it can be observed that the thermal load is definitely not satisfiable, differently from what performed by mGTs. It can also be seen that the load is equally divided among the various FCs; this is because this distribution allows taking full advantage of the increasing efficiency of the Fuel Cells at partial load. It is important to underline that, for the type of PEMFC technology, it is preferable not to subject them to excessive oscillatory and ON/OFF loads in order to avoid a greater usage and therefore a decrease in their lifetime. In this sense Table 59 shows the number of ON/OFF for the various Fuel Cells on a monthly basis.

Table 59 PEMFCs ON/OFFs on a monthly basis, cold ambient

MVZ 1-2 (ZG 1)	MVZ 3-4-5 (ZG 2)	MVZ 6-7 (ZG 3)
0-0	0-0-0	25-25-25-25

It is, therefore, possible to highlight how, for the first two zonal groups, no PEMFC is subjected to switching on and off during its weekly operation, a considerable advantage in terms of costs and maintenance. Further analysis of the above figures shows that it is interesting to analyse the percentage of load, and therefore the efficiency, at which the optimization software operates the different cells. Such data are reported in Table 60 in relation to the hours of operation in a given circumstance.
Looking at the graphs in Table 60, what has been stated previously is confirmed. A detailed analysis of the percentages of use of the various PEMFCs for the different zonal groups shows how the various curves within the graphs are overlapped for most of the time period considered. However, it is good practice, even in this case, to " alternate " the various cells in order to standardize their use. Focusing now on the graphs relating to the efficiency, it can be seen that rather flat curves are obtained, with an average value well above 50%.

Table 60 Partial Loads and efficiency of PEMFCs for each ZG in a cold ambient (in descending order)

	MVZ 1-2 (ZG 1)
1	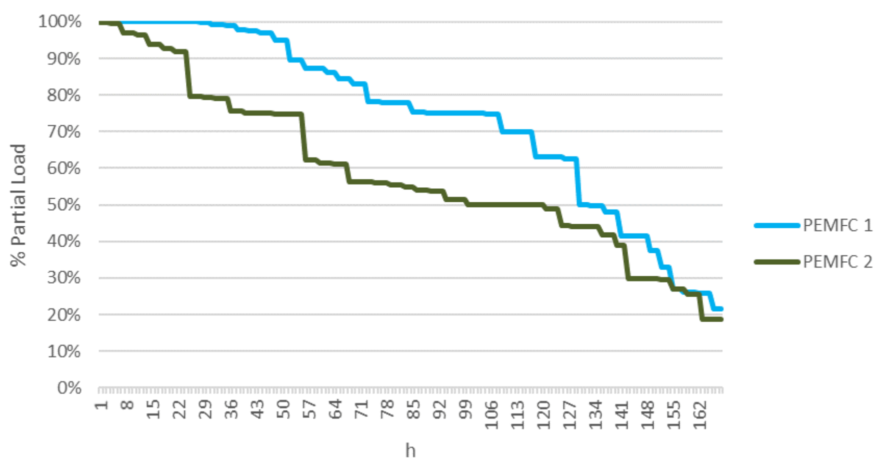

2	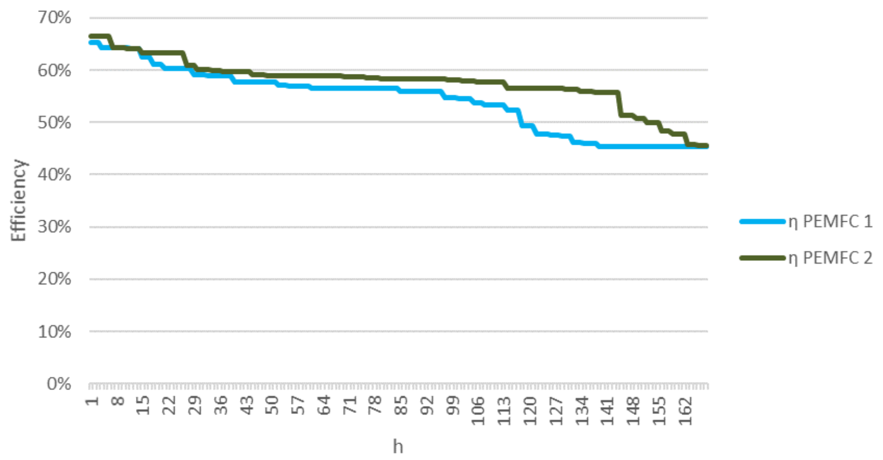
	MVZ 3-4-5 (ZG 2)
3	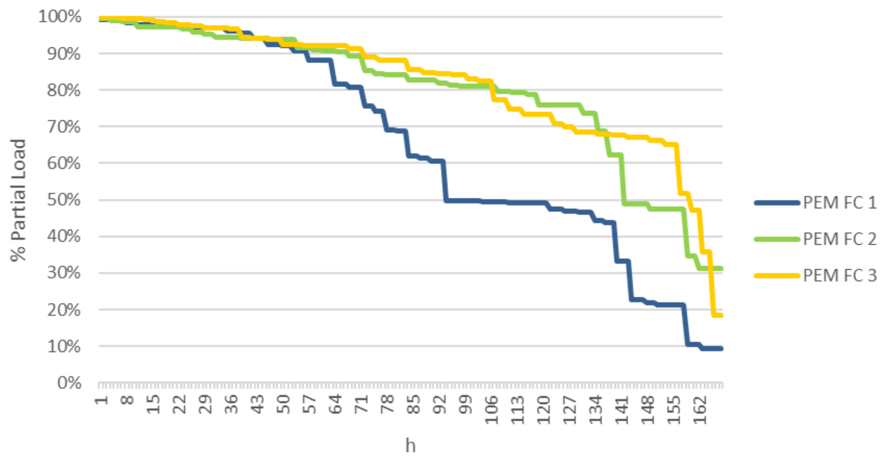
4	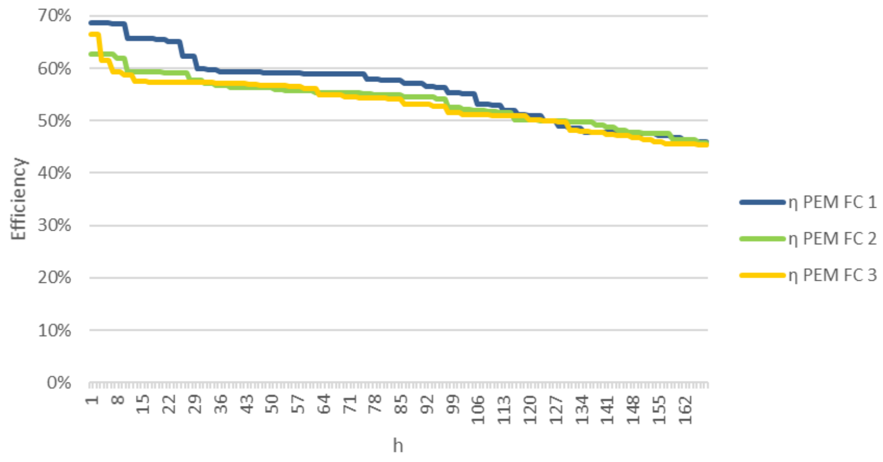
	MVZ 6-7 (ZG 3)

5

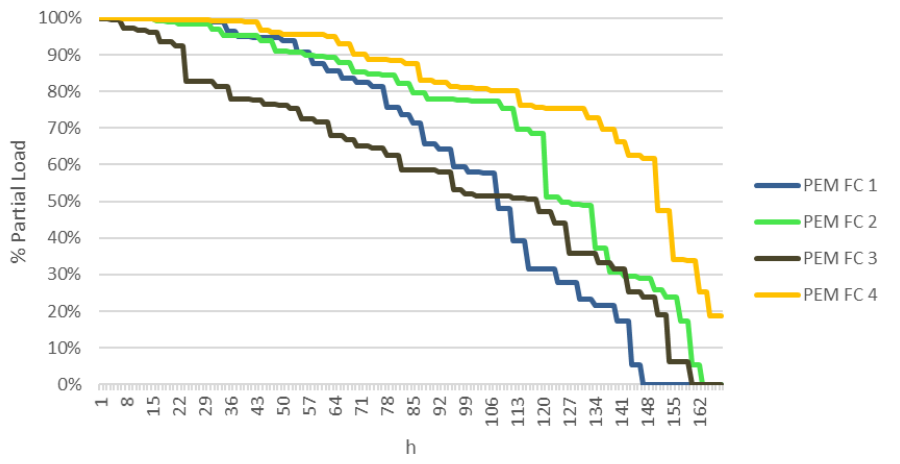

6

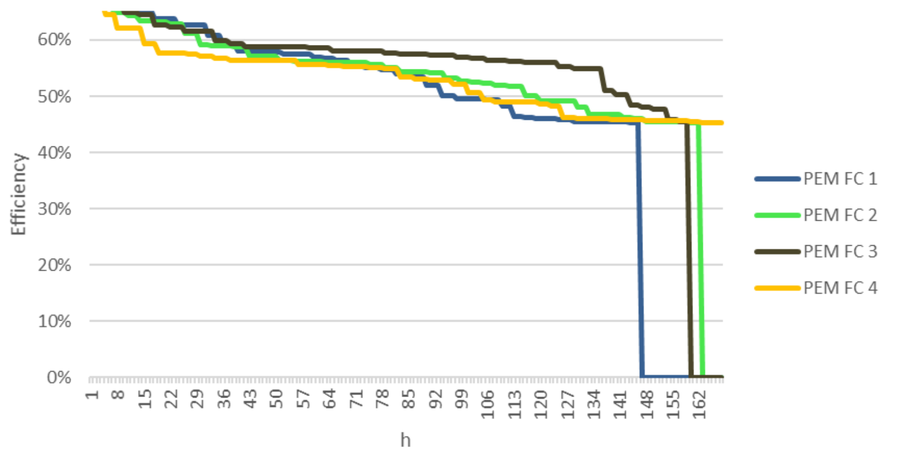

It can therefore be asserted that, in terms of efficiency, consumption and emissions, the fuel cell solution is highly advantageous compared to the mGT solution (average efficiency around 27% with a combustion process and consequent CO_2 emissions).

- **<u>Warm scenario</u>**

From the point of view of the PEM Fuel Cells, the scenario with a warm external environment leads to better management of the system in terms of cogeneration, since a higher electrical demand corresponds to lower thermal demand than in the case with a cold external environment. We can therefore expect a decrease in the thermal deficit, but a corresponding increase in costs due to greater use of the cells to compensate for the increase in electrical load. It may therefore be interesting in the following sections to go over the economic impact of the thermal deficit on the system.

Table 61 Electrical and thermal management of PEMFCs in the three different ZGs in warm ambient

<table>
<tr><th colspan="2">MVZ 1-2 (ZG 1)</th></tr>
<tr><td>1</td><td>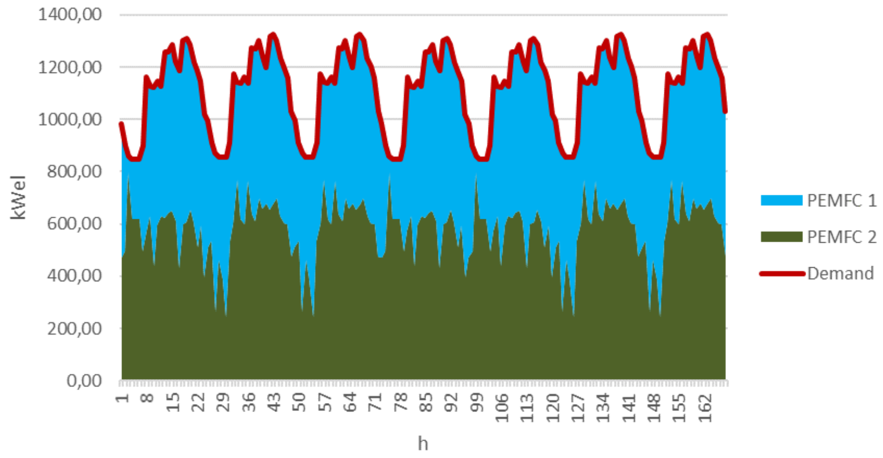

Figure 184 ZG 1 Electric management warm ambient</td></tr>
<tr><td>2</td><td>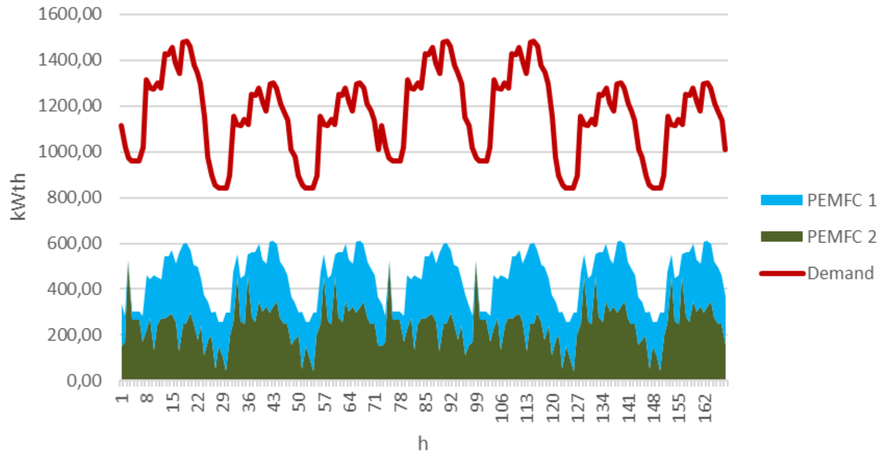

Figure 185 ZG 1 Thermal management warm ambient</td></tr>
<tr><th colspan="2">MVZ 3-4-5 (ZG 2)</th></tr>
</table>

3

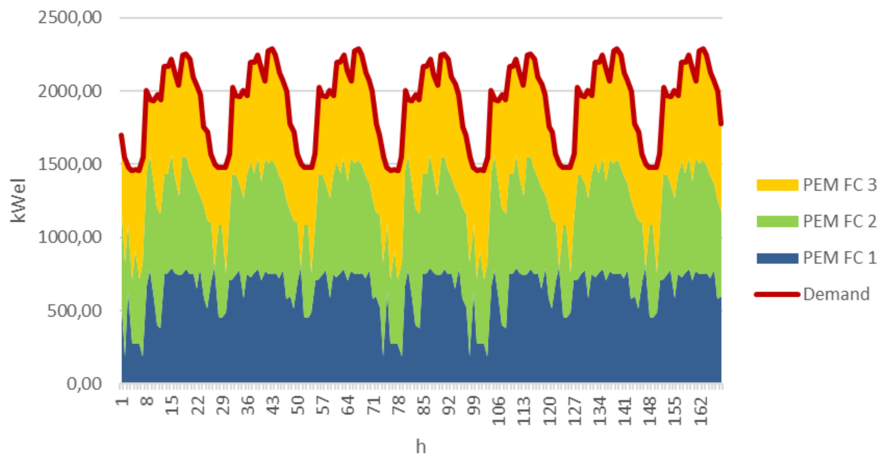

Figure 186 ZG 2 Electric management warm ambient

4

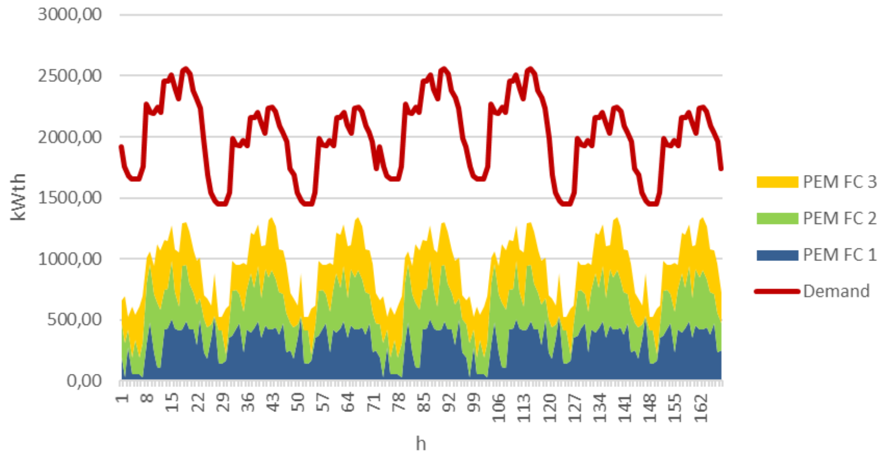

Figure 187 ZG 2 Thermal management warm ambient

MVZ 6-7 (ZG 3)

5

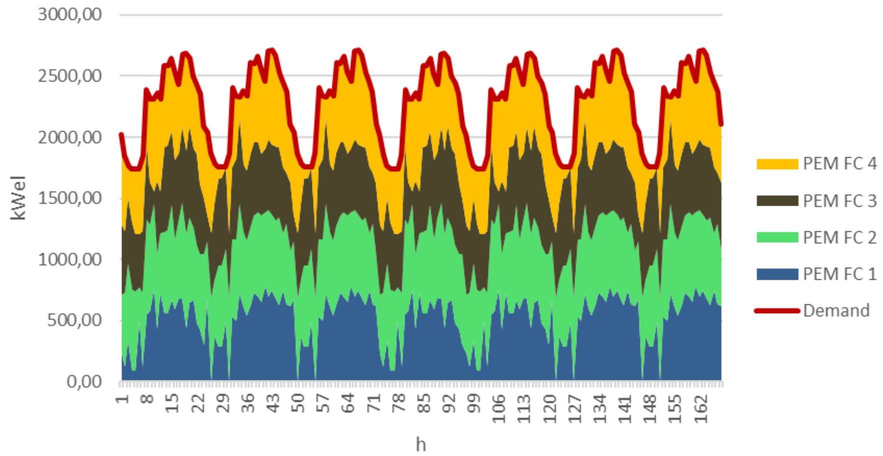

Figure 188 ZG 3 Electric management warm ambient

6	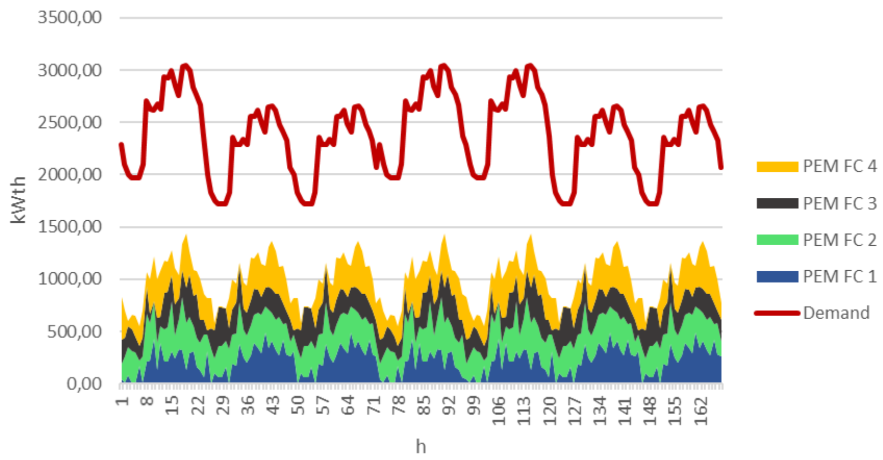 Figure 189 ZG 3 Thermal management warm ambient

Table 58 shows the system operation in a scenario with a warm outdoor environment. Even for these higher electrical loads, the size chosen for the machines turns out to be sufficient to satisfy the electrical demand. Focusing then on the thermal aspect, it is possible to see how the generation curves get closer to the red line, related to the demand, compared to what happened for the cold scenario. This proves how the cogeneration aspect is more exploited in the case of a hot external environment. Focusing on the zonal group 3, it is possible to notice the very strong use of the fuel cells. It is therefore interesting to evaluate the possible ON/OFF of the cells during operation. The results are shown in Table 62.

Table 62 PEMFCs ON/OFFs on a monthly basis, warm ambient

MVZ 1-2 (ZG 1)	MVZ 3-4-5 (ZG 2)	MVZ 6-7 (ZG 3)
0-0	0-0-0	12-12-12-12

A numerical analysis of zonal group 3 shows 12 ON/OFFs distributed over two cells on a weekly basis. This aspect, therefore, leads to opt for a "rotation" on a weekly basis in the use of the various PEMFC in order to have a uniform and delayed deterioration of the system. It can be interesting also in this case to examine the percentages of use of the various cells and to estimate the efficiency with which they work. These data are reported in Table 8.37.

Table 63 Partial Loads and efficiency of PEMFCs for each ZG in a warm ambient (in descending order)

MVZ 1-2 (ZG 1)	
1	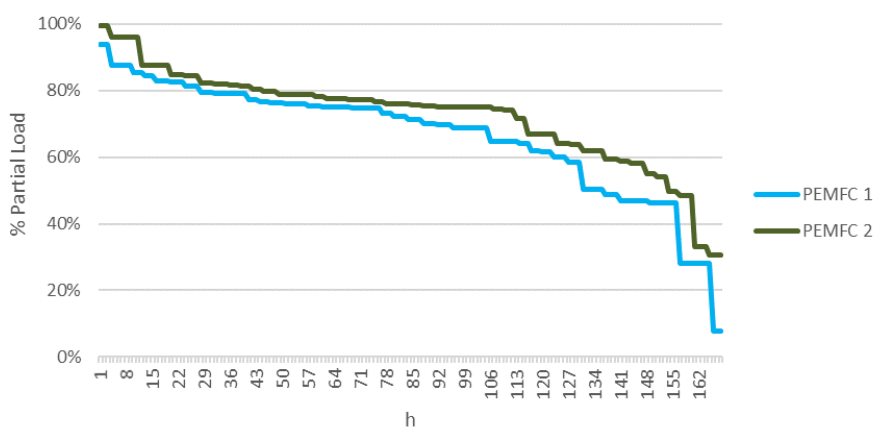
2	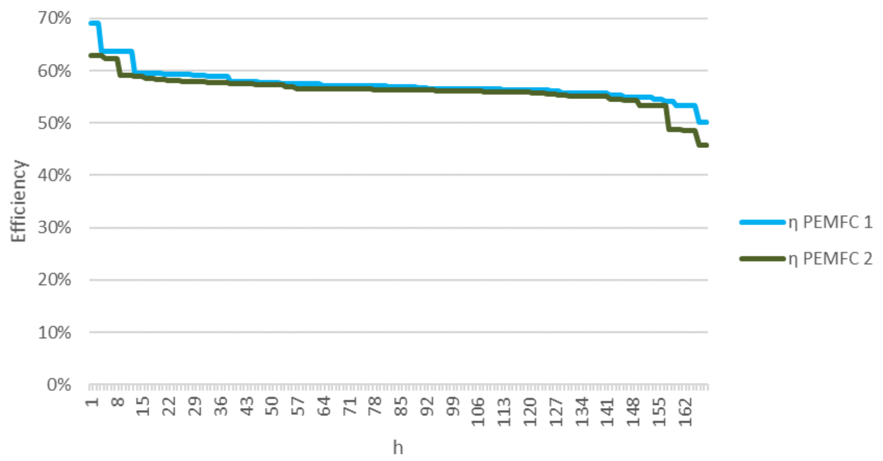
MVZ 3-4-5 (ZG 2)	
3	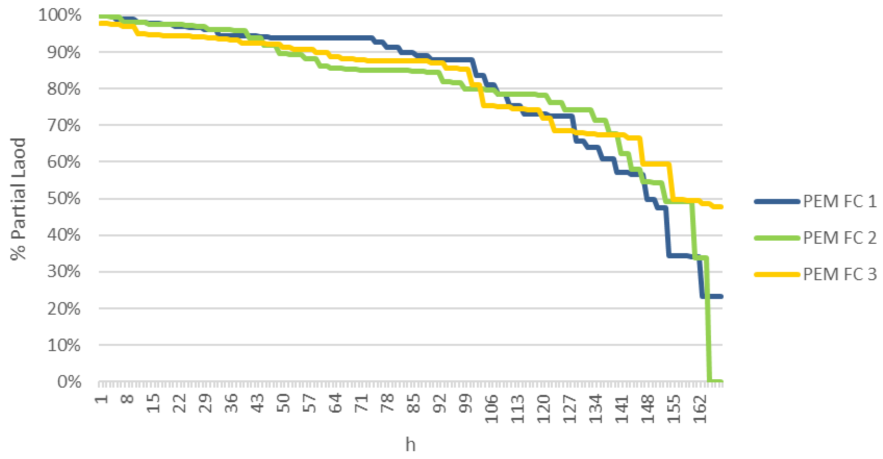

4

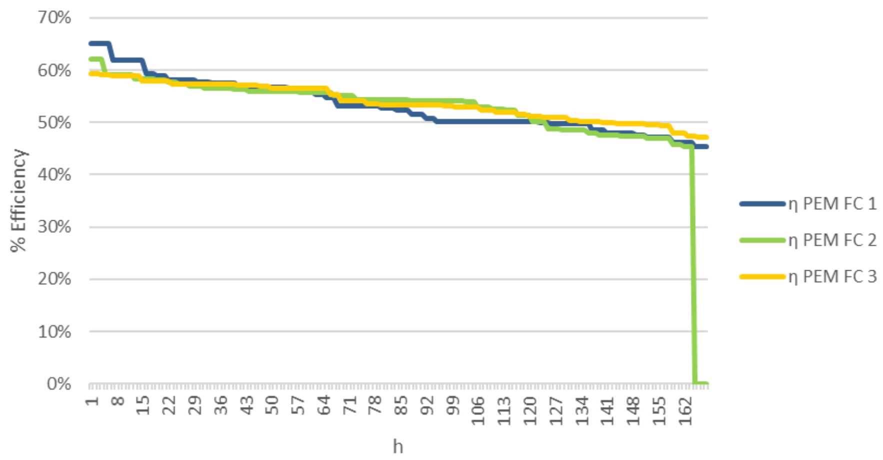

MVZ 6-7 (ZG 3)

5

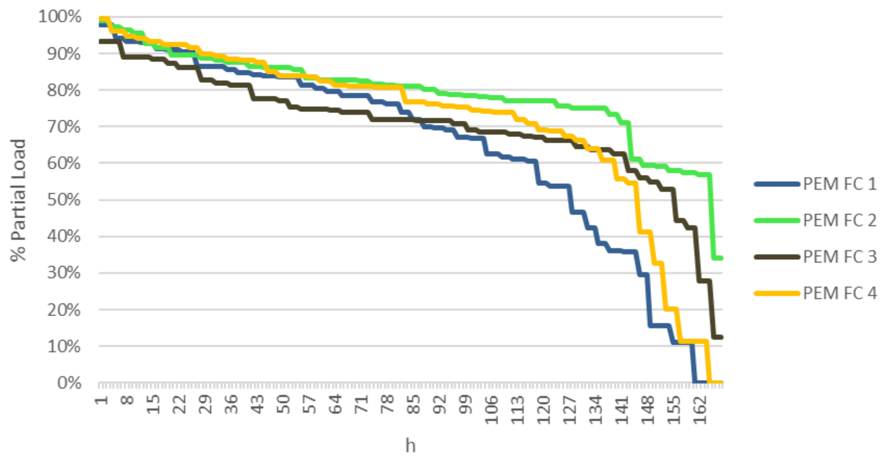

6

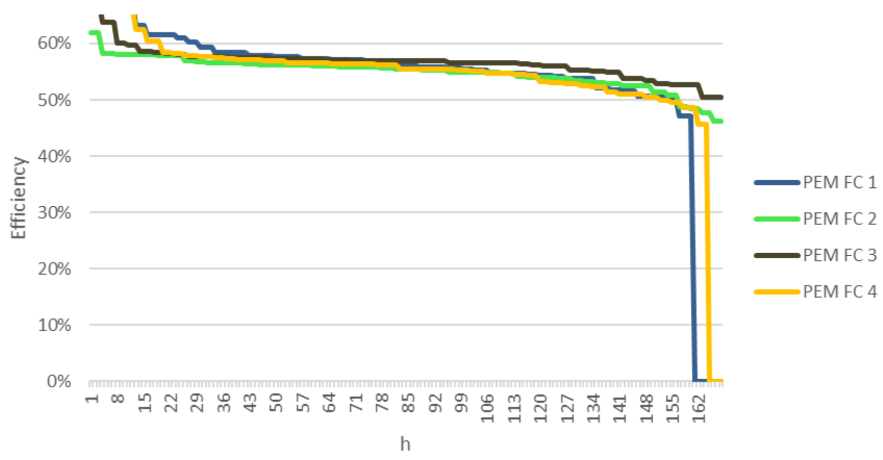

The partial loads, which are higher than in the scenario with a cold outdoor environment, lead to slightly lower efficiency values given the rather flat shape of the off-design curve of PEMFCs in which efficiency increases as power output decreases.

Table 64 shows the economic assumptions made on the basis of the economic values described in the dedicated section.

Table 64 Economic hypothesis

Economic Hypothesis	
LH_2 cost [€/ton]	300
Discount rate	2%
Inflation	1%

Naturally, in this case, the CO_2 emission cost does not appear as the system does not imply CO_2 emissions. In order to appreciate from an economic point of view the performance of the system with PEM Fuel Cells directly fuelled by hydrogen, Table 8.34 shows the calculation of the operating costs of the system on a weekly basis, for each zonal group.

Table 65 Cold ambient weekly costs per ZGs

Cold ambient (weekly)						
ZG1	*El produced [MWh]*	*El demand [MWh]*	*Th produced [MWh]*	*Th demand [MWh]*	*CO_2 Emissions [ton]*	*Thermal dissipations [MWh]*
	178.09	176.39	79.15	236.42	0.00	-157.27
	On/Off	*O&M [€]*	*Fuel cons [ton]*	*Fuel Costs [€]*	*CO_2 costs [€]*	***Total costs [€]***
	0	2,137.1	9.99	21,370.6	0.0	**23,507.7**
ZG2	*El produced [MWh]*	*El demand [MWh]*	*Th produced [MWh]*	*Th demand [MWh]*	*CO_2 Emissions [ton]*	*Thermal dissipations [MWh]*
	304.22	304.33	149.14	408.07	0.00	-258.93
	On/Off	*O&M [€]*	*Fuel cons [ton]*	*Fuel Costs [€]*	*CO_2 costs [€]*	***Total costs [€]***
	0	3,650.7	17.43	37,298.0	0.0	**40,948.7**
ZG3	*El produced [MWh]*	*El demand [MWh]*	*Th produced [MWh]*	*Th demand [MWh]*	*CO_2 Emissions [ton]*	*Thermal dissipations [MWh]*
	364.50	361.66	177.34	485.04	0.00	-307.70
	On/Off	*O&M [€]*	*Fuel cons [ton]*	*Fuel Costs [€]*	*CO_2 costs [€]*	***Total costs [€]***
	25	4,374.0	20.97	44,878.0	0.0	**49,252.0**

Table 66 Warm ambient weekly costs per ZGs

Warm ambient (Weekly)						
ZG1	*El produced [MWh]*	*El demand [MWh]*	*Th produced [MWh]*	*Th demand [MWh]*	*CO_2 Emissions [ton]*	*Thermal dissipations [MWh]*
	186.85	187.14	76.50	195.73	0.00	-119.23
	On/Off	*O&M [€]*	*Fuel cons [ton]*	*Fuel Costs [€]*	*CO_2 costs [€]*	***Total costs [€]***
	0	2,242.2	10.01	21,426.6	0.0	**23,668.7**
ZG2	*El produced [MWh]*	*El demand [MWh]*	*Th produced [MWh]*	*Th demand [MWh]*	*CO_2 Emissions [ton]*	*Thermal dissipations [MWh]*
	322.72	322.84	160.09	337.65	0.00	-177.55
	On/Off	*O&M [€]*	*Fuel cons [ton]*	*Fuel Costs [€]*	*CO_2 costs [€]*	***Total costs [€]***
	4	3,872.6	18.46	39,502.6	0.0	**43,375.2**
ZG3	*El produced [MWh]*	*El demand [MWh]*	*Th produced [MWh]*	*Th demand [MWh]*	*CO_2 Emissions [ton]*	*Thermal dissipations [MWh]*
	383.56	383.66	168.39	401.32	0.00	-232.94
	On/Off	*O&M [€]*	*Fuel cons [ton]*	*Fuel Costs [€]*	*CO_2 costs [€]*	***Total costs [€]***
	12	4,602.8	20.98	44,898.8	0.0	**49,501.6**

The costs in Table 66 are significantly higher than those obtained for the cold scenario in Table 65. This result is due to the combination of two factors: the increase of the load (therefore of the consumption) and a decrease of the efficiency due to the off-design behaviour of the cell. It is necessary to consider how, at an economic level, in this phase, the influence of the ON/OFF is not calculated because already limited by the code and difficult to quantify numerically as the economic impact on the system even if it is an interesting data to report. The study done on a weekly basis is now extended to an annual basis, with the same assumptions made for the microturbine analysis. The number of weeks in which the vessel is estimated to be used in a year is 50 (25 for each scenario). A clear and immediate view of costs and consumption is given in a single table where data for the whole ship over the whole year are included (Table 67).

Table 67 Costs and fuel consumptions on a yearly basis for the whole cruise ship

Cruise Ship (Annual)						
El produced [MWh]	*El demand [MWh]*	*Th produced [MWh]*	*Th demand [MWh]*	*CO_2 Emissions [ton]*	*NOx Emissions [ton]*	*Thermal dissipations [MWh]*
43498.50	43400.50	20265.25	51605.75	0.00	0.98	-31,340.50
On/Off	*O&M [€]*	*Fuel cons [ton]*	*Fuel Costs [€]*	*CO_2 costs [€]*	*NOx costs [€]*	***Total costs [€]***
1025	521,985.0	2,446.00	5,234,365.0	0.0	0	**5,756,347.5**

.

From the data of Table 67, we have therefore a direct and global evaluation of the management costs of the system in the case of use of the technology with PEM Fuel Cells directly powered by hydrogen. It is immediate to notice how this configuration results to be therefore more expensive than the solution with microturbines. Also for the configuration with fuel cells with hydrogen stored directly on board it will be interesting to develop a more detailed economic analysis that takes into account the fixed costs, the useful life of the system and the various aspects of savings compared to the various technologies that will be studied in the following paragraphs. It will also be important to evaluate the advantages and disadvantages of the use of innovative technologies with respect to the state of the art and environmental regulations introduced.

3.1.4.3 Thermal management

As highlighted, the cogenerative application of fuel cells involves a thermal energy deficit compared to what is required. Therefore, in order to meet both requirements, it is necessary to introduce corrective measures. The most interesting appear to be:

- The introduction of a natural gas-fired boiler with the aim of covering the gap between demand and thermal energy production in the application case of Fuel Cells;
- A plant solution that we can call "hybrid": it provides for the equal division of the power size installed in each MVZ between mGT and PEM Fuel Cell. In this way it is possible to combine the thermal dissipations of the mGTs with the deficits of the PEMFCs, getting considerably closer to demand. For simplicity of on-board fuel management, it has been chosen to use LNG-fuelled PEMFCs, with the installation of a reforming system.

The integration of an **LNG-fuelled boiler** to produce the heat needed to meet the thermal demand logically leads to an increase in variable costs and emissions. In the application case of hydrogen-fueled PEMFCs, we obtain the annual values shown in Table 68 regarding the boiler integration based on what reported in [100].

Table 68 Boiler consumption, costs and emissions with PEMFC application

Boiler Data for PEMFC+LH_2 Application	
Annual LNG consumption [ton]	2,667
Annual LNG cost [€]	800,182
Annual CO_2 emissions [ton]	6,311
Annual Nox emissions [ton]	5

For what concerns the **<u>"hybrid" solution</u>**, as a reference only the simulations results for ZG 3 in a cold ambient are reported, since this condition represents the most difficult in terms of tracking both thermal and electrical demand. The size of the installed generation units is reported in detail in Figure 190.

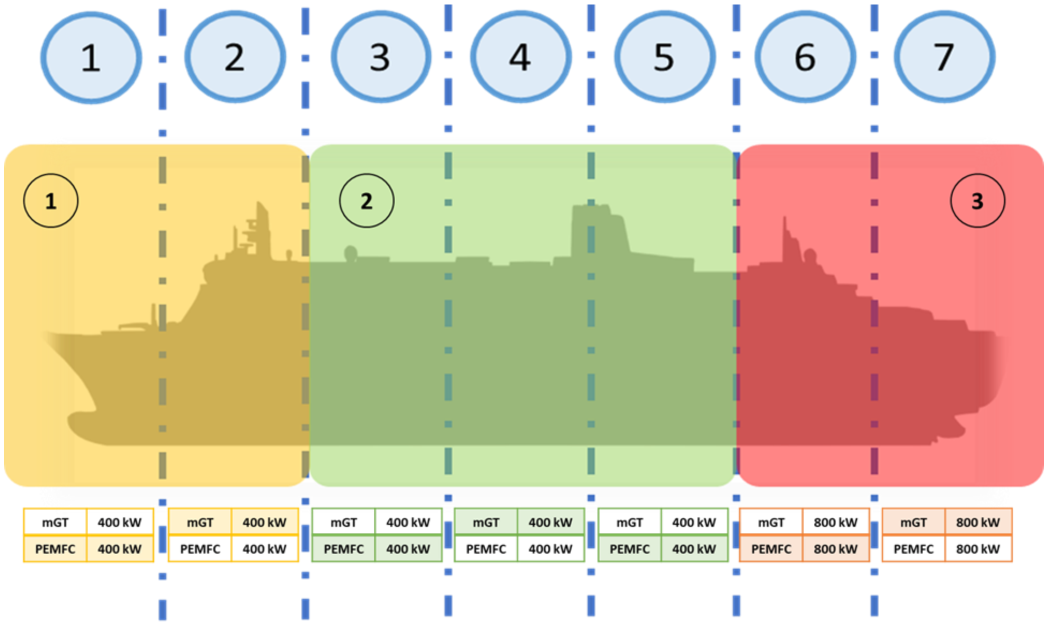

Figure 190 Hybrid solution layout

Table 69 reports the results of the simulation with W-ECoMP for ZG 3 in a cold ambient. From the charts included, it is possible to observe the supply of energy demands for the ZG 3 in a cold outdoor environment scenario (high thermal demand). It can be pointed out that the tracking of both loads is difficult to obtain even with hybrid configuration. This aspect can be explained by the fact that the size division between mGT and PEMFC is not sufficient to satisfy both energy demands, since from the thermal point of view the cells provide a much lower contribution than the microturbines. In order to obtain better coverage of the thermal demand, it will be necessary to consider a larger use of mGT instead of PEMFC (through a different distribution of the total size of each MVZ); however, this would lead to a decrease in system efficiency and consequently an increase in variable costs. When a more precise thermal load profile is available, it will be possible to consider the benefits and disadvantages of different size distribution between mGTs and PEMFCs. Finally, the possibility of filling the thermal gap with a boiler or a thermal recovery from the internal combustion engines (used for propulsion) should be considered.

Table 69 Electrical and thermal management of Hybrid solution in ZG 4 in cold ambient

MVZ 6-7 (ZG 3)

1

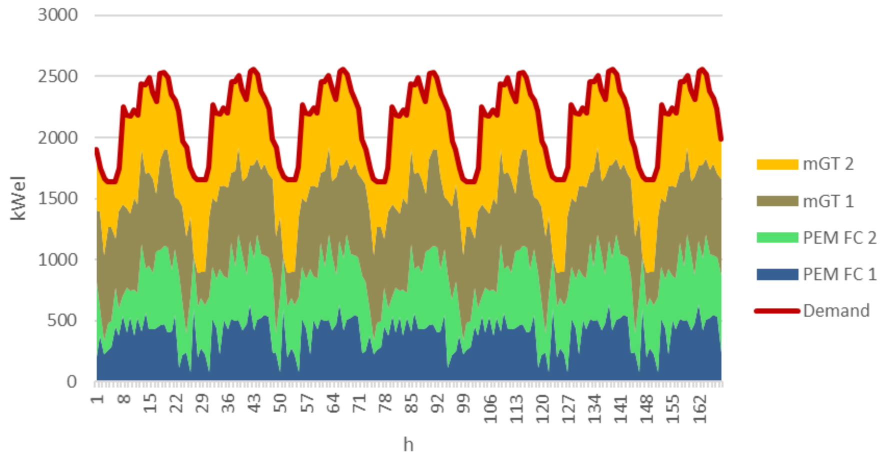

Figure 191 ZG 3 Electric management for hybrid solution in cold ambient

2

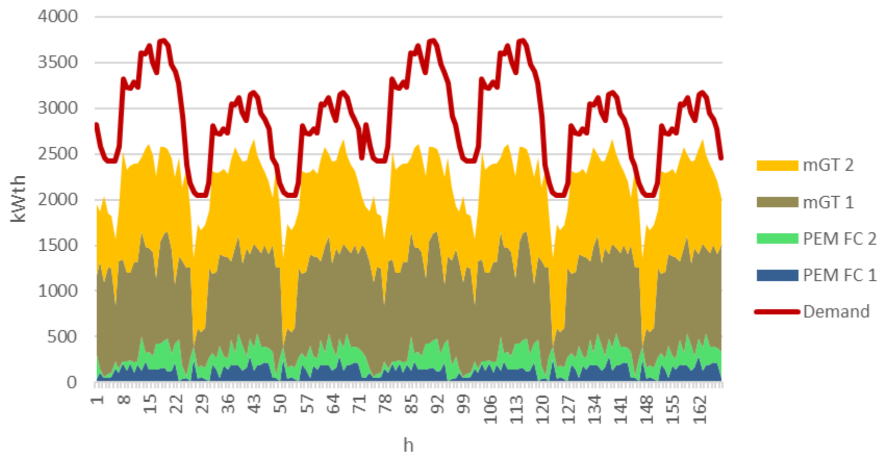

Figure 192 ZG 3 Thermal management for hybrid solution in cold ambient

Table 70 underlines how, in order to maximize the efficiency of the overall system and the tracking of both demands, the mGTs are used more than PEMFCs. It also worth remembering that, at maximum power, the mGTs have higher efficiency than PEMFCs (see Table 39).

In detail: working at partial load, the cell + reformer system can achieve significantly higher efficiencies than mGTs (visible in the charts for the efficiencies). On the contrary, the microturbines maximize their efficiency by working in nominal conditions. This aspect, therefore, implies a more intensive use of mGTs. Furthermore, taking into account the significantly high thermal efficiency of mGT compared to cells, it is necessary to use them intensively in order to maximize the thermal production to meet the demand.

Table 70 Partial Loads and efficiency for PEMFCs and mGTs in ZG 3, cold ambient

	MVZ 6-7 (ZG 3)
1	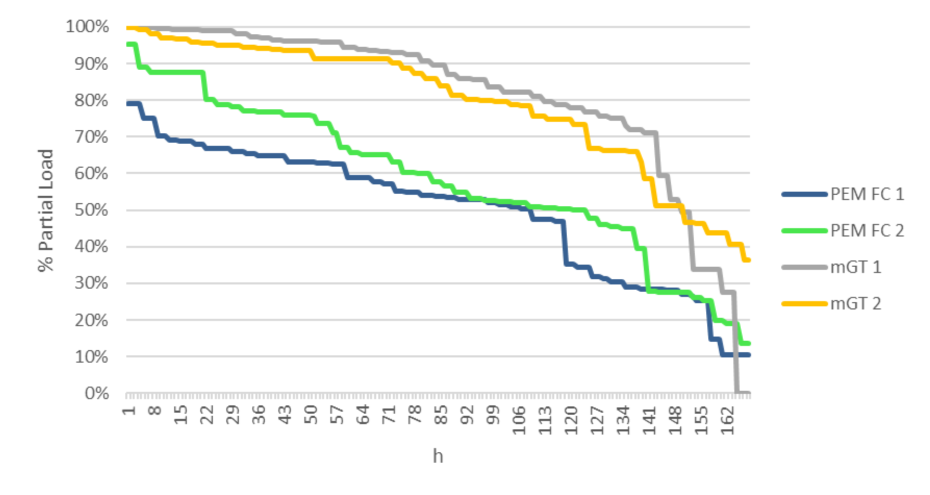
2	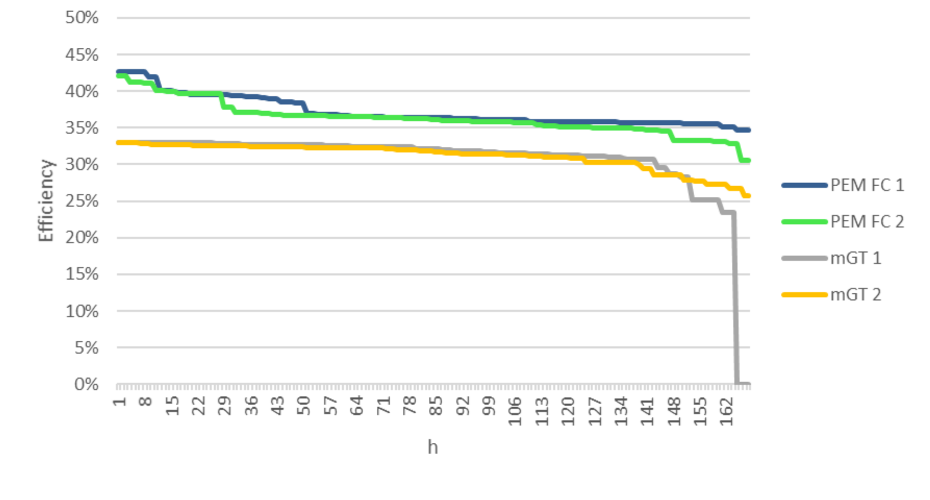

Moving to the economic aspects, overall consideration related to the whole cruise ship are provided in Table 71. It is, therefore, possible to see how the "hybrid" solution presents moderate total variable costs with annexed thermal deficits rather contained compared to what has been shown for only fuel cell configuration. In this sense, the application of this configuration to vessels that are used throughout the year in warm environments may be of interest (both demands could be satisfied). It would therefore be possible to exploit a technology that also foresees the use of fuel cells, which would make it possible to satisfy both energy requirements. In this case, the use of a single fuel already covered by international maritime regulations such as liquid natural gas is also contemplated.

Table 71 Costs and fuel consumptions on a yearly basis for the whole cruise ship, Hybrid solution

Overall Ship (Annual)						
El produced [MWh]	*El demand [MWh]*	*Th produced [MWh]*	*Th demand [MWh]*	*CO_2 Emissions [ton]*	*NOx Emissions [ton]*	*Thermal dissipations [MWh]*
43,386.89	43,401.29	44,626.75	51,609.15	27,605.63	5.54	-6,982.40
On/Off	*O&M [€]*	*Fuel cons [ton]*	*Fuel Costs [€]*	*CO_2 costs [€]*	*NOx costs [€]*	***Total costs [€]***
825	451,943	10,038	3,011,523	0	0	**3,463,467**

Considering the limited, but still present, thermal deficits, calculations related to the installation of a boiler are reported in Table 72.

Table 72 Boiler consumption, costs and emissions with Hybrid application

Boiler Data for Hybrid Application	
Annual LNG consumption [ton]	594
Annual LNG cost [€]	178,274
Annual CO_2 emissions [ton]	1,406
Annual Nox emissions [ton]	1

3.1.4.4 Final Considerations

After having analysed the different configurations in detail, we will now proceed with a more general view that will allow us to make a comparison between them in order to be able to evaluate which can be the best technology in consideration of the requirements of the scenario in which it is applied. Table 73 shows the most relevant data of the different configurations (in brackets the data including the use of the boiler). These values can be conveniently compared with the use of an internal combustion engine for marine application, fuelled by LNG, that satisfies the same electrical demand.

Table 73 Different technologies comparison (in brackets the data including the use of the boiler)

	mGT	PEMFC	PEMFC + mGTs	LNG Engine
LNG consumption [tons]	10,732	(2,667)	10,038 (10,632)	11,081
H_2 consumption [tons]	-	2,446	-	-
CO2 emissions [tons]	29,513	(6,311)	27,605 (29,011)	30,474
NOx emissions [tons]	9.57	0.98 (5.98)	5.54 (6.54)	43
Weight [tons]	771	1,642	915	-
Volume [m^3]	1,960	3,415	3,051	-

The use of hydrogen-fuelled PEMFCs guarantees almost zero emissions coupled with high efficiency, however, it requires high volumes and weights, as well as the management of liquid hydrogen on board ship. The configuration with micro-turbines, definitely more compact, can be interesting because it would allow a significant cogenerative contribution to the energy management of the ship. The "hybrid" application represents a compromise between the use emissions of a Fuel Cell with reformer (especially contained as regards NOx) and the limited overall dimensions of an mGT.

In order to compare numerically the different configurations studied in this chapter, a comparison is proposed in economic terms between the various solutions. To complete the analysis, the use of boilers will also be taken into account, where necessary, in order to satisfy the thermal demand. One of the main comparison parameters will therefore be the LCOE, already presented in the initial part of this chapter in the "full load" analysis, reported in Table 74.

Table 74 LCOE of the considered technologies

	mGT	PEMFC	PEM + mGT
LCOE [€/MWh]	101.70	286.68	187

Taking into account the considerations that have just been made from the point of view of emissions and overall dimensions, Table 74 allows highlighting the configuration with microturbines as the winning one in purely economic terms. The use of Fuel Cells involves an important economic impact on the system mainly linked to the capital cost of this technology and of the auxiliary aspects to its operation (Liquid Hydrogen). On the other hand, the so-called hybrid solution presents competitiveness from the economic point of view since it allows to lower the initial fixed costs with respect to the only PEMFC + reformer (halving the number of fuel cells and reformer) and at the same time decrease also the variable costs thanks to the higher global efficiency of the system with respect to the only mGT (since at partial loads the PEMFC + reformer system assumes higher efficiency than the mGT) annexed to the exclusive use of LNG.

In order to have a uniformity of conditions in the considerations, in this case, the value of LCOE for the time-varying case does not include the costs related to the use of the boiler; in fact, in the "steady-state" analysis these additional costs were not taken into account. Consider initially the configuration with mGT shown in Figure 193, it can be seen how the LCOE assumes a higher value in the case of time-varying use, i.e. with machines working at partial load.

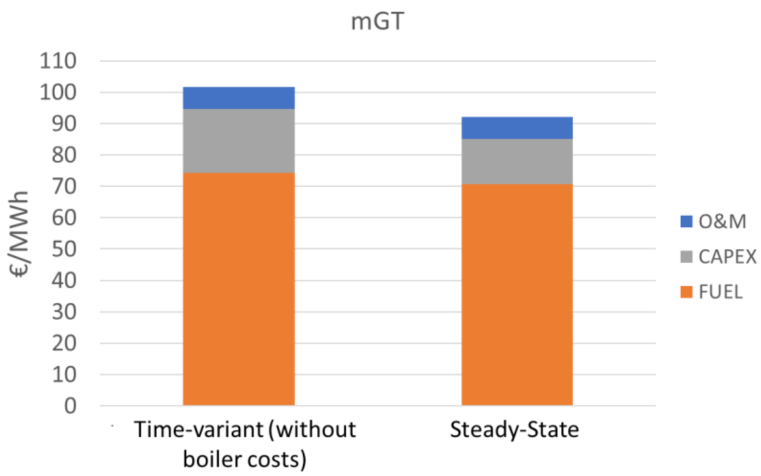

Figure 193 mGT LCOE comparison

Investigating the different components of the LCOE it is possible to highlight the fact that less intense use of the system (time-varying case) involves a greater impact of fixed costs (CAPEX); recalling also the characteristic curve of the microturbines, which provides a decrease in their efficiency at partial loads, it can be seen that even the component related to the cost of FUEL shows a slight increase in the time-varying case. On the other hand, the costs related to maintenance (O&M) maintain a constant weight on the LCOE since they are proportional to the energy produced by the system. It is interesting to note that the FUEL component is definitely preponderant compared to the others.
Then, the technological solution involving the direct use of hydrogen-fuelled PEMFCs is discussed. As previously highlighted, this solution has higher capital costs than the mGT, and high fuel costs due to the high cost of liquid hydrogen used as fuel. On the other hand, higher efficiencies and zero emissions can be obtained. Figure 8.105 shows the LCOE value in the two different scenarios considered.

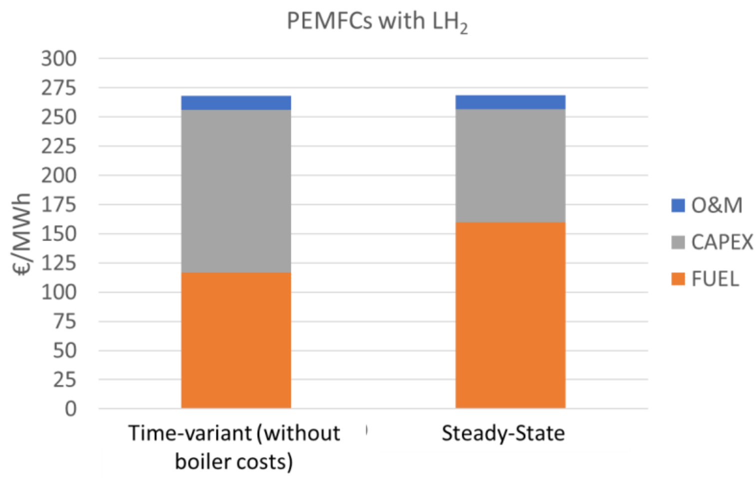

Figure 194 PEMFC LCOE comparison

It is clear, in comparison with the previous configuration, that this time the LCOE value remains substantially unchanged. In fact, in the time-varying case, despite the lower exploitation of the cell involves a greater influence of fixed costs on the LCOE, the possibility of working at higher efficiency allows a lower specific fuel consumption; therefore, the savings in economic terms is significant given the high cost of liquid hydrogen.

The work developed within the GEI project underlines that many simultaneous aspects could affect the choice of the best generation technologies to be installed on board in a maritime scenario. Indeed, this choice has to take into account economic aspects, volume and weights, and compliance with emissions regulation. Therefore, from this activity came out the idea to develop a comparison methodology that, using an immediate interface, is able to suggest the most promising generation technology for a considered scenario.

3.2 HELM Tool

To evaluate the general performances of different energy generation technologies on board ships, the software "HELM" (Helper for Energy Layouts for Maritime applications) has been specially developed. This program allows making a first assessment of the different technologies suitable for specific marine application.

Figure 195 HELM Logo

As highlighted from the activity developed within GEI Project, during the early stages of ship design, the choice of the best applicable technical solution is mainly influenced by weight, the volume occupied, cost and related pollutant emissions. The priority assigned to each of these performance parameters depends on the context in which the vessel is intended to operate.

With HELM software, it is possible to deal with this preliminary phase of analysis and comparison of different technical solutions. Among the strengths of the software are its user-friendly interface and the possibility of updating the data to technical innovations progressively introduced in the market. This program is designed to support the user in the preliminary stages of design, allowing to focus only on the technologies emerging as most promising for a more in-depth evaluation of the systems (e.g. time-transient behaviour). In this way it is then possible to save a huge amount of time, and also to address external users to the proper set of technology.

The core of the present software is a large database, which collects information on power units, fuels and storage systems, obtained through extensive market surveys and by the interaction with companies active in the maritime sector [101] [102].

The data put together in the database has been appropriately processed to create maps that allow the software to assign the values of weight, volume and cost corresponding to the system size, entered as input by the user. Emissions are calculated through maps dedicated to each technical solution; to access them, it is necessary to know the amount of fuel consumed or the power produced. Figure 196 shows an example of a map used to define the characteristics of fuel oil tanks: entering the abscissa with the required fuel capacity, the weight and dimensions of the storage units are obtained on the left ordinate axis, while the right ordinate axis provides the related cost.

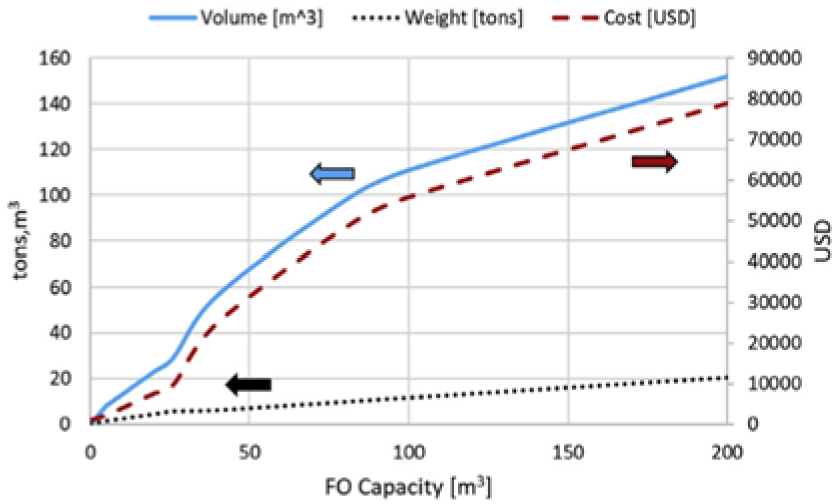

Figure 196 Fuel Oil Tank Map

It can be observed that the curves have different slopes as the fuel capacity varies; this is due to the use of different specific functions, extrapolated from data obtained from market analyses. In this case, three classes of storage units have been defined: the first for capacities below 5 cubic meters, the second for capacities between 5 and 20 cubic meters, and the third for capacities above 20 cubic meters.
The algorithm throughout the different values for each technology are calculated is reported schematically in Figure 197.

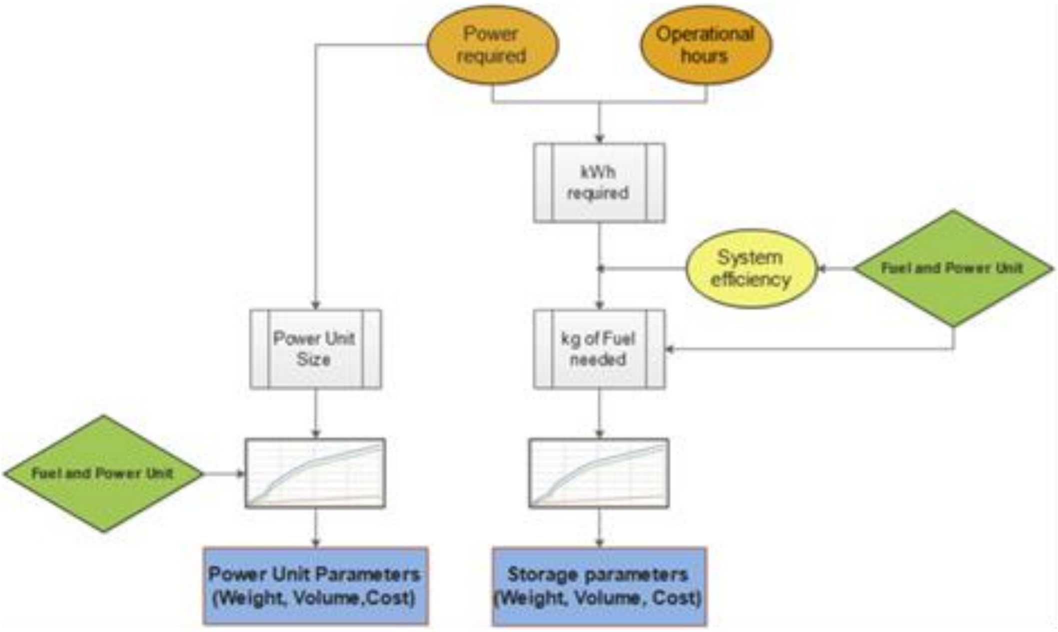

Figure 197 HELM Tool logical scheme

The main input data are the hours of non-stop navigation and the power required; in order to make a precautionary dimensioning, the maximum power required by the ship's operational profile is entered, even if the power actually delivered most of the time will be lower. The product of power required and operating hours returns the mechanical energy expended during navigation; dividing this value by the reference efficiency of the technical solution considered, the amount of energy required in the form of fuel is obtained, allowing access to maps to determine the costs, weights and dimensions of the storage units. The general parameters of the power unit are obtained by an immediate procedure since the size and costs can be obtained by entering the maps directly with the required power. This procedure is repeated for each technical solution implemented in the program.

In order to identify the best technical solution, the software assigns to each technology a score, which takes into account the performance in terms of weight, volume, cost and emissions: for each of these parameters (e.g. the total weight of the system), a score from 1 to 10 is assigned. The maximum score is given to the technical solution with the highest performance value (in the case of weight, therefore, the lightest system is assigned 10 points). The scores of the other technologies are assigned by comparison with the technology that has received the highest evaluation, referring to the parameter:

$$X_i = \frac{V_i}{V_{best}} \quad (33)$$

Where:

V_i is the value reported by the i-th technology (for a specific performance parameter, e.g. weight);

V_{best} is the value reported by the optimal solution (for a specific performance parameter, e.g. weight).

As an example, Figure 198 shows the range of Xi used to assign the points related to the evaluation of system performance in terms of weight.

Value	Score	Value	Score
$1 < X \leq 1.1$	10	$3 < X \leq 4$	5
$1.1 < X \leq 1.3$	9	$4 < X \leq 5$	4
$1.3 < X \leq 1.6$	8	$5 < X \leq 6$	3
$1.6 < X \leq 2$	7	$6 < X \leq 8$	2
$2 < X \leq 3$	6	$X > 8$	1

Figure 198 X_i Values for the weight performance parameter

Depending on the scenario considered for the considered vessel, it is possible to set a specific relevance to each one of the performance parameters (weight, volume, costs and emissions). This allows characterizing the result of the best solution specifically in the context assigned. For each performance parameters, it is possible to give relevance (R) between 1 and 5. The highest the value of the relevance for a performance parameter, the larger the priority given to this parameter during the evaluation process. Then the obtained total score, for the i-th technology is calculated as:

$$TotalScore^i = R_{weights} * Score^i_{weights} + R_{costs} * Score^i_{costs} + R_{emissions} * Score^i_{emissions} + R_{volumes} * Score^i_{volumes} \quad (34)$$

Generally, during the preliminary design phases of a vessel, the choice of the best applicable technical solution to produce energy onboard is mainly influenced by the weight, the volume occupied, the cost and the related pollutant emissions. The priority given to each of these performance parameters depends on the context in which the ship is to operate: if constant navigation in ECA zones is required, the environmental parameter will have a higher weight than the others; if, on the other hand, the ship is designed for the transport of goods, greater priority will be given to the compactness of the installed systems.

Furthermore, by selecting the ship size on the tool, it is also possible to consider if the volume and weights of the technology are feasible with the available size of the considered vessel.

All these mentioned aspects can be observed from the user interface reported in Figure 199.

Figure 199 HELM User interface

When the scenario in which the vessel operates is known, the user can enter the power required and the hours of navigation in the orange cells at the top right; the size of the vessel is taken into account by selecting one of the three options available: "Small", "Medium", "Large". If the resulting weights or volumes are not compliant with the available space on board, the relative cells are highlighted in red.

The software reports a default value for the efficiency of each system, equal to the average value obtained from market analysis; however, the user can modify the efficiency to obtain results comparable with the systems at his disposal.

At the bottom right, it is possible to assign to each of the performance parameters the respective relevance index, which depends on the scenario in which you want to conduct the simulation.

Clicking on "Calculate", the data processing begins, ending with the projection of the obtained results on the screen: for each technology, the required quantity of fuel (mass and volume), the general characteristics of the plant (weight, overall dimensions and costs) and the environmental performance (CO_2 and NOx emissions) are reported.

The score is then reported in the bottoming line as the main result. The technology with the highest score is then the most promising technologies for the energy generation on board of the considered vessel.

3.2.1 HELM Applications and studies

Once that the database and the code have been implemented in HELM, it allows performing easily many different studies related to a maritime application, considering different technologies. The easy user-interface gives the chance to create a strong interaction with the students, letting them the possibility to analyse independently some applications. Anyway, it is worth underlining that expert supervision in the use of this tool is needed. The choice of the relevance parameters and the system efficiencies requires experience in the energy and maritime fields.

3.2.1.1 Yacht application

The boat chosen to represent a small size case study is the Azimut Magellano 76 [103]. This yacht is 24 m length and 6.13 width with a total weight (full load) of 66 tons. The boat is equipped with two MAN V8 engines for a total power of 1470 kW and has a fuel tank capacity of 7500 L, therefore around 15 hours of navigation without docking can be estimated. In this scenario, the main relevance can be related to the chance to navigate wherever without any issues, especially in touristic zones (most of them are included in ECAs). Volumes represent another significant parameter in terms of comfort: small system volumes allow for larger space for services and rooms. Weights have a lower relevance, while costs are not really significant for yachts. HELM points out, with red coloured cells, that the use of PEMFC with compressed hydrogen and PEMFC metal hydrides are not feasible for the considered scenario, the first one in terms of volume and the second for the weights. Hence these solutions are omitted in the analysis.

The system efficiency for the PEMFC+LH_2 system has been set to a lower value (40%) than the other PEMFC application, (45%) in this way, the energy needed for keeping the tank at cryogenic temperature (-253 °C) is taken into proper account. The most performant solution suggested by HELM is the PEMFCs+LH2 one. The second acceptable solution is ICE+FO, which represents the state of the art. The use of LNG with mGTs or ICEs leads to worse overall scores. The main advantage given by the use of PEMFC is certainly its zero emissions, leading to great advantages in terms of free navigation areas. Moreover, storing H2 in a liquid form it is possible to minimize the system volumes and weights being quite competitive with the solutions with ICEs. The use of mGT in this application is less competitive because of large weights and volumes without significative emissions reduction. Indeed, in this scenario, the power units (high value for the required power and few operational hours) mainly affect the results. Considering this aspect, the mGTs are the power units with the highest volume and weight values. It is also possible to see how the use of LNG (especially with mGT) allows for very low values of NOx emissions. Comparing the ICEs solutions, the one with LNG has lower values for the emissions but, on the other hand, the LNG storage system has higher volumes and weights if compared with FO tanks. As predictable, PEMFCs have the highest costs, while the most developed technologies for maritime application (ICEs) have lower costs.

3.2.1.2 Hotel load ferry cruise ship

The ship considered for a large size case is the Viking Sky ferry built by Fincantieri [103]. This ferry has a length of 228 m and a moulded beam of 28.8 m with a total gross weight of 47800 tons. The ferry is equipped with two MAN 9L32/44CR engines and two MAN 12V32/44CR engines for a total installed electric power of 23.5 MW. The propulsion requests around 14.5 MW, hence it can be approximately considered that the electrical loads related to hotel services and supply systems have a peak value of 9 MW. The operational hours for this application can be assumed for about 24 hours. In this application, the innovative technologies (PEMFC, mGT and ICE) are considered only to cover the loads referred to hotel services and supply systems. This choice derives from the need for reducing pollutant emissions mainly in ports, during the docking period, when the propulsion load is zero. The ferry applications have different needs and requirements respect to the small/medium size case. In this context, emissions are still a significant parameter but not preponderant on volumes. Indeed, in ferry applications is extremely important to have most space as possible for rooms and for commercial onboard activities like restaurants and bars. Therefore, these two aspects are considered as the most relevant for this scenario. From an economic point of view, costs cannot be neglected, while weights do not significantly affect the choice of the best solution. The overall efficiencies for FC systems have been increased if compared with the small/medium case because the systems for this application are usually significantly oversized; therefore, fuel cells work mainly at partial loads, where their efficiency is higher (as highlighted during GEI Project activities). The simulation provided by the tool suggests LNG ICE as the best solution (total score 69): this is, in fact, the best compromise in terms of emissions, volumes and costs. All the studied technologies are feasible with the considered application even if the use of compressed H_2 and metal hydrides is not very competitive with the other technologies. PEMFC+LH_2 application (total score 67) is the best in terms of emissions without being significantly competitive in terms costs and volumes, while the use of ICE+FO (total score 64) is the most performant in terms of volumes, weights and costs but it is significantly penalized in terms of emissions. Using ICE+LNG it is possible to obtain a good compromise.

3.2.1.3 Kattamaram ferry boat

In this section, the case study considered is the Kattamaram passenger vessel [102]: the catamaran's length is about 35 m, with a capacity of 200 passengers and a cruising speed of 5.4 knots. Typically, the propulsion system for this kind of craft is an internal combustion engine, fuelled by Marine Gas Oil (MGO), with a total power of about 360 kW, this capacity is used as a reference. In this work, the choice is to give the highest priority to pollutant emission minimization since the application on a lake belongs to inland waters. Another relevant parameter is the volume minimization that guarantees more space for passengers and much higher profit for every single trip. The results obtained show how the PEMFC+LH_2 solution can be considered the most suitable for the application requirements. In fact, the use of PEMFCs guarantees no pollutant emissions; the hydrogen storage in a liquid form reduces volumes in a significant way if compared to the other hydrogen storage technologies (compressed hydrogen or metal hydrides). The second most competitive solution is the state-of-the-art one, with ICE fed by FO. This suggests how an improvement in the actual scenario is really challenging to reach. In fact, the “state-of-the-art” solution is intrinsically related to cost minimization, also guaranteeing very compact solutions specifically designed for naval applications. On the other hand, the penalizing parameter for this technology is pollutant emissions that will be more and more restricted in future by IMO rules.

The “state-of-the-art” solution leads to the highest score for what concerns costs, weight and volume minimization, while it is strongly penalised in terms of pollutant emissions. Focusing on PEMFC solutions, the use of LH2 guarantees space and weight improvement if compared with CH2 storage. Figure 200 shows how the choice of the relevant parameter related to pollutant emissions affects the total score results. Moving from the minimum value of 1 up to the maximum value of 5, it is possible to note that the PEMFCs’ application, at the present day, is the best solution only in scenarios characterized by a high priority in terms of pollutant emissions minimization. In other scenarios, the ICE + FO solution is the best one, since its clear advantages in terms of low costs, volumes and weights for the storage tanks.

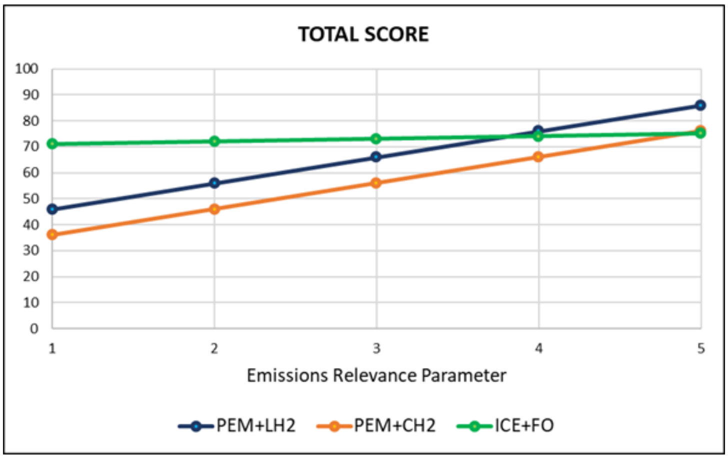

Figure 200 Impact of Emissions relevance parameter on the overall score for the main technologies

3.2.1.4 Modular storage system

In this study, the idea is to develop a low emission ship in compliance with the current normative for onboard energy generation, avoiding the refuelling process and its issues [104]. In order to reach this goal, the storages have to be placed inside standard containers in order to guarantee safe and easy operations during the substitution process. The empty storages will be re-filled in-land, respecting all the already existing normative, making them available for being used on the incoming ships. The considered ship for this application requires a power generation of 2 MW and an entire week period without docking. Considering the peculiarities of this application, the relevance parameters in HELM have been set in order to minimize costs and emissions, without neglecting the impact of volumes and weights. The state of the art (ICE+FO), in this scenario, represents the best solution nowadays. While the application of mGT and ICEs with LNG can be considered promising alternatives. Considering also the next future, with expected restrictions on pollutant emissions, it is worth to understand the potential of the studied technologies in this context. The scores detail shows that ICE+FO is the most compact and economic, while the PEMFC, and secondly the mGT, represent the most competitive solution from the environmental point of view. Among these, the PEMFC is strongly penalised by their high costs, while mGT is competitive also in economic terms. Therefore, it can be concluded that, for the cited application, mGT are the most interesting solution. Focusing on the application of this case study, the use of 40 ft containers for energy storages (internal volume of 66 m3) is considered. Table 75 shows the impact of this configuration on the system dimensions. The Ratio between the volume using containers and one of the storage system itself is also provided in the table.

Table 75 Containers for storage system

	PEMFC + LH2	mGT+LNG	ICE + LNG	ICE + FO
Storage system [m^3]	1116	284	267	121
N° of Containers	17	5	5	2
Containers [m^3]	1122	330	330	132
Ratio	1.00	1.16	1.24	1.01

It can be noticed that not a huge impact on the overall volumes can be expected by using containers for modular system storage. Only the LNG solutions, moving to the use of containers can have an increase of 16% or 24% in terms of overall volumes.

3.2.1.5 Use of innovative fuels onboard cruise ships

In this research work, innovative solutions, based on ammonia and methanol fuels, which are attracting research in these years [73] [74], have been implemented in HELM and investigated considering a specific maritime application [105].

Methanol (CH_3OH) is liquid at ambient pressure and temperature, making it much easier to manage and store onboard compared to gaseous fuels (i.e. H_2, CH_4), which require pressurization and/or refrigeration techniques in order to store it in liquid form. Methanol has the highest hydrogen to carbon (H/C) ratio among liquid fuels, thus allowing for a significant reduction in terms of CO_2; this aspect has recently attracted the attention for applications in the maritime sector. Furthermore, methanol does not present SOx emissions since it has not sulphur part in its composition. Methanol has a Lower Heating Value (LHV) and an energy density lower than traditional marine fuel oils (HFO and MGO): with the same energy required, the use of methanol needs a storage volume 2.5 times higher than the one for traditional marine fuels. This aspect is partially compensated by methanol high octane number, which allows for more complete combustion and higher efficiency. The retrofitting of infrastructure used for conventional marine fuels to methanol is possible with minor modifications. Recently, the Stena Germanica RoPax ferry was retrofitted to run its engines (24 MW) with a mix of 95% methanol and 5% MGO. The ship represents the world's first methanol powered ferry [106].

Ammonia (NH_3) is a chemical compound based on nitrogen and hydrogen, naturally present in vapour state at ambient pressure and temperature. It can be easily stored as a liquid in pressurized tanks at ambient temperature and modest pressure (10 bar) or at ambient pressure by refrigeration (-33 °C). The second solution is the most employed at an industrial scale, as it presents lower initial investments. Liquefied ammonia is an easy solution for transportation and storage, as it is not flammable, and it does not show a tendency to ignition. Ammonia has an LHV comparable to methanol and its volumetric energy density is lower than the one of traditional marine fuels: for the same amount of energy stored, NH_3 storage requires a space 2.5 times larger than HFO and MGO, which represent the state of the art.

NH_3 utilization is an interesting solution from the environmental standpoint, as it does not contain carbon, thus it presents zero CO_2 emissions in its combustion. Moreover, it does not present SOx, particulate matter and CO pollutant emissions. Ammonia is identified as one of the most interesting alternative fuels in a long-term scenario (2050) by IMO, as it would allow for reducing GHG emissions, as it is carbon-free. Although it has remarkable potential, its combustion in internal combustion engines needs an energy input for the ignition and heavy modifications to the engine. Furthermore, its combustion generates emissions in terms of NOx, therefore a system to manage the NOx is mandatory in order to respect the limits set by IMO. In the end, it is worth notice that Ammonia is a dangerous fuel for human health, therefore it has to be properly managed onboard and during the refuelling phases. The use of ammonia in ICE requires the presence of an ignition fuel; usually, hydrogen directly obtained from ammonia by installing a cracking unit. This aspect leads to additional volume, weights and costs in the application of NH_3 on board.

To define the data required as input by HELM, reference was made to the Costa Diadema, in navigation since October 2014. The ship is divided into 7 Main Vertical Zones (MVZ), i.e. vertical sectors designed to confine damage caused by accidents (e.g. flooding, fires) to the affected area only, safeguarding areas not affected. In order to size the generation system that takes charge of the hotel services demand, it is necessary to know the power loads: the power required by the Diadema during the day reaches 8.5 MW, while the annual average is 7.5 MW. As a precautionary measure, an installed capacity of 9 MW is considered, which guarantees the operation of the services even in the heaviest conditions, i.e. in the warmer season, when the power absorbed by the air conditioning systems is maximum. 30 hours of autonomy have been set. For what concerns the relevance of the performance parameters, taking into account the scenario of this application, the priority is given to volume and costs minimization despite the emissions.

The hotel load of the entire ship is served by a single, large plant, which is applied in a scenario where the volume and cost of the systems have a higher priority than the emissions.

In this work, the main goal has been to compare PEMFC applications with ICEs using different fuels. It is worth considering that the use of PEMFC with metal hydrides will be omitted in the next considerations since not compliant with the available volumes and weights for the vessel analysed.

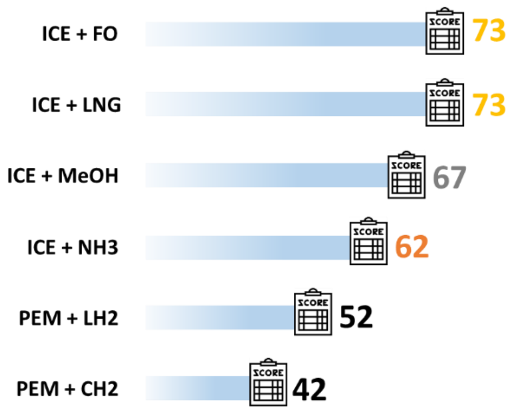

Figure 201 HELM resulting scores

Observing the scores, solutions with H_2 and fuel cells are quite far from endothermic engine solutions. The "ICE+FO" technology stands out due to its low weight, cost and volume. The "ICE+LNG" technology manages to compensate the lower score in volume and weight with better environmental performance, thus achieving the same score as the fuel oil engine.

The "ICE+MeOH" and "ICE+NH_3" innovative technologies are ranked second and third respectively. As mentioned, methanol and ammonia have low energy densities: for the same stored energy, the use of these fuels requires a higher storage volume than conventional marine fuel oils. For this reason, these two solutions obtain a low score for what concerns the volume. Methanol engines benefit from the low cost, similar to the cheapest solution ('ICE+FO'), while ammonia treatment section (cracking unit) has a negative impact on the investments required by the 'ICE+NH_3' technology, which receives a lower score in the 'cost' category.

Compared to conventional technology, the use of a methanol engine provides a modest reduction in carbon dioxide emissions, while NOx is significantly lower. The ammonia engine is disadvantaged by a high level of NOx emissions (equal to conventional marine fuel oils) but largely offsets this with zero CO_2 emissions.

The lowest scores are obtained by fuel cell technologies "PEM+LH_2" and "PEM+CH_2". The volume, weight and cost are greatly disadvantaged by the storage units used to store high-density hydrogen (by liquefaction at -253 °C in the first case, by pressurization up to 700 bar in the second). Fuel cells guarantee the zero-emission of pollutants, but this aspect is not very valued in the scenario considered, in which the most compact and convenient solutions are prioritized.

3.2.2 HELM in a maritime Distributed Generation application

In this section, HELM tool has been implemented to identify the best solutions applicable for supplying the hotel load of a cruise ship for the duration of the port stop. The hotel load includes passenger and crew services and auxiliary services on board and is connected to the low-voltage electric grid.

In order to define the data required as input by the program, reference was made to the "Costa Diadema" (Figure 202), belonging to the company Costa Crociere: launched on October 30, 2014, she was the flagship of the fleet until March 3, 2019, when she gave way to the more recent "Costa Venezia" [107].

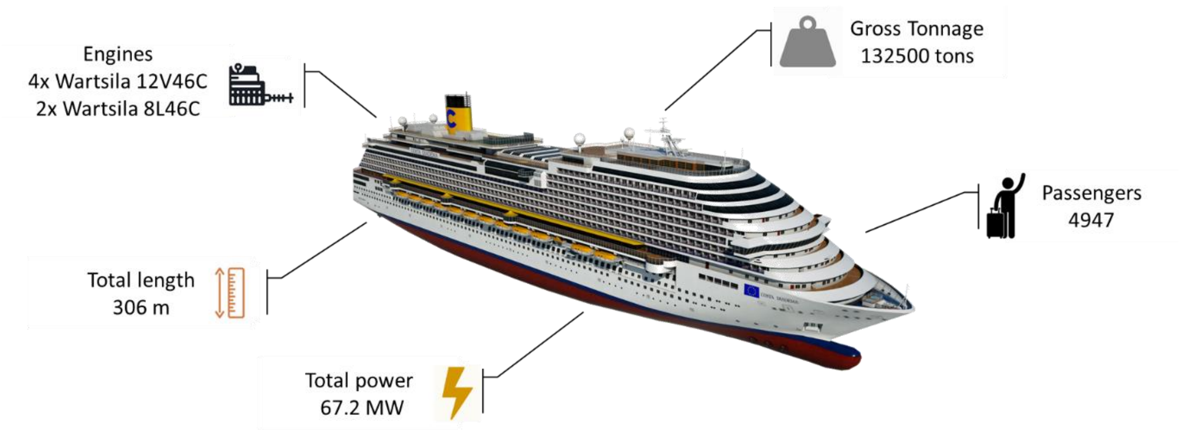

Figure 202 Costa Diadema main characteristics

The significative technical data referred to the considered vessel are reported in Table 76.

Table 76 Costa Diadema Technical Data

Gross Tonnage (GT)	132500
Deadweight (DWT) [t]	11118
Length over all [m]	306
Length between perpendiculars [m]	269,1
Molded breadth [m]	37,2
Persons onboard	6200
Passengers (max)	4947
Number of cabins	1862
Crew	1253
Max speed [knots]	22,5
Cruise speed [knots]	20
Engines (type, power)	4 x Wärtsilä 12V46C 2 x Wärtsila 8L46C
Generators total output [kW]	67200
Propulsion (machinery type)	diesel – electric
Power (propulsion, [kW])	42000
Propellers (number/type)	2 x fixed pitch
Bow/stern thrusters (number)	6

The vessel is structured in 7 Main Vertical Zones (MVZs), i.e. vertical sectors designed to confine damages due to possible accidents (e.g. flooding, fire) to the affected area only, safeguarding the uninvolved areas. In order to size the generation system that will take charge of the electrical demand of the hotel services, it is necessary to properly estimate the power required. Figure 203 shows that the power required by Diadema cruise ship during the day reaches over 8.5 MW.

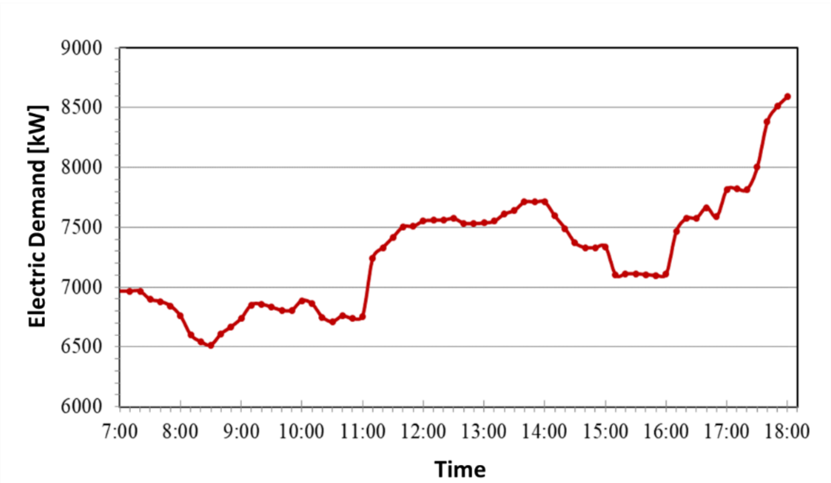

Figure 203 Hotel electrical load

As a precautionary measure, an installed power of 9 MW is considered, which guarantees the operation of services even in the most severe conditions, which can be reached, for example, in the hottest seasons, when most of the power is absorbed by the air conditioning systems. The average length of the stopover in ports is 12 hours, thus the installed systems must be able to supply the hotel load for 15 hours to be conservative. However, in order to guarantee autonomy for two stopovers, the sizing of the storage systems is carried out considering 30 hours of autonomy. For what concerns the relevance parameters definition the chosen values are here reported and motivated:

- Volume (3): for a cruise ship, it is preferable to use compact systems in order to maximize the space available for rooms and hotel services.
- Weight (1): since it is not a critical point for a vessel, its relevance is set to the lowest value. Furthermore, this value is somehow linked to the volumes, therefore giving a high value to this parameter it is possible to overestimate these aspects.
- Cost (3): in a commercial application, the limitations of cost is important in order to make feasible the investment and the management of a cruise ship.
- Emissions (4): considering a future scenario, where limitation of pollutant emission will represent a fundamental aspect, high priority is given to the reduction of pollutant emissions.

The technologies considered in this study are:

- **Fuel Cells:** the main FC application for the transport context is related to PEMFC technology directly fuelled by hydrogen. Two hydrogen storage systems are taken into account: LH_2 and CH_2. Furthermore, in this study, it is also considered the use of SOFC fuelled by LNG, even if this technology presents some drawbacks for transport application (i.e. low vibrations resistance due to the presence of ceramic material.
- **mGTs:** as emerged also from GEI project, the use of natural microturbine seems promising for maritime applications, especially in a mid-term scenario.
- **ICEs:** as state of the art and most employed technology in maritime applications, internal combustion engines cannot be neglected. Anyway, with the aim of minimizing the pollutant emissions of ICE applications, different fuels are considered (FO, LNG, MeOH and NH_3).

Figure 204 HELM screenshot with the implemented technologies

In order to better understand the impact of distributed generation, the evaluation has been carried out considering the two cases commented below:

- Case 1: the electrical demand of the hotel services is supplied by a single 9 MW plant;
- Case 2: each MVZ is equipped with a dedicated plant, with a size of 1.3 MW each (distributed electrical generation).

3.2.2.1 Case 1 Simulation and results

In this case, HELM is applied in order to perform the evaluation of a centralized generation unit with a size of 9 MW. In this scenario, the evaluation regards a centralized system installed on board. Once that the inputs have been properly implemented, the results of the comparison are computed by HELM and reported in Figure 205.

In the considered scenario, giving priority to the minimization of emissions, HELM tool suggests as most promising technology the use of PEMFC coupled with Liquid hydrogen storage. This solution is indeed related to zero emissions even if has some limitations concerning weights, volumes and costs (in particular due to the storage system). It is anyway worth considering the application of ICE+LNG that represents a more economical solution linked to limited pollutant emissions. Also in this case, even if more limited, some drawbacks in terms of volume and weights are present (mainly due to the LNG storage system) as reported in Figure 206. Below the two most promising technologies, it is possible to consider as intermediate solutions the use of ICE with different fuels (NH_3, MeOH and FO) or the application of mGT with LNG. The use of NH_3 is really performant in terms of CO_2 emissions, but the need for a cracking system leads to additional costs and volume if compared with the FO solution that is the most compact and economic but also affected by highest emissions. The use of MeOH is really competitive in terms of costs, but in terms of volume and weights, the lower energy density of MeOH respect to FO leads to lower scores.

Furthermore, the presence of NOx and CO_2 emissions, even if limited, slightly penalizes this solution.

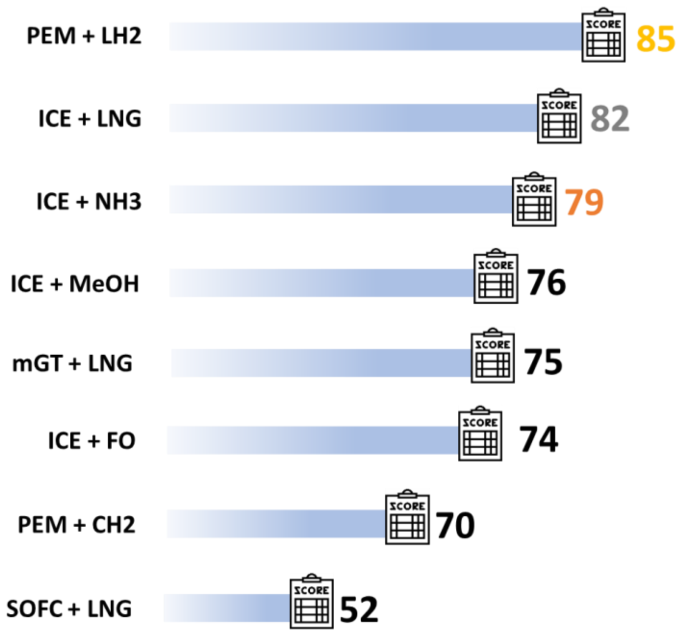

Figure 205 HELM Score results for Case 1

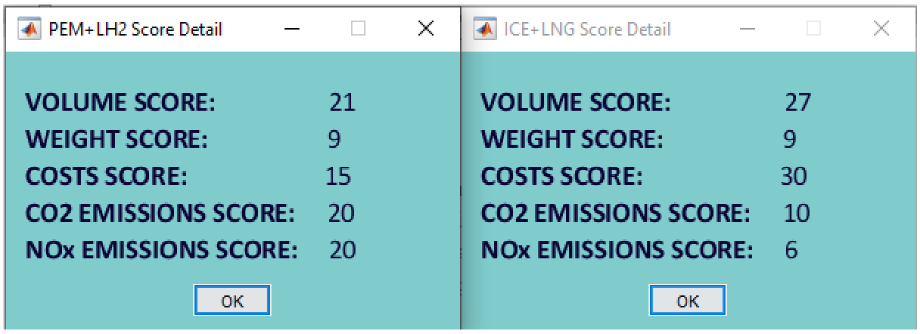

Figure 206 Score detail for PEM+LH2 and ICE+LNG solutions

In the end, the application of mGT is a really intermediate solution. In this sense, this solution is linked to rather limited emissions; while the mGT unit is compact but slightly costly (if compared to ICE). The presence of an LNG storage system, in addition, requires additional volumes and weights.

The solution of PEMFC+CH2 and SOFC+LNG are not significant for this application because of the huge storage volumes (CH_2) and the high technology costs (SOFC), as highlighted by the detailed results provided by HELM in Figure 207, where the SOFC solution is compared with the mGT one.

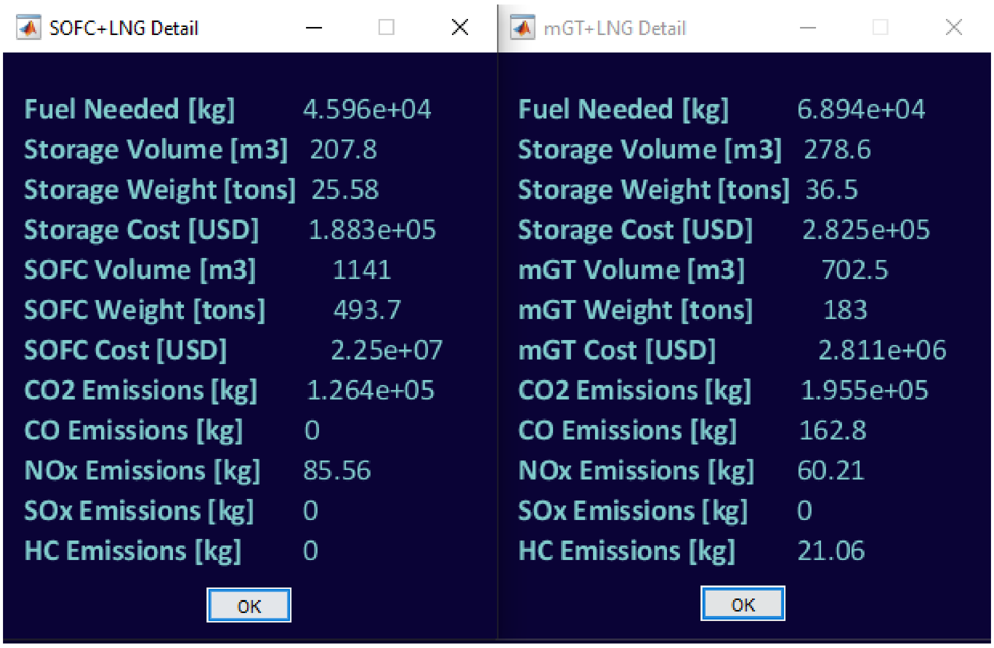

Figure 207 Detailed data for mGT and SOFC solutions

The higher system efficiency of SOFC (45%) respect to mGT (30%) leads to better storage system performances, since the same fuel is used. Anyway, moving to the power units, the mGT shows significant better performances in terms of volumes and weights. Considering the costs, SOFC appears still like a more prototypal solution; therefore, this technology can be considered as not already mature for a maritime application.

3.2.2.2 Case 2 Simulation and results

The second case is the real scope of this study: the development of a distributed generation scheme on board of a cruise ship, similarly to what has been presented in the GEI Project. Furthermore, this time, thanks to the use of HELM tool, there is the chance to evaluate and compare properly all the solutions taking into account all the main aspects with their respective relevance. As mentioned before, moving from a centralized scheme to a distributed one, the power installed decreases from 9 MW to 1.3 MW; while the relevance parameters remain the same as before. The results of the comparison provided by HELM are reported in Figure 208.

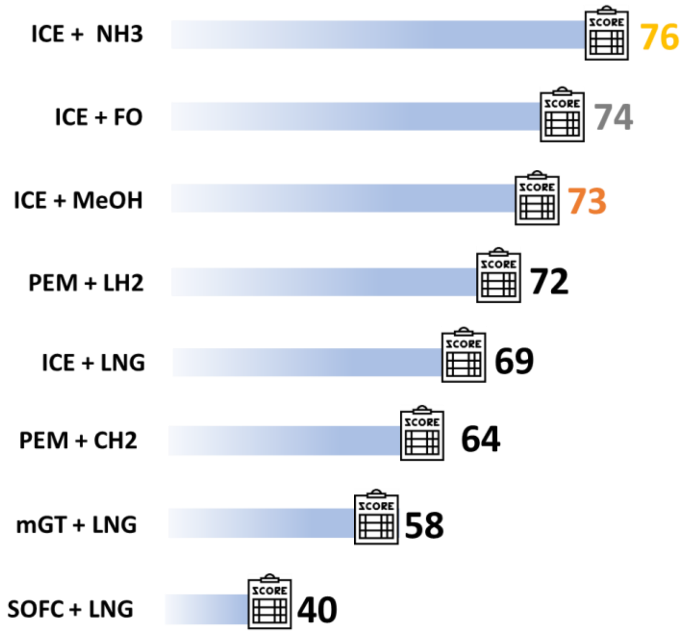

Figure 208 HELM score results for Case 2

It is worth noting that, moving from centralized to distributed generation, the cryogenic storages are strongly penalized respect to the other kind of storages. Therefore, this time, the solution suggested by HELM is the application of ICE with ammonia. This solution, indeed, allows to a promising CO_2 emissions reduction, without being strongly penalized by the storage system. The state-of-the-art technology (ICE+FO) is really performant in a distributed generation scenario, despite its high emissions, thanks to the well-proven technology that guarantees compact and economic solution at any scale. Anyway, methanol application and PEMFC+LH_2 are really competitive. The use of ICE+MeOH leads to a promising volumes and weights limitation linked to small emissions, furthermore this can be considered as a really economic solution. On the other hand, the use of PEMFC+ LH_2 owes its high score to its zero emissions, but it is penalized by costs and storage dimensions. Figure 209 confirms what has been stated in the previous lines. In particular, concerning volumes and weights, the ICE+FO solution gets the highest score; while the MeOH solution presents performant volumes even rather penalized by the lower energy density of methanol if compared with FO.

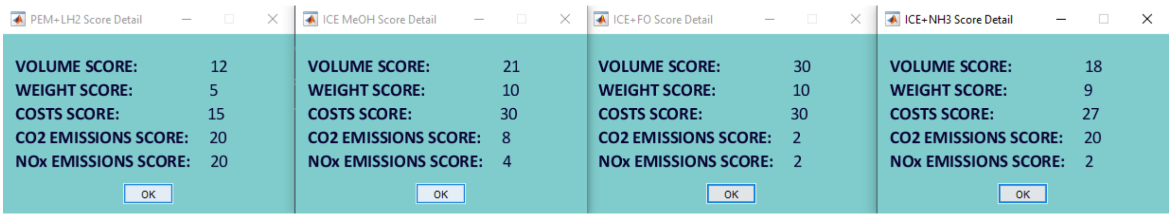

Figure 209 Case 2 Score detail for PEM+LH_2, ICE+MeOH, ICE+FO, ICE+NH_3

Considering the NH_3 solution, the performances are affected by the presence of the cracking system that leads to additional volume, weights and costs if compared to MeOH solution. The presence of the cracking system affects also the score related to costs, that for NH_3 solution is slightly lower than the similar technologies (ICE+MeOH and ICE+FO). As mentioned before, the solution with PEMFC+LH_2 does not present excellent performances in terms of weights and volumes (mainly due to the cryogenic storage system), and also the costs are quite high if compared with SoA solutions (mainly due to the PEMFC cost). Concerning the emissions, the PEMFC solution is obviously the best, since no emissions are observed. As mentioned, ICE+FO has the worst performances in terms of emissions, while the MeOH and NH_3 solutions are an intermediate solution. The latter one has zero CO_2 emissions but needs some treatment in order to reduce NOx emissions; MeOH on the other hand has no zero emissions, but both CO_2 and NOx emissions are limited.

For what concerns the LNG technologies it is worth considering more in detail the values reported in Figure 210.

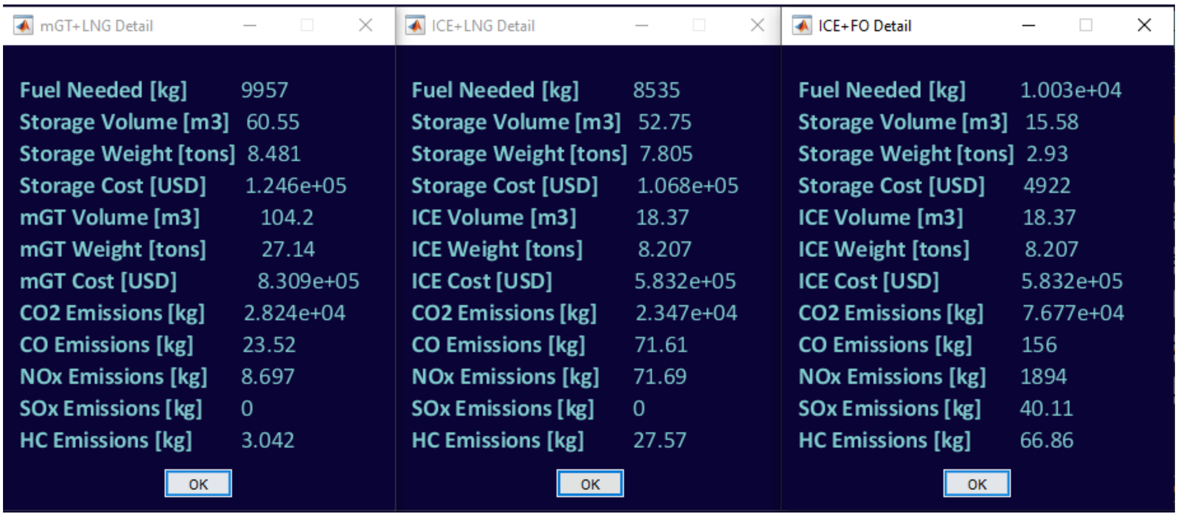

Figure 210 Details on the values provided by HELM for mGT+LNG, ICE+LNG, ICE+FO

Starting from a comparison between ICE+LNG and ICE+FO, considering that the power unit is the same in terms of volumes, weights and costs, it can be seen that the main difference between this technology is the storage system performances. The LNG tank indeed requires higher volume, costs and weights than the FO ones. From this aspect derives the main differences in terms of overall scores between the two technologies.

On the other hand, the mGT has similar values in terms of storage system compared to the ICE+LNG one; in fact, the storage system is the same. The most penalizing aspect for this technology is related to the generation unit. The mGT requires higher volumes, weights and costs if compared to ICE. In this aspect resides the low overall performances of this solution for the considered maritime application; on the other hand, in terms of emissions the presence of mGT is really competitive, especially for NOx.

In order to confirm the detailed values obtained using the database implemented in HELM tool, it is possible to compare the data of mGT reported in the GEI project detailed study with the one provided by HELM simulation. Table 77 collects the obtained results.

Table 77 HELM Database validation on GEI Data

	HELM result (1300 kW)	GEI analysis (800 kW)
Volume [m^3]	104.2	65.25
Weight [tons]	27.14	14.10
Cost [kUSD]	830	816

In accordance with what seen in the simulations, we can evidence that the motorization with natural gas is more suitable to the realization of centralized plant, promoted by the smaller total weight and from a considerable saving of space.

It can be observed that the distributed electric generation is always associated to greater investments, due to aspects such as the employment of a greater quantity of material, greater labour charges etc.

However, the advantages of distributed power generation should not be ignored, thanks to which (for instance) the problems caused by the failure of a single plant are limited.

The ICE+MeOH technology has obtained good results thanks to its reduced weight and cost. Moving on to a scenario focused on environmental performance, methanol motorization overcame the traditional solution, standing out for lower carbon dioxide and nitrogen oxide emissions. With distributed electric generation, the methanol engine becomes one of the solutions recommended by the software: already advantaged by its light weight, low cost and modest polluting emissions, this technology prevails over gaseous fuels (Hydrogen and Natural Gas) thanks to the greater ease of storage, which is not affected by the reduction in plant size.

From the results of the first simulation, it emerges that PEMFC+LH_2 and ICE+LNG powered solutions are preferable to the ammonia engine, whose environmental performance has limited relevance in the considered context.

Moving on to subsequent simulation, the ICE+NH_3 technology overcomes the other solutions, becoming the first technical solution recommended by the software in the case of distributed power generation. The strengths of the technology ICE+NH_3 are the relatively low weight, the competitive cost and the absence of CO_2 emissions, particularly appreciated in this mid/long-term scenario. In addition, it should be noted that ammonia, compared to other liquefied gaseous fuels, is easier to bring to a liquid state, as it is sufficient to reach -34 °C, compared to -166 °C in the case of LNG and -253 °C in the case of hydrogen.

In all the simulations, the fuel oil engine is shown to be the reference solution for weight, volume and low cost. The higher priority currently given to these aspects is the reason why this technology remains the most applied solution today. However, as environmental awareness becomes more prevalent, it will be complicated for this powertrain to meet the increasingly stringent emissions regulations expected in the future, as shown in Figure 205.The only solution to justify a future application of fuel oil engines is the one related to distributed generation on board, that with a proper management could guarantee and increase of the overall system efficiency (as demonstrated in GEI project).

Fuel cell technologies fail to compete with endothermic engine solutions in a current scenario, where greater priority is given to compactness and system cost. The metric used in this study values the complete absence of polluting emissions guaranteed by fuel cells, which therefore manage to obtain promising scores. The PEM+LH_2 solution, in particular, succeeds in containing the overall dimensions and weights of its storage units, managing to compete with endothermic engine technologies both in the case of a single plant and in the case of distributed electricity generation. Considering the strong modularity of PEMFC technology, it can be observed that, apart from the difference in the investments required, the performances offered by the technology PEM+LH_2 do not change passing from the single plant to the distributed electric generation system. It is worth noting, however, that the power typically delivered by fuel cells requires to employ several units to reach the centralized power of 9 MW (since that currently there are no systems available larger than 1 MW), so it could be more convenient to collect the entire plant in a single electrical generation system, avoiding the installation of a dedicated voluminous cryogenic unit in each MVZ.

4 Conclusions

In this work, it has been analysed in detail the use of micro Gas Turbines in distributed generation. As an introduction it has been necessary to describe the current regulation, constraints and incentives that distributed generation has to face with a particular focus on the Italian scenario, that reports European directives on the Italian territory. A particular focus on the most employed or promising technologies has been also developed, focusing in particular on the micro Gas Turbines benefits and drawbacks. This technology is in fact, in this work, investigated in two different innovative scenarios: a residential and a maritime one.

The residential application takes place within the H2020 project ENVISION, that aims to accelerate the development of Zero or Positive Energy Building and to test its integration in a Distributed Generation Network. The first step has been, therefore, to properly design the system that will be tested in Savona Campus, where a mGT will be installed together with an HP supplied by façade thermal solar panels. The choice of Savona Campus allows, indeed, to interact with the Smart Poly-generation Microgrid present in this venue of the University of Genoa. The preliminary evaluations led to the definition of system size, giving the input for a market investigation with the aim of purchasing the necessary elements to prepare the Savona demo site. In parallel, it has been necessary to develop models of the components involved in the Savona Demo with the aim of optimizing the system configuration in a general context. Then, once the optimized layout of the demo site has been decided, proper management of the system, on a district scale, has to be developed. To do that, in order to provide general best practices of system management, different simulations have been done using the optimization software (W-ECoMP) developed by the author's research group. In the end, based on these guidelines and the developed models, a Model Predictive Control has been implemented. It is worth considering that these analyses will have a complete validation of the results once that the experimental campaign will be developed at Savona Campus. Unfortunately, due to COVID-19 pandemic, this experimental campaign has been postponed to the second half of 2021.

Considering the obtained results, the demo site consists of:

- 100 m^2 of façade solar thermal panels, for a thermal power of around 20 kW
- 10 kWe Heat Pump, using as a working fluid R134a since that the required temperature allows the use of standard fluids
- 100 kWe micro Gas Turbine, in a CHP configuration able to produce also 150 kWth
- 500 l Thermal Energy Storage

For what concerns the economic consideration, the cost related to the electricity consumptions of the HP is the most relevant. In parallel, the cost of solar façade panels has to decrease in order to make the ENVISION technology package a promising solution also under the economical point of view. Anyway, in order to maximize the overall system performances, it is necessary to maximize the façade surface involved in panels installation. The management strategy confirms that the presence of thermal storage is necessary in order to guarantee proper tracking of both thermal and electric demands. Furthermore, the calculations suggest the use of seasonal thermal storage in order to maximize the overall efficiency of the system. The economic aspect, calculated in terms of LCOE, suggests that the definition of the mGT size has to be precisely designed in order to maximize its exploitation during the overall system operation since the mGT represents the major voice of costs. In order to guarantee proper management of the system and advanced MPC has to be implemented in order to take into account both energetic and economic aspects. The architecture of control, developed in Matlab Simulink ambient, will be tested and tuned during the experimental campaign. It is worth noting that, a preliminary test campaign has been already performed in order to evaluate the impact of insulation in the back of a panel in order to avoid dissipation, despite decreasing the possibility to use the thermal panels as an external ambient heat exchanger. The results obtained confirm that it will be promising the provision of proper insulation in the back of the panel.

An innovative application of distributed generation has been considered for maritime application, in particular on board of cruise ship in order to supply the hotel loads, within the context of GEI project in collaboration with Fincantieri and CNR.
Moving to the maritime application, the choice of the most promising technology has to consider also aspects related to volumes and weight, in addition to the common energetic and economic evaluation. A detailed analysis has been performed with the aim of evaluating, among different technologies (such as mGT), which can be the most interesting for a distributed generation application on board of cruise ship. After a preliminary comparison, a detailed analysis has been performed in a time-dependent analysis that highlights the good performances of PEMFC in partial load.
From GEI project it has been deduced the necessity of developing a comparison tool able to consider the different priority to be given to economic, environmental and volume aspects. HELM tool aims to cover this necessity, on activities that are getting more and more interesting in the maritime sector. A description of the tool is developed, and then some case studies are cited.
A particular focus is given to the study of a distributed generation application, in comparison with the same power supply in a centralized configuration.
Among the considered technologies for power generation on board, in order to be compliant with future emissions restrictions, the most promising solutions are represented by innovative fuels with internal combustion engines and PEMFC application with Liquid Hydrogen Storage. In this context, the use of micro Gas Turbine is quite penalized by the need of Liquid Natural Gas Storage.

Considering the interesting in the use of PEMFC in maritime applications, more detailed studies have been performed in research projects for Fincantieri. The main aim of these activities is to study the dynamics related to hydrogen and oxygen supply to the fuel cell system in order to avoid issues on the delicate operation of the PEMFC. The results related to these activities are not included in this work, since represents a trade secret of Fincantieri included in its intellectual property.

The presented study can represent a basis for the development on field of DG technologies, testing the real benefits of the proposed management strategies. In particular, for what concerns ENVISION project, the designed plant will be implemented and tested also under the management rules suggested in this work. Evaluating the most relevant Key Performance Parameters (KPIs) of the system over a yearly basis, it will be then possible to understand the benefits (economic and environmental) given by both technologies and management strategies. It is worth noting that the proposed methodology has a general value. Modifying the boundary conditions (ambient conditions and energy demands), it will be possible to perform the proposed methodology in different scenarios, using the same models. This last aspect could be promising when considering the potential of the technology in different geographic locations.

Furthermore, the study performed within the maritime sector reports relevant and significant results towards the reduction of onboard emissions. The presented study within GEI project has been used by Fincantieri as a milestone in order to understand which are actually the technologies that worth effort for being used on board of cruise ship. The next step will consider a detailed analysis of these relevant technologies. Some of these studies have been already performed by the author inside studies funded by Italian Navy and, therefore, the obtained results can not be published.

On the other hand, the presented tool HELM, developed by the author, gives the possibility to exploit relevant results on a wide scale, involving many stakeholders. Using HELM, it is then possible to evaluate many different technologies in various applications in a short time. HELM can be easily enhanced including additional technologies or updating the database. One of the most relevant enhancements that will be done in the future is the introduction of batteries in stand-alone mode or coupled with Fuel Cell.

Concluding, the ambition of this work has been to demonstrate the main constrains and potentialities of innovative technologies in both residential and maritime sector, describing which can be the most promising technologies and the best way to manage it on order to satisfy the energetic loads reducing operational costs and emissions.

5 References

[1] "Share of renewables in power generation in the Sustainable Development Scenario, 2000-2030 – Charts – Data & Statistics - IEA." https://www.iea.org/data-and-statistics/charts/share-of-renewables-in-power-generation-in-the-sustainable-development-scenario-2000-2030 (accessed Nov. 23, 2020).

[2] "Renewable power generation by technology in the Sustainable Development Scenario, 2000-2030 – Charts – Data & Statistics - IEA." https://www.iea.org/data-and-statistics/charts/renewable-power-generation-by-technology-in-the-sustainable-development-scenario-2000-2030 (accessed Nov. 23, 2020).

[3] I. J. Pérez-Arriaga, "The Transmission of the Future," *IEEE Power and Energy Magazine*, pp. 41–53, 2016.

[4] Sweco, "Study on the effective integration of Distributed Energy Resources for providing flexibility to the electricity system," no. April, 2015.

[5] M. G. Prina, D. Moser, U. Filippi, R. Vaccaro, and M. Gazzani, “Economic and environmental impact of photovoltaic and wind energy high penetration towards the achievement of the Italian 20-20-20 targets,” 2015.

[6] G. Terna, “Dati provvisori di esercizio del sistema elettrico nazionale 2017,” 2018.

[7] Ministero dello Sviluppo Economico, Ministero dell’Ambiente e della Tutela del Territorio e del Mare, and Ministero delle Infrastrutture e dei Trasporti., “Piano Nazionale Integrato per l’Energia e il Clima,” 2019, [Online]. Available: https://www.mise.gov.it/images/stories/documenti/PNIEC_finale_17012020.pdf.

[8] MISE and MATTM, “Strategia Energetica Nazionale (SEN), 2017,” *Mise; Mattm*, no. 10 November 2017, pp. 1–308, 2017.

[9] Italian Legislative Decree n.28., “Implementazione Direttiva europea 2009/28/EC su l’energia rinnovabile.” 2011, [Online]. Available: https://www.gse.it/documenti_site/Documenti GSE/Servizi per te/CONTO ENERGIA/Normativa/_D.LGS+03032011+N.+28.PDF.

[10] “Gazzetta Ufficiale.” https://www.gazzettaufficiale.it/eli/id/2019/04/30/19G00043/sg (accessed Nov. 23, 2020).

[11] RSE, “A snapshot of smart grids achievements in Italy,” 2014, [Online]. Available: http://www.rse-web.it/notizie/cloneIn-sintesi-il-punto-di-RSE-sulle-reti-intelligenti.page.

[12] “Gazzetta Ufficiale.” https://www.gazzettaufficiale.it/eli/id/2014/12/29/14G00203/sg (accessed Nov. 23, 2020).

[13] “Decreto legislativo numero 257 del 16/12/2016 | mit.” https://www.mit.gov.it/normativa/decreto-legislativo-numero-257-del-16122016 (accessed Nov. 23, 2020).

[14] F. Luiso, “La normativa nazionale per le smart grid,” 2017.

[15] M. Valenti, M. di Somma, and G. Graditi, “LINEE GUIDA TECNICHE SUL QUADRO REGOLATORIO E NORMATIVO DELLE SMART GRID,” 2019.

[16] “GUIDA TECNICA SUI SISTEMI DI ACCUMULO CONNESSI ALLA RETE ELETTRICA DI DISTRIBUZIONE.” Accessed: Nov. 24, 2020. [Online].

[17] “DELIBERAZIONE 18 DICEMBRE 2014 642/2014/R/EEL.” https://www.arera.it/allegati/docs/14/642-14.pdf (accessed Nov. 24, 2020).

[18] A. Galliani, “Evoluzione del mix produttivo di energia elettrica e suoi effetti sul sistema Ripasso di elementi attinenti al funzionamento dei mercati elettrici,” pp. 1–50, 2018.

[19] “DELIBERAZIONE 5 MAGGIO 2017 300/2017/R/EEL PRIMA APERTURA DEL MERCATO PER IL SERVIZIO DI DISPACCIAMENTO (MSD) ALLA DOMANDA ELETTRICA ED ALLE UNITÀ DI PRODUZIONE ANCHE DA FONTI RINNOVABILI NON GIÀ ABILITATE NONCHÉ AI SISTEMI DI ACCUMULO. ISTITUZIONE DI PRO.” Accessed: Nov. 24, 2020. [Online].

[20] A. Galliani, “Evoluzione delle modalità di approvvigionamento delle risorse necessarie per i servizi ancillari,” pp. 1–42, 2020.

[21] "The coronavirus crisis reminds us that electricity is more indispensable than ever – Analysis - IEA." https://www.iea.org/commentaries/the-coronavirus-crisis-reminds-us-that-electricity-is-more-indispensable-than-ever (accessed Nov. 24, 2020).

[22] I. Benoit, "DISTRIBUTED GENERATION : DEFINITION , BENEFITS AND ISSUES Pepermans G ., Driesen J ., Haeseldonckx D ., D ' haeseleer W ., Belmans R . secretariat : DISTRIBUTED GENERATION : DEFINITION , BENEFITS AND ISSUES," *Energy*, vol. 32, no. 0, pp. 0–21, 2003.

[23] "DIRETTIVA 2009/72/CE." https://eur-lex.europa.eu/legal-content/IT/TXT/PDF/?uri=CELEX:32009L0072&from=EN (accessed Jan. 15, 2021).

[24] "Distributed Generation of Electricity and its Environmental Impacts | Energy and the Environment | US EPA." https://www.epa.gov/energy/distributed-generation-electricity-and-its-environmental-impacts (accessed Nov. 24, 2020).

[25] E. F. El-Saadany, H. H. Zeineldin, and A. H. Al-Badi, "Distributed Generation : Benefits and Challenges," *International Conference on Communication, Computer & Power*, pp. 115–119, 2007.

[26] Terna s.p.a, "Contesto ed evoluzione del sistema elettrico," pp. 42–45, 2019.

[27] W. El-Khattam and M. M. A. Salama, "Distributed generation technologies, definitions and benefits," *Electric Power Systems Research*, vol. 71, no. 2, pp. 119–128, 2004, doi: 10.1016/j.epsr.2004.01.006.

[28] A. Poullikkas, "Implementation of distributed generation technologies in isolated power systems," *Renewable and Sustainable Energy Reviews*, vol. 11, no. 1, pp. 30–56, 2007, doi: 10.1016/j.rser.2006.01.006.

[29] T. Phelps, S. David Wrightsman, and B. Development Manager, "INTERNAL COMBUSTION ENGINES Combined Heat and Power," 2017. Accessed: Dec. 01, 2020. [Online].

[30] M. A. R. do Nascimento, L. D. O. Rodrigues, E. E. B. G. E. C. Dos Santos, F. L. G. Dias, E. I. G. Velásques, and R. a. M. Carrillo, "Micro Gas Turbine Engine: A Review," *Progress in Gas Turbine Performance*, no. June 2019, pp. 108–142, 2013.

[31] "Model-Based Control of Micro Gas Turbines – Institute for Dynamic Systems and Control | ETH Zurich." https://idsc.ethz.ch/research-guzzella-onder/research-projects/ProjectArchive/micro-gas-turbine.html (accessed Dec. 02, 2020).

[32] "New Energy Outlook 2020 | BloombergNEF." https://about.bnef.com/new-energy-outlook/ (accessed Dec. 02, 2020).

[33] L. van Biert, M. Godjevac, K. Visser, and P. v. Aravind, "A review of fuel cell systems for maritime applications," *Journal of Power Sources*, vol. 327, no. X, pp. 345–364, 2016, doi: 10.1016/j.jpowsour.2016.07.007.

[34] M. Rivarolo, D. Rattazzi, T. Lamberti, and L. Magistri, "Clean energy production by PEM fuel cells on tourist ships: A time-dependent analysis," *International Journal of Hydrogen Energy*, vol. 45, no. 47, pp. 25747–25757, 2020, doi: 10.1016/j.ijhydene.2019.12.086.

[35] M. Ronchetti, “Ente per le Nuove tecnologie, l’Energia e l’Ambiente CELLE A COMBUSTIBILE Stato di sviluppo e prospettive della tecnologia.” Accessed: Dec. 03, 2020. [Online].

[36] R. E. Rosli *et al.*, “A review of high-temperature proton exchange membrane fuel cell (HT-PEMFC) system,” *International Journal of Hydrogen Energy*, vol. 42, no. 14, pp. 9293–9314, Apr. 2017, doi: 10.1016/j.ijhydene.2016.06.211.

[37] “Market Review of Energy Storage Systems.” https://www.victanis.com/market-review-of-energy-storage-systems (accessed Dec. 03, 2020).

[38] S. Al-Thyabat, T. Nakamura, E. Shibata, and A. Iizuka, “Adaptation of minerals processing operations for lithium-ion (LiBs) and nickel metal hydride (NiMH) batteries recycling: Critical review,” *Minerals Engineering*, vol. 45, pp. 4–17, Mar. 2013, doi: 10.1016/j.mineng.2012.12.005.

[39] G. Fitzgerald, C. Nelder, J. Newcomb, J. Lazar, R. A. Project, and R. Allen, “ELECTRIC VEHICLES AS DISTRIBUTED ENERGY RESOURCES ELECTRIC VEHICLES AS DISTRIBUTED ENERGY RESOURCES | 2 AUTHORS ADDITIONAL CONTRIBUTORS SUGGESTED CITATION.” Accessed: Dec. 03, 2020. [Online]. Available: http://www.rmi.org/pdf_evs_as_DERs.

[40] “Data & Statistics - IEA.” https://www.iea.org/data-and-statistics?country=WORLD&fuel=Energy%20consumption&indicator=TFCShareBySector (accessed Jan. 18, 2021).

[41] “ENERGY-EFFICIENT BUILDINGS PPP MULTI-ANNUAL ROADMAP AND LONGER TERM STRATEGY.” Accessed: Dec. 04, 2020. [Online]. Available: http://ec.europa.eu/research/research-eu.

[42] C. F. O. R. E. Buildings, “Horizon 2020 Call : H2020-EEB-2016-2017 (CALL FOR ENERGY-EFFICIENT BUILDINGS) Topic : EEB-03-2016 Type of action : IA (Innovation action) Proposal number : 723562 Proposal acronym : THERMOSS Deadline Id : H2020-EEB-2016 Table of contents,” 2017.

[43] A. N. Traverso, “Comparison of different approaches for control and optimization systems of a cogenerative microgrid,” *PhD Thesis*, no. February 2015, p. 31, 2014.

[44] S. J. Rees, “An introduction to ground-source heat pump technology,” in *Advances in Ground-Source Heat Pump Systems*, Elsevier Inc., 2016, pp. 2–25.

[45] Y. Bulut, “Performance Assessment of Colored Façade Integrated Solar Collectors and Numerical Analysis of Solar Collector- Heat Pump System with TRNSYS Performance Assessment of Colored Façade Integrated Solar Collectors and Numerical Analysis of Solar Collector-Hea.”

[46] G. F. Frate, L. Ferrari, and U. Desideri, “Analysis of suitability ranges of high temperature heat pump working fluids,” *Applied Thermal Engineering*, vol. 150, no. January, pp. 628–640, 2019, doi: 10.1016/j.applthermaleng.2019.01.034.

[47] “REFPROP | NIST.” https://www.nist.gov/srd/refprop (accessed Dec. 10, 2020).

[48] F. J. Lorenzini, “Model Predictive Control of a real cogenerative system with energy storage,” 2018.

[49] T. A. Horst, H. S. Rottengruber, M. Seifert, and J. Ringler, “Dynamic heat exchanger model for performance prediction and control system design of automotive waste heat recovery systems,” *Applied Energy*, vol. 105, pp. 293–303, 2013, doi: 10.1016/j.apenergy.2012.12.060.

[50] R. Sangi, P. Jahangiri, and D. Müller, “A combined moving boundary and discretized approach for dynamic modeling and simulation of geothermal heat pump systems,” *Thermal Science and Engineering Progress*, vol. 9. pp. 215–234, 2019, doi: 10.1016/j.tsep.2018.11.015.

[51] R. Joshi, “A Comparative Study of the Effect of Variation of Inside Diameter of Condenser and Mass Flow Rate on the Heat Transfer Coefficient in a Domestic Refrigerator.,” *Material Science*, 2014, Accessed: Dec. 11, 2020. [Online].

[52] A. L. Abdullah, S. Misha, N. Tamaldin, M. A. M. Rosli, and F. A. Sachit, “Photovoltaic thermal /solar (PVT) collector (PVT) system based on fluid absorber design: A review,” *Journal of Advanced Research in Fluid Mechanics and Thermal Sciences*, vol. 48, no. 2, pp. 196–208, 2018.

[53] T. Dembeck-Kerekes, J. P. Fine, J. Friedman, S. B. Dworkin, and J. J. McArthur, “Performance of variable flow rates for photovoltaic-thermal collectors and the determination of optimal flow rates,” *Solar Energy*, vol. 182, no. February, pp. 148–160, 2019, doi: 10.1016/j.solener.2019.02.032.

[54] F. Negro, “Accumulo termico per un Energy-Hub : modello e validazione sperimentale Thermal storage for an energy-hub : model and experimental validation,” 2013.

[55] M. Tammaro, C. Montagud, J. M. Corberán, A. W. Mauro, and R. Mastrullo, “A propane water-to-water heat pump booster for sanitary hot water production: Seasonal performance analysis of a new solution optimizing COP,” *International Journal of Refrigeration*, vol. 51, pp. 59–69, 2015, doi: 10.1016/j.ijrefrig.2014.12.008.

[56] “EUR-Lex - 52019DC0001 - EN - EUR-Lex.” https://eur-lex.europa.eu/legal-content/EN/TXT/?qid=1548155579433&uri=CELEX:52019DC0001 (accessed Jan. 19, 2021).

[57] S. Barberis, “Università degli Studi di Genova Scuola Politecnica Ph . D . Thesis in Fluid Machinery Engineering Polygenerative Smart Grids and interaction with energy storage systems PhD Candidate :,” 2016.

[58] “Emissioni inquinanti legate alla produzione di elettricità in Italia.” https://scienzaverde.it/cronaca-ambientale-blog/emissioni-inquinanti-produzione-elettricita-italia/#Paesi_Bassi (accessed Jan. 19, 2021).

[59] “Netherlands natural gas prices, June 2020 | GlobalPetrolPrices.com.” https://www.globalpetrolprices.com/Netherlands/natural_gas_prices/ (accessed Jan. 19, 2021).

[60] "QUANTO COSTA INSTALLARE UNA CALDAIA A GAS NUOVA: IL PREZZO DI UNA CALDAIA A GAS NORMALE O A CONDENSAZIONE, COSTI CALDAIE IVA COMPRESA - CONSULENTE-ENERGIA.COM." http://www.consulente-energia.com/am-quanto-costa-installazione-caldaia-a-gas-nuova-prezzo-di-acquisto-caldaie-a-gas-metano-normali-o-a-condensazione-iva-inclusa.html (accessed Jan. 20, 2021).

[61] R. Gubiani, G. Pergher, D. Dell'antonia, and D. Maroncelli, "Convegno Nazionale IV Sezione AIIA La produzione di energia da biomasse agroforestali e' sempre una proposta attuale?" Accessed: Jan. 20, 2021. [Online].

[62] D. Connolly *et al.*, "Heat roadmap Europe: Combining district heating with heat savings to decarbonise the EU energy system," *Energy Policy*, vol. 65, pp. 475–489, 2014, doi: 10.1016/j.enpol.2013.10.035.

[63] M. A. Sayegh, P. Jadwiszczak, B. P. Axcell, E. Niemierka, K. Bryś, and H. Jouhara, "Heat pump placement, connection and operational modes in European district heating," *Energy and Buildings*, vol. 166, pp. 122–144, 2018, doi: 10.1016/j.enbuild.2018.02.006.

[64] "Capstone Turbine Corporation (CPST)." https://www.capstoneturbine.com/ (accessed Dec. 13, 2020).

[65] "How do I use electricity during the day - the load curve." https://www.solarchoice.net.au/blog/how-do-i-use-electricity-throughout-the-day-the-load-curve/ (accessed Dec. 14, 2020).

[66] F. Veynandt, F., Ramschak, T., Louvet, Y., Kohl, M., Fisher, "LCoH Calculation Method : Comparison Between Task 54 and Solar Heat WorldWide INFO Sheet A013 LCoH Calculation Method : Comparison Between Task 54 and Solar Heat WorldWide INFO Sheet A013," pp. 1–5, 2018.

[67] R. M. Tien Nguyen , Jacob Spendelow, "The levelized costs of electricity (LCOE) from CHP and PV," pp. 1–6, 2014.

[68] Lazard, "Lazard's Levelised Cost of Energy Analysis," *Lazard.Com*, no. November, pp. 0–21, 2017, [Online]. Available: https://www.lazard.com/perspective/levelized-cost-of-energy-2017/.

[69] W. R. Sultana, S. K. Sahoo, S. Sukchai, S. Yamuna, and D. Venkatesh, "A review on state of art development of model predictive control for renewable energy applications," *Renewable and Sustainable Energy Reviews*, vol. 76, no. June, pp. 391–406, 2017, doi: 10.1016/j.rser.2017.03.058.

[70] S. Kemaloğlu, E. Ö. Kuzu, and D. G. Ö. Çetin, "Model predictive control of a crude distillation unit an industrial application," *IFAC Proceedings Volumes (IFAC-PapersOnline)*, vol. 7, no. PART 1, pp. 880–885, 2009, doi: 10.3182/20090712-4-tr-2008.00144.

[71] "Solar Forecasting & Solar Irradiance Data." https://solcast.com/ (accessed Dec. 18, 2020).

[72] DNV GL, "Assessment of Selected Ternative Fuels and technologies," *Imo*, vol. 391, no. June, pp. 1–48, 2018, [Online]. Available:

http://www.imo.org/en/KnowledgeCentre/IndexofIMOResolutions/Maritime-Safety-Committee-(MSC)/Documents/MSC.391(95).pdf.

[73] ABS, "Low Carbon Shipping Setting the Course To Pathways To Sustainable Shipping."

[74] E. Lewenhaupt, "Methanol as an alternative fuel in shipping Stena Line at a glance," *Maritimes Cluster Norddeutchland*, 2017.

[75] "SECA & ECA - Thor Marine Trading." https://www.thormarinetrading.com/bunker-trading/seca-eca/ (accessed Dec. 22, 2020).

[76] "Fincantieri | FINCANTIERI E CNR: INNOVAZIONE IN CAMPO NAVALE." https://www.fincantieri.com/it/media/comunicati-stampa-e-news/2019/fincantieri-e-cnr-innovazione-in-campo-navale/ (accessed Dec. 26, 2020).

[77] "C800S :: Capstone Turbine Corporation (CPST)." https://www.capstoneturbine.com/products/c800s (accessed Dec. 27, 2020).

[78] E. K. Boulougouris and L. E. Chrysinas, "LNG Fueled Vessels Design Training," no. July, 2015, [Online]. Available: https://www.onthemosway.eu/wp-content/uploads/2015/06/Lecture-Notes.pdf.

[79] "Cryo Systems." https://sweden.man-es.com/products/cryo (accessed Dec. 28, 2020).

[80] L. van Biert, M. Godjevac, K. Visser, and P. v. Aravind, "A review of fuel cell systems for maritime applications," *Journal of Power Sources*, vol. 327, pp. 345–364, 2016, doi: 10.1016/j.jpowsour.2016.07.007.

[81] J. J. de-Troya, C. Alvarez, C. Fern andez-Garrido, and L. Carral, "Analysing the possibilities of using fuel cells in ships," *International Journal of Hydrogen Energy*, vol. 41, pp. 2853–2866, 2016, doi: 10.1016/j.ijhydene.2015.11.145.

[82] T. Tronstad, H. Høgmoen, Å. Gerd, P. Haugom, and L. Langfeldt, "Study on the use of fuel cells in shipping DNV GL 1 MARITIME STUDY ON THE USE OF FUEL CELLS IN SHIPPING EMSA European Maritime Safety Agency." Accessed: Dec. 28, 2020. [Online]. Available: www.dieselduck.net.

[83] M. Ronchetti, "Ente per le Nuove tecnologie, l'Energia e l'Ambiente CELLE A COMBUSTIBILE Stato di sviluppo e prospettive della tecnologia." Accessed: Dec. 28, 2020. [Online].

[84] Hydrogenics, "Fuel Cell Megawatt Power Generation Platform," *Hydrogenics' HyPMTM-HD30*, 2019, [Online]. Available: https://www.hydrogenics.com/hydrogen-products-solutions/fuel-cell-power-systems/stationary-stand-by-power/fuel-cell-megawatt-power-generation-platform/.

[85] "HyPM HD 30 - Hydrogenics - PDF Catalogs | Technical Documentation | Brochure." https://pdf.directindustry.com/pdf/hydrogenics/hypm-hd-30/33492-420319.html (accessed Dec. 28, 2020).

[86] J. W. Pratt and L. E. Klebanoff, “Feasibility of the SF-BREEZE: a Zero-Emission, Hydrogen Fuel Cell, High-Speed Passenger Ferry.” Accessed: Dec. 28, 2020. [Online]. Available: http://www.ntis.gov/search.

[87] D. P. Carmela Maria *et al.*, “Leadership T.- GEI - D4.4,” 2018.

[88] Hexagon, “Compressed Hydrogen Solutions Flyer.” http://www.hexagonlincoln.com/resources/brochures (accessed Feb. 17, 2018).

[89] Helbio, “Helbio HHG series.” .

[90] BlueGold, “BlueGold Research LNG prices.” .

[91] “Hydrogen economy - Wikipedia.” https://en.wikipedia.org/wiki/Hydrogen_economy (accessed Dec. 30, 2020).

[92] Alexander Körner, “Technology Roadmap: Hydrogen and Fuel Cells (Technical Annex), International Energy Agency (IEA),” p. 81, 2015.

[93] M. Melaina and M. Penev, “Hydrogen Station Cost Estimates: Comparing Hydrogen Station Cost Calculator Results with other Recent Estimates,” 2013. Accessed: Dec. 30, 2020. [Online]. Available: www.nrel.gov/publications.

[94] “Buycylinder.” http://www.buycylinder.com/product/search.do?HYFL=natural%20gas&select=2&SHOW_TYPE=%20list&SPGJC (accessed Dec. 30, 2020).

[95] U.S. Department of Energy *et al.*, “Energy Hydrogen Storage Cost Analysis,” 2013, [Online]. Available: https://www.osti.gov/servlets/purl/1082754.

[96] “EMEA Bunker Prices - Ship & Bunker.” https://shipandbunker.com/prices/emea (accessed Dec. 30, 2020).

[97] “TRADING ECONOMICS | 20 million INDICATORS FROM 196 COUNTRIES.” https://tradingeconomics.com/ (accessed Dec. 30, 2020).

[98] AEEG, “Costi di produzione di energia elettrica da fonti rinnovabili.” https://www.autorita.energia.it/allegati/docs/13/RappPolitecnicoRinn.pdf (accessed Dec. 30, 2020).

[99] “» Natural Gas and the Environment NaturalGas.org.” http://naturalgas.org/environment/naturalgas/ (accessed Jan. 02, 2021).

[100] D. Rattazzi, M. Rivarolo, T. Lamberti, and L. Magistri, “A design tool for the performances comparison of innovative energy systems for naval applications,” in *E3S Web of Conferences*, Aug. 2019, vol. 113, doi: 10.1051/e3sconf/201911302005.

[101] M. Rivarolo, D. Rattazzi, T. Lamberti, and L. Magistri, “Clean energy production by PEM fuel cells on tourist ships: A time-dependent analysis,” *International Journal of Hydrogen Energy*, vol. 45, no. 47, pp. 25747–25757, Sep. 2020, doi: 10.1016/j.ijhydene.2019.12.086.

[102] D. Rattazzi, M. Rivarolo, T. Lamberti, and L. Magistri, “A design tool for the performances comparison of innovative energy systems for naval applications,” in *E3S Web of Conferences*, Aug. 2019, vol. 113, doi: 10.1051/e3sconf/201911302005.

[103] D. Rattazzi, M. Rivarolo, T. Lamberti, and L. Magistri, “PRELIMINARY DESIGN OF INNOVATIVE LOW EMISSIONS SYSTEMS FOR DIFFERENT MARITIME APPLICATIONS,” 2019, pp. 9–10.

[104] D. Rattazzi, M. Rivarolo, and A. F. Massardo, “An innovative tool for the evaluation and comparison of different fuels and technologies onboard ships,” pp. 1–6, 2020.

[105] “Methanol: The marine fuel of the future.” Accessed: Jan. 05, 2021. [Online].

[106] P. Gualeni and A. Rubattino, “Distributed generation for naval application : energetic and environmental analysis,” 2016.